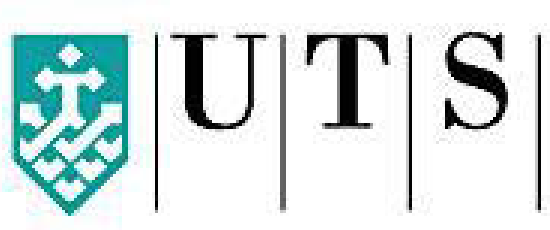

School of Civil and Environmental Engineering

University of technology, Sydney

Sydney, Australia

PERFORMANCE OF POLYMER-CONCRETE COMPOSITES IN SERVICE LIFE OF MARITIME STRUCTURES

By

Seyed Farhad Nabavi

A thesis submitted in fulfillment of the requirements for the degree of

Doctor of Philosophy

December 2014

CERTIFICATE OF AUTHORSHIP/ORIGINALITY

I hereby declare that this submission is my own work and to the best of my knowledge it contains no material previously published or written by another neither person, nor material which to a substantial extent has been accepted for the award of any other degree or diploma at the University of Technology, Sydney or any other educational institution. Any contribution made to the research by others, with whom I have worked at the University of Technology, Sydney or elsewhere, is explicitly acknowledged in the thesis.

I also certify that the intellectual content of this thesis is the product of my own work. Any assistance that I have received in my research work and the preparation of the thesis itself has been acknowledged. In addition, I certify that all information sources and literature used are indicated in the thesis.

Seyed Farhad Nabavi

December 2014

ABSTRACT

Premature deterioration of Reinforced Concrete (RC) structures exposed to severe environment has become a global problem with serious economic consequences, environmental impact, and safety issues. According to the enormous investigations, it is evident that the dominant factor of this process is the chloride-induced corrosion of the steel reinforcement in RC structures. Diffusion of the chloride into the concrete occurs through the interconnected pores and surface cracks generated by different sources such as external loading and shrinkage. Large number of the wide cracks not only can accelerate the diffusion process but also enhance the probability of the steel corrosion leading to decreasing the service life of structures. In spite of many conducted studies, records and case studies confirm that the problem still exists.

In this study, current significant corrosion preventing methods have been investigated and their advantages and disadvantages have been examined. Based on this investigation, modifying and improving the microstructure of the concrete, to reduce its permeability, gives the impression to be the most leading method due to easy implementation and lower cost.

In the experimental program of this research two main research areas consisting (i) effect of polymer-concrete composites on mechanical properties of the concrete, and (ii) effect of polymer-concrete composites on service life of RC structures exposed to severe environmental exposure conditions have been investigated. In addition, two different categories of polymer-concrete composites including synthetic fibres and latex polymer have been selected to investigate their effects on mechanical properties and durability performance of the composites. According to the result of this study, polymer-concrete composites reveal enhancement on the mechanical properties of the concrete such as compressive strength, flexural strength, and tensile strength.

Furthermore, to assess the durability performance of the polymer-concrete composites series of long-term tests (up to 720 days) have been conducted in the concrete laboratory of University of Technology Sydney. In this research, service life of the

RC structure has been taken either as time of corrosion initiation (corrosion free service life) or time of cracking of the concrete cover due to steel corrosion (corrosion time). Chloride content measurement was utilized in this study to find the chloride diffusion rate in polymer-concrete composites exposed to high concentrated chloride solution for 24 months. Results of chloride content tests revealed that the polymer-concrete composites can significantly reduce the chloride diffusion rate in concrete and extend the corrosion-free service life of RC structures. To estimate the corresponding service life to corrosion time, an accelerated electrochemical method was deployed in order to obtain the results in relatively shorter time. The results of corrosion time also confirmed that the polymer-concrete composites can increase the service life of the structure considerably.

Most of the previously proposed models available in the literature, consider the chloride diffusion coefficient as a constant parameter. In this study, a new mathematical model was proposed to determine the chloride diffusion coefficient as a time-dependent parameter. In the proposed model the effects of water cement ratio, cement type, cement content, and coarse aggregate proportion were investigated and included

Finally, finite element analysis by Utilizing ABAQUS has been performed to verify the mathematical model. The results of the computer modeling and long-term experimental program are in reasonably good agreement.

To My Lovely Wife

And

To Soul of My Beloved Mother

ACKNOWLEDEMENT

The research presented in this thesis was carried out in the School of Civil and Environmental Engineering at the University of Technology, Sydney (UTS).

I wish to express my deep appreciation and gratitude to my supervisor, Dr. Shami Nejadi for his patient supervision, valuable guidance, critical suggestions, and continuous support throughout this research. I would also like to thank my co-supervisor, Professor Bijan Samali, for his support and many discussions during the study.

I thank the manager, Mr. Rami Haddad, and staff, David Hooper and David Dicker, of UTS Concrete Laboratory.

I would like to express my deepest gratitude to my father and to soul of mother for their love, support, and encouragement.

Eventually, I wish to thank my wife, Dayrak Ahmadipour, who has always accompanied me throughout this journey. Without her love, patience, support, and encouragement the completion of this thesis would not have been possible.

TABLE OF CONTENTS

LIST OF TABLES

LIST OF FIGURES

CHAPTER 1

INTRODUCTION

CHAPTER 1. INTRODUCTION

1.1 BACKGROUND

Reinforced concrete (RC) structures are generally exposed to various environmental conditions during their lifetimes. Therefore, degradation and deterioration of concrete structures may occur that can significantly affect the service life of the structures. Degradation processes influence both concrete and steel strongly depends on diffusion processes of moisture and aggressive species such as carbon dioxide, chlorides, and sulfates from environment into the concrete (GjØrv, 2009). Particularly, premature deterioration of reinforced concrete (RC) structures exposed to marine environment has become a worldwide problem with serious economic consequences regarding to maintenance, repair, and replacement of the RC structures and also environmental impact and safety issues (Ann et al., 2009, Song and Kwon, 2009).

According to the vast investigations throughout the literature, it is found out that the dominant factor of degradation process is the chloride-induced corrosion of the steel reinforcement in concrete (Zornoza et al., 2009, Costa and Appleton, 1999). Chloride diffusion into the concrete occurs through the concrete interconnected pores and surface cracks resulted from different sources such as loading and shrinkage. When the concentration of chloride ions around the steel reinforcement surface reaches to the chloride threshold level, destruction (depassivation) of high alkaline protective layer leads to steel corrosion initiation (Ann and Song, 2007, Koleva et al., 2007, Hussain et al., 1995, Glass and Buenfeld, 1997, Angst et al., 2009). Consequently, the

corrosion products occupy the space four to five times more than the initial state of steel. This expansion generates tensile stresses in concrete leading to cracking, delamination, and spalling of concrete cover. In addition, the corrosion of steel reinforcement causes the reduction of reinforcement cross section, loss of bond between steel and concrete, strength reduction, and ductility. Accordingly, the durability and serviceability of concrete structures are decreased, and their service lives shortened.

Indeed the premature deterioration of RC structures causes many serious repair and rehabilitation problems resulting in a huge annual cost to the construction industry. The main consequences can be classified as follows. First problem is economic impact and financial problem due to repair and/or reconstruction of some parts or even the whole structure (Virmani, 2002). Generally, the repair of structures is an expensive issue and for marine and water front structures due to the presence of water and difficulties in access to damage portion, is much more expensive and time consumer.

Second problem is the safety of concrete structures due to the presence of cold joint between the old concrete and fresh concrete. In June 1999 the repaired (replaced) lining-concrete-block (length of 2m, weight of 200kg) of a tunnel hit the Shinkasen super express at the Fukuoda-tunnel of Sanyo Shinkasen Line. In two incidents, concrete blocks of another tunnel and the concrete wall of an apartment fell down (Sue, 2001).These accidents gave rise to increase uncertainties of about the safety of concrete structures. Sue's experimental observations show that the bending strength of the repaired member remarkably decreases due to the cold joint between the top layer (old concrete) and the lower layer (repaired and replaced part).

According to recent systematic study commissioned by the United States Federal Highway Administration (FHWA), the annual direct cost of corrosion in the United States was $276 billion in 1998, or 3.1% of the gross domestic product (GDP) (Koch et al., 2001). Corrosion cost studies were also conducted in other countries, such as the United Kingdom, Japan, Australia and Kuwait. Even though the level of effort varies greatly among these studies, all of them estimated the total annual cost of corrosion as ranging between 1% and 5% of each country's gross national product (GNP) (Virmani, 2002). As a rapidly increasing number of new important concrete

infrastructures are being produced, an increasing and precisely controlled corrosion of reinforcement is not only a technical and economic issue, but also a very significant environmental and sustainability issue.

In spite of the numerous conducted studies, investigations, and proposed various methods to prevent the chloride-induced corrosion of steel reinforcement, the records and case studies confirm that the problem still exists (Costa and Appleton, 2002, Khayat et al., 2005). In this study the most significant current corrosion preventing methods are investigated and their advantages and disadvantages are reported.

Among the proposed methods for extension of the service life, improving the microstructure of concrete with the aim of reducing the concrete permeability can be the most appropriate method due to relatively easy implementation and life time cost (Val and Stewart, 2003). One of the methods to improve the concrete microstructure is the polymer-concrete composites to modify the cementitious matrix by means of reducing the microcracks and blocking the pores.

Two different following polymer-concrete composites are implemented in this research:

- Fibre Reinforced Concrete (FRC) incorporating polypropylene (PP) fibres to reduce the number and size of cracks specially surface cracks.
- Polymer Modified Concrete (PMC) incorporating Styrene Butadiene Rubber (SBR) which is classified as latex to block the interconnected pores.

In this research, an extensive experimental program is employed to investigate the durability performance of polymer-concrete composites exposed to severe conditions.

A mathematical model to express chloride diffusion coefficient as a time-dependent parameter is proposed. A computer model utilising ABAQUS software is conducted and eventually is verified by experimental results of this study.

1.2 RESEARCH OBJECTIVES

Due to growing number of RC infrastructures, there exists a need for both analytical and experimental research on extending the service life of the RC structures. Precise prediction of service life requires understanding the influencing parameters on deterioration of RC structures.

The objectives of this thesis can be expressed as follows:

- To study the deterioration mechanisms of reinforced concrete structures.
- Better understanding of the influencing parameters and factors on durability and service life of the structures.
- Conducting a comprehensive experimental investigation on the durability performance of polymer-concrete composites exposed to severe environmental exposure conditions.
- Developing optimized mix design and methods to cast and curing of the polymer modified concrete
- Proposing a mathematical model to determine chloride diffusion coefficient as a time-dependent parameter to predict RC structures service life more precisely.
- Conducting a FE analysis to determine the chloride content in concrete at different depths by utilizing ABAQUS software (computer modelling).
- To verify the proposed mathematical model by comparison of FE analysis results with the experimental results obtained in this study.

1.3 OUTLINE OF THESIS

This thesis is presented in ten chapters which is organised as follows:

Chapter 1 presents an introduction to work and the objectives of the study

Chapter 2 includes literature review regarding the existing problems, conducted investigations, different methods, and previously proposed mathematical models to increase the service life of the RC structures emphasising on polymers in concrete.

Chapter 3 gives a vast and extensive investigation on mathematical and analytical models to predict the diffusion rate, steel corrosion in concrete, and service life.

Chapter 4 presents two different analyses conducted in this research including technical assessment and cost impact of the most common corrosion prevention methods. In addition, performing data analysis and comparison of previously proposed mathematical models presented with the experimental database in the literature.

Chapter 5 investigates the polymers in concrete, their physical and mechanical properties and different applications of polymers in concrete.

Chapter 6 illustrates the experimental program including material properties, sample preparations, test methods and assessment of the mechanical and durability properties of the selected polymer-concrete composites in this research.

Chapter 7 Discusses the experimental results of this investigation comprehensively.

Chapter 8 presents the analytical model of chloride diffusion coefficient as a time-dependent parameter proposed in this study.

Chapter 9 expresses the FE analysis (computer modeling) utilising ABAQUS software to determine the chloride content in the concrete at different depths over time applying both chloride diffusivity and surface chloride concentration as time-dependent parameters.

Chapter 10 presents a brief summary of the research and conclusions drawn from this study and suggestions for further research.

CHAPTER 2

LITERATURE REVIEW

CHAPTER 2. LITERATURE REVIEW

2.1 INTRODUCTION

Premature deterioration of reinforced concrete structures exposed to severe environment is a worldwide problem. Corrosion of embedded reinforcing steel caused by the ingress of chloride ions into the concrete is the dominant factor of the problem in many countries. Chloride ions derived from de-icing salts or marine environment diffuse into the concrete and contact the steel reinforcement. When the chloride concentration at the reinforcing steel reaches the critical level or the Chloride Threshold Level (CTL), the pH of the concrete around the steel bars decreases and depassivation can take place. Depassivation in the presence of oxygen and moisture at the steel surface, initiates the corrosion of the steel reinforcement. The penetration of chloride into the concrete occurs via different mechanisms depending on the exposure environment. In order to overcome this problem and prevent the initiation of corrosion of reinforcing steel, it is necessary to understand how chloride ions are transported through concrete.

This chapter contains a review of the current knowledge of the structure of Portland cement concrete. More specifically, the review addresses the microstructure of concrete, its durability and service life, the deterioration mechanisms of reinforced concrete structures, the mechanism of chloride ion transport in concrete, CTL, surface chloride concentration, and chloride diffusion coefficient. In addition, mathematical

models that predict the service of concrete structure are investigated. the next section gives some real-world background to the problem.

2.2 BACKGROUND

Reinforced concrete structures have indicated high strength but many of them have shown durability problems which consequently generates high cost maintenance and repair issues. Many reported collapses of in-service structures can be attributed to material degradation caused by environmental exposure conditions (Enright and Frangopol, 2000).

To ensure the reliability of these structures and the safety of the public, health monitoring, condition assessment and safety evaluation have become necessary (Chong et al., 2003).

In 2006, U.S. Department of Transportation identified about 25% of almost 600,000 bridges in the United States as structurally deficient. It was estimated that more than US $65 billion of investment would be needed to replace these bridges or address the existing deficiencies. Australia has about 50,000 public bridges, most of which are considered old and functionally obsolete (O'Connor, 2007). This clearly represents a major challenge to the civil and structural engineering community.

The collapse of the I-35W Bridge in Minneapolis, (Minnesota, U.S.A.) in 2007 provided a stark reminder, to the governments and the structural engineering community alike, about the importance of structural health diagnostics. According to the Australian public road departments (Sumitomo 2000), it is estimated that on average more than AUD 220 million per annum is allocated solely to bridge maintenance. A recent survey by the Roads and Maritime Services (RMS) of New South Wales found that about 63% of their bridges were unsatisfactory and required repairs and remedial work. It is apparent that techniques of damage detection and structural health monitoring are necessary for routine maintenance of the current “distressed” civil infrastructure in Australia and other parts of the world.

2.3 STRUCTURE OF CONCRETE

Concrete, in the broad sense, is a composite material composed of Portland cement as a binder, water, coarse and fine aggregate. The binder (cement paste) "glues" the aggregate together to form a synthetic conglomerate (Neville and Brooks, 1987).

Portland cement is the most common type of cement in general usage. It consists of a mixture of oxides of calcium, silicon, and aluminum. Aggregates can be obtained from many different sources and kinds of material. The cement may be Portland cement or a mixture of Portland cement and pozzolanic materials such as fly ash, blast-furnace slag, and silica fume (Mindess and Young, 1981).

Mixing water with a cementitious material forms a cement paste by the process of hydration. The cement paste glues the aggregate together and fills the voids between particles. A lower water cement ratio (W/C) yields a stronger concrete. The quality of mixing water should be close to that of drinking water because impure water can cause problems in setting time or premature failure of the structure. Coarse and fine aggregates make up the bulk of a concrete mixture. Sand (natural/artificial) and gravel (natural/crushed stone) are typically used in concrete mix (Shetty, 2005).

The properties of concrete are influenced not only by the properties of the constituent materials but also by their interfacial properties. The volume occupied by a properly compacted fresh concrete is slightly greater than the compacted volume of aggregate which the concrete contains. This volume difference means that the aggregate particles are not in a point-to point contact but are separated from one another by a thin layer of cement paste (Neville and Brooks, 1987).

2.3.1 Chemical Composition of Portland Cement

The chemical composition of a general-purpose (ordinary) Portland cement is given in Table 2-1. Noted that the quantities do not add up to 100%, impurities accounted for the missing percentages (Neville and Brooks, 1987).

The chemistry of the Portland cement used in concrete is an important factor in the concrete microstructure. Cements vary considerably in chemical characteristics. These chemical variations affect the developing pore solution chemistry and the paste structure.

Table 2-1 Typical composition of ordinary Portland cement (Neville and Brooks, 1987)

Chemical Name	Chemical Formula	Shorthand Notation	Weight Percent
Tricalcium silicate	$3CaO.SiO_2$	C_3S	50
Dicalcium silicate	$2CaO.SiO_2$	C_2S	25
Tricalcium aluminate	$3CaO.Al_2O_3$	C_3A	12
Tetracalcium aluminoferrite	$4CaO.Al_2O_3.Fe_2O_3$	C_4AF	8
Calcium sulfate dehydrate	$CaSO_4.2H_2O$	CSH_2	3.5

The alkaline nature of concrete pore solutions provides high protection against corrosion of the embedded steel reinforcement. The specific content of the minor alkali-bearing components such as potassium sulfates or potassium calcium sulfates in the composition of the cement, strongly influences concrete pore solution chemistry (Bye, 1999, Goñi and Andrade, 1990).

Also, chemical composition variations in the Portland cement have a considerable effect on the concrete permeability and chloride binding properties. For instance, very small differences in *CaO* contents make major differences in the relative proportions of the calcium silicate components, namely C_3S and C_2S. The relative proportions of the two mentioned calcium silicates induce significant influence on paste microstructure. Similarly, the proportions of the aluminum-bearing phases C_3A and ferrite (nominally"C_4AF") in the cement, influence the rate and extent of the ettringite (ettringite is the mineral name for calcium sulfoaluminate) production (Bullard et al., 2011).

2.3.2 Hydration Reaction

The setting and hardening of concrete are the result of chemical and physical processes that take place between cement and water. Explicit understanding of the chemistry of the hydration is necessary for full appreciation of the properties of cement and concrete. It is assumed that the hydration of each component of Portland cement takes place independently. When cement is brought into contact with water the constituents hydrate at different rates and make contributions to the overall strength of the concrete at different times. For instance, C_3S assists in the initial set and continues hydrating for the first few days. The hydration reaction can be represented as follows (Bullard et al., 2011, Scrivener and Nonat, 2011):

$$2C_3S + 7H \rightarrow C_3S_2H_4 + 3CH \tag{2.1}$$

This reaction makes a significant contribution to the early strength of the concrete. However, C_2S hydrates at a much slower rate with similar products to those of C_3S but much less calcium hydroxide, as a comparison of Equations 2.1 and 2.2 shows:

$$2C_2S + 5H \rightarrow C_3S_2H_4 + CH \tag{2.2}$$

This reaction proceeds for an extended period and is thought to be the main contributor to strength beyond and after 28 days.

In contrast to C_2S, C_3A undergoes to a very rapid reaction in the presence of water which can result in flash set. Gypsum is added to cement to control this reaction. In the presence of sulfate, C_3A reacts with water to form ettringite:

$$C_3A + 3CSH_2 + 26H \rightarrow C_6AS_3H_{32} \tag{2.3}$$

If most of the sulfate is consumed in the reaction, the ettringite will become unstable and will convert to a different sulphoaluminate hydrate:

$$C_6AS_3H_{32} + 2C_3A + AH \rightarrow 3C_4ASH_{12} \tag{2.4}$$

Since C_3A undergoes a very rapid chemical reaction, it gains most of its strength in one day and little thereafter. Similarly, C_4AF reacts rapidly with water but is not thought to add much to the strength of the concrete.

In summary, C_3A has the main effect on the rheology of the fresh mix and the setting of the concrete. Generally, C_3S gains most of its strength in the first seven days and little increase occurs afterwards. C_2S contributes little to early strength but continues gaining strength after 28 days. Finally, C_4AF makes little contribution to the strength of the concrete.

2.3.3 Microstructure of Concrete

Noted earlier, concrete consists of aggregates which are held together by a porous binder (porous media), specifically a complex of solids and pores called *hydrated cement paste*. Since this porous media is a continuous phase in the composite, it is critical with respect to movement of water and chemical substances into or out of the concrete. This is a feature extremely relevant to the durability of the concrete in service.

The microstructure of concrete is complex and its transport properties are influenced by many interacting parameters such as the W/C ratio, the use of chemical admixtures, variation in aggregate size and proportion, and curing method (Diamond, 2004). More water is added to concrete than that required for the hydration reaction with the cement, the extra water is required for workability as the concrete is mixed and placed in position. In water the cement grains tend to join together in small groups leaving water-filled gaps between each group and the next. As each cement grain hydrates, a halo of cement gel form around it and calcium hydroxide crystals grow in some of the gaps. The haloes reduce the contact between the cement grains and the water, but the reaction proceeds and gradually the space between the grains begins to fill with gel. Pores within the gel trap some of the water and there may be relics of unhydrated cement at the locations of the centers of the original grains.

The cement gel is not able to fill the space between the groups of grains completely. As the gel grows and the cement paste sets, water is trapped in capillary passages.

Hydration continues and consequently the volume of water decreases as it is used up in the reaction until there is insufficient to fill the capillaries, and so pockets of water vapour form. The process of structure formation is shown schematically in Figure 2-1.

At first, the capillaries are interconnected and this remains the case if the concrete original water content was too high or if hydration is not permitted to continue over a sufficiently long period. So, as long as sufficient water is provided, the interconnected pores in concretes with a low W/C ratio will eventually become blocked. However, as the W/C ratio increases, the time for which water curing must be provided increases substantially until for values in excess of 0.7 it is not possible to block the pores.

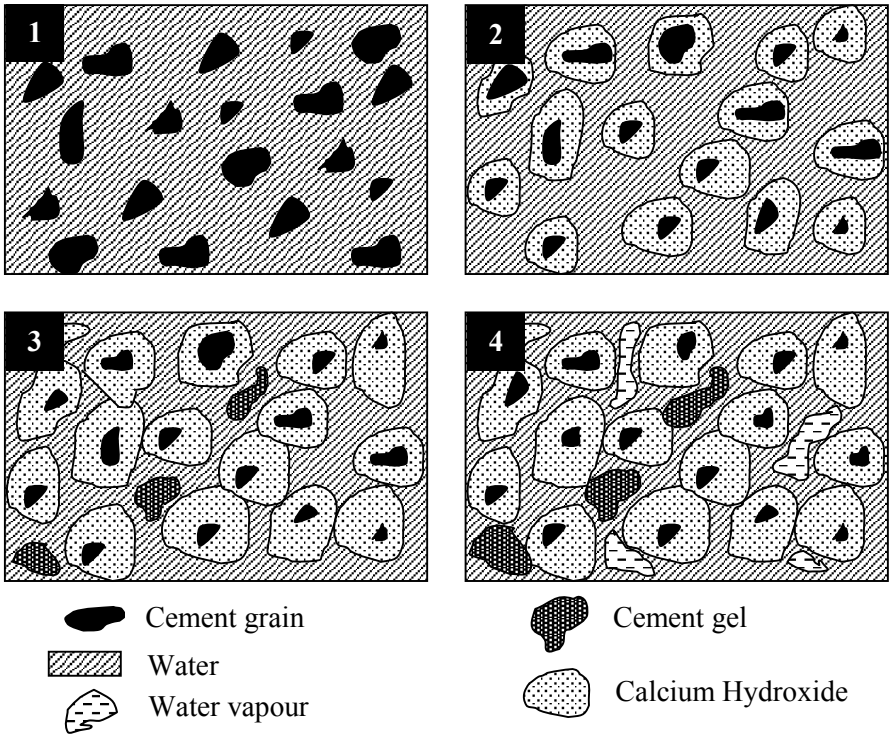

Figure 2-1 Development of capillary pores in cement paste structure

The presence or absence of interconnected pores within the cement paste is as important in consideration of the durability of concrete as they control permeability. In general, permeable concretes are much less durable because the pore structure allows gases, liquids, and any dissolved salts to penetrate deep into the body of the concrete.

2.3.4 Porosity

Porosity is one of the basic properties of hardened cement paste. Commonly, similar to the other porous materials, the strength of the cement paste depends primarily on its porosity. The exact chemical nature of the hydration products is less significant. As long as there is enough water (theoretically) to fully hydrate the cement, the cement gel porosity remains independent of W/C ratio. It depends only on the degree of hydration, or maturity, of the paste. Thus, the additional water in the normal range of w/c ratio affects only the capillary porosity (Winslow et al., 1994).

Since the gel porosity is an intrinsic part of the paste structure, the changes in many concrete properties will be directly related to changes in the capillary porosity. Porosity also dominates the permeability of the concrete paste. Pastes with high capillary porosities have high permeability (Powers et al., 1954), as water flows easily through the larger pores. The capillary pore network has the greatest influence on the penetration of fluids into the concrete. The capillary pores are the remnants of water-filled space that exists between the partially hydrated cement grains whereas the gel porosity can be regarded as part of the Calcium Silicate Hydrate (C-S-H) (Roy et al., 1993a). The porosity seen in Scanning Electron Microscope (SEM) micrographs is capillary porosity: gel porosity cannot be resolved by the SEM and would be included in the volume occupied by C-S-H (see Figure 2-2). Well-hydrated paste with low W/C ratio has permeability approximately three orders lower than a paste with a high W/C ratio.

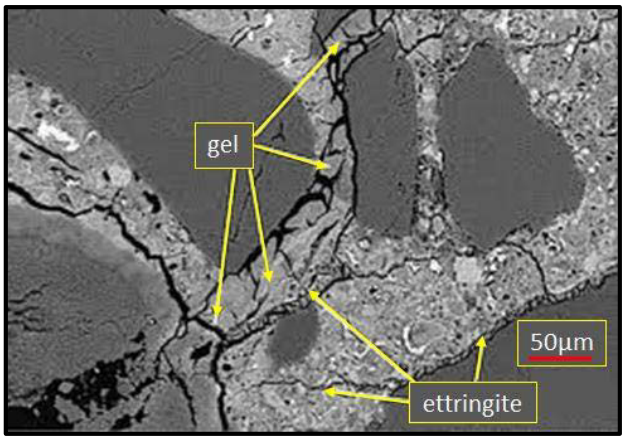

Figure 2-2, SEM micrographs of pores in concrete provided (Roy et al., 1993a)

The cement paste surrounding each aggregate particle, the interfacial transition zone (ITZ), contains higher porosity and lower cement content relative to the bulk cement paste farther away. The ITZ thickness is normally around 50 nm and can occupy 30% to 50% of the total volume of cement paste in concrete and so the property of this phase is expected to have an influence on overall behaviour of the composite (Zheng et al., 2009) .

Most of properties of hardened concrete are related to the quantity and characteristics of various types of pores in the cement paste. The total volume of pores, not their size or continuity, affects the strength and elasticity of the concrete, whereas concrete permeability is influenced by pore volume, size and continuity. It is believed that capillary voids larger than 50μm (referred to as macro pores) are detrimental to the strength and impermeability, whereas voids smaller than 50μm (micro pores) are more related to drying shrinkage and creep of the concrete.

From a pragmatic standpoint, the porosity of a material is not of interest as an end in itself. Rather porosity is of interest because it directly influences both the mechanical and permeability properties of the cementitious materials.

2.3.5 Pore Size and Distribution

There are a variety of "types" of porosity in concrete. These types may be classified in terms of their origin or in terms of their anticipated effect on measurable parameters such as strength or permeability. Sources of porosity in concrete include gel pores, smaller capillary pores, larger capillary pores, large (air) voids, porosity associated with paste-aggregate ITZ, micro-cracks and discontinuities associated with dimensional instabilities, and porosity in aggregate (Ohama et al., 1991).

When concrete has hardened, four types of void and micro-cracking may be recognisable. The smallest of these are gel pores with diameter of 1×10^{-6} mm to 8×10^{-6} mm. Capillary pores are formed by the space originally occupied by the mixing water, and have diameters between 8×10^{-6} and 0.013 mm (Winslow et al., 1994). Air voids are formed through entrapment during compaction and normally have diameter range from

1×10^{-6} mm to 2 mm in diameter. Finally, aggregate pores may exist from 0% to 20% for normal aggregate (Roy et al., 1993a).

The capillary pores network has the greatest influence on the concrete permeability. Gel pores are very small. Air voids are usually isolated as they represent trapped air. Aggregate pores are usually very small or are isolated from the permeability network by being completely surrounded by cement paste.

Concrete porosity is usually expressed in terms of its percentage by volume of concrete. The interconnectivity of pores, rather than total porosity determines a concrete's permeability. Concrete with a high proportion of disconnected pores may be less permeable than concrete with a much smaller proportion of connected, or continuous pores. With greater particularity, it is the overall nature of the matrix pore structure that ultimately affects its permeability, sorptivity, and diffusivity. The size, distribution, interconnectivity, shape, and tortuosity of pores are all determining factors in the overall permeability of a concrete matrix (Roy et al., 1993a). Thus, the distribution of pores significantly influences the permeability of concrete. If the distribution of the pores enables interconnection of the pores, permeability will be increased considerably. It has been observed that pores distribution depends on the several factors such as W/C ratio, curing time and method.

2.3.6 Cracks in Concrete

To identify or develop methods of preventing concrete deterioration, it is important to gain an understanding of the main causes and basic mechanisms of the various forms of deterioration. Deterioration of concrete and its rate may be affected by the presence of defects which the time of construction, or in the very early stages and/or in the long term of the life of the structure (Kwon et al., 2009). These defects permit the atmosphere and other environmental agents to penetrate the surface of the concrete and to take part in the chemical and physical processes which give rise to deterioration (Aldea and Shah, 1999).

One of the most effective concrete deterioration phenomena is surface cracks (Win et al., 2004). Cracks can occur during any stage of the life of a concrete structure. They can be due to the concrete material itself, as in the case of restrained shrinkage, or due to external factors such as excessive loading, displacement, temperature, or design error. During its service life, concrete can be subjected to many different environmental conditions such as different relative humidity, temperature, wet and dry cycles and chemical substances such as salt solutions, acidic gases and liquids can vary widely and in different combinations, resulting in deterioration of the concrete (Jaffer and Hansson, 2008). At the time of placing in the formwork, concrete is a fluid mixture mainly consisting of water, cementitious material, and aggregate. With development of the cement hydration this paste will be gradually converted to a stiff and strong mass. The setting time depends on the type of cement, the presence of admixtures, the curing system, and ambient conditions. Loss of moisture while concrete is in the paste (plastic) state can cause cracks and other defects (Kelly, 1981).

As mentioned above, the cement matrix contains different kinds of pores and capillaries through which harmful chemical substances can diffuse and penetrate into the concrete. In addition, surface cracks assist this process. Some categories of cracks are defined in the following sections:

2.3.6.1 Plastic Shrinkage Cracking

A concrete surface exposed to the atmosphere is subjected to evaporation and loss of the mix water. The rate of evaporation is dependent on the atmosphere conditions such as temperature, presence and speed of wind, relative humidity, and sunny hours in the day. The water lost near the surface will be replaced by water rising from inside the concrete by capillarity action. With continuing surface evaporation, a local reduction in volume will occur. The concrete immediately below the region of reduced volume will resist the decrease in volume. This resistance generates tensile stress in the surface layer and since the concrete is in the early-age and has not gained the sufficient strength, cracking can result (Cohen et al., 1990). These kinds of cracks are called plastic shrinkage cracks and form in a random pattern on the concrete surface. In reinforced concrete if the top reinforcement is close to the surface, the cracks pattern will most

likely follow the reinforcement pattern. Plastic shrinkage cracks can be quite wide (1 to 3 mm) on the surface and can be seen easily, but the depth of the cracks reduces rapidly (shallow cracks) (Uno, 1998).

2.3.6.2 Plastic Settlement Cracking

When concrete is in the plastic form, the aggregate can move in the paste, so the upward bleeding of water may be accompanied by the downward movement of the solids due to gravity. This downward movement will be resisted by the top layer which contains steel reinforcement. In this case, the top layer becomes draped over the bars and separates from the lower surface of the bars, resulting in cracks. The cracks pattern on the surface tends to mirror that of the reinforcement (Shetty, 2005).

If the settlement of solids in the concrete can freely take place without hindrance there will be a reduction in depth and volume of the cast concrete but no cracking. However, any restraint to this movement, e.g. reinforcement, can result in plastic settlement cracks.

Where the solids continue to settle in comparison to those which are prevented from further downward movement, the concrete will 'break its back' and a tear appears in the surface as it is forced into tension. Cracks may develop at regular spacing reflecting the reinforcement layout. These crescent-shaped voids may initially be filled with bleed water. Consequently, the contact area between reinforcing steel and concrete is reduced.

Cracks caused when the settlement of fresh concrete is restrained by reinforcement or formwork. Plastic settlement cracks can form in concrete surface, within the first few hours after placing. As water moves upward through the mixture, the denser constituents move downward. This downward movement may be obstructed by the top layer of reinforcement or by the shuttering.

The plastic concrete may arch over the top of individual reinforcing bars, bringing the surface into tension. Cracks may develop at regular spacing and usually follow the line of the uppermost bars, giving a series of parallel cracks; there may also be shorter cracks at right angles over the bars running in the opposite direction.

It is sometimes possible for plastic settlement cracks to form on a vertical face where reinforcement has restricted the free flow of concrete within the formwork. In such cases it is possible that the cracks are formed between the lines of the reinforcement.

The concrete can also be supported by the shuttering, causing restraint to the concrete in connected members. This typically happens at mushroom-heads on columns but can also occur at other locations, such as under spacer blocks. Cracks at mushroom heads of columns are generally horizontal. They are also typically 1 mm wide and can cross the full section.

The most common restraint in slabs is from the reinforcement. The cracks occur on the top surface and usually follow the line of the uppermost bars, giving a series of parallel cracks; there may also be shorter cracks at right angles over the bars running in the opposite direction. Cracks are typically 1 mm wide and usually run from the surface to the bars. The settlement may also result in visible undulations on the concrete surface, with the high points over the top reinforcing bars.

In some cases where the bars in the top layer of reinforcement are close together, the whole surface layer of the concrete may be ‘suspended’ on the reinforcement while the concrete below settles. This can lead to a horizontal discontinuity beneath the bars, resulting in a loss of bond and with time delamination of concrete cover that protects the reinforcing steel against corrosion.

Unlike cracks in hardened concrete, due to overloading for instance, these cracks form at a very early age and pass through the cement paste and do not pass through aggregate particle pieces. The path is therefore more tortuous. This form of crack can be potentially serious as it passes longitudinal with the reinforcement and extends to the steel, negating the resistance to corrosion provided by the concrete.

Fine cracks can occur in relatively narrow formed surfaces such as columns. The concrete may arch between the containing form faces. Settlement below the restrained concrete results in a crack being formed, generally coinciding with the links.

The concrete can also be supported by the formwork face. This causes restraint to the concrete between connected members and is especially evident where changes in

section cause differential settlement, the concrete in the deeper section settling more than the shallower section resulting in a crack.

2.3.6.3 Dry Shrinkage Cracking

The temperature of concrete will be equal to the surrounding ambient temperature several days after pouring, but the volume changes will continue. Water content in concrete mixes is much greater than the amount required for cement hydration reaction. This additional water enables the mix to have sufficient workability, to be placed and compacted in the shutters easily. This additional water may be trapped in the mix as the concrete sets; it is gradually released to the atmosphere resulting in shrinkage. In this case, the volume reduction is associated with the cooling from the hydration peak temperature. Any restraint of the movement can result in tensile stresses which are sufficiently great to cause cracks (Kalousek, 1954, Kraai, 1985).

Long-term drying shrinkage cracks are formed when drying shrinkage is restrained; typical locations are thin slabs and walls. The main causes of shrinkage cracking are inefficient joints, inadequate reinforcement, poor curing and too high a water content in the original concrete mix (Altoubat and Lange, 2001).

2.4 PERMEABILITY OF CONCRETE

Permeability is the capability of transmissibility of a solid, meaning how much fluid or gas penetrates in a specific time, dependent on the type of permeate, pressure, temperature, thickness of the solid and the exposed area. Permeability in concrete depends on the size, type, distribution, continuity and interconnection of the pores (Hausmann, 1967).

The pores that belong to the sub-distribution representing the finest porosity are created by the hydration process. Because the majority of this porosity exists in the hydration products that are forming, these pores control the kinetics of hydration. Alternatively, from the viewpoint of permeability-pore structure or fracture mechanics-pore structure relationships, the majority of porosity in this range is not important. It is well recognized

that only interconnecting capillary pores significantly contribute to permeability because moisture cannot easily move through the nano-scale gel pores (Aldea et al., 1999).

The movement of gases, liquids and ions through concrete is important because of their interactions with concrete constituents and the pore water which can alter the integrity of concrete directly and indirectly, leading to the deterioration of structures. In reinforced concrete, this deterioration is mainly due to the corrosion of reinforcement, freezing-thaw cycle, and chemical attack (Kollek, 1989).

The air permeability of concrete can be decreased by a relatively low average aggregate size (Caré, 2003, Basheer et al., 2005). When the size and proportion of coarse aggregates increase in a mix, there will be an associated increase in permeability (Wee et al., 1999). Microstructural analysis at the Interfacial Transition Zone (ITZ) of aggregate and cement paste clearly indicates that the coarser the aggregate the more porous at the ITZ, This is in line with the results of permeability and durability studies (Basheer et al., 2005). The W/C ratio factor has an important role in permeability because as the W/C ratio decreases, the porosity of the paste is decreases and the decrement in volume of pores will reduce.

Porosity controls permeability and the most significant affecting parameters which control the total porosity of a composite are the aggregate content, water cement ratio, and curing time. The total effect of ITZ on the overall permeability is low, although its porosity and local diffusivity are higher than those of bulk paste. This indicates that permeability can be governed by the volume fraction and micro-geometry of the entire pore structure within the cement paste, not just that within the porous ITZ (Zheng et al., 2009).

Scholars interested in determination of the diffusivity of aggressive ions, particularly chloride ions, in concrete (Güneyisi et al., 2009) have employed the Nernst-Einstein equation to evaluate the permeability of concrete and predict the service life of the reinforced concrete structures (Lu, 1997).

Permeability can be described by Darcy's law (Equation 2.1) which states that steady-state rate of flow is directly proportional to hydraulic gradient (Hausmann, 1967).

$$v = \frac{Q}{A} = \frac{k\rho g}{\eta} \cdot \frac{\Delta h}{L} \tag{2.5}$$

where, v is the apparent velocity of flow or volume of water per unit time per unit area [m/s], Q is the flow rate [m^3/s], A is the cross-sectional area of the sample [m^2], k is the intrinsic permeability of materials [m^2], ρ is the density of the fluid [kg/m^3], g is the acceleration due to gravity [m/s^2], η is the dynamic viscosity of the fluid [kg/m.s], Δh is the drop in hydraulic head through the sample [m], and L is the thickness of the sample [m].

The intrinsic permeability coefficient "K" is independent of the fluid involved.

$$K = \frac{k\rho g}{\eta} \tag{2.6}$$

Thus

$$v = \frac{Q}{A} = K \cdot \frac{\Delta h}{L} \tag{2.7}$$

where K is the coefficient of permeability or hydraulic conductivity (*m/s*).

When the flow is of an unsteady state, the hydraulic head may not decrease linearly along the direction of flow and in such case the flow velocity is given by:

$$v = K \cdot \Delta h \tag{2.8}$$

And in one-dimensional system:

$$v = K \cdot \frac{dh}{dx} \tag{2.9}$$

Permeability has been used as the criterion to characterise the penetrability of concrete regardless of the environmental situation. There are situations in which permeability is highly relevant to hydraulic pressure, such as submerged concrete where water hydraulic pressure forces water through. However, in concrete structures which are not in contact with water under pressure, permeability is generally not one of the most important mechanisms (Hausmann, 1967, Basheer et al., 2001).

2.5 DURABILITY AND SERVICE LIFE OF REINFORCED CONCRETE STRUCTURES

Durability can be defined as the capability of a building, assembly, component, structure or product to maintain minimum performance over at least a specified time under the service loads and influence of degradation factors (Sarja, 2000). In another words, durability is an indicator which informs of the extent to which a material maintains its original requirements over time.

Degradation factor is any of the group of external factors, including weathering, biological agents, stress, incompatibility and use that adversely affects the performance of building materials and components (Fagerlund, 1979). After construction of a structure, concrete is exposed to in-service conditions that may alter both pore solution composition and pore structures. Penetration of chemical substances, leaching, repeated wetting and drying, freezing events, and carbonation, can induce significant internal changes in pore fluid composition and in pore structure. Some of these alterations may induce specific durability problems (Trocónis de Rincón et al., 2007).

The durability of reinforced concrete structures has become extremely significant task as a quality factor of concrete due to its considerable effect on service life of the structures, and consequently maintenance and repair costs of structures (Liang et al., 1999, Apostolopoulos and Papadakis, 2008, Ferreira, 2010). Most of the problems, which (onshore/offshore) concrete structures such as bridges, dams, and marine structures are involved, have been arisen due to lack of systematic durability design. Due to importance of durability issue and its very high cost effects, in most of countries

over the world many national and international associations such as DURACON (Trocónis de Rincón, 2006) have been established to investigate on the improvement of the durability of concrete structures. Good performance of concrete in service, including durability, is the second important characteristic after the usual required mechanical properties, such as strength. However, in the last decades the problems of unsatisfactory durability of reinforced concrete are in a dramatic increase which causes economic impacts. In general, concrete repair expenses of the deteriorated structures are almost equal to the cost of construction of new ones. In addition, it causes environmental and social problems due to decrease of reliability and safety (Apostolopoulos and Papadakis, 2008, Xi and Ababneh, 2000).

The durability of reinforced concrete structures in chloride environments is a serious challenge to design engineers, infrastructures owner, and researchers. Sustainability has become an increasingly important characteristic for concrete infrastructure, as the production of Portland cement (the most common binder in concrete) is an energy-intensive process that accounts for a significant portion of global carbon dioxide emissions and other greenhouse gases (Mehta, 2002, Peris Mora, 2007)

Durability of a concrete structure directly depends on the microstructure of the concrete and the degree of concrete porosity. However, the other parameters such as concrete cover, quality of finished surface, amount of reinforcement and dimensions of structure are the other durability parameters as well (Hilsdorf and Kropp, 2004, Basheer et al., 2005).

In general, transportation of aggressive ions into the concrete has a great influence on the service life of the concrete structures. For example, the ingress of chloride ions may cause the corrosion of reinforcement leading to the deterioration of structures. Therefore, the diffusion coefficient or diffusivity of the aggressive ions may be one of the most important parameters for evaluating the durability and predicting the service life of a concrete structure (Lu, 1997, Chatterji, 1994, Khatri and Sirivivatnanon, 2004).

Naturally, the high alkalinity of the concrete pore solution (pH > 12.5) due to hydration reaction products leads to form a thin passive layer surrounding the steel bars that prevents the corrosion of steel reinforcement (Glass and Buenfeld, 2000a). As long as

this passive layer is sustained, corrosion will not occur. When the chloride concentration on the reinforcing steel surface exceeds the Chloride Threshold Level (CTL), the pH level is considered to be low enough that the corrosion of steel may take place (Ahmad, 2003). This point is referred to depassivation state. As shown in Figure 2-3, service life of reinforced concrete structure can be modeled as a summation of two separate phases: corrosion initiation time (t_0) and corrosion propagation time (t_p) (Tuutti, 1982). During the initiation time, chlorides migrate from the surface of member through the concrete cover to steel reinforcement. During propagation time, corrosion rate will be accelerated after cracking of the concrete cover. Propagation stage continues until an unacceptable level of steel loss occurs, or concrete cover spalls off which is considered as the end of structure service life (Bertolini, 2008).

Among these three stages, corrosion initiation time usually takes the longest time. It can last for many years depending on the corrosion resistance of the steel, the thickness and quality of concrete cover, and other corrosion protection methods applied to the structure (Funahashi, 1990). The second stage is shorter than the first one, depending on the porosity of the ITZ. The third stage is the shortest one among the three stages, since a crack is formed around the steel bar, it can quickly propagate to the surface.

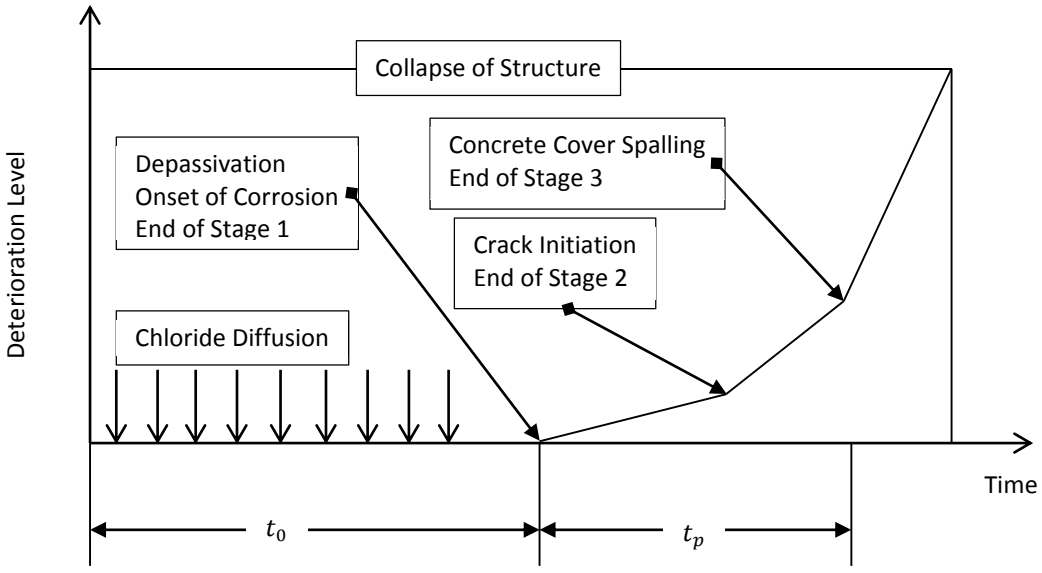

Figure 2-3 Modified model of service life of RC structures (Tuutti, 1982)

Predicting the service life of RC structures has been a great focused area among scholars and scientists in the recent years. Developing various mathematical models to increase the accuracy of the estimations, and also utilizing finite element methods to simulate processes through numerous recently published papers and books, confirms that this area has attracted a great concern (Gulikers, 1997, Martín-Pérez et al., 2000, Ahmad, 2003, Qing Li, 2004, Trocónis de Rincón, 2006, Nokken et al., 2006, Alonso and Sanchez, 2009, Luc The Ngoc et al., 2010, Shafei et al., 2012, Nogueira and Leonel, 2013, Stipanovic Oslakovic et al., 2010).

2.6 MARINE ENVIRONMENT AND CONCRETE STRUCTURES INTERACTION

Marine environment is generally characterized by its high relative humidity which in most cases is accompanied by high temperature. Marine concrete structures such as floating, mobile drilling, near/onshore and offshore, jetties, piers, docks, harbor structures, bridges are subjected to different conditions and factors resulting in premature deterioration of them (GjØrv, 2009).

Corrosion initiates in marine environment with higher rate compared to other climate conditions (Khatri and Sirivivatnanon, 2004). The most effective factors in deterioration of concrete structures exposed to marine environment, rather than relative humidity and temperature, are surface chloride concentration, sulfate attack, carbonation, wetting-drying cycle, and abrasion in this process (Song et al., 2008). These severe environmental conditions and presence of aggressive substances on the concrete surface make the structure service life be much lesser than the normal environmental exposure conditions (Al-Amoudi, 2002).

The environmental conditions of maritime structures vary significantly from the lowest level of construction, usually beneath the seabed, to the highest level of construction, often well above the level of extreme waves. They alter the physical loading on the structure in terms of water pressure, waves and currents and also the environmental

loading in terms of abrasion, temperature, rainfall, frequency of wetting by seawater and exposure to drying conditions (Polder and Peelen, 2002, Meira et al., 2010).

The physical loading will dictate the size of members and the robustness of temporary works needed during construction but the environmental loading will determine the long term durability of the structure within each exposure zone (Sandberg et al., 1998). Because the environmental loading determines the degree of risk of corrosion and risk of abrasion, it also influences the curing of the concrete before its exposure to degrading conditions (Güneyisi et al., 2009, Hooton et al., 2002).

Generally, diffusion of oxygen from air cannot occur, or it occurs at a negligible rate, in a fully and continuously water-saturated cement matrix, as concrete permanently is under sea water. Therefore, an intermittent presence of water due to discontinuous exposure to sea water and air (such as those in the tidal and splash zone of a marine structures) is the most favorable condition to supply both the chloride ions needed to depassivate the metallic reinforcements and the reactant products (H_2O, O_2) needed to feed the corrosion process (Melchers and Li, 2009).

In the submerged zone, concrete is in saturated condition and moisture occupies pores, then dissolved oxygen and carbon dioxide, and chloride ions cannot penetrate to concrete rapidly (Luping, 2008). In the tidal zone, the condition is different, in this zone wetting-drying altering cause a severe condition for corrosion of steel reinforcement. In wetting time moisture (H_2O, O_2) will penetrate to concrete and in dry time due to decreasing of saturation around 85% to 90% chloride ions diffuse to concrete (Roy et al., 1993b).

In the splash zone, the situation turns to extreme condition because of high concentration of chloride on the concrete surface and also diffusing of carbon dioxide when the saturation reduces to 50-60%. In this zone the relative humidity varies between 85% (convenient condition for chloride diffusion) and 50% (convenient condition for carbon dioxide penetration). After splashing of water to the concrete surface, wind firstly, assists the moisture to penetrate deeper and secondly, with accompanying of sunlight the surface becomes dry resulting to decrement of relative humidity to about 50% (Sandberg et al., 1998).

This cycle repeated thousands of times, results in rapid corrosion of steel reinforcement and reduces service life considerably. In this zone, influencing factors on RC structures deterioration such as moisture, accumulated chloride ions and carbon dioxide perform more severely. The corrosion rate, from top level of tidal zone till 1.5 meter above the sea level, has shown the maximum magnitude as shown in Figure 2-4 (Meira et al., 2010).

Figure 2-4 Severe corrosion in tidal zone

2.7 DETERIORATION MECHANISMS AND THEIR PROCESSES

As already discussed, deterioration of concrete and its rate can be affected by the presence of defects which originates at the time of construction, in the very early stages or later in the life of the structure. These defects permit the atmosphere and other environmental agents to penetrate the surface of the concrete and to promote the chemical and physical processes which give rise to deterioration.

Concrete structures may experience many different environmental conditions during their life time and be attacked by various harmful substances in the form of liquids and gases (GjØrv, 2009). Diffusion of these harmful substances through the concrete surface and then distribution of them in the concrete body will cause premature deterioration of structure. There are different causes of deterioration of reinforced concrete structures such as corrosion of reinforcement bars due to carbonation front or chloride ingress, freezing and thawing action, sulfate attack, alkali aggregate reaction,

etc. (Cabrera, 1996, Hossein M. Shodja 2010). The use of wrong materials or imprecise design, improper detailing, insufficient quality control, and inadequate curing system can reduce the service life of the structures or can force extensive repairs with huge economic costs.

Chloride-induced corrosion of reinforcing steel is the major and dominant cause of premature deteriration of RC structures exposed to seawater resulting in shortening of their service life (Gjørv and Vennesland, 1979, Glass and Buenfeld, 2000a, Ahmad, 2003, Anwar Hossain et al., 2009, Brenna et al., 2013).

In chloride-rich environments, like marine environment, concrete is exposed to wetting and drying cycles in tidal and splash zones which accelerates the deterioration of the structure (Polder and Peelen, 2002). In this situation, chloride will penetrate the concrete initially by absorption and produce an accumulation of chloride ions close to the concrete surface, from which diffusion can occur (Ye et al., 2012). The chloride reservoir will be topped up by periodic absorption processes. If the concrete dries out to a greater depth, subsequent wettings carry the chlorides deeper into the concrete. Thus, absorption and diffusion are the most significant transport mechanisms associated with chloride ingress in maritime structures (Hong and Hooton, 1999). However, models based solely on diffusion have been found acceptable for long-term monitoring of chloride ingress in concrete structures (Bamforth et al., 1997, Tang and Gulikers, 2007).

2.7.1 Corrosion Process in RC Structures

Corrosion can be defined as the disintegration of a material into its constituent atoms due to chemical reactions with its surroundings. A loss of electrons of metals due to reaction with water and oxygen weakens the iron due to oxidation of iron atoms which is an example of electrochemical corrosion, commonly known as rusting. This type of damage typically produces oxide(s) and/or salt(s) of the original metal. Corrosion can lead to failure of the plant infrastructure which is usually costly. Failure can be in terms of lost or contaminated products, environmental damage and human safety (Raupach, 1996).

The decrease in pH to certain level may cause depassivation of concrete and commencement of reinforcement corrosion. The state of corrosion at various pH levels is illustrated in Table 2-2 (Pullar-Strecker, 1987).

Table 2-2 State of reinforcement corrosion at various pH levels (Pullar-Strecker, 1987)

pH of concrete	State of reinforcement corrosion
9.5	Commencement of steel corrosion
At 8.0	Severe corrosion
Below 7	Catastrophic corrosion

Corrosion of steel embedded in concrete is an electrochemical process. The corrosion process is confirmed to be similar to the action, which takes place in a battery. The surface of the corroding steel functions as a mixed electrode that is a composite of anodes and cathodes which is electrically connected through the body of steel itself, upon which coupled anodic and Cathodic reactions take place (Morris et al., 2004). Concrete pore water functions as an aqueous medium, i.e. a complex electrolyte. Therefore, a reinforcement corrosion cell is formed, as shown in Figure 2-5 (Hansson, 1984).

Corrosion, as an electrochemical process, is driven by a potential or voltage difference between the anode and cathode. Steel is a heterogeneous material, with a patchwork of sites of slightly different potentials on the surface. Potential differences (great enough to drive corrosion) can be found in areas of residual stress, and even in places where there are scratches on a bar. The electrolyte, or concrete pore solution, surrounding the steel reinforcement may have different concentrations of chloride ions, oxygen, moisture, and hydroxyl ions. These differences can set up microscopic electrochemical cells (microcells), where both the anode and the cathode exist on the same bar. These may be caused by different local concentration of salts or varying availability of oxygen along the bar's length.

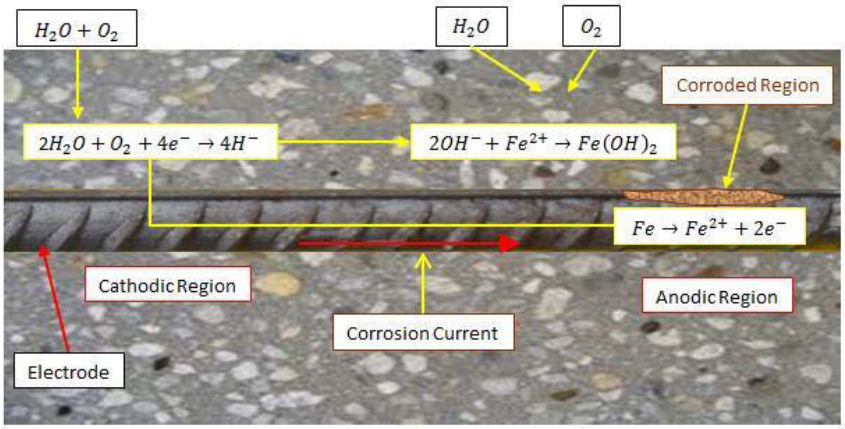

Figure 2-5 Galvanic corrosion of the steel reinforcement in concrete

Reactions at the anodes and cathodes are broadly referred to as "half-cell reactions". The "anodic reaction" is the oxidation process, which results in dissolution or loss of metal whilst the "Cathodic reaction" is the reduction process which results in reduction of dissolved oxygen forming hydroxyl ions.

For steel embedded in concrete, several anodic reactions are possible depending on the pH of the interstitial electrolyte, presence of aggressive anions, and the existence of an appropriate electrochemical potential at the steel surface is shown by Equation 2.10. At the anode site, the iron dissociates to form ferrous ion and electrons (Chitty et al., 2005).

$$Fe \rightarrow Fe^{++} + 2e^- \tag{2.10}$$

The electrons move through the metal towards the cathodic site while the ferrous ions are dissolved in the pore solution. At the Cathodic site, oxygen in the pore solution combines with the electrons to form hydroxyl ions as shown in Equation 2.11:

$$2H_2O + O_2 + 4e^- \rightarrow 4OH^- \tag{2.11}$$

The ferrous and hydroxyl ions move in opposite directions through the pore solution (concrete acts as an electrolyte). When they meet, ferrous hydroxide is precipitated:

$$Fe^{++} + 2OH^- \rightarrow Fe(OH)_2 \tag{2.12}$$

Further, since moisture and oxygen are present, the ferrous hydroxide is oxidized to form ferric oxide or rust as shown in Equations 2.13 & 2.14:

$$4Fe(OH)_2 + 2H_2O + O_2 \rightarrow 4Fe(OH)_3 \quad (2.13)$$

$$2Fe(OH)_3 \rightarrow Fe_2O_3 + 3H_2O \quad (2.14)$$

The precipitated corrosion products occupy 2 to 4 times of the volume of the original steel. As the corrosion products build up they exert a gradually increasing internal tensile stresses in the concrete cover until it cracks. In most cases the cracks propagate from the bar to the adjacent surface, and the cracks on the surface follow the pattern of reinforcement. In this stage, penetration of carbon dioxide, chloride, moisture and oxygen accelerate corrosion progress (Neville and Brooks, 1987).

As corrosion continues and cracks propagate, corners of beams and columns may first become detached and spall. On slabs, the cracks may form at a shallow angle to the surface and be intercepted by cracks from adjacent bars before reaching the surface. Consequently, a plate of concrete above the reinforcement becomes detached from the main body with a few surface cracks only intermittently visible on the surface. This phenomenon is known as lamination or delamination (Otieno et al., 2011).

Corrosion of concrete reinforcement may also take place in chloride affected concrete when little oxygen is available. In this case corrosion is localized and forms deep pits. The volume of generated corrosion products may be insufficient to cause surface cracking, and it is possible that there could be severe loss of cross-section of some bars with very little prior warning from visible signs on the surface. Therefore, in addition to loss of concrete cover, a reinforced concrete member may suffer structural damage due to loss of bond between steel and concrete and loss of rebar cross-sectional area (Shetty, 2005, Johannesson, 2003, Fang et al., 2004).

Electrical resistivity (or conductivity) of concrete is of importance to certain diffusion of aggressive ions and corrosion process, since concrete in the corrosion process contributes as an electrolyte (solid electrolyte). The electrical resistivity of the concrete is very much dependent on the moisture content of the concrete. With moisture content

of over 4%, the concrete resistivity drops below the electrical value of about 10,000 [ohm.cm]. Excessive moisture can reduce the resistivity due to absorption of the water into the dry concrete pores (Browne, 1980).

2.8 MASS TRANSFER

When a system contains two or more components whose concentrations vary from point to point, there is a natural tendency for mass to be transferred, minimising the concentration differences within the system. The transport of one constituent from a region of higher concentration to that of a lower concentration is called mass transfer. Mass transfer underlies the various chemical separation processes where one or more components migrate from one phase to the interface between the two phases in contact (Luikov, 1975).

Migration or *transport* of the various substances that participate in the mechanism of corrosion is facilitated by the network of interconnected pores in the material's structure. Species diffuse through the pore water due to concentration gradients that exist between the exposed surface and the pore solution of the cement matrix in saturated concrete. Another transport mechanism is that of capillary sorption (or desorption) which occurs when concrete is partially saturated. As water flows from saturated to partially saturated areas, it carries along dissolved chlorides or oxygen that add to the total concentration (Martín-Pérez et al., 2001).

Transfer of chloride ions through concrete cover is the most significant factor in reducing and shortening the service life of RC structures due to depassivation and corrosion of steel reinforcement. When concrete is completely saturated, chloride penetrates by a pure diffusion mechanism due to concentration gradient as the driving force. However, in partially saturated concrete, chloride can penetrate by absorption and capillary forces (Saremi and Mahallati, 2002, Castellote et al., 2002).

Diffusion process can be mathematically modelled by Fick's laws of diffusion. According to Fick's laws, the diffusion flux is proportional to the gradient of concentrations, it goes from regions of higher concentration to the region of lower

concentration (Philibert, 2005). Most mathematical models for predicting chloride ingress through saturated cement-based materials have been proposed based on the Fick's second law (Gjørv and Vennesland, 1979, Khitab et al., 2005).

2.8.1 Fick's Laws of Diffusion

Fick's laws of diffusion can be used to solve the chloride diffusion coefficient (D). They were derived by Adolf Fick in 1855.

Fick's first law relates the diffusive flux to the concentration under the assumption of steady state. It postulates that the flux goes from regions of high concentration to regions of low concentration, with a magnitude that is proportional to the concentration gradient or spatial derivative (Philibert, 2005). The law can be expressed as follows;

$$J = -D\frac{\partial \emptyset}{\partial x} \tag{2.15}$$

where J is the "diffusion flux" (amount of substance per unit area per unit time $\frac{mol}{m^2 \cdot s}$). J measures the amount of substance that will flow through a small area during a small time interval, D is the diffusion coefficient or diffusivity ($\frac{m^2}{s}$), $\emptyset$ is the concentration (amount of substance per unit volume $\frac{mol}{m^3}$), and x is the depth from concrete surface (m).

Fick's second law predicts how diffusion causes the concentration to change with time:

$$\frac{\partial \emptyset}{\partial t} = D\frac{\partial^2 \emptyset}{\partial x^2} \tag{2.16}$$

Collepardi and colleagues (Collepardi et al., 1970) were the first to use Fick's laws to model ingress of chloride ions into concrete from de-icing salts.

Crank's solution (Crank, 1975) for Fick's second law states that the chloride concentration in the concrete (C_x), at any depth (x) from the concrete cover surface, is

a function of the boundary surface chloride concentration (C_s), an intrinsic chloride diffusion coefficient of the concrete (D), and the period of exposure (t):

$$C_x = C_s \left[1 - erf\left(\frac{x}{\sqrt{4tD}}\right)\right] \tag{2.17}$$

C_s quantifies the chloride load or severity of the exposure conditions and D the resistance of the concrete to chloride penetration, while erf is the mathematical Gaussian error function complement.

The equation assumes the surface to be a plane and the area and depth to be effectively infinite. In a pure application of diffusion theory to a porous material such as concrete, Crank's solution would describe the concentration of the chloride ions in the pore solution directly. However, because extraction and analysis of the pore fluid is difficult, chloride ingress profiles are usually obtained by milling discrete increments of the concrete at specified depth from surface. The resulting powders are then analysed for their total chloride concentration. This value includes both the free ions in the pore fluid and those that are physically absorbed or have chemically react with the cement gel. Glass and colleagues' investigation (Glass et al., 2000) suggested that total chloride is in fact the most appropriate parameter for determining risk of reinforcement corrosion.

Eventually, to predict the corrosion-free service life of a structure, three following parameters should be determined:

- Chloride threshold level (CTL) at the surface of steel reinforcement ($C_x = C_{th}$).
- Surface chloride concentration or the chloride load on the concrete surface (C_s).
- Chloride diffusion coefficient (D).

2.9 CHLORIDE THRESHOLD LEVEL (CTL)

The significance of chloride content in the corrosion of reinforcing steel bars in concrete, has led to the concept of a critical chloride content or Chloride Threshold

Level (CTL). The CTL can be defined as the level of chloride content at the steel reinforcement surface that is necessary to destroy the passive protective layer (depassivation) and initiation of corrosion (Angst et al., 2009, Deb, 2012).

The CTL is usually presented as the ratio of chloride to hydroxyl ions (Cl^-/OH^-) or percentage of the total chloride content relative to the cement weight (Schiessl and Raupach, 1990). CTL is a key element to predict the service life of structures exposed to chloride environment. The Cl^-/OH^- ratio seems to be the most rigorous expression, since it conveys the critical chloride content, and informs on the ability of concrete to maintain the passivity of the reinforcement and inhibits corrosion initiation. However, due to difficulty in measuring OH^- in concrete, the free and total chloride contents have been more vastly used (Alonso and Sanchez, 2009).

In addition, Song et al. (Song et al., 2010) based on their study, came to conclusion that the best representation of the CTL is the total chloride content as a percentage by weight of cement. This presentation of the CTL is favoured because it is relatively easy to determine and it involves the corrosion risk of bond chloride and inhibitive effect of cement hydration products.

The first measurement of CTL was conducted by (Hausmann, 1967) using a synthetic concrete solution with a Cl^-/OH^- ratio of 0.6. The CTL measured for bridges in UK ranges from 0.2% to 1.5% by the weight of cement (Vassie et al., 1985). The British Standard limits the chloride content to less than 0.2% for reinforced concrete structures exposed to chloride environment and 0.1% for prestressed concrete structures. Whereas in ACI 357 the CTL has been defined as 0.06% and 0.1% for RC structures and prestressed concrete structures, respectively (See Table 2-3).

Despite the importance of the CTL, conservative values such as 0.2% or 0.4% by the weight of cement have been used in predicting the service life, because of uncertainty in regard with the actual limits in various environments for chloride-induced corrosion (Hooton et al., 2002, Funahashi, 1990, Mullard and Stewart, 2011).

A considerable number of studies have been performed to establish the CTL initiation of corrosion, but the measured values cover an extremely wide range which does not

make feasible to define a unique and representative value. The reason for this extensive differences in reported CTL includes the type and content of cement, the type of steel, presence of air voids, cracks, the method of measurement, method of presentation of CTL, condition of the steel-concrete interface, oxygen availability at the rebar surface, and influence of environmental factors such as exposure conditions, temperature, and relative humidity (Ann et al., 2009, Alonso and Sanchez, 2009).

Thus, it is not possible to give any general value for critical chloride content. When certain values for the critical chloride content is nevertheless given in existing concrete codes and recommendations, this is only based on empirical results of the chloride content which may give a certain risk for the development of corrosion.

Generally, very small chloride concentration in the pore solution of a concrete is able to destroy the passivity of the steel, but the risk of the development of corrosion may be very low both in very dry concrete due to ohmic control of the corrosion process and in very wet or submerged concrete due to very low availability of oxygen (GjØrv, 2009). Table 2-3 illustrates the risk of corrosion with different amount of the chloride content at the steel reinforcement surface (Angst et al., 2009).

Table 2-3 Risk of corrosion with different amount of chloride content at reinforcing steel surface

Chloride content (%)		Risk of corrosion
By wt. of cement	By wt. of concrete	
> 2.0	> 0.36	Certain
1.0 - 2.0	0.18 - 0.36	Probable
0.4 - 1.0	0.07 - 0.18	Possible
< 0.4	< 0.07	Negligible

An analysis of the data obtained on bridge structures in UK suggested that chloride levels below 0.2% (by weight of cement) represent minimal corrosion risk, while level above 1.5% represent a very high corrosion risk (Figure 2-6). The results of similar work on the US bridges suggested a range between 0.17 and 1.4% by weight of cement and on the Danish bridges 0.3 and 0.7% by the weight of cement (Glass and Buenfeld, 1997).

The diffusion process of chloride in concrete is a slow and complex process involving many material and environmental variables. Many experimental studies indicate that the concentration level of chloride at the depth of steel bar varies in a very broad range (Alonso et al., 2000, Ann and Song, 2007, Angst et al., 2009, Trejo and Monteiro, 2005).

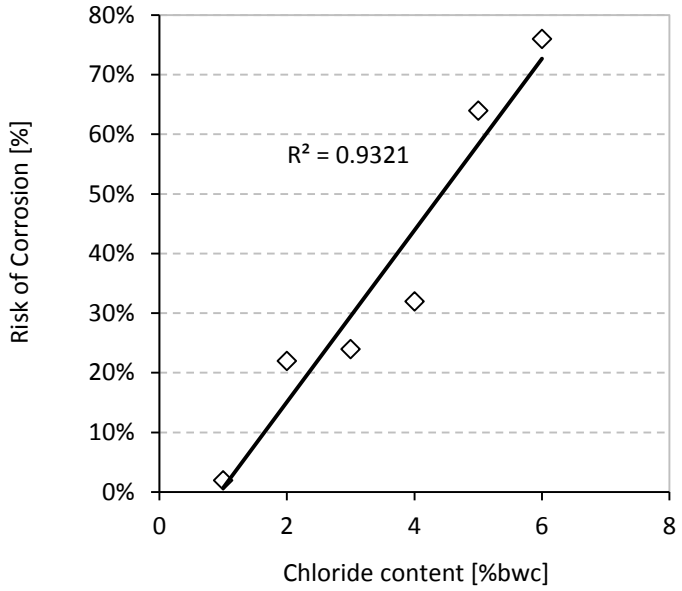

Figure 2-6 Risk of corrosion as a function of chloride content (Glass and Buenfeld, 1997)

Li et al. (Li et al., 2007) investigation proved that under the same conditions, there was no influence to the chloride ion critical content when fly ash and slag were added to concrete.

The chloride threshold level is commonly expressed by using the total chloride level approach which has been adopted in the standards. Table 2-4 exhibits the limit of the total chloride content of concrete from ACI and BS point of view (Ahmad, 2003).

The conservative values, as the chloride threshold level, such as 0.2% or 0.4% by weight of cement has been often used in predicting the corrosion-free life (Hooton et al., 2002, Funahashi, 1990) because of the uncertainty regarding the actual limits in various environments for chloride-induced corrosion, whereas chloride transport in terms of the chloride diffusion has been considered as being time-dependent (Bentz et al., 1996).

Table 2-4 Chloride threshold level of the reinforcing steel surface set by ACI and BS documents

Type of Concrete	Maximum chloride content (%, cement)			
	BS 8110	ACI 201	ACI 357	ACI 222
Prestressed Concrete	0.1		0.06	0.08
Reinforced Concrete exposed to chloride in service	0.2	0.1	0.1	0.2
Reinforced Concrete protected from moisture in service	0.4			
Other reinforced concrete		0.15		

Following parameters affect the value of CTL and many of them are interrelated (Bertolini et al., 2013):

- Steel-concrete interface
- Concentration of hydroxide ions in the pore solution
- Electrochemical potential of the steel
- Binder type
- Surface condition of the steel
- Moisture content of the concrete
- Oxygen availability at the steel surface
- Water binder ratio
- Electrical resistivity of concrete
- Degree of hydration
- Chemical composition of the steel
- Temperature

The variety of influencing factors indicates that the concept of critical chloride content confronts some difficulties regarding to a unique chloride threshold value applicable to a wide range of structures.

The recently published paper by Castro et al. (Castro-Borges et al., 2013) shows that in addition to the abovementioned factors, the method of evaluation of the chloride threshold is also important. The Castro et al.'s study, five water/cement ratios of 0.46, 0.53, 0.59, 0.7, and 0.76 with three different curing time duration of 1, 3 and 7 days were selected to be investigated. Chloride threshold values were determined by measuring the corrosion rate using polarization resistance technique. The results were presented by using instantaneous i_{corr}, i_{mean} and i_{accu} to find out the differences in the threshold value depending on the utilized method. The summary of Castro et al.'s test results are presented in Table 2-5.

Table 2-5 The ranges and average of CTL obtained by three different way of measurements (Castro-Borges et al., 2013)

W/C	CTL, i_{corr} (%bwc)	Average	CTL, i_{mean} (%bwc)	Average	CTL, i_{accu} (%bwc)	Average
0.46	0.38-0.54	0.46	0.40-0.61	0.50	0.26-0.33	0.30
0.53	0.55-0.79	0.67	0.65-1.10	0.87	0.39-0.53	0.46
0.59	0.52-0.68	0.60	0.49-0.61	0.55	0.56-0.73	0.65
0.70	0.35-0.47	0.41	0.33-0.47	0.40	0.37-0.50	0.44
0.76	0.35-0.49	0.42	0.30-0.43	0.36	0.38-0.50	0.44

Table 2-6 summarises most of the reliable publications in regard with CTL. However, results of field studies revealed that, it is not clear whether the corrosion state is close to depassivation or corresponds to a later stage in the propagation period. However, in the case of laboratory studies, corrosion was mostly detected close to depassivation due to the application of electrochemical techniques (Angst et al., 2009).

Table 2-6 Summary of test results in the literature regarding the CTL

CTL	Experimental details				Reference
%bwc	Chloride Introduction	w/b	Cement type	Remarks	
0.32	MIX*	NG	NG	Submerged	(Kaesche, 1959)
0.57-1.09	MIX	0.7	NG	Submerged	(Bäumel, 1959)
>0.4	MIX	0.45	OPC	No corrosion	(Richartz, 1969)
0.45	MIX	0.6	OPC	NG	(Gouda and Halaka, 1970)
0.15	MIX	0.6	GGBS	NG	(Gouda and Halaka, 1970)
0.4-0.8	MIX	0.4	OPC	Air exposure	(Locke and Siman, 1980)
0.25-0.5	MIX	0.5	OPC	Submerged	(Elsener and Böhni, 1986)
0.1-0.19	MIX	0.45	OPC	Wet/dry cycle	(Hope and Ip, 1987)
0.2-0.68	DIF**	0.5	OPC, FA		(Hansson and Sorensen, 1988)
0.48-2.02	MIX, DIF	0.4-0.6	OPC, FA, SF	Macro-cell	(Schiessl and Raupach, 1990)
1.5-2.5	CAP*** + DIF	0.5	OPC		(Page et al., 1991)
0.4-2.0	MIX	0.5	OPC		(Lambert et al., 1991)
0.5-1.8	CAP + DIF	0.4-0.6	OPC, FA, SF	Air exposure	(Pettersson, 1992)
0.5-1.0	MIX, DIF	0.5-0.7	OPC	Air exposure	(Schiessl and Breit, 1996)
1.0-1.5	MIX, DIF	0.5-0.7	GGBS, FA	Air exposure	(Schiessl and Breit, 1996)
0.25-0.75	DIF	0.5-0.6	OPC, FA, SF	Submerged	(Breit, 2003)
0.25-1.25	CAP + DIF	0.6	OPC		(Zimmermann et al., 2000)
0.74	CAP + DIF	0.5	OPC, FA		(Alonso et al., 2002)
0.62	CAP + DIF	0.37	SRPC	95% RH	(Castellote et al., 2002)
0.42	MIG****	0.37	SRPC	95% RH	(Castellote et al., 2002)
0.04-0.24	MIG	0.5	OPC	Submerged	(Trejo and Pillai, 2003)
0.68-0.97	MIX	0.35-0.55	OPC, FA, GGBS	95% RH	(Oh et al., 2003)
0.45	MIX	0.35-0.55	SRPC	95% RH	(Oh et al., 2003)
0.4-1.3	MIX, CAP + DIF	0.4, 0.6	OPC	Submerged	(Morris et al., 2004)
0.52-0.75	CAP + DIF	0.45	OPC		(Nygaard and Geiker, 2005)
0.05-0.15	MIG	0.5	OPC	Submerged	(Trejo and Monteiro, 2005)
1.1-2.0	MIX	0.6	OPC	Air exposure	(Manera et al., 2008)
0.6-1.2	MIX	0.6	SF	Air exposure	(Manera et al., 2008)
0.15-0.23	DIF, MIG	NG	OPC	NG	(Alonso and Sanchez, 2009)
0.4	MIX	0.55	OPC	Submerged	(Xu et al., 2009)

*Chloride added to the mix
**Chloride introduced by diffusion
***Chloride introduced by capillary suction
****Chloride introduced by migration

2.10 SURFACE CHLORIDE CONCENTRATION (C_s)

Surface chloride concentration is another important factor in the Fick's second law which is vital to be determined in order to estimate the service life. Surface chloride concentration affects the chloride diffusion process in concrete significantly.

The surface chloride concentration value may vary to a large degree by environmental exposure conditions such as degree of chloride concentration, wetting and drying cycles, and weathering condition, location from sea level and concrete quality (Pack et al., 2010).

Normally, C_s is defined as shown in Figure 2-7, which is the result of regression analysis of observed data on chloride penetration and curve fitting to the Fick's second law. The chloride content within a couple of millimeters inside the outer surface of concrete cover is decreased because of "skin effect". Concrete skin is considered as the closest concrete zone to the surface of reinforcements. It is usually has a different composition than the internal concrete due to phenomena such as contact with mould or segregation of aggregates.

In addition, environmental actions induce a gradient of moisture along the depth of concrete cover. These circumstances sometimes produce an irregular chloride profile in the cover. A theoretical study presented by Andrade et al (Andrade et al., 1997) revealed that, if the diffusivity of the skin and the bulk concrete were very different, an error would introduce when the "skin effect" was not taken into account. They concluded that the existence of a skin having different chloride diffusivity than the bulk concrete may result in different profiles than those obtained from the usual solution of the Fick's second law. However, from this hypothesis it cannot be stated that the skin effect can justify all the reported deviations from a pure error function profile. Other parameters such as progression of hydration or nonlinear binding ability or climate cycles may also be important and effective.

This study has collected an extensive data from the significant published reports regarding the surface chloride content of concrete exposed to marine environment.

Accordingly, the influencing parameters as well as time dependency of C_s will be investigated broadly.

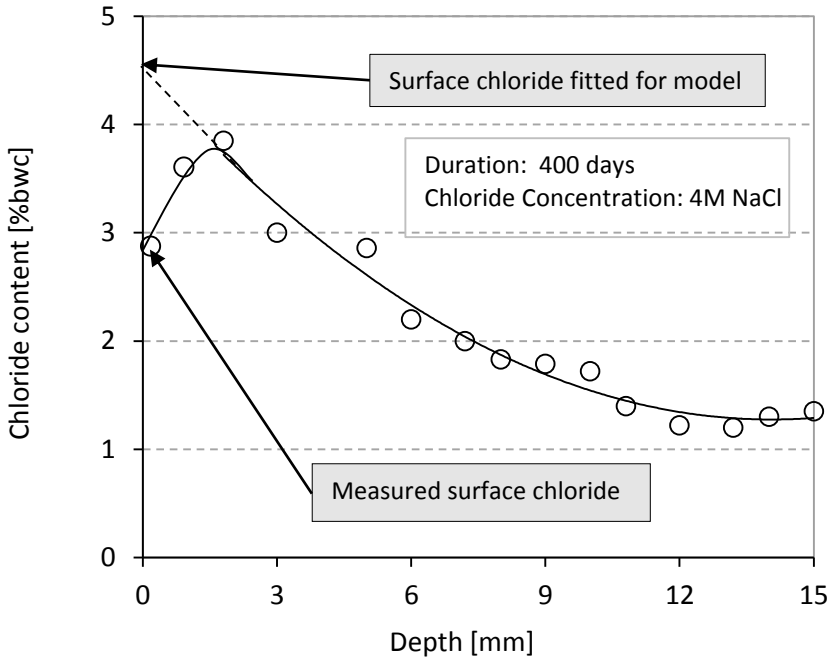

Figure 2-7 A typical example of the chloride content with fitted curves for surface chloride content (GjØrv, 2009)

The influencing factors on surface chloride content such as exposure conditions, concrete mix proportion, and curing are investigated in this section.

2.10.1 Exposure Conditions

For marine concrete structures, the vicinity to seawater could mainly govern the chloride transport behaviour. However, there are limited studies in the literature concerning the effect of location from sea level, except a few limited data (Liam et al., 1992, Castro et al., 2001) as shown in Figure 2-8 the height from sea level was limited within 2 m higher or about 1 m lower from sea level. It seems that splash zone near the sea level is the easiest for chlorides to accumulate on the surface of concrete, while a build-up of C_s took place the least at sea level. This may be due to the wet and dry cycles, resulting in a successive supply of chloride by wetting with seawater and later evaporation and salt crystallisation by drying. However, from a long term monitoring

from 23 to 58 years Uji et al. (Uji et al., 1990) showed that the order of C_s with regard to the level from seawater is in the order of tidal > splash > atmospheric zone. The difference of C_s developed between these data is not clearly known, but presumably different weathering and concrete mix may have affected process of the chloride concentration.

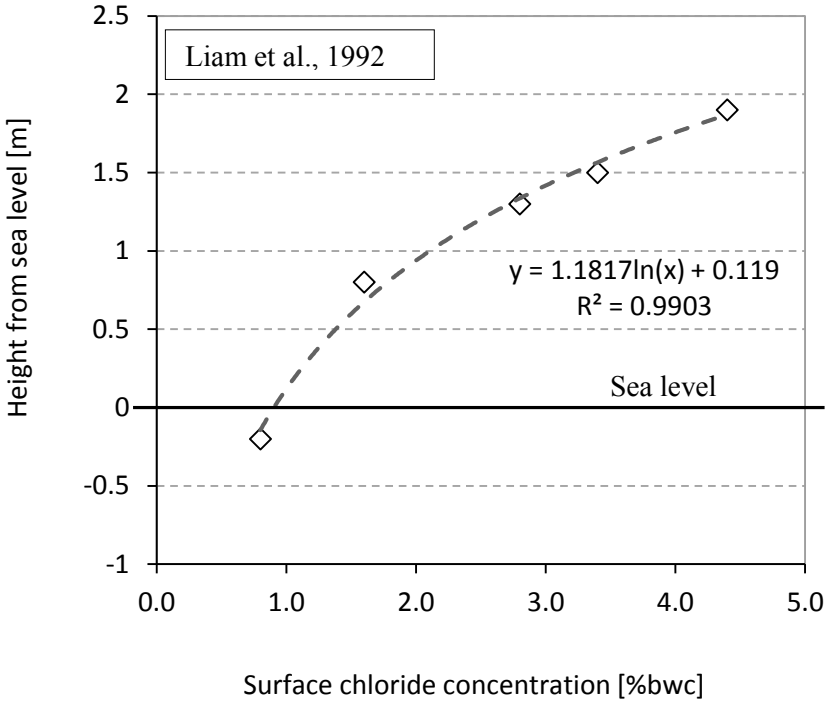

Figure 2-8 Surface chloride concentration of a jetty concrete structure exposed to splash/tidal conditions for 24 years (Liam et al., 1992).

Figure 2-9 illustrates effect of the exposure conditions in tidal and splash zones. As can be seen, the surface chloride content for the tidal zone is higher than the splash zone.

The distance of structure from the sea is another factor related to exposure condition. Figure 2-10 shows build-up of C_s measured from the specimens and structures exposed to a chloride aerated environment for 30 years. The distance from sea can strongly influence the magnitude of C_s. For instance; from 0.20% to 2.43% by weight of cement, for the distance of 50 to 1000 m, respectively (Morinaga, 1992). Structures about 1 km away from coast may be free from chloride-induced corrosion deterioration, because it would take extremely long for chloride ions, with a lower level of C_s, to reach the CTL steel corrosion at the depth of steel.

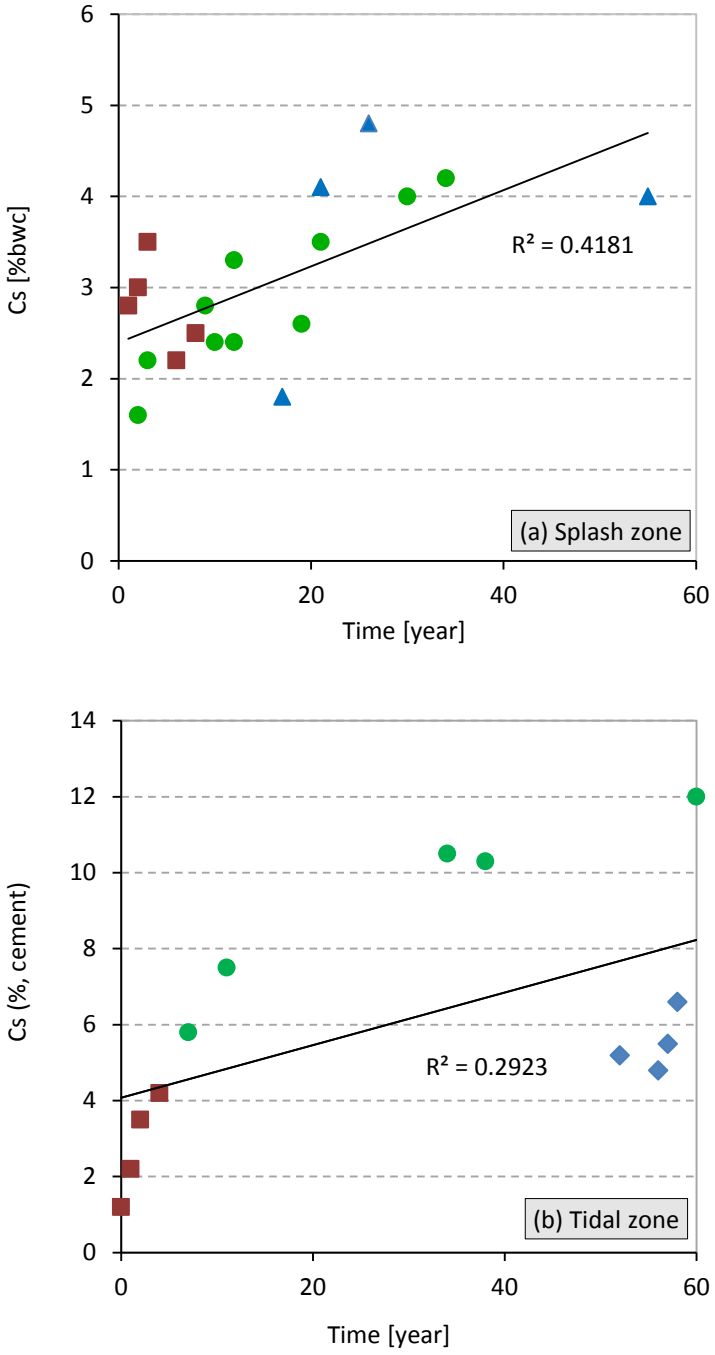

Figure 2-9 Surface chloride content exposed to splash zone (a) and tidal zone (b)

Meira et al. (Meira et al., 2007) provided additional information on chloride accumulation in concrete due to natural exposure to marine aerosols. Marine aerosols are mainly generated along the seashore by breaking waves movement and carried inland by wind (Fitzgerald, 1991).

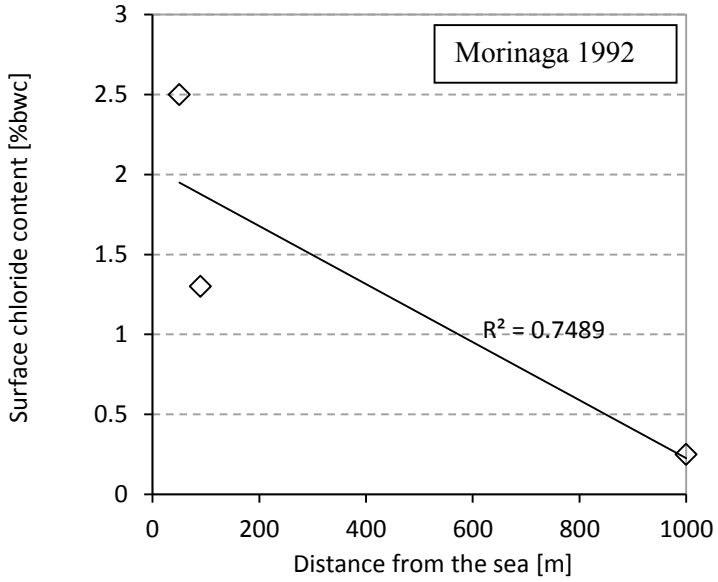

Figure 2-10 Surface chloride content in aerated conditions with the distances from sea (Morinaga, 1992)

When wind speed increases, there is an increase in both the number of marine particles generated and the percentage of larger drops in the aerosol spectrum (McDonald et al., 1982). As a consequence, salt concentrations increase exponentially with wind speed. Moreover, stronger winds enable larger particles to cover longer distances before settling (Lovett, 1978). Thus higher salt concentration can be observed at the same distances from the sea when wind speed increases (Gustafsson and Franzén, 1996). Figure 2-11 depicts the relationship between chloride deposition measurements and distance from the sea in the different countries.

Figure 2-12 shows the influence of the climate on surface chloride content. Three different series of C_s were measured in UK, Japan, and Venezuela where the specimens were placed in different latitudes (Uji et al., 1990, de Rincón et al., 2004b, Luo et al., 2003). The specimens from UK were submerged in seawater and the others were placed in the tidal/splash zones. The C_s from UK was the lowest because of the submerged condition as well as higher latitude, compared to the measured C_s from Japan and Venezuela. Also, the C_s from Venezuela showed much higher value than that from Japan, despite a similar exposure conditions and duration. This difference may be related to the climate difference of the two countries, since tropical climate fosters

chloride ion movement into concrete due to high level of relative humidity, temperature, and chloride concentration.

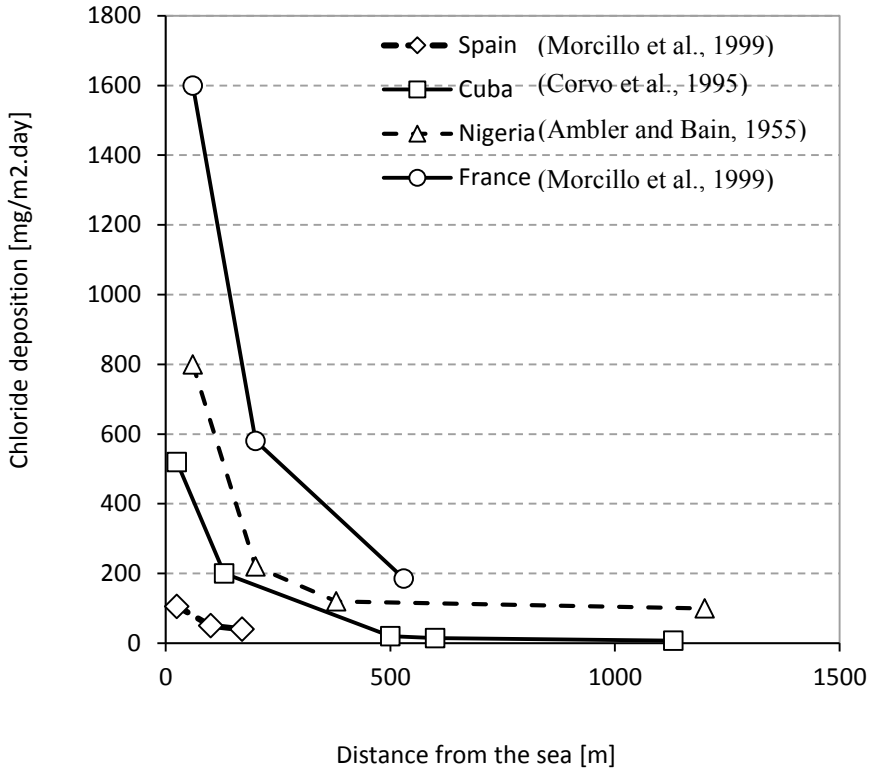

Figure 2-11 Relationship between chloride deposition from marine aerosol and distance from the sea

Recently, a study was conducted by Zhao et al. (Zhao et al., 2013) on the influence of the alternation of the natural seasons on the variation of the surface chloride concentration. They concluded that the surface chloride content (chloride load) varies with seasons. They observed peak of the surface chloride surface in summer. The highest temperature together with the wildest wind and wave conditions in summer causes the accumulation of chloride ions at the surface. The average values of the surface chloride content in different seasons are demonstrated in Figure 2-13. It can be observed that surface chloride concentration values are 0.58%, 0.66%, 0.87%, and 0.59% in winter, spring, summer, and autumn, respectively. It should be noted that this results are based on the data from a dock at the north coast of Hangzhou bay in the east part of China.

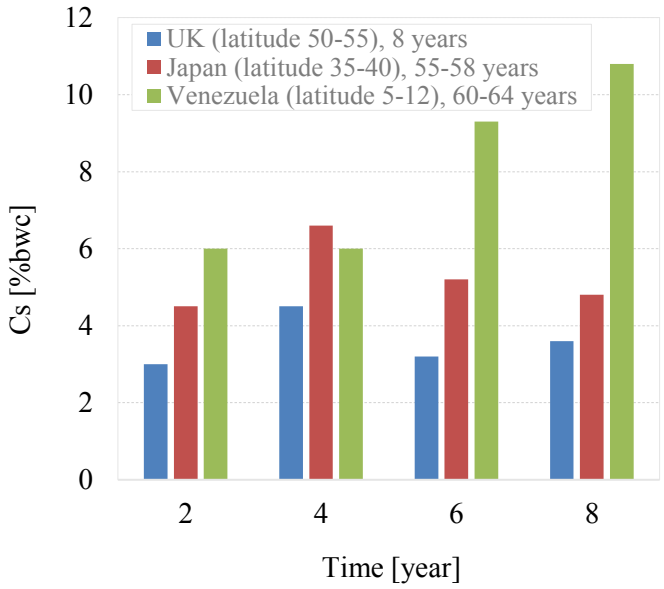

Figure 2-12 Surface chloride content of concrete structures measured in different countries with different climate (Uji et al., 1990, de Rincón et al., 2004a, Luo et al., 2003)

Relatively, limited research has been conducted on the effect of the salt solution concentration on C_s. An investigation carried out by Singhal et al. (Singhal et al., 1992) showed a linear relationship between C_s and salt concentration Figure 2-14.

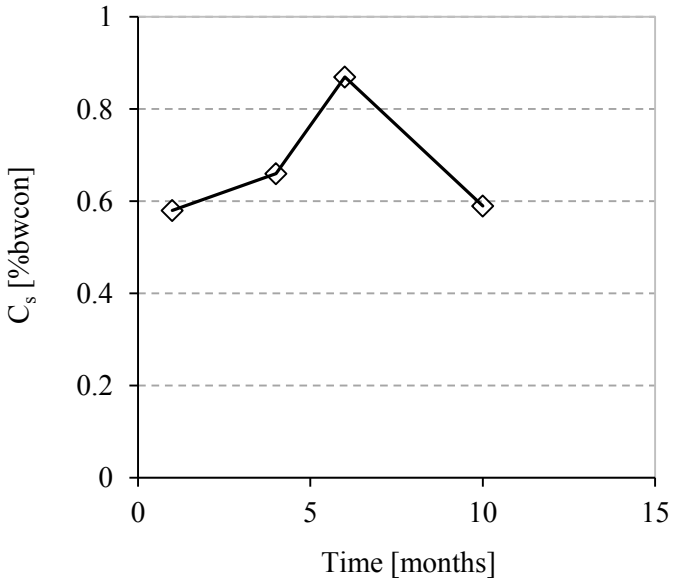

Figure 2-13 Monthly average of the surface chloride content

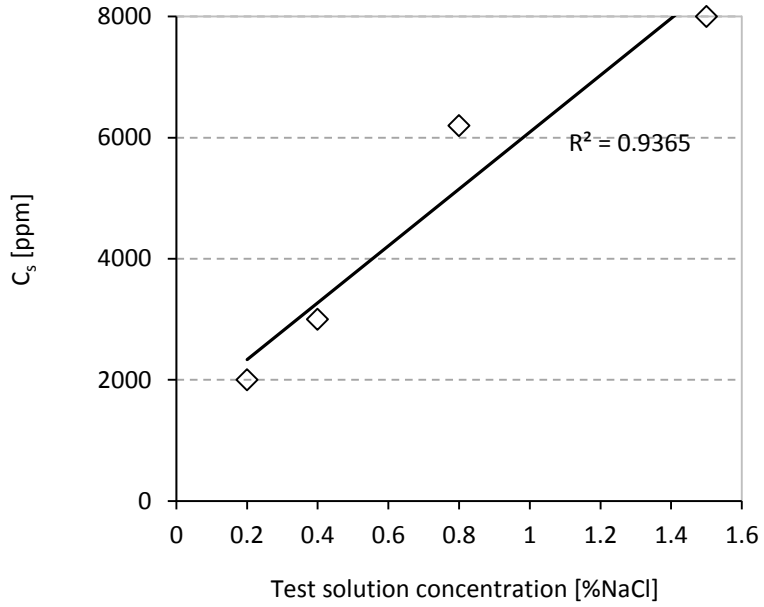

Figure 2-14 The relationship between surface chloride concentration and the test solution concentration (Singhal et al., 1992)

2.10.2 Concrete Mix

It is well proven that binder type, water/binder ratio (W/B), and mix proportion significantly affect chloride transfer into concrete since formation of pore structure is completely dependent upon these factors.

Figure 2-15 shows that by increasing W/B ratio reduces C_s. For instance; a single study of Gjørv and Vennesland (Gjørv and Vennesland, 1979) has shown that the C_s at a given cement content can be reduced by an increase in W/B ratio for two-year submerged concrete specimens. This can be explained by the fact that higher W/B ratio means to form thicker cement paste layer on the concrete surface, so that the layer would enhance the dielectric activity between hydroxyl ions in the concrete skin and chloride ions in the solution. Thus the increased repulsive force removes chloride ions from the concrete surface.

Figure 2-15 also illustrates that C_s is influenced by binder type. Irrespective of exposure condition and duration, C_s for blended cement concretes was greater than that for ordinary cement (OPC) concrete. This phenomenon can presumably occur due to the

higher capacity of chloride binding and sorptivity associated with blended cement concrete. With increased chloride binding capacity, total concentration of chloride increases at the concrete surface (Glass and Buenfeld, 2000b).

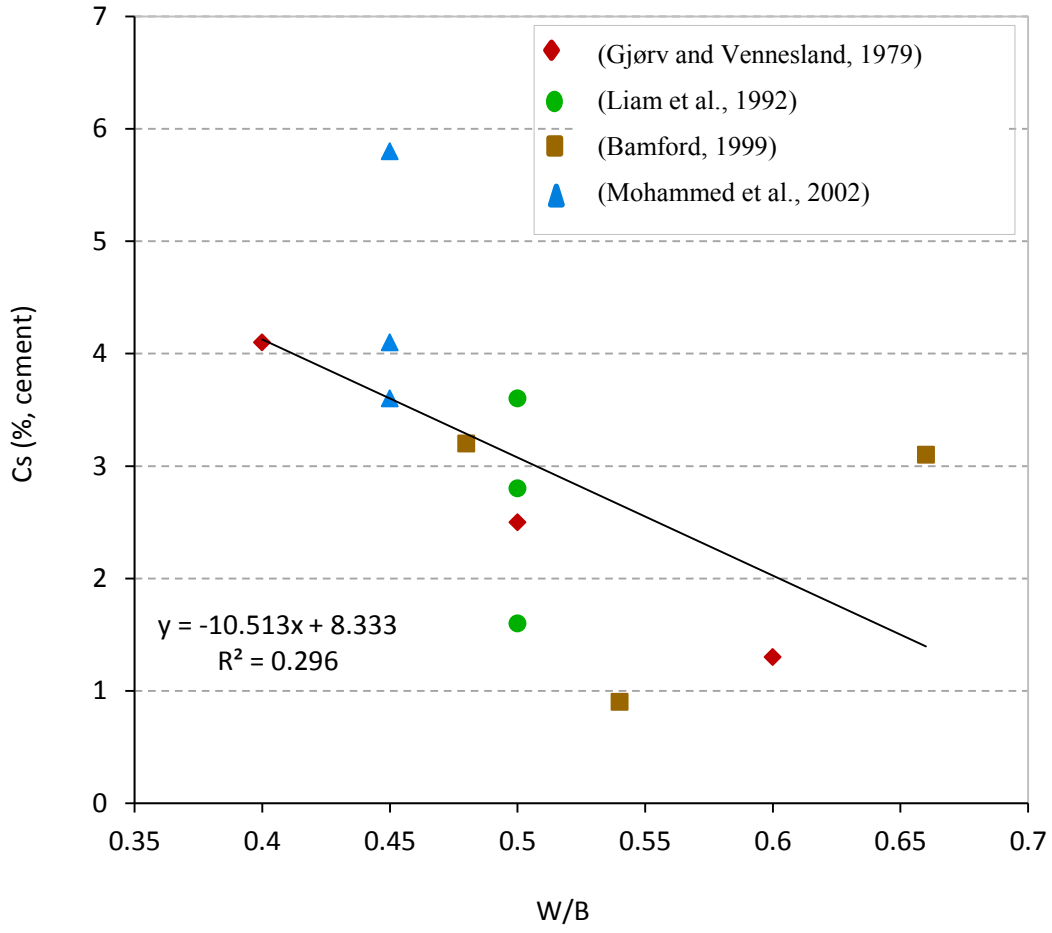

Figure 2-15 Relationship between C_s and *W/B* ratio

Results derived from in-situ marine structure by Pack et al. (Pack et al., 2010) confirmed the results of these previously conducted investigations (see Figure 2-16).

Cement content also affects the C_s. A study conducted by Buenfeld and Okundi (Buenfeld and Okundi, 1998) showed that increasing the cement content increases C_s. They expressed that increased activity by higher cement content would bring the higher level of chloride ions near the concrete surface. Figure 2-17 illustrates their results.

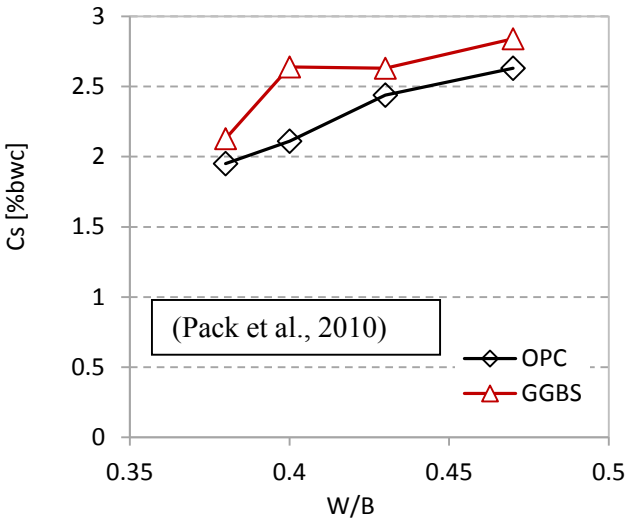

Figure 2-16 Effect of binder type and W/B ratio on C_s (Pack et al., 2010)

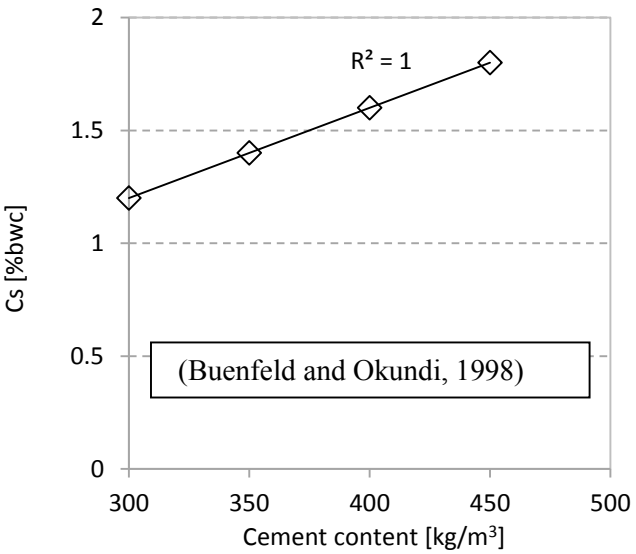

Figure 2-17 Effect of cement content on C_s (Buenfeld and Okundi, 1998)

2.10.1.1 Curing Methods

Curing method affects the surface chloride content as well. Bamford (Bamford, 1999), and Bamford & Price (Bamforth and Price, 1993) studied the influence of curing methods on surface chloride content. Figure 2-18 shows the various level of C_s for different curing methods when the concrete specimens were submerged in seawater for eight years period. Based on the results, it can be stated that surface chloride

concentration for OPC in all curing methods was lower than the samples incorporating supplementary cementitious materials (Fly Ash, Slag, and Silica Fume). The highest surface concentration of chloride is related to concrete samples with 30% of Fly Ash. Moreover, it can be observed that using Non Aeration curing method revealed the lower surface concentration of chloride except for Fly Ash concrete.

As a conclusion, it can be expressed that curing method has some effect on surface chloride concentration but, it is not significant. Also, concrete samples incorporating SCMs showed higher surface concentration of choride.

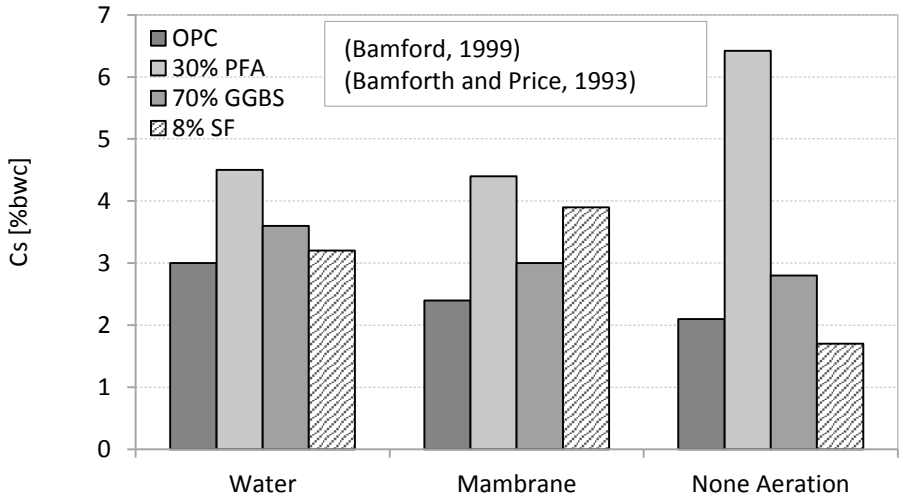

Figure 2-18 Effect the curing method on C_s

2.10.3 Mathematical Models for C_s

Fick's second law has been the most utilized equation by scientists and scholars attempting to predict the chloride content at the certain time and distance from the concrete surface so far. Investigation on predicting the service life of RC structures exposed to chloride environment has been conducted based on that equation in general.

Many authors have used Fick's second law to determine the time of chloride-induced corrosion with a constant value for diffusion coefficient (D) and surface chloride content (C_s) assuming that cement matrix in concrete is chemically inert and evenly

porous (West and Hime, 1985, Clear, 1976, Funahashi, 1990, Mangat and Molloy, 1994b, Hooton et al., 2002, Zhang and Lounis, 2009).

The other reason for using a constant value for C_s to model a chloride profile was due to intuitive support that chemical equilibrium at the concrete surface sustains a certain concentration of chloride when a concrete is subjected to a direct contact with seawater. Increasing the C_s for concrete structures exposed to seawater was observed in previous surveys (Liam et al., 1992, Uji et al., 1990, Ann et al., 2006). Also, this hypothesis and models have been challenged since Bamforth and Price (Bamforth and Price, 1993) addressed the time-dependent characteristic of chloride transport in terms of D and C_s. Immediately after being exposed to a chloride environment, the concrete surface is surrounded by a reservoir of chloride ions. The chemistry between cement matrix and chloride ions forces a certain concentration of chlorides to set at the concrete surface. Then, the surface chloride ranges between 2.0% and 2.5%, even at an early age of exposure.

The first mathematical model for C_s primarily was suggested by Amey et al. (Amey et al., 1998). In this model a linear build-up of C_s over time was proposed as shown in Equation 2.18. For a square root build-up of C_s over time, Equation 2.19 was used to determine the surface chloride concentration.

$$C_s(t) = k_1 t \tag{2.18}$$

$$C_s(t) = k_2 \sqrt{t} \tag{2.19}$$

where $C_s(t)$ is the surface chloride concentration at time t $(\%/m^3)$ and k_1 and k_2 are constant values .

However, these models do not consider an initial build-up of chloride on the concrete surface at an early age of chloride exposure. For example, the C_s would be negligibly small for one year of exposure, ranging between 0.1% and 0.77% by weight of cement from Equations 2.13 and 2.14, respectively. Whereas, case studies confirm that the magnitude of C_s is 2% to 2.5% after only 28-day exposure time. on the other hand, after 60 years of exposure, Equations 2.13 and 2.14 overestimate C_s concentration as 7.6%

to 8.2%, comparing to 6% obtained from exposure test data (Bentz et al., 1996). Hence, these models may not be able to predict service life of RC structures exposed to marine environment both for short-term and long-term of exposure accurately.

Song et al. (Song et al., 2008) proposed an empirical mathematical models as shown in Equation 2.20 which has been proved that is more realistic than the other two models as shown in Figure 2-19. Experimental results have been taken from Benz et al. (Bentz et al., 1996)

$$C_s = C_0 + \alpha \cdot ln(t) \tag{2.20}$$

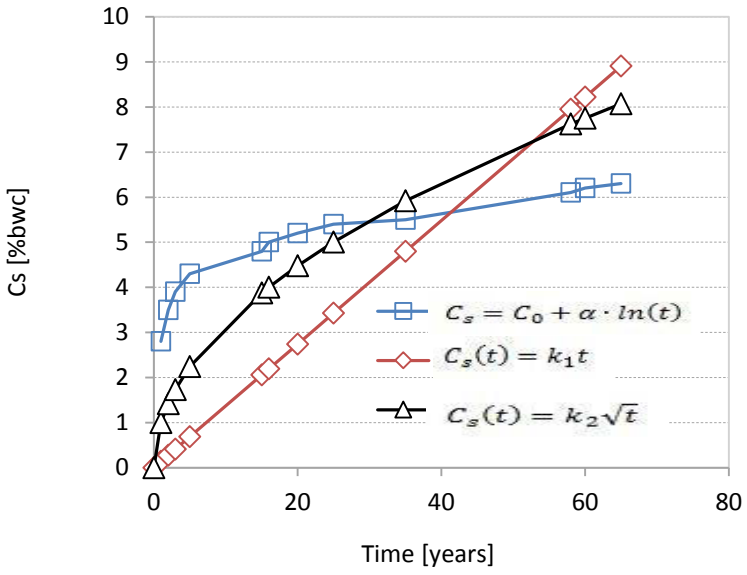

Figure 2-19 Mathematical models and empirical measurement of surface chloride concentration

Recently conducted study by Pack et al. (Pack et al., 2010) also has revealed the time dependency of surface chloride content.

2.11 CHLORIDE DIFFUSION COEFFICIENT (D)

Diffusion is the process by which ions or molecules move from a higher concentration in media to lower concentration. The durability of concrete structures exposed to chloride environment depends mainly on the ability of concrete to resist against the

chloride ingress. The chloride diffusion coefficient of a concrete (D) is a material property that is a measure of chloride penetration into the concrete. This complex phenomenon depends on many parameters related to the concrete properties and environmental characteristics (Costa and Appleton, 1999).

In this part, chloride diffusion coefficient, the influencing parameters, and mathematical models are surveyed and discussed.

Concrete consists of a graded mix of aggregate particles in cement matrix. Song et al. (Song et al., 2010) believe that the aggregates usually have very low permeability and therefore have little effect on chloride transport in concrete. Hence, the rate of transport in a concrete is largely dependent on the characteristics of the cement paste, which may include its porosity and pore size distribution, primarily controlled by its W/C. Capillary pores are the most important parameters when considering solution or diffusion transport in concrete, and are the main means of transport of ions if they are interconnected and filled with pore solution. Capillary porosity is found to decrease as hydration proceeds (Song et al., 2010). However, apart from the abovementioned parameters, Zhang and Lounis (Zhang and Lounis, 2009) stated that the aggregate fraction is an influencing factor as well.

The influencing factors on D are discussed separately below:

2.11.1 Concrete mix

W/C ratio significantly affects D since formation of pore structure is strongly dependent on the concrete mix proportion. Figure 2-20 shows an increase in the W/C ratio resulted in a significant increase in D due to increased porosity of the concrete matrix and pore network. The results depicting the influence of W/C ratio on the chloride diffusion coefficient (D) collected from JSCE (Japan Society of Civil Engineers, 1999), Han (Han, 2007), and Pack et al. (Pack et al., 2010) have been illustrated in Figure 2-20. The figure clearly shows that increase in W/C ratio increases the chloride diffusion coefficient sharply. It can be concluded that W/C ratio is the most effective parameter in the chloride diffusion coefficient.

The interface between coarse aggregate and cement paste provides an easier path for chloride ions to transport into the concrete (ITZ). It has been established that ITZ is profoundly different from the bulk cement paste in terms of morphology, composition, and density (Mehta and Monterio, 1993, Barnes et al., 1979). Since the porosity of ITZ is higher than that of bulk paste, the ITZ has a significant effect on the permeability and durability of concrete. As the proportion of the 20 mm aggregate increases in the mix the cumulative chloride scaling also increases, indicating a decrease in durability (Scrivener, 1989, Zhang et al., 1988).

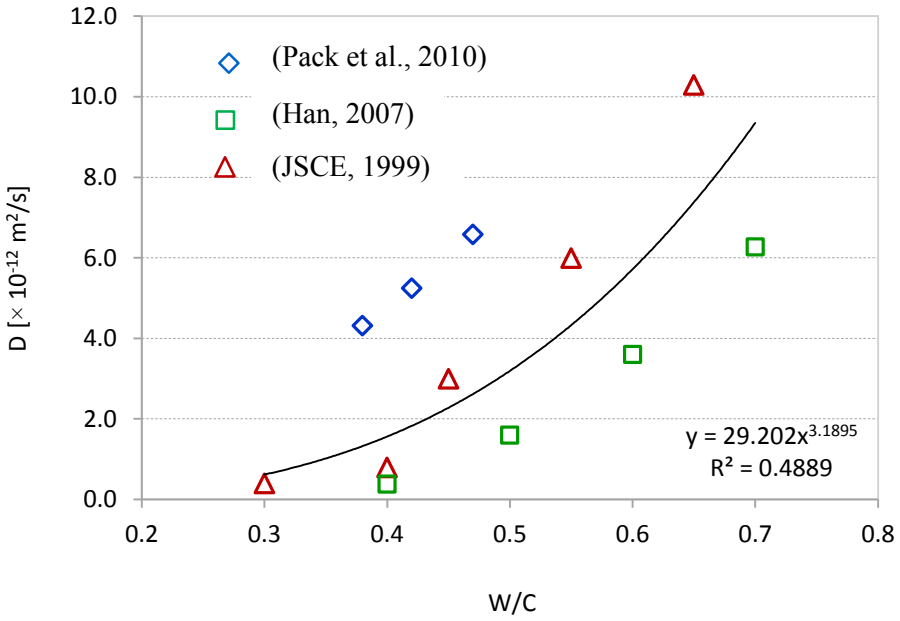

Figure 2-20 Influence of W/C on D

Figure 2-21 shows the effect of changing aggregate content on the chloride diffusion coefficient with the minimum aggregate content of 50% of the concrete volume and water cement ratio of 0.55 (Yunping Xi, 1999).

Zheng and Zhou (Zheng and Zhou, 2007) investigations showed that the chloride diffusion coefficient of concrete decreases with the increase of the aggregate area fraction and the maximum aggregate diameter, but increases by increasing the thickness of ITZ. It should be pointed out that the inclusion of aggregate in the hydrated cement paste has two opposite effects on the transport properties of concrete. The dilution and tortuosity effects reduce the chloride diffusion coefficient of concrete while the ITZ and

percolation effects increase the chloride diffusion coefficient of concrete. When the aggregate fraction is larger than a certain value, a percolation ITZ cluster will form across the concrete samples. Since the ITZ is much more porous than the cement paste, chloride ions will diffuse mainly along the percolated ITZ cluster.

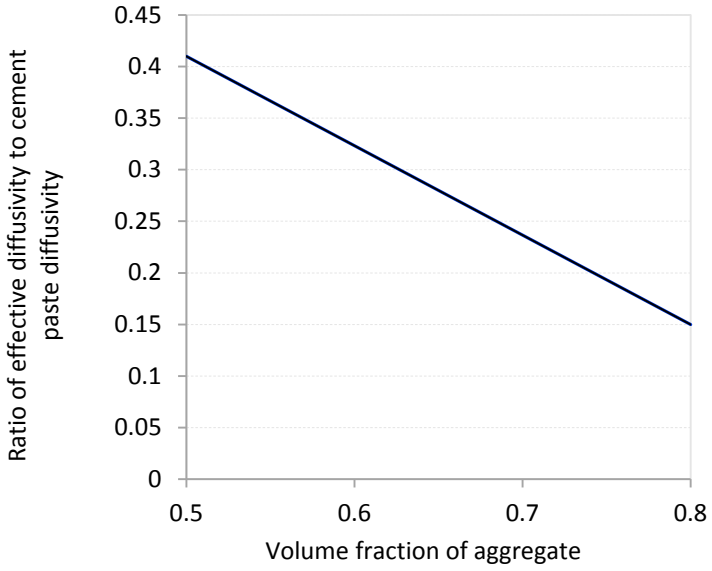

Figure 2-21 Effect of aggregate content on chloride diffusion coefficient (Yunping Xi, 1999)

2.11.2 Exposure Condition

Liam et al. (Liam et al., 1992) have investigated the effect of location from sea level on diffusion coefficient. Their study outcome is shown in Figure 2-22.

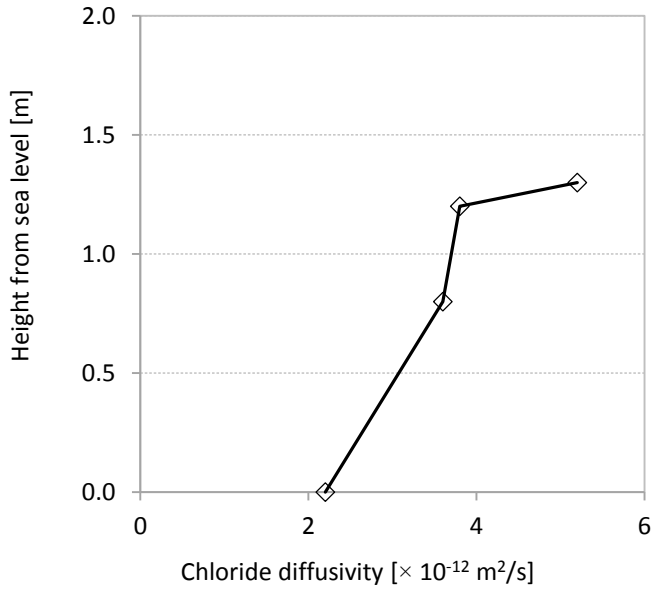

Figure 2-22 the effect of the height from sea level on chloride diffusion coefficient (Liam et al., 1992)

Investigation conducted by Zhao et al. (Zhao et al., 2013) shows that the diffusion coefficient varies in different season. The values of *D* at different elevations from sea level in the same month are averaged and results are shown in Figure 2-23.

On the other hand, the temperature and the surface chloride content are assumed to explain the seasonal variation of chloride diffusion coefficient. The maximum of temperature obviously occurs in summer. However, the maximum D does not occur in the summer but occurs in spring. The reason might be that the peak value of concrete surface chloride ion concentration in summer hinders the penetration of the chloride ion due to the ion-ion interaction. In the following time, although the concrete surface chloride content declines, the chloride diffusion coefficient keeps the relatively low value because of the gradually decreasing temperature. This chloride diffusion situation does not change until the next spring comes when the temperature increases again (Zhao et al., 2013).

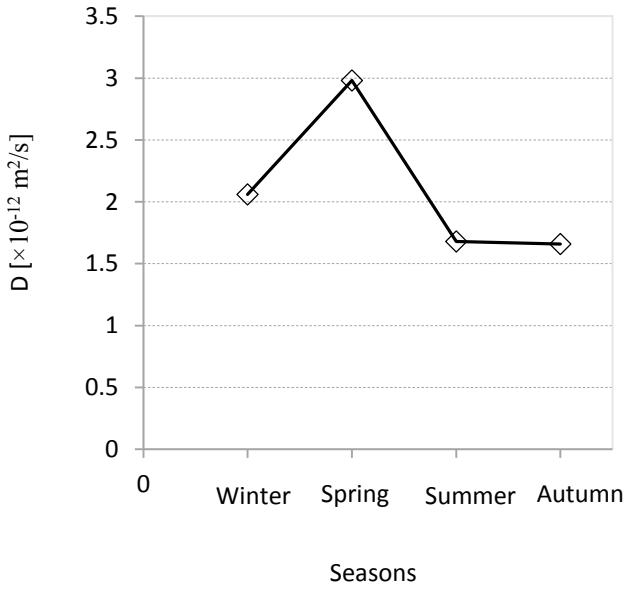

Figure 2-23 Seasonal average of the chloride diffusion coefficient value (Zhao et al., 2013)

2.11.3 Effect of Chloride Binding

When chloride ion from environment penetrates into the concrete, some of them are captured by the hydration products, which is called chloride binding. The effect of chloride binding is significant in study of the service life of concrete structures due to three reasons: (1) reduction of the free chloride concentration in the vicinity of the reinforcing steel which reduce the chance of corrosion; (2) removal of chloride from the diffusion flux, thus retarding the penetration of chloride to the level of the steel; and (3) formation of Friedel's salt which results in a less porous structure and slows the transport of chloride ions (Yuan et al., 2009).

Chloride ions can exist either in the pore solution, chemically bond to the hydration products, or physically held to the surface of the hydration products (Berman, 1972). Some researchers (Suryavanshi et al., 1998, Kayyali and Haque, 1995) believe that only free chloride ion in the pore solution is responsible for initiating corrosion. However, Reddy et al. (Reddy et al., 2002), Glass and Buenfeld (Glass and Buenfeld, 1997, Glass and Buenfeld, 2000b), and Glass et al. (Glass et al., 2000) indicated that bound chloride may also be responsible for the corrosion initiation due to the release of some bound chloride ions into the pore solution. Also, Tang and Nilson (Tang and Nilson, 1993)

suggested that most of the bound chloride is physically bound to ion exchange sites of C-S-H gel. They also stated that a significant degree of reversibility exists and therefore, reducing the pore solution chloride concentration could result in desorption of bound chlorides. Thus, the total chloride, instead of free chloride, is used to evaluate the service life of reinforced concrete structures.

The binding of chloride ion by cementitious materials is very complicated and is influenced by many factors including chloride concentration, cement type and composition (Arya and Xu, 1995, Rasheeduzzafar et al., 1991), mineral additives (Byfors et al., 1986), hydroxyl concentration in pore solution (Tritthart, 1989), cation of chloride salt (Arya et al., 1990), and temperature (Luping and Nilsson, 1993a).

Predicting and modelling of chloride binding accurately needs comprehensive data on chemically and physically bound of chloride and influencing factors. Also relationship between free chloride and binding chloride has to be modelled precisely.

2.11.4 Determination and Mathematical Models of *D*

There exist several different methods of calculating the chloride diffusion coefficient based on the different principles. When trying to calculate D, two kinds of diffusion coefficients are currently used. One of them is obtained from steady-state experiments using migration cells (Page et al., 1981, Andrade et al., 1994, Castellote et al., 2002, Friedmann et al., 2004), and the other obtained from non-steady-state experiments (Andrade et al., 2000, Castellote et al., 2001). These coefficients are called as effective chloride diffusion coefficient, D_{eff}, and apparent chloride diffusion coefficient, D_{app}, in the literature.

The calculation of *D* from the chloride profile is a common method since this parameter is said to account for the resistance of the concrete to the transport of chlorides (Andrade et al., 2000). The most common practice to measure the chloride penetration depth is obtaining the chloride profile after predetermined time. Fitting of this profile to the so called error function (see Eq. 2.17), enables the calculation of the diffusion coefficient (Tuutti, 1982). Since the procedure of conducting this method is relatively slow, the

application of electrical fields to accelerate ionic transport can be justified (Whiting, 1981).

The long-term performance of most reinforced concrete structures is determined by chloride-initiated reinforcement corrosion. To design new durable structures reliable prediction models for chloride initiated steel reinforcement corrosion should be developed and utilised.

A model for predicting chloride ingress into concrete always aims to predict the chloride profile $C_{(x,t)}$ or at least the chloride content at the depth of the reinforcement after a certain exposure time t. The output is always meant to be compared to the CTL that is relevant to reinforcement corrosion (Nilsson, 2009). Numerous chloride diffusion models have been proposed during the last 10 to 15 years (Nilsson and Ollivier, 1995a, Nilsson, 2006, Luping and Gulikers, 2007).

One of the major achievements in service life modelling of structures exposed to chloride environment has been the insight that the chloride ingress decreases with time (Buenfeld and Newman, 1987, Mangat and Gurusamy, 1987, Mustafa and Yusef, 1994).

The chloride diffusion coefficient of a concrete typically decreases as time passes since the capillary pore system is altered as the hydration products continue to form. Also, some chloride ions will become chemically or physically bound as they penetrate into the pore system (Hooton and McGrath, 1995).

Haynes (Haynes, 1982) showed that the permeability of concrete exposed to sea water decreases with exposure time. More recently, Takewake and Mastumoto (Takewake and Mastumoto, 1988) are probably the first researchers who stated the dependency of D on the exposure period t and employed a purely empiric equation to describe the decrease of diffusion coefficient with time as proportional to $t^{-0.1}$.

Since Takewake and Matsumoto's study was published, the error function solution has been used with the apparent diffusion coefficient $D_a(t)$, in an exposure interval (t_{a0}, t) that decreases with time. A commonly used equation for this purpose, originally proposed by Takewaka and Matsumoto (1998) is shown in Equation 2.21:

$$D_a(t) = D_a(t_{a0}, t) = D_{a0}\left(\frac{t_{a0}}{t}\right)^a \quad (2.21)$$

where t is the age of the concrete, t_{a0} is a reference period, a is the aging exponent, and D_{a0} is the apparent diffusion coefficient at time t_{a0}.

Some researchers use t as the exposure time and t_{a0} as the age at exposure, which causes some discrepancies at early ages. Of course, D_{a0} cannot be determined directly and series of chloride profiles from different exposure times are needed. D_{a0} and a are merely looked upon as parameters that must be quantified from exposure data (Nilsson, 2009).

Tang and Nilson (Tang and Nilsson, 1992) applied a rapid diffusivity test and found that the measured diffusion coefficient in the young concrete decreased dramatically with age. They used a migration test method to determine a migration coefficient within 24 hours at different ages. This make it possible to measure the instantaneous diffusion coefficient D(t) from early ages after a certain curing time, without exposure to the chloride. Tang and Nilson (1992) showed that the diffusion coefficient measured in this way decreases with time, but only for six months. They used an expression similar to Equation 2.21 as follows:

$$D(t) = D_0\left(\frac{t_0}{t}\right)^n \quad (2.22)$$

where D_0 is the instantaneous diffusion coefficient at the age of t_0 which can be measured directly, and n is the age factor.

Mangat and Molloy (Mangat and Molloy, 1994b) presented their models as Equation 2.23. They obtained an empirical relationship between D and exposure time (t) as follows:

$$D_c = D_i t^{-m} \quad (2.23)$$

where t is the exposure time (seconds), m is an empirical coefficient, D_c is the effective diffusion coefficient at time t, and D_i is the effective initial diffusion coefficient.

By plotting the coefficient m against W/C ratio Equation 2.24 can be obtained as follows:

$$m = 2.5\left(\frac{w}{c}\right) - 0.6 \tag{2.24}$$

Then, by substituting m from Equation 2.24 in Equation 2.23, Equation 2.25 can be written as follows:

$$D_c = D_i t^{\left[2.5\left(\frac{w}{c}\right)-0.6\right]} \tag{2.25}$$

Equation 2.22 can also be rewritten as follows (Nokken et al., 2006):

$$D(t) = D_{ref}\left(\frac{t_{ref}}{t}\right)^m \tag{2.26}$$

where D_{ref} is reference diffusion coefficient at the reference time t_{ref} which can be assumed to be 28 days or one year.

Equation 2.26 accounts for the influence of time (concrete maturity) on diffusivity. The coefficient "m" is a constant dependent on variables such as type of the cementitious materials and concrete mix proportions. Values for "m" for different types of concrete should be accurately established, although some values have been published (Bamford, 1999, Stanish and Thomas, 2003, Thomas and Bamforth, 1999, Mangat and Molloy, 1994b)

Since changing in the pore structure is considered in terms of development of cement hydration process, this model can fit with a chloride environment. However, the model has not considered the change of D over time and this may lead to an erroneous judgment (Ann et al., 2009).

In order to remedy this defect, Pack et al. (2010) has used the mean value of the D for exposure duration to a marine environment to predict a chloride profile. Thus, the mean value was calculated by integrating the definite D for a given exposure duration, divided by the exposure duration, as shown in Equation 2.27.

$$D_m(t) = \frac{1}{t}\int_0^t D(T) \cdot dT \tag{2.27}$$

Where $D_m(t)$ is the mean diffusion coefficient for exposure duration, t. In this model, the time dependency of D was expressed as a power function shown Equation (2.27). Thus, the mean D can be obtained as follows:

$$D_m(t) = \frac{D_R}{1-m}\left(\frac{t_R}{t}\right)^m \tag{2.28}$$

This equation is more applicable to solving the Fick's 2nd law appropriately for a chloride profile, rather than a constant D. Since both the time dependency and historic change of the diffusivity are taken into account (Pack et al., 2010).

2.12 SUMMARY

A comprehensive literature review on the concrete microstructure, porosity and generation of cracks, with respect to their influence on concrete durability and service life (RC) structures service life has been conducted.

The main determinant of the premature deterioration of RC structures has been specified as chloride-induced corrosion of the steel reinforcement embedded in concrete. Therefore, the corrosion-free service life of the RC structures is defined as the initiation time of the corrosion of the reinforcing.

Also, based on the published papers, among the mass transport mechanisms, diffusion is the dominant transfer mechanism of the chloride ions into the concrete. For this reason, the Fick's 2nd law has widely been used by scholars to predict the service life of the structures exposed to chloride environment. To predict the free-corrosion service life of the RC structures based on the Fick's 2nd law, three parameters have to be identified. These parameters are chloride threshold level (CTL), surface chloride concentration (C_s), and chloride diffusion coefficient (D). In this chapter, all the above

mentioned factors were investigated and discussed extensively and also the most significant available relevant published articles were reviewed.

The reviewed experimental investigations have proved that both surface chloride content (C_s) and chloride diffusion coefficient (D) are time-dependent factors. In this chapter the most frequently used mathematical models in the literature were discussed to determine these factors.

Discussion continues about the time-dependency of the D and how it should be presented mathematically. Existing mathematical models are not enough accurate and induce mathematical errors. For instance; Tang and Gulikers (2007) (Tang and Gulikers, 2007), and Goltermann (2008) (Goltermann et al., 2008).

General conclusions on existing empirical models based on the Fick's 2nd law can be summarised as follows.

- The effect of the other ions in the pore system is completely neglected in empirical models utilising the Fick's 2nd law.
- The meaning of regression parameters in empirical models is not always easy to understand. They must be very clearly defined.
- The background for a number of the assumptions made in empirical models could be questioned. This is especially important for the continuous time-dependency of the diffusion coefficients and the surface chloride contents.
- Empirical models need enormous databases on surface chloride content for every new concrete, new environment, and new marine environment.

CHAPTER 3

MATHEMATICAL MODELS

CHAPTER 3. INVESTIGATION ON MATHEMATICAL MODELS IN THE LITERATURE

3.1 INTRODUCTION

The current practice of design of durable concrete structures is mainly based on prescriptive rules, such as specifying minimum concrete cover, maximum water/cement ratio (W/C), use of corrosion resistant reinforcing steels, limitation of crack width, etc. These rules are deemed-to-comply the design life requirements of safety and serviceability without explicitly specifying the relationship between performance and service life. However, the observed extensive deterioration and failure of a large number of reinforced and pre-stressed concrete structures before the end of their design lives have illustrated the serious inadequacy of the current ‘‘deemed-to-comply” rules (Costa and Appleton, 2002, Mehta, 2001, Meira et al., 2010, Mohammed et al., 2004).

Computer and analytical modelling has become a powerful tool used by researchers and engineers to understand the response of RC structures to service loads and to predict their performance especially with respect to deterioration and residual load-carrying capacity under different service conditions.

The durability design of concrete structures that are built in chloride-laden environments should be based on practical models (Zhang and Lounis, 2009, Glasser et al., 2008). These models require an adequate and clear understanding of the physicochemical processes that induce deterioration in concrete structures. These models can be classified as follows:

- Simplified diffusion-based model for chloride ingress into the concrete (Bentz et al., 1996, Thomas and Bamforth, 1999, Shin and Kim, 2002); and
- Reinforcement corrosion model (Bertolini, 2008, Chen and Mahadevan, 2008, Funahashi, 1990, Hsu et al., 2000, Hussain and Ishida, 2011).

The deterioration process of RC structures due to chemical-physical phenomena can be profitably analysed by means of simulated models, utilizing mathematical/numerical approach (Hossein M. Shodja 2010, Saetta, 2005). The prediction of the expected service life of reinforced concrete structures exposed to severe marine environment is the main objectives of this research. To predict service life of RC structures in chloride environment, the flow rate of chloride ions through a unit area (diffusion coefficient) of concrete must be known. However, the main focus of this research is development of a mathematical model to determine the chloride diffusion coefficient as a time-dependent factor.

Service life (t_l) can be expressed by means of time needed to initiate corrosion (depassivation time, t_p) plus time required to corrosion-induced crack (corrosion propagation time, t_{corr}) (Liang et al., 2002). Initiation time of the steel reinforcement corrosion is completely dependent on the diffusion process rate and can be predicted by diffusion models. This time period is also called corrosion-free service life. The propagation time extends from the time when corrosion products form to the stage where they generate sufficient stress to disrupt the concrete cover by cracking can be predicted by means of steel corrosion models (Ahmad, 2003).

$$t_l = t_p + t_{corr} \tag{3.1}$$

In this chapter both diffusion-based and steel reinforcement corrosion models are investigated and the most significant models are presented. Due to difficulties in understanding the physio-chemical reactions that occur during the propagation period, in most cases the initiation of corrosion is defined as the limiting condition in estimating the expected service life of the concrete.

3.2 DIFFUSION MODELS

Transport of the various species that participates in the mechanism of corrosion is facilitated by the network of interconnected pores in the material structure. Species diffuse through the pore water due to concentration gradients that exist between the exposed surface and pore solution of the cement matrix in saturated concrete. Another transport mechanism is that of capillary sorption which occurs in the partially saturated concrete. As water flows from saturated to partially saturated areas, it carries along dissolved chlorides or oxygen that add to the total concentration (Martín-Pérez et al., 2001).

Diffusivity is the relationship between the concentration flux (*J*), of diffusing material and the gradient of the chemical potential that is assumed to drive the mass diffusion process. Most of the studies on diffusion-based mathematical models have been conducted supported by Fick's law (Equation 2.16) of diffusion (Philibert, 2005). Fick's law of diffusion describes diffusion and can be used to determine the diffusion coefficient of ions into porous media like concrete. Fick's law relates the diffusive flux to the concentration field, by postulating that the flux goes from the regions of high concentration to the region of low concentration, with a magnitude that is proportional to the concentration gradient dimension.

Fick's Second Law can be expressed as follows:

$$\frac{\partial \emptyset}{\partial t} = D \frac{\partial^2 \emptyset}{\partial x^2} \tag{3.2}$$

where $\emptyset$ (mol/m^3) is the concentration rate of diffusive flux, t (s) is the time, D (m^2/s) is the diffusion coefficient, and x is the distance from concrete surface (m).

If the diffusion coefficient is not constant and depends upon the coordinate and/or concentration ratio, Fick's Second Law can be defined as Equation 3.3:

$$\frac{\partial \emptyset}{\partial t} = \nabla \cdot (D \cdot \nabla \emptyset) \tag{3.3}$$

Since the diffusion of the chloride ions into RC structures is the main cause of deterioration of RC structures (Costa and Appleton, 2002, Bamforth et al., 1997), this study will focus on this phenomenon. As a result of chloride diffusion, a concentration gradient develops near the concrete surface. The time at which the chloride concentration at the steel reinforcement surface reaches to chloride threshold level (CTL) and depassivates it, can be regarded as the initiation time of corrosion. The gradient of chloride content is often described by an error function model (Crank, 1975) which fulfils the condition of Fick's second law of diffusion as shown in Equation 3.4:

$$C_{(x,t)} = C_s \left[1 - erf\left[\frac{x}{2(Dt)^{\frac{1}{2}}}\right]\right] \tag{3.4}$$

where $C_{(x,t)}$ (%/m^3) is the chloride content (gradient) at depth x (m) at time t (s), C_s (%/m^3) is the chloride concentration at the concrete surface, x (m) is the depth from concrete surface, D (m^2/s) is the diffusion coefficient, erf is the error function, and t (s) time.

Bazant (Bazant, 1979) proposed a model to determine the initiation time of corrosion based on Fick's second law as follows:

$$t_0 = \frac{1}{12D}\left[\frac{c}{1 - (C_{th}/C_s)^{1/2}}\right]^2 \tag{3.5}$$

where t_0 (s) is the initiation time of corrosion, D (m^2/s) the diffusion coefficient, C_{th} (%/m^3) the chloride threshold level, and C_s (%/m^3) the surface chloride concentration.

Siemes and Polder (Siemes et al., 1998) stated a simplified formula for estimating the initiation time of corrosion as shown below:

$$L_i = \frac{d^2}{(A \cdot D_{Cl})} \tag{3.6}$$

where L_i (year) is the time until initiation of corrosion, d the depth of concrete cover, and A the constant depending on C_s and C_{cr} where $A = 1.8$ ($C_s = 3\%, C_{cr} = 1\%$); $A = 2.65$ ($C_s = 4\%, C_{cr} = 1\%$), and D_{Cl} the diffusion coefficient for chloride penetration.

Clear (Clear, 1976) proposed that the time prior to chloride induced corrosion may be empirically modelled as following:

$$RT = 129(S_i/25.4)^{1.22}/[K^{0.42}(w/c)] \tag{3.7}$$

where RT (*year*) is the time to onset of corrosion, S_i (*mm*) the concrete cover, and K (*ppm*) the chloride concentration of water deposited on concrete surface.

The onset of corrosion of the reinforcing steel is assumed to occur when the concentration of chlorides at the level of the reinforcement has reached the CTL. Therefore, the duration of the initiation stage can be considered from time zero to the onset of corrosion. Based on the concept of chloride threshold level for corrosion initiation and the assumptions of the Fick's second law process of chloride diffusion, a deterministic model of the time to corrosion initiation was expressed by Zhang and Lounis (Zhang and Lounis, 2009) as a function of four key parameters (Tuutti, 1982, Zhang and Lounis, 2006) as follows:

$$T_i = f(C_s, C_{th}, D, d_c) = \frac{{d_c}^2}{4D\left[erf^{-1}\left(1 - \frac{C_{th}}{C_s}\right)\right]^2} \tag{3.8}$$

where T_i is the onset time of corrosion (corrosion initiation time), C_s is surface chloride concentration, C_{th} is chloride threshold level, D the chloride diffusion coefficient, d_c is depth of concrete cover, and erf is the error function.

The model is a transformation of Crank's solution to the Fick's second law of diffusion for one-dimensional flow, under the assumptions of a constant diffusion coefficient, constant surface chloride content, and the initial chloride concentration condition specified as zero.

In this deterministic model (Equation 3.8) the following four parameters are assumed to be four independent design variables that are critical for corrosion protection as follows:

- Concrete cover depth d_c as structural parameter
- Chloride diffusion coefficient D, which is an indicator of the rate of chloride penetration into concrete.

- Chloride threshold value C_{th}, as environmental parameter which is an indicator of the corrosion resistance of reinforcing steel.
- Surface chloride concentration C_s, which is a measure of the corrosion load or exposure risk on concrete structures.

Recently, an inclusive ion transport process for predicting of the chloride ingress into concrete structures has been described as the Nernst–Planck's Equation (Samson and Marchand, 2008, Krabbenhøft and Krabbenhøft, 2008, Samson et al., 2003). This equation, which is well established on the traditional electrochemical theorem (Yang and Cho, 2003, Lizarazo-Marriaga and Claisse, 2009), describes the ion transport as a combination of three different mechanisms, including: (i) diffusion; (ii) convection; and (iii) electrical migration. Although, the mechanism of electrical migration under an imposed electrical potential has been used as an accelerated method (Rapid Chloride Permeability Test) to determine the diffusion coefficient of concrete (Andrade, 1993, Zhang and Gjørv, 1994, Yang and Cho, 2003) long time ago, however the study of its contribution to chloride ingress under normal service condition has been performed recently (Samson and Marchand, 2008).

Nernst and Einstein's equation cited by (Yang and Cho, 2004) proposed the relationship between the diffusion and electro-migration of ions in the same electrolyte. If concrete is considered to be a solid electrolyte, the diffusion of charged species i in concrete is related to its partial conductivity σ_i, and this relationship is called the Nernst-Einstein Equation.

$$D_i = \frac{RT\sigma_i}{{Z_i}^2 F^2 C_i} \tag{3.9}$$

where D_i (cm^2/s) is the diffusivity of species i, R (8.314 J/mol.K) the ideal gas constant, T (°K) the absolute temperature, σ_i (S/cm) the partial conductivity of species i, Z_i the charge of species i, F (96500 Coul/mol) Faraday's constant, C_i (mol/cm^3) the concentration of species i.

If the partial conductivity σ_i and the concentration C_i are determined, the diffusivity of species i, D_i can be calculated from Equation 3.9. However, the partial conductivity σ_i can be defined as:

$$\sigma_i = t_i \cdot \sigma \tag{3.10}$$

where σ is the conductivity of concrete, and t_i the conversion of species i, which can be defined as,

$$t_i = \frac{Q_i}{Q} = \frac{I_i}{I} \tag{3.11}$$

where Q_i and I_i are the electric quantity and current contribution of species i to the total electric quantity Q and current I, respectively.

If the diffusivity of an ion is to be determined by the Nernst-Einstein Equation, the transference number of this ion should be known (Yang et al., 2002). A simple and proper approach is to make the transference number approximately equal to 1.0. For example, if the concrete be saturated with a concentrated salt solution, the transference number may be assumed as 1.0, and C_i may be considered equal to the chloride concentration in the pore solution, or in the solution used to fill the concrete. Where $T = 298\,K$, $C_{cl^-} = 0.005\,mol/cm^3$.

Depending on the exposure condition as well as on the moisture content of the concrete element, the ingress of chlorides into concrete occurs through coupled multiple transport mechanisms (Kropp, 1995, Wang et al., 2005, Sandberg et al., 1998). However, most models for chloride ingress into the concrete are still based on the Fick's second law of diffusion as the main transport mechanism. Moreover, diffusion-based models have been found broadly acceptable for long-term monitoring of the chloride ingress in concrete structures (Bamford, 1999, Tang and Gulikers, 2007, Bentz et al., 1996).

Basheer et al. (Basheer et al., 1996) expressed their mathematical model based on Fick's law and incorporated the quantity of chloride binding with the matrix. The equation applies the principle of mass conservation to the concentration of chloride ion couple utilizing the Fick's diffusion law as shown in Equation 3.12.

$$\frac{\partial C}{\partial t} = div[D_i \nabla(C)] - \frac{1}{\omega} \cdot \frac{\partial S}{\partial t} \tag{3.12}$$

where C (mol/cm^3) is the free chloride concentration in the porous media; S is the quantity of bound chloride ions (mol/cm^3); ω is the content of water in which diffusion occurs (per unit mass of cement), and D_i (cm^2/s) is the chloride diffusion coefficient in the pore solution.

In addition, the diffusion-reaction-equilibration is represented by the Langmuir-type relationship between the free and bound chloride as shown in Equation 3.13.

$$S = C_t - w_e C \tag{3.13}$$

where C_t (mol/cm^3) and w_e are the total chloride concentration and the evaporable water content, respectively.

Therefore, the ionic binding may be approximated by the Langmuir adsorption isotherm relationship, as following:

$$S_{Cl^-} = \frac{\propto C_{Cl^-}}{1 + \beta C_{Cl^-}} \tag{3.14}$$

where $\propto$ and β are constants from Equations 3.12 to 3.14 by assuming that the free water is the evaporable water. Consequently, the concentration profile of chloride ions can be obtained using Equation 3.15.

$$\left[1 + \frac{\propto}{w_e(1 + \beta C)^2}\right]\frac{\partial C}{\partial t} = div[D_i \nabla(C)] \tag{3.15}$$

However, for long term predictions, it has been suggested that the constant diffusion coefficient in Equation 3.3 should be modified using the mix water/cement ratio (Mangat and Molloy, 1994a).

$$D_i^* = D_i \times t^{\left[0.6 - 2.5\left(\frac{w}{c}\right)\right]} \tag{3.16}$$

where the governing differential equation can be expressed as:

$$\left[1 + \frac{\propto}{w_e(1 + \beta C)^2}\right]\frac{\partial C}{\partial t} = div[D_i^* \nabla(C)] \tag{3.17}$$

For total chloride concentration, Equation 3.9 can be rewritten as following:

$$\left[1+\frac{\propto}{w_e(1+\beta C)^2}\right]\frac{\partial C_t}{\partial t}=div[D_i^*\nabla(C)] \tag{3.18}$$

Equations 3.17 and 3.18 approximate the free and total chloride concentration for a fully saturated concrete under isothermal conditions. The solution of Equations 3.17 and 3.18, as nonlinear differential equations, requires a finite element method utilizing a Newton-Raphson iterative solution. The total chloride content C_t can be obtained in accordance with ASTM C114.

Since the diffusion and concentration of chloride ions into concrete and on the reinforcement surface are long-term processes, accelerated electrochemical diffusion has been established to determine the diffusivity in relatively shorter time. Liang et al. (Liang et al., 1999), by using Tang and Nilson (Tang and Nilsson, 1992) equation and considering the influence of the added potential for accelerated diffusion, suggested that the Fick's second law can be re-expressed as:

$$J_{ix}=-D_e\left[\frac{\partial C_f}{\partial x}-\frac{eFE}{RT}C_f\right] \tag{3.19}$$

where $\mathrm{J_{ix}}$ is the flux of chloride ion, $\mathrm{D_e}$ the effective diffusion coefficient for the free chloride ion, $\mathrm{C_f}$ (mol/L) the construction of free chloride ion, e the valency of ion, F (96500 Coul/mol) the Faraday's constant, E (volt/m)the electrical field density, $\mathrm{R} = 8.31\ (\mathrm{j/mol.\,K})$ the ideal gas constant, and T the absolute temperature (°K).

The total chloride ion concentration C_t, in $\delta V = A \times \delta x$ can be obtained from Equation 3.20.

$$C_t = C_b + \varepsilon.d.C_f \tag{3.20}$$

where C_b (mol/L) is the bound chloride ion, ε the total porosity of concrete, and d the degree of saturation by the pore water solution.

The mathematical model of continuity of the chloride ion is presented by Equation 3.21 and shown in Figure 3-1.

$$\delta(C_t)A.\delta x = J_x \cdot A \cdot \delta x - J_{(x+\delta x)} \cdot A \cdot \delta x \tag{3.21}$$

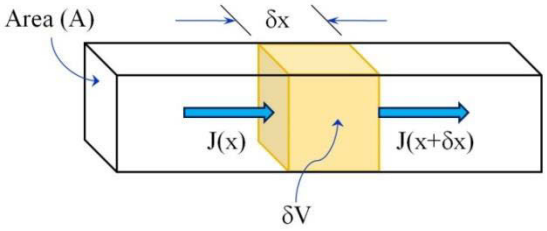

Figure 3-1 Continuity for the chloride ion diffusion

By expanding the Taylor's series and substituting in Equation 3.21, it can be rewritten as follows:

$$\frac{\partial(C_b + \varepsilon C_f)}{\partial t} = \frac{\partial}{\partial x}\left[D_e\left(\frac{\partial C_f}{\partial x} - \frac{eFE}{RT}C_f\right)\right] \tag{3.22}$$

Assuming that C_f and C_b are parts of a reversible process, the forward and backward absorption rates can be written as Equations 3.23 and 3.24, respectively.

$$r_a = k_a \cdot \varepsilon \cdot d \cdot C_f \tag{3.23}$$

$$r_b = k_b \cdot C_b \tag{3.24}$$

where k_a and k_b are forward and backward deposition coefficients, respectively. The net absorption rate can be determined by Equation 3.25:

$$\frac{\partial C_b}{\partial t} = r = r_a - r_b = k_a \cdot \varepsilon \cdot d \cdot C_f - k_b \cdot C_b \tag{3.25}$$

Substituting Equations 3.24 into Equation 3.25 yields:

$$\frac{\partial(\varepsilon d C_f)}{\partial t} = \frac{\partial}{\partial t}\left[D_e\left(\frac{\partial C_f}{\partial x} - \frac{eFE}{RT}C_f\right)\right] - r \tag{3.26}$$

If both porosity and the effective diffusion coefficient for mature concrete are independent of space and time (both ε and D_e are constant with respect to x and t), then Equation 3.26 can be rewritten as:

$$\varepsilon \frac{\partial C_f}{\partial t} = D_e \left[\frac{\partial^2}{\partial x^2} C_f - \frac{eFE}{RT} \frac{\partial C_f}{\partial x} \right] - r \tag{3.27}$$

where

$$C = \frac{C_f}{C_{en}} , \omega = \frac{C_b}{C_{b,sat}} , z = \frac{x}{L} , \tau = \frac{D_e}{\varepsilon d L^2} \cdot t , \lambda = \frac{eFEL}{RT} , \beta = \frac{C_{b,sat}}{\varepsilon d C_{en}} \tag{3.28}$$

C_{en} is the chloride concentration at the interface of the concrete surface exposed to the external environment (surface chloride concentration), $C_{b,sat}$ the maximum concentration that can be absorbed by concrete, and L the cover thickness of concrete.

From Equations 3.25, 3.27, and 3.28 the non-dimensional Equations 3.29 and 3.30 can be driven as follows:

$$\frac{\partial C}{\partial \tau} = \frac{\partial^2 C}{\partial z^2} - \lambda \frac{\partial C}{\partial z} - \beta \frac{\partial \omega}{\partial \tau} \tag{3.29}$$

and;

$$\beta \frac{\partial \omega}{\partial \tau} = \alpha C - \mu \omega \tag{3.30}$$

where

$$\alpha = \frac{k_a L^2 \varepsilon}{D_e} \tag{3.31}$$

$$\mu = \frac{k_b L^2 C_{b,sat}}{D_e C_{en}} \tag{3.32}$$

Equations 3.21 and 3.22 are driven simultaneously from the diffusion of accelerated chloride ions in an electric field. For absorption in the concrete pores α, β, λ, and μ are all constant with respect to z and τ.

If $C_b \to 0$, then $\omega \to 0$, then Equation 3.30 should be modified as follows:

$$\beta \frac{\partial \omega}{\partial \tau} = \alpha C \tag{3.33}$$

By substituting Equation 3.33 into Equation 3.29, the governing Equation 3.34 can be obtained:

$$\frac{\partial C}{\partial \tau} = \frac{\partial^2 C}{\partial \tau} - \lambda \frac{\partial C}{\partial z} - \alpha C \tag{3.34}$$

Eventually, Liang et al. (Liang et al., 1999) expressed an analytical solution by using Laplace transform equation as following:

$$C_{(z,\tau)} = \frac{1}{2} exp\left\{\left[\frac{\lambda}{2} - \sqrt{\frac{\lambda^2}{4} + \alpha}\right] z\right\} \cdot \left\{erfc\left[\frac{z}{2\sqrt{\tau}} - \sqrt{\left(\alpha + \frac{\lambda^2}{4}\right)\tau}\right] + exp\left(z\sqrt{4\alpha + \lambda^2}\right) \cdot erfc\left[\frac{z}{2\sqrt{\tau}} + \sqrt{\left(\alpha + \frac{\lambda^2}{4}\right)\tau}\right]\right\} \tag{3.35}$$

$erfc(x)$ is the complementary error function and can be defined by Equation 3.36 as follows:

$$erfc(x) = 1 - erfc(x) = \frac{2}{\sqrt{\pi}} \int_x^{\infty} e^{-u^2} du \tag{3.36}$$

Jastrzebski (Jastrzebski, 1976) pointed out that 30% to 40% of the volume of a permeable concrete consists of pores which means that the porosity is 30% to 40%. The diameter of pores ranges from 0.002 μm to 10 μm, and area of the porous surface per unit gram is

approximately 200 m^2 to 400 m^2. Thus, the porosity of the concrete can obviously have a significant impact on the absorption of chloride ions. The porous diffusion coefficient D_p can be defined as shown in Equation 3.37:

$$D_p = \frac{D_e}{\varepsilon} \tag{3.37}$$

However, rearranging Equations 3.34 and 3.35 yields the following Equations, respectively:

$$\tau = \frac{D_p}{dL^2} t, \tag{3.38}$$

$$\alpha = \frac{k_a L^2}{D_p} \tag{3.39}$$

Many researchers have used Fick's second law to predict the time of chloride induced corrosion with a given diffusion coefficient D and surface chloride content C_s, assuming that cement matrix in concrete is chemically inert and evenly porous (Hooton et al., 2002, Funahashi, 1990, Nguyen et al., 2008). However, these hypothesis and models have been challenged since Bamforth and Price (Bamforth and Price, 1993) addressed the time-dependent characteristic of chloride transport in terms of D and C_s. Later, Bentz et al. (Bentz et al., 1996) and Luping and Gulikers (Luping and Gulikers, 2007) confirmed the change of D with time.

The C_s for a concrete exposed to seawater may not change with time due to the chemical equilibrium, but at the tidal/splash zone the chloride content on the concrete surface can be increased by a number of wet and dry cycle resulting in a successive supply of chlorides by wetting with seawater, and water evaporation which makes salt crystallization by drying (Song et al., 2008, Ye et al., 2012).

Song et al. (Song et al., 2008) introduced their mathematical model based on the time-dependent diffusion coefficient and surface chloride concentration effect (Equation 3.40). Capillary pores reduce due to partially blockage as the cement matrix hydrates (Winslow

et al., 1994), which implies loss of paths for chloride ions. Thus, D can be decreased and C_s can be increased by accumulation of chloride ions on the concrete surface.

$$D_{(t)} = D_0 \left(\frac{t_0}{t}\right)^m \tag{3.40}$$

where $D_{(t)}$ (m^2/s) is the diffusion coefficient at time t, D_0 (m^2/s)the diffusion coefficient at time t_0, t_0 the standard time (one year or 28 days), t (s), and m the constant value.

3.3 MODELS FOR CORROSION STEEL REINFORCEMENT

Factors that influence the service life of structures are material properties, environmental conditions, and construction method. The service life of a reinforced concrete structure can be estimated by adding two periods of the corrosion time, namely initiation period and propagation period of steel reinforcement corrosion.

After initiation of corrosion, formation of hydrated red rust causes increase in the size of reinforcement bar due to volume expansion. This expansion causes tensile stresses and consequently initiation and propagation of cracking and eventually spalling of the concrete cover. The concrete behaviour is dominated by tensile cracking at a low level of compressive stresses and in this case the constitutive behaviour of concrete can be modeled using an elastic cracking model. The crack initiation is defined based on the Rankine criterion, according to which a crack forms in the direction normal to the maximum major tensile stress when this stress exceeds the tensile strength of concrete (parallel to the principal plane-Mohr circle) (Chitty et al., 2005).

Although, the steel reinforcement corrosion takes place non-uniformly in the concrete as pitting corrosion, it is assumed that uniform corrosion products are formed around the steel surface to simplify the analysis and modelling. The uniform corrosion products result in a uniform expansive stress applied to the surrounding concrete. Not all of corrosion products are responsible for the expansive pressure; some of them may fill the voids around the steel-concrete interface (Weyers, 1998). Due to complexity of the problem, corrosion cracking is only restricted to the stresses resulting from the expansion of corrosion

products. Figure 3-2 shows a schematic diagram of the basic model for the corrosion-induced cracking processes (El Maaddawy and Soudki, 2007).

When the total amount of corrosion products (W_T) is less than the amount of the corrosion products required to fill the porous zone around the steel-concrete interfacial zone (W_P), the formation of corrosion products at this stage (stage b. in Figure 3.2) cannot create any stress on the surrounding concrete (Zhang et al., 2010, Markeset, 2008, Otieno et al., 2011).

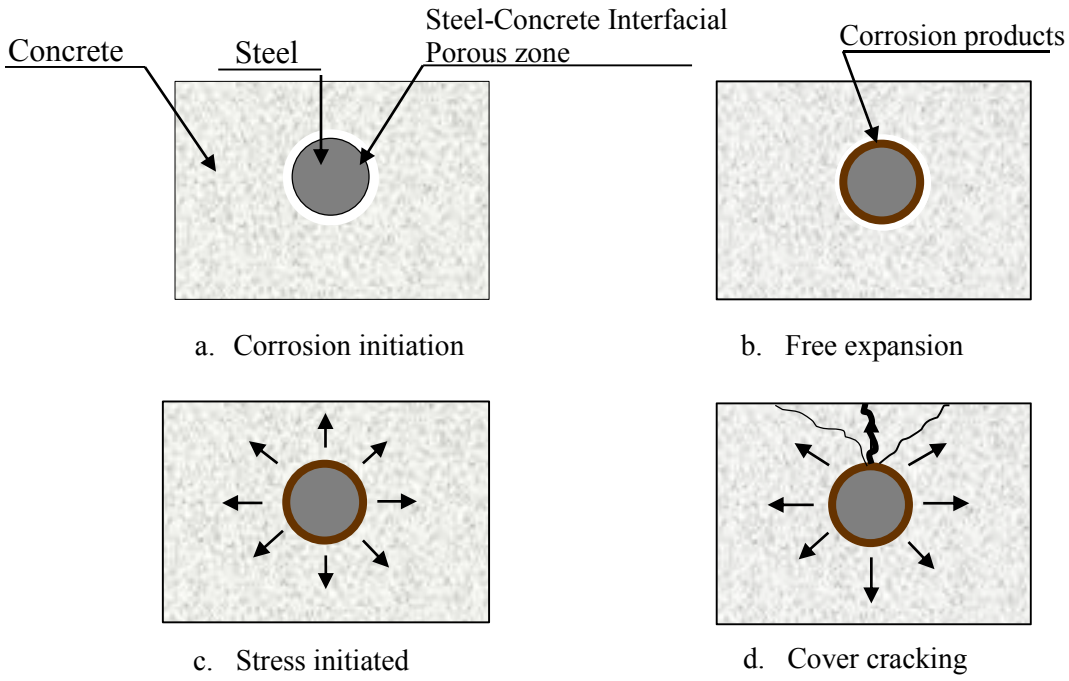

Figure 3-2 Schematic diagram of the corrosion-cracking process

As W_T exceeds W_P the expansive pressure on the concrete surrounding the steel is created. When W_T reaches the critical amount of the corrosion products (W_{cr}), internal stress from the volume increase of rust will exceed the tensile strength of the concrete and the cracks are generated.

$$W_P = \rho_{rust} \cdot V_P \tag{3.44}$$

where ρ_{rust} is the density of the corrosion products and V_P the total volume of pores in the steel-concrete interfacial zone.

If assume that d_0 is the thickness of porous zone, the original diameter of the steel bar (D) will increase by $D + 2d_0$ when the amount of corrosion products reaches to W_P. Since $d_0 << D$, W_P can be estimated from Equation 3.45.

$$W_P = \rho_{rust} \cdot \pi \cdot d_0 \cdot D \tag{3.45}$$

As can be seen, W_P is a function of the size of steel reinforcement, density of rust and characteristics of the steel-concrete interfacial. The critical amount of corrosion products can be written as:

$$W_{cr} = \rho_{rust}\left[\pi(d_s + d_0)D + \frac{W_{st}}{\rho_{st}}\right] \tag{3.46}$$

where ρ_{rust} is the density of corrosion products, d_s the thickness of corrosion products to generate the tensile stresses, d_0 the thickness of porous zone around the steel, D original diameter of the steel, W_{st} mass of the steel corroded, and ρ_{st} density of the steel.

$$W_{st} = \alpha \cdot W_{cr} \tag{3.47}$$

where α is the molecular weight of the steel divided by the molecular weight of the corrosion products. The value of α depends on the type of corrosion products. For instance $\alpha = 0.523$ when the corrosion products are considered as $Fe(OH)_3$ and $\alpha = 0.622$ for $Fe(OH)_2$.

For constant corrosion rate, the time to cracking (t_{cr}) can be estimated as follows:

$$t_{cr} = \frac{W_{cr}^2}{2k_p} \tag{3.48}$$

where k_p is the rate of rust production which may be expressed in terms of corrosion current density (i_{corr}) as shown in Equation 3.49.

$$k_p = 2.59 \times 10^{-6}(1/\alpha)\pi D i_{corr} \tag{3.49}$$

Also, the increment of reinforcing bar diameter has been modelled by Bazant (Bazant, 1979) shown in Equation 3.50.

$$\Delta D = t_{corr} \frac{s j_r}{D \rho_{corr}} \tag{3.50}$$

where D is the original reinforcing bar diameter, ΔD is the increase in the diameter, t_{corr} the duration of steady state corrosion, s the spacing of bars, j_r the rate of rust production per area, and $\rho_{corr} = (\pi/2)[(1/\rho_r) - 0.538/\rho_{st}]^{-1} = 3.6\ \ g/cm^3$. Here ρ_r and ρ_{st} are mass densities of $Fe(OH)_2$ and steel, respectively. Equation 3.50 is simplified further by assuming that the rate of increase in bar diameter is linearly proportional to time over the initial bar diameter.

$$\Delta D = \frac{t}{D} \tag{3.51}$$

where t represents the time when steady state corrosion begins.

According to Lundgren (Lundgren, 2002), the increase in the radius of a reinforcing bar due to corrosion (δ) can be estimated from Equation 3.52.

$$\delta = \sqrt{r^2 + (\propto_v - 1)(2 r p_{corr} - {p_{corr}}^2)} - r \tag{3.52}$$

where $r = d/2$ is the radius of the reinforcing bar, p_{corr} the corrosion penetration, and $\propto_v$ the volumetric expansion ratio of corrosion products. If $p_{corr} \ll r$, then instead of using Equation 3.52 it is possible to estimate δ accurately by using Val et al. (Val et al., 2009) Equation as follows:

$$\delta = (\alpha_v - 1) p_{corr} \tag{3.53}$$

and if the corrosion rate is constant, the corrosion penetration in mm at time *t* (*year*) after corrosion initiation can be found using the Faraday's law of electrolysis from Equation 3.54.

$$p_{corr} = 0.0116\, i_{corr} t \tag{3.54}$$

where, i_{corr} is the corrosion current density ($\mu A/cm^2$).

The structural consequences of the deterioration mechanisms can be addressed by means of simple models as given by Goltermann (Goltermann et al., 2008). Following the Goltrermann's approach, contact pressure between the reinforcement bar and the cement paste can be computed from Equation 3.55 which has been expressed by Basheer et al. (Basheer et al., 1996).

$$p = \Delta D \cdot G_a K_0 \tag{3.55}$$

where

$$G_a K_0 = E_p / \left[\left(1 + v_p/2\right) + \left(E_p/E_s\right)(1.2 v_s) \right] \tag{3.56}$$

and E_p is the modulus of elasticity of the paste, E_s the modulus of elasticity of steel, and v_p and v_s the Poisson's ratio of paste and steel, respectively. When the value of p exceeds the fracture strength of concrete, cracks are initiated.

Meanwhile, from structural point of view, the effective cross-sectional area of reinforcement is decreased due to the corrosion process which results a reduction in load bearing capacity of structure.

Pfeifer (Pfeifer, 2000) reported that concrete would crack and spall after 25 μm of the steel reinforcement diameter has corroded although, this is likely not the case for all concrete.

$$t_{cr}(year) = \frac{25\ \mu m}{corrosion\ rate\ \left(\frac{\mu m}{year}\right)} \tag{3.57}$$

3.3.1 Corrosion Measurement Parameters

In general, information about the state of reinforcement corrosion is usually obtained in terms of three measurement parameters, namely corrosion potential (E_{corr}), concrete resistivity (ρ), and corrosion current density (I_{corr}).

The parameters are briefly described as follows.

3.3.1.1 Corrosion potential (E_{corr})

The corrosion potential, also called half-cell potential is measured at several distinct points over a given area to be surveyed. It is used as a qualitative index for ascertaining whether reinforcement is likely to be corroding or not. In addition, it can be used for obtaining a contour plot to delineate anodic (corroding) and cathodic (noncorroding or passive) portions of the RC structure under investigation.

Interpretation of half-cell potential test results according to ASTM C876 (1991) guidelines, are presented in Table 3-1.

Table 3-1 Interpretation of half-cell potential values as per ASTM C876

Half-cell potential (mV) relative to Cu/CuSO4 reference electrode	Percentage chance of active corrosion
$\mathrm{E_{corr}} < -350$	90
$-350 < E_{\mathrm{corr}} < -200$	50
$\mathrm{E_{corr}} > -200$	10

3.3.1.2 Concrete resistivity (ρ)

The corrosion of a specific length of reinforcement is dependent on the algebraic summation of the electrical currents originating from the corroding sites on the steel through the surrounding concrete to the non-corroding sites. Hence, the electrical resistance of concrete plays an important role in determining the magnitude of the corrosion at any specific location (Berkeley and Pathmanaban, 1990). This factor is measured in terms of electrolytic resistivity of concrete and is usually expressed in ohm-centimeters. Classification of the likelihood of corrosion can be obtained on the basis of the values given in Table 3-2. These values are best suited when half-cell potential measurements indicates that corrosion is possible (Carino, 1999).

Table 3-2 Interpretation of reinforcement corrosion regard to concrete resistivity

Resistivity (Ω cm)	Probability of significant corrosion
$\rho < 5000$	Very high
$5000 < \rho < 10000$	High
$10000 < \rho < 20000$	Moderate
$\rho > 20000$	Low

3.3.1.3 Corrosion current density (I_{corr})

The corrosion rate is measured in terms of the corrosion current density, I_{corr}, and is a quantitative index, which represents an overall estimation of the corrosion attack of reinforcement. The I_{corr} is measured electrochemically. According to the previously established corrosion models (Lu et al., 2011), when corrosion of reinforcement is controlled by the diffusion of oxygen; the corrosion current of reinforcement can be estimated by Equation 3.58.

$$i_{corr} = i_{diff} = nFD_o \frac{[O_2]}{\delta} \tag{3.58}$$

where, i_{corr} is the corrosion current density of reinforcement, i_{diff} the electrical diffusion current of oxygen, n the electrons loss of oxygen during the cathodic reaction, D_o the diffusion coefficient of oxygen in the different layer, O_2 the soluble oxygen concentration at the outside surface of diffusion layer, and δ the effective thickness of the diffusion layer on the reinforcement surface.

The Linear Polarization Method (Scully, 2000) is one of the most rapid test for estimating the corrosion current density which is based on the Stern-Geary equation.

$$i_{corr} = \frac{\beta_a \beta_c}{2.3(\beta_a + \beta_c)} \cdot \frac{1}{R_p} = \frac{B}{R_p} \tag{3.59}$$

where, $\beta_a \; and \; \beta_c$ are Tafel's constants for anodic and cathodic reaction, respectively, B usually is in the range of 6.5 mV to 52 mV (for steel in concrete 26 mV for active and 52 mV for passive), and R_p linear polarization resistance.

Tafel slopes, β_a and β_c, may be determined by minimizing the error function of Z as shown in Equation 3.61, which is the square of the difference between LHS and RHS of the Equation 3.60 (polarization equation):

$$2.3R_pI_i = \frac{\beta_a\beta_c}{(\beta_a+\beta_c)}\left[exp\left(\frac{2.3\varepsilon_i}{\beta_a}\right) - exp\left(\frac{-2.3\varepsilon_i}{\beta_c}\right)\right] \tag{3.60}$$

$$Z = \sum_{i=1}^{n}\left[A_i - \frac{1}{\left(\frac{1}{\beta_a}+\frac{1}{\beta_c}\right)}\left[exp\left(\frac{B_i}{\beta_a}\right) - exp\left(\frac{-B_i}{\beta_c}\right)\right]\right]^2 \tag{3.61}$$

where $A_i = 2.3R_pI_i$ and $B_i = 2.3\varepsilon_i$.

The minimization of Z may be carried out using a simple method of tabulation, whereby the values of Z may be tabulated for a large number of possible values of $1/\beta_a$ and $1/\beta_c$ at equal spacing within the feasible region, i.e., $0.02 < \left((2.3/\beta_a) + (2.3/\beta_c) < 0.12\right)$, and the minimum value of Z is then sought. The values of $1/\beta_a$ and $1/\beta_c$ in the error function of Z will give the actual value of β_a and β_c. This minimization may be conducted by using a short computer programming. The time required for the computing procedure described above was found to be less than one minute.

Once β_a and β_c are determined, the Stern–Geary constant, B may be calculated using Equation 3.62.

$$B = \frac{\beta_a\beta_c}{2.3(\beta_a+\beta_c)} \tag{3.62}$$

The electrochemically measured value of I_{corr} can be converted to the instantaneous corrosion rate, J_r, and penetration rate, P_r through Faraday's law (Ahmad, 2003), as shown in Equations 3.63 and 3.64.

$$J_r = \left(\frac{W}{F}\right)I_{corr} \tag{3.63}$$

$$P_r = \left(\frac{W}{F\rho_{st}}\right)I_{corr} \tag{3.64}$$

where, W is the equivalent weight of steel, F the Faraday's constant (96488 C or A.s), ρ_{st} the density of steel (7.85 g/cm^3), I_{corr} the corrosion current density (A/cm^2), J_r the corrosion rate (g/cm^2/s), and P_r the penetration rate (cm/s).

3.4 SERVICE LIFE PREDICTION MODELS

Tutti (Tuutti, 1982) described the corrosion of concrete structures as a two-stage process consisting corrosion initiation and corrosion propagation. The corrosion initiation stage corresponds to the process of chloride ingress into concrete and depassivation of protective layer surrounding the steel bars after reaching to the Chloride Threshold Level (CTL). The corrosion propagation stage starts after the initiation of active corrosion which results the generation of cracks and then spalling of concrete cover (Val, 2007). Therefore, the duration of the initial stage, which is often used as a quantitative indicator of service life or durability of concrete structures, depends on the rate of chloride penetration in concrete (Shafei et al., 2012). The needs to predict the service life of existing structures and to design more durable structures have been the objectives of the extensive investigations to simulate and model the chloride ingress, corrosion initiation, and corrosion propagation in concrete structures for the last three decades (Enright and Frangopol, 1998, Khatri and Sirivivatnanon, 2004, Liang et al., 2002, Lin et al., 2010, van der Wagen et al., 2012).

Aggressive agents such as chlorides, water, and oxygen penetrate into concrete through the capillary pores and micro-cracks in the cement paste matrix as well as at the interfacial transition zone of paste and aggregate (Ustabas, 2012, Kropp, 1995). The rate of penetration is dependent primarily on the quality of concrete particularly on the W/C ratio of the concrete mix, and/or protective systems that delay or slow down chloride ingress. In porous solids, such as concrete, chlorides can penetrate in concrete via different physical mechanisms, such as diffusion, capillary absorption, electrical migration, and permeation due to hydraulic pressure heads (Boddy et al., 1999, Buenfeld and Glass, 1998, Conciatori et al., 2008). Furthermore, the penetration process is also influenced by chemical reactions such as chloride binding (Luping and Nilsson, 1993a, Tritthart, 1989, Saetta, 2005).

Service life is directly related to the material characteristics, cover depth and severity of the exposure conditions (Zimmermann et al., 2000, Yiğiter et al., 2007). The first

influencing factor in service life is the material characteristics (Song et al., 2010). In any structure, there is bound to be variation in the quality of concrete due to variation on water/binder ratio, different levels of compaction, variation in extent of curing or the variation in the hydration of cement due to changes in temperature (Morinaga, 1992). The second influencing factor is the variation in the thickness of cover depth values. Variation in the exposure conditions of service environment is another influencing factor of scatter in service life (Amey et al., 1998). A part of the structure could be in tidal zone and another part could be in the splash zone. Also, some portions of structure could be continuously immersed in the seawater and some portion could be exposed to airborne chloride (Khatri and Sirivivatnanon, 2004, Ye et al., 2012).

In the next section the most significant models published in the literature are investigated as follows:

3.4.1 Bazant's Model

Bazant's model (Bazant, 1979) for the prediction of corrosion damage, considers the volume expansion due to the formation of hydrated red rust, ($Fe(OH)_3$), over the residual rebar core. This red rust is expansive in nature and occupies four times the volume of parent steel. Thus, a uniform radial pressure is exerted onto the surrounding concrete resulting in outward radial expansion of concrete. This expansion is same as the increase in diameter ΔD of the rebar (due to geometrical compatibility), and increases with an increase in the volume of rust till the cover concrete cracks and is rendered functionally unsatisfactory. When corrosion is in a steady state with a constant rate, the unacceptable deformation of concrete at cracking can be related to the duration of the steady-state corrosion, as expressed in Equation 3.65.

$$t_{corr} = \rho_{corr} \frac{D \cdot \Delta D}{p J_r} \tag{3.65}$$

where, t_{corr} is the steady-state corrosion period, ρ_{corr} the combined density factor for steel and rust, D the original diameter of reinforcing bar, ΔD the increase in diameter of reinforcing bar, p the perimeter of reinforcing bar, and J_r the corrosion rate as given by Equation 3.63.

3.4.2 Morinaga's Model

Morinaga (Morinaga, 1990) has developed an empirical model to compute the amount of corrosion, Q_{cr}, when concrete cover cracks due to expansion by means of rust formation on rebar surface. The expression to estimate Q_{cr} is shown by Equation 3.66.

$$Q_{cr} = 0.602\left(1 + \frac{2C_v}{D}\right)^{0.85} D \tag{3.66}$$

where, Q_{cr} is the amount of corrosion when concrete cracks ($\times 10^{-4}\, g/cm^2$), C_v the concrete cover thickness (mm).

The duration of steady-state corrosion, t_{corr} corresponding to Q_{cr} can be obtained from Equation 3.67.

$$t_{corr} = \frac{Q_{cr}}{J_r} \tag{3.67}$$

3.4.3 Wang and Zhao's Model

Wang and Zhao (Wang and Zhao, 1993) have suggested a step method by using finite element analysis to determine the thickness of the corrosion product, Δ, corresponding to the time duration when the surface concrete cracks. Furthermore, by analysing a large number of rebar corrosion data collected from laboratory and comparing to the results of the finite element analysis, they have established an empirical expression to determine the ratio of thickness of corrosion product, Δ, to the depth of rebar penetration, H in the concrete cover. The ratio (Δ/H), as given below, is termed as expansion coefficient, and γ has been expressed as a function of cube strength of concrete, f_{cu}, in Equation 3.68.

$$\frac{\Delta}{H} = \gamma = 0.33\left(\frac{D}{C_v}\right)^{0.565} {f_{cu}}^{1.436} \tag{3.68}$$

By using the value of Δ the value of H corresponding to cracks in the concrete cover can be obtained. In addition, the value of H can be used to determine the time necessary for longitudinal cracking of concrete cover, t_{corr} by Equation 3.69.

$$t_{corr} = \frac{H}{P_r} \tag{3.69}$$

where P_r is the penetration rate of rebar due to corrosion, as given by Equation 3.64.

3.4.4 Ahmad et al.'s Model

An experimental methodology, suggested by Ahmad et al. (Ahmad et al., 1997), for service life prediction based on cumulative damage theory can be presented as follows:

If a RC specimen is allowed to corrode for a time duration, L_c at its natural corrosion rate, I_{corr} from the time of depassivation, t_p onward and then the same is subjected to an impressed anodic current, I_a up to the time of cracking, t_{corr}, according to the cumulative damage theory, the following expression can be written;

$$\frac{L_c}{L_t} + \frac{L_a}{L_l} = 1 \tag{3.70}$$

where L_c/L_t is fraction of damage due to the natural corrosion, L_a/L_l the fraction of damage due to externally applied current, L_a the time taken by the specimen for its complete damage under the effect of external current being applied after the natural corrosion that had already taken place, L_l the time taken by the specimen for its complete damage under applied current alone excluding the effect of natural corrosion, L_c the duration of the natural corrosion starting from the time of depassivation of rebar to the date of application of external current, and L_t the total life of specimen against corrosion cracking of concrete cover.

The expression of L_t can be determined by Equation 3.71.

$$L_t = L_c \Big/ \left\{1 - \left(\frac{K_2}{K_1}\right)\left[\frac{F_0 f(C_v/D)}{EI_a}\right]\right\} \tag{3.71}$$

where

$$L_a = \frac{F_0 f(C_v/D)}{E I_a K_1} \tag{3.72}$$

and

$$f(C_v/D) = \frac{4.72\left(\frac{C_v}{D}\right)^2 + 4.72\left(\frac{C_v}{D}\right)+1}{\left(\frac{C_v}{D}\right)+1} \tag{3.73}$$

In the above Equations, F_0 is the failure tensile stress of concrete, I_a the applying anodic current for a time period of T, E the modulus of elasticity of concrete, K_1 and K_2 constant, C_v cover thickness, and D reinforcing bar diameter.

K_1 may be determined using Equation 3.74.

$$\frac{F_T}{F_0} = 1 - K_1\left[\frac{E \cdot T \cdot I_a}{F_0 f\left(\frac{C_v}{D}\right)}\right] \tag{3.74}$$

where F_T is the failure tensile stress of concrete after applying I_a for duration of T. K_2 may be determined utilising Equation 3.75.

$$\frac{1}{L_a} = K_2 + NCF \tag{3.75}$$

where NCF is the natural corrosion factor, which can be computed using Equation 3.76.

$$NCF = \frac{E \cdot L_c I_{corr}}{f_t' f\left(\frac{C_v}{D}\right)} \tag{3.76}$$

where f_t' is cylindrical tensile strength of concrete, I_{corr} the corrosion rate before application of I_a.

3.5 SUMMARY

In this chapter the current most significant models were investigated in order to obtain the main concepts, influencing factors, and procedures of modelling the service life of RC structures.

The service life models should consist of two phases, corrosion initiation time which is dependent on the diffusion process, and corrosion propagation time. The models regarding to both processes were investigated. This investigation proved that most of the proposed models for diffusion process have used Fick's 2nd law as the base concept and model. In these models two effective factors including chloride diffusion coefficient D and surface chloride concentration C_s have been assumed as constant factors. However, few studies and models have been proposed these two parameters as time-dependent factors.

A brief review of this chapter can be summarised as follows:

- Significant models of chloride diffusion in concrete to estimate the corrosion initiation time and models of corrosion propagation were investigated.
- The models' criteria, assumptions, and influencing parameters were presented.
- The initiation time of corrosion (depassivation time) is dependent on water cement ratio, curing method, environmental exposure conditions, surface chloride content, chloride diffusion coefficient, cover depth, and wetting-drying cycles.
- The propagation time is dependent on the cover thickness, concrete conductivity, steel-concrete interface, type of corrosion products, and reinforcing steel diameter.
- Although, the type of steel reinforcement corrosion in the concrete is pitting corrosion, in all corrosion models, it is assumed that uniform corrosion products are formed around the steel surface to simplify the analysis and modelling.
- Not all of corrosion products are responsible for the expansive pressure; some of them may fill the voids around the steel-concrete interface.
- Concrete can be considered as a solid electrolyte thus, the diffusion of charged species (e.g. Cl^-) in concrete is related to its partial conductivity (σ_i).

The most significant mathematical models for diffusion process in concrete, presented in the literature review, are summarized in Table 3-3.

Table 3-3 Mathematical models for diffusion process in concrete

	Mathematical Model	Reference
1	$\frac{\partial \emptyset}{\partial t} = D\frac{\partial^2 \emptyset}{\partial x^2}$ D, constant	Fick's Second Law
2	$t = \frac{1}{12D}\left(\frac{d_c}{1-\sqrt{\frac{C_{th}}{C_s}}}\right)^2$ D, constant	Bazant (1979b)
3	$C_{(x,t)} = C_s\left[1 - erf\left[\frac{x}{2(Dt)^{\frac{1}{2}}}\right]\right]$ D, constant	RILEM Report 14, (1996)
4	$C_{(x,t)} = S\sqrt{t}\left[1 - erf\left(\frac{x}{2\sqrt{Dt}}\right)\right]$ D, constant	Weyers (1998)
5	$J_{ix} = -D_e\left[\frac{\partial C_f}{\partial x} - \frac{eFE}{RT}C_f\right]$	Liang et al. (1999)
6	$D_i = \frac{RT\sigma_i}{{Z_i}^2F^2C_i}$	Nernst-Einstein (1975),
7	$\frac{\partial C}{\partial t} = div[D_i\nabla(C)] - \frac{1}{\omega}\cdot\frac{\partial S}{\partial t}$	Basheer et al. (1996)
8	$T_i = f(C_s, C_{th}, D, d_c) = \frac{{d_c}^2}{4D\left[erf^{-1}\left(1-\frac{C_{th}}{C_s}\right)\right]^2}$ D, constant	Zhang and Lounis, (2009)
9	$L_i = \frac{d^2}{(A\cdot D_{Cl})}$ D, constant	Siemes and Polder, (1998)

The mathematical models for corrosion of steel reinforcement in concrete have been summarized in Table 3-4.

Table 3-4 Corrosion of steel reinforcement models

	Mathematical Model	Reference
1	$RT = 129(S_i/25.4)^{1.22}/[K^{0.42}(w/c)]$	Clear, (1976)
2	$t_{corr} = \rho_{corr}\dfrac{D \cdot \Delta D}{pJ_r}$	Bazant's model (1979b)
3	$t_{corr} = \dfrac{\delta \rho_{st} ZF}{Ai_{corr}}$	Fontana (1987)
4	$\mathrm{t_{corr}} = \dfrac{\mathrm{W_{cr}^2}}{2\mathrm{k_p}}$	Liu (1996)
5	$\delta = \sqrt{r^2 + (\propto_v - 1)(2rp_{corr} - {p_{corr}}^2)} - r$	Lundgren, (2002)

The mathematical models for service life prediction have been summarized in Table 3-5.

Table 3-5 Service life prediction models

	Mathematical Model	Reference
2	$t_{corr} = \dfrac{Q_{cr}}{J_r}$, $Q_{cr} = 0.602\left(1 + \dfrac{2C_v}{D}\right)^{0.85} D$	Morinaga's model (1990)
3	$t_{corr} = \dfrac{H}{P_r}$, $\dfrac{\Delta}{H} = \gamma$ $= 0.33\left(\dfrac{D}{C_v}\right)^{0.565} {f_{cu}}^{1.436}$	Wang and Zhao's model, (1993)
4	$L_t = L_c/\left\{1 - \left(\dfrac{K_2}{K_1}\right)\left[\dfrac{F_0 f(C_v/D)}{EI_a}\right]\right\}$	Ahmad et al. (1997)

The main weakness of the transport processes models up to now is the assumption of constant diffusion coefficient. As a consequence, a single value of diffusion coefficient can never obtained from the measured concentration profiles, particularly if the measurements are performed over longer periods. The diffusion coefficient then appears as a function of time.

3.6 CONCLUSIONS

So far, two following mathematical relations for expressing of diffusion coefficient as a time-dependent function have been suggested.

Mangat and Molloy (1994) have suggested the following mathematical relation between diffusion coefficient of concrete and water cement ratio:

$$D_i^* = D_i \times t^{\left[0.6-2.5\left(\frac{w}{c}\right)\right]} \tag{3.77}$$

where D_i (cm^2/s) is the chloride diffusion coefficient in the pore solution.

Song et al. (2008) suggested their mathematical model based on time-dependent diffusion coefficient and surface chloride concentration as well. Capillary pores reduce and are partially blocked as the cement matrix hydrates (Winslow et al., 1994), which implies a loss of paths for chloride ions. The so-called time-dependent model can be obtained based on an empirical Equation as follows:

$$D_{(t)} = D_0 \left(\frac{t_0}{t}\right)^m \tag{3.78}$$

where $D_{(t)}$ (m^2/s) is the diffusion coefficient at time t, D_0 (m^2/s) is the diffusion coefficient at time t_0, t_0 is the standard time (one year or 28 days), t (s) is the time, and m is the age factor.

CHAPTER 4

DATABASE ANALYSIS & ASSESSMENT

CHAPTER 4. DATABASE ANALYSIS AND ASSESSMENT

4.1 INTRODUCTION

In this chapter analysis of the available database is described and assessed. The first conducted analysis is the technical assessment and economic evaluation of the most commonly used corrosion prevention methods in RC structures exposed to severe environment. The second performed investigation is analysis and assessment of the mathematical models of chloride diffusion coefficient in concrete exposed to marine environment.

4.2 STATE OF PROBLEM

Many civil structural elements are required to be repaired due to various mechanical, physical, and chemical deterioration processes such as steel reinforcement corrosion, cracking and spalling in order to extend the service life or restore the original strength and serviceability of the structures.

In recent years, the growing need to maintain and repair structures has brought about a definite variation in the expenditure for restoration compared to the investment for new structures. The expenditure for restoration has nearly doubled compared to the last decade, when it was seen to be between 25% and 30% (Coppola, 2000).

Despite the inherent durability of concrete, the premature deterioration of concrete structures has caused many serious problems (Costa and Appleton, 2002, Khayat et al., 2005, Villain et al., 2012). These problems can be classified as follows:

First problem is the financial problems due to repair and/or reconstruction some parts or even whole of structure (Koch et al., 2001). Generally, the repair of structures is an expensive issue and for marine and water front structures due to presence of water and difficulties in access to damage portion, will be much more expensive and time consuming (Pullar-Strecker, 1987, Schiessl and Breit, 1996).

Second problem is the presence of cold joints between old concrete and fresh concrete. Experimental observations conducted by Sue (Sue et al., 2001) showed that the bending strength of the repaired member remarkably decreased due to the age difference (cold joint) between the top layer (old concrete) and the lower layer (repaired and replaced part). Despite of all progress and improvement of material science in this field, this problem still exists.

An interface appears whenever a repair material is applied to an structural system after rehabilitation. Usually the interface is relatively weaker than the material on either side of it in a repaired system. The performance of the repaired system is strongly dependent on the performance of the interface (Chandra Kishen and Rao, 2007). In a repaired system, the chances of failure by cracking along the interface is higher because of the stress concentration and rapid change of stress levels along the interface (Lim et al., 2001).

Therefore concrete structures should be protected from premature deterioration in order to be more safe and economic. For achieving this purpose many investigation have been performed and many prevention attempts and methods have been proposed and carried out.

Since late 1960s, when corrosion of steel in reinforced concrete structures was first recognized as a problem in reinforced concrete structures, many methods have been developed to prevent the corrosion of steel bars. These methods, which have been applied up to now, can be divided into four different main categories, based on the protection mechanism (Kepler et al., 2000) as follows:

- Alternative reinforcement includes materials that electrically isolate the steel from the concrete and create a barrier for chloride ions, materials that protect steel galvanically, and materials that have significantly higher corrosion thresholds than conventional reinforcing steel. Epoxy-coated reinforcement, galvanized steel bars, and fibre reinforced polymer reinforcement are the most utilized methods in this category.
- Barrier methods protect reinforced concrete from corrosion damage by preventing water, oxygen, and chloride ions from reaching the reinforcement and initiating corrosion such as surface treatment of concrete.
- Electrochemical methods use current and an external anode to protect the reinforcement, even when the chloride ion concentration is above the corrosion threshold. Cathodic protection is the most famous methods in this category.
- Corrosion inhibitors offer protection by raising the threshold chloride concentration level chemically. Calcium nitrite is the most applied inhibitor in for corrosion prevention.

Some of the most commonly used methods including electrochemical techniques, epoxy coated bars, galvanized steel bars, fibre reinforced polymer bars, corrosion inhibitors, and silica fume concrete are investigated and assessed in the this study.

4.3 TECHNICAL ASSESSMENT OF METHODS

4.3. 1 Electrochemical Methods

Electrochemical methods include cathodic protection and electrochemical chloride extraction. Both of these methods have the ability to stop corrosion in chloride contaminated concrete and are most often used as rehabilitation methods, although cathodic protection is also be used for structures (Berkeley and Pathmanaban, 1990).

The advantages and disadvantages of the electrochemical methods can be listed as follows (Orellan et al., 2004, von Baeckmann et al., 1997, Macknick et al., 1985):

Advantages

- Effective performance to stop corrosion
- Can be applied to prestressed concrete members as well

Disadvantages

- It may be difficult to achieve sufficient protection at locations where resistivity is high without generating hydrogen in areas of low resistance (Bennett and Schue, 1995)
- Any disconnection in circuit may result in non-sufficient protection.
- A continuous monitoring has to be applied.
- A regular technical inspection needs to be conducted.
- Any initial errors during the installation may cause failure of the system.

Cathodic protection can be divided into two separate procedures including sacrificial anode and impressed current (Bertolini et al., 2002, Page and Sergi, 2000, Fang et al., 2004) Table 4-1 presents comparison of the two methods.

Table 4-1 Technical comparison of two electrochemical techniques

Impressed Current	Sacrificial Anode
External power supply needed	External power supply is not required
Driving voltage can be varied	Fixed driving voltage
Current can be varied	Limited current
Can be designed for almost any current	Usually used where current requirements are small
Can be used in any level of resistivity	Usually used in low-resistivity electrolytes

4.3. 2 Epoxy-Coated (EC) Steel Reinforcement

Epoxy coatings of the reinforcing steel are generally prepared by one of the following methods (Brown, 2002):

- **Liquid Resin:** Liquid epoxy is commonly prepared by mixing stoichiometrically balanced proportions of a two-part system, epoxy resin and polyamine. The liquid epoxy is applied by brushing or spraying, or by immersing the bars to be coated. The former method is most appropriate for field dressing of observed damage on reinforcing bars prior to concrete placement. The liquid coatings commonly contain solvents that, upon evaporation, may result in pore formation within the cured coating. Shrinkage due to solvent loss and curing is also a concern with the use of liquid epoxy coatings (Salparanta, 1988).

- **Fusion-Bonded Powder:** The most commonly used fabrication method for EC involves fusion bonding of epoxy. In this method, the steel bar is cleaned by blasting with grit to a near-white finish to remove millimetre scale, rust and contaminates. The bar is then heated to the temperature required for the application of the epoxy powder, typically 230°C, and passed through an electrostatic spray that applies charged, dry epoxy powder to the steel. The epoxy melts flows and cures on the bars, which then are quenched, usually with a water spray bath (Seymour and Mark, 1990).

Epoxy coatings are effective in two ways, first by acting as a barrier, keeping the oxygen and chloride ions away from accessing the surface of the steel, and second by increasing the electrical resistance between adjacent steel locations (Clear, 1976).

Epoxy resins are thermosetting plastics that have good long-term durability when added to concrete and resistance to solvents, chemicals and water (Pike, 1973). However, epoxy based coatings are not impermeable to water (Neville and Lee, 1967). Epoxy coatings function in two ways, first by acting as a barrier, keeping away oxygen and chloride ions from contacting the surface of the steel, and second by increasing the electrical resistance between adjacent steel locations. Epoxy coatings reduce the magnitude of macro-cell currents, which are responsible for extensive deterioration when they develop in bridge decks. Since the protective ability of epoxy coatings depend on their ability to act as both a physical and electrical barrier, effective quality control measurements must be taken during coating of the bars and subsequent handling, shipping, storage and assembling of the bars (Clear et al., 1995).

As use of epoxy-coated reinforcement increased, some problems were revealed, such as cracking of the coating during bending and damage of the coating during shipping,

placement of the bars, and handling on construction site (Manning, 1996). New methods, such as bending the bars before coating, increasing the number of supports during shipping, padding the bundles, and using nylon slings for loading and unloading, were developed to overcome these problems (Virmani and Clemena, 1998).

The advantages and disadvantages can be expressed as follows:

Advantages:

- The higher quality of concrete and adequate cover, the better performance in severe environmental exposure conditions (Clear et al., 1995).
- Acting as a barrier to keep the aggressive species away from steel
- Decreasing the conductivity of adjacent steel bars in different locations

Disadvantages:

- Epoxy coatings lose their bond (adhesion) to steel reinforcement when exposed to moisture condition (Singh and Ghosh, 2005, Smith and Virmani, 1996).
- The defects (pinholes) directly affect the electrical resistivity of the reinforcement (Manning, 1996)
- Most reported problems with epoxy-coated reinforcement have occurred in the environments where the concrete is continuously wet, and oxygen is still available (splash zones on piers, or areas of high humidity) (Weyers et al., 1997). Often these environments have a high average temperature which accelerates the damage.

4.3. 3 Galvanized Reinforcement (zinc-coated or sacrificial coating)

Zinc-coated or galvanized bars are produced by a hot-dip process. This process consists of cleaning the steel bars by pickling and then immersing them in the molten zinc. Typically, in accordance with ASTM A767, galvanized bars are placed in a chromate bath after coating to passivate the zinc surface from reacting with the hydroxide in fresh cement paste. Similar to steel, zinc has corrosion products which occupy additional volume and as a result can cause cracking of the concrete. An advantage of galvanized reinforcement can

be explained as; when zinc corrodes sacrificially, a hydrated oxide [$Zn(OH)_2$] is formed on the surface that acts as an electrical insulator. This insulator is thought to form a barrier layer at active corrosion sites that will prevent further corrosion occurrence (Macias and Andrade, 1987).

The cost of galvanizing is significant relative to the base price of the reinforcing steel. Depending on the bar dimensions (length and diameter), the form of the product (straight lengths or pre-bent components) and the location of the plant, the cost of galvanizing may vary from about $180 to $500 per tonne. Assuming an average cost of $300 per tonne, the cost of galvanizing represents about a 50% surcharge on the cost of the steel (Yeomans, 1987).

The advantages and disadvantages of this method can be illustrated as follows:

Advantages:

- Since zinc has a higher chloride threshold level than steel, the initiation time of corrosion in galvanized bars may occur with delay (Manning et al., 1982, Darwin et al., 2009).
- This method increases the service life of structure by five years in addition to the typical 10-15 years that corrosion damage occurs on the typical unprotected reinforcing steel (Gowripalan and Mohamed, 1998).

Disadvantages:

- Results from laboratory and field studied on galvanized reinforcement are disagree (Virmani and Clemena, 1998). Laboratory studies with aqueous solutions have shown that zinc has a higher chloride concentration level than steel at the onset of corrosion. This higher threshold helps to explain why galvanizing can delay the onset of corrosion in outdoor specimens. There is, however, an indication from these outdoor specimens that once corrosion begins on galvanized bars, corrosion-induced distress in the concrete occurs faster than for specimens containing black bars. It is difficult to use laboratory performance to predict service life in the field because of a lack of standardization in laboratory tests (Darwin et al., 2009).

- Rapid corrosion in concrete structures comprising interconnected black and galvanized reinforcement exposed to marine environment.
- If corrosion begins, corrosion-induced distress in the concrete occurs faster than uncoated steel bars due to pitting corrosion (Virmani and Clemena, 1998).
- Increasing the life-time cost of structure considerably (Manning et al., 1982)

4.3. 4 Fibre Reinforced Polymer Reinforcement (FRP)

The use of Fibre Reinforced Polymers (FRPs) as reinforcement in RC elements is a viable option to prevent corrosion effects that reduce the service life of members employing steel reinforcement. FRP bars generally made of longitudinal fibers and a polymeric resin, namely Polyester and Vinylester. The fibers provide strength and stiffness while the resin matrix binds and protects the fibers from damage, and transfer stresses between the fibers (Ceroni et al., 2006). The mechanical properties of the FRP bars strongly depend on the type and volume of fibers, while the polymeric resin plays an important role in the transverse direction. Recently, many studies have been carried out on durability of FRP bars (Balázs and Borosnyói, 2001). However, there are still many aspects to be investigated to provide reliable design guideline to be implemented in codes of practice.

Since the various types of polymeric fibre bars available in the market have been made with different materials, then different long-term behaviour under different environment conditions are can be expected. Three types of FRP bars which mainly have been used in concrete are Carbon Fiber Reinforced Polymer (CFRP), Glass Fiber Reinforced Polymer (GFRP), and Aramid Fiber Reinforced Polymer (AFRP). Durability of concrete members reinforced with FRP bars depends on the effect of environment on the composite material, cracking, and concrete-bar bond (Robert et al., 2009).

Unfortunately durability of FRP bars is not straightforward subject; it tends to be more complex than corrosion of steel reinforcement, because degradation of the material could depend both on resin and fibres and their interface bond behaviour. Furthermore, the types of bars available on the market are various and the commercial products are continuously changed. Different fibres are characterized by different behaviour under high temperature, environmental effects and long-term phenomena. In addition, concrete could be an

unfavourable environment due to alkali and moisture absorption (Ceroni et al., 2006). The durability of FRP materials has not been yet assessed thoroughly and hence reliable design rules for RC structures are still lacking (Steckel et al., 1998, Bank et al., 1995).

Beside the cost issues, the most significant technical obstacle, preventing the extended use of FRP materials in civil engineering, is lack of long-term and durability performance data comparable to that available in traditional construction materials (Micelli and Nanni, 2004).

Over the past decade, many investigations have been carried out on the behaviour of concrete members reinforced or strengthened by FRP materials subjected to applied mechanical loads. FRP possesses not only high tensile strength but also anti-seismic behaviour, electromagnetic neutrality, versatility, excellent fatigue behaviour, and ease of installation.

The difference in thermal expansion in transverse direction may cause significant splitting stresses in concrete around the bars under temperature increase, or separation of the bars from the concrete under temperature decrease (Elbadry et al., 2000). This may affect the bond between the FRP reinforcement and the surrounding concrete and cause cracking of the concrete cover around the reinforcement (Galati et al., 2006). Abdalla's investigation (Abdalla, 2006) showed that the high transverse coefficient of thermal expansion of the GFRP bars creates bursting tensile stresses in the concrete surrounding the bars at high temperatures. Also concrete specimens reinforced with GFRP exhibited wide cracks around the bars at high temperatures and these cracks in the vicinity of the bars resulted in weakening of bond between the concrete and GFRP. But the thermal behaviour of CFRP is similar to that of steel and better than GFRP. Abdalla concluded that a concrete cover ranging between $1.5d_b$ and $2d_b$can satisfy both the loading and temperature requirements for beams in hot climates.

There exist two elements that compose a fibre reinforced polymer bar as following:

- Fibrous materials such as carbon, glass, and aramid;
- resinous synthetic polymer as adhesive and coupling agent to enhance the bond between the other two components (Phong, 1997, Bakis et al., 2002).

Advantages:

- FRPs present a much higher corrosion resistance compared to steel reinforcement.
- Deformed FRPs show similar bond strength to that of deformed steel bars (Cosenza et al., 1997).

Disadvantages:

- Water and salt solutions reduce the life of the structures exposed to long-term fatigue loading in glass fibres reinforcement (Kootsookos and Mouritz, 2004).
- Freeze-thaw cycles in 2% sodium chloride solution result in decreasing the dynamic modulus, flexural modulus, flexural strength, and toughness of the composite (Liao et al., 1997)
- Carbon fibre exhibits higher fatigue behaviour, high tensile modulus, and lower relaxation; but also has a low tensile strain in cyclic loadings.
- Temperature affects the bond strength between FRP bars and concrete. Cold or hot environmental conditions can weaken the bond strength between FRP bars and concrete dramatically.
- Durability of the RC elements with FRP bars is a complex phenomenon due to variety of products available in the market in terms of constituents (resin and fibres) and surface treatment.
- The main weakness of FRPs to environmental agents (water, alkali, salt solution) is related to degradation of resin that protect the fibres.

4.3. 5 Corrosion Inhibitors (CI)

Corrosion inhibitors are chemical additives that can slow down or prevent corrosion of reinforcing steel in the concrete (Söylev and Richardson, 2008). Corrosion inhibitors are typically divided into three categories: anodic inhibitors, cathodic inhibitors, and organic inhibitors. Currently, there are only a few commercially available corrosion inhibiting admixtures. The most commonly used example of corrosion inhibitors are calcium nitrite

(Trépanier et al., 2001) which contains 30 percent calcium nitrite and 70 percent water, mixture of amines and esters, and mixture of alcohol and amine. Calcium nitrite raises the corrosion threshold at the reinforcement surface rather than blocking the chloride ions from entering the concrete and has shown better performance compared to two other inhibitors (PYC, 1998).

Advantages:

- Versatility and cost effect
- Corrosion inhibitor such as calcium nitrite can extend service life of the concrete structures (Berke and Hicks, 2004).
- The effectiveness of the protection is dependent to the ratio of chloride-to-nitrite ions, which should be kept below 1.0 for the life of structure. Accordingly, enough amount of the calcium nitrite should be added to the concrete mix to maintain the ratio of chloride –to-nitrite ions less than 1.0 during service life of the structure (Nmai, 2004) .

Disadvantages:

- After corrosion initiation, their effectiveness is less significant (Söylev and Richardson, 2008).
- In cracked concrete, which usually concrete cracks under the service loads, significant localised corrosion was noted after only one year of marine exposure (Kondratova et al., 2003).
- Calcium nitrite is water soluble and may leach out of the concrete cover over time.
- Using CI not an independent method, since the quality of the concrete plays an important role in the effectiveness of this method.
- It acts as a set accelerator. Therefore, a set retarder must be added to the concrete mix to neutralize the acceleration of the calcium nitrite (Sherman et al., 1993).
- The data regarding the long-term performance of inhibitors are very limited.

4.4 COST ANALYSES OF THE CORROSION PREVENTIVE METHODS

To compare the cost of different discussed corrosion preventive methods, the Present Value (PV) cost analysis method was used. PV comprises the initial cost of construction and installation; plus maintenance, repair, and operation cost for each technique. The assumptions considered in this assessment are as follows (Kepler et al., 2000):

- 40 years is considered in this investigation.
- After 25 years, repair or replacement in some methods should be conducted on structure.
- The annual interest rate is assumed 4% based on average of several annual data.
- Inflation is excluded in these analyses. Because, the fluctuations of inflation in different countries are so different and cannot be considered in a general estimation.

For cost analysis in this study, a typical conventional reinforced concrete bridge deck with the following assumptions is investigated:

- Thickness of 250 mm,
- Concrete cover 50 mm, and
- N20 galvanized reinforcing bars.
- The average density of reinforcement is 36 kg/m^2 [0.25 m^3/m^2 × 143 kg/m^3 = 35.75 kg/m^2].

The cost for this deck with galvanized reinforcement is calculated by converting the in-place cost of concrete for superstructures in Australia in 2011.

Step 1: The concrete, formwork, and labor costs: 0.250 m^3/m^2 × \$600 /m^3 = \$150 /m^2

Step 2: The reinforcement cost with galvanized bar: \$11 /kg × 36 kg/m^2 = \$396 /m^2

Therefore, the initial cost for reinforced concrete deck will be: P_0 = \$546 /m^2

McCrum and Arnold (McCrum and Arnold, 1993) stated that corrosion damage in unprotected steel reinforcement usually appears after 10-15 years of service life.

Furthermore, Bentur et al. (Bentur et al., 1997) estimated that a deck with 50mm of cover over black steel would need repair after 20 years.

According to McCrum and Arnold (1993), galvanized reinforcement can enhance five years to the time to corrosion damage compared to black steel. Therefore, in this study the time to repair for the typical deck with galvanized reinforcement is assumed to be 25 years (see Figure 4.1).

Repair cost can be determined as follows:

- Full depth repair cost including concrete removal (cutting and cleaning) cost: \$361/m^2
- Partial depth repair cost: \$246 /m^2
- Machine preparation of area: \$35 /m^2
- Overlay execution (by silica fume): \$86 /m^2

The total cost of repair (including 10% of full depth and 25% of partial depth repair) is presented in Table 4-2.

Table 4-2 Total cost of the partial repair of the typical bridge deck

Item Description	Cost (\$/m2)
Full depth repair	361*0.1=36
Partial depth repair	246*0.25=61
Machine preparation of area	35
Overlay execution (silica fume)	86
Incidental cost	90
Total repair cost	308

Consequently, the cash flow of the initial cost (P_0 = \$546/m^2) and repair cost after 25 years of the service life (\$308/m^2) of a reinforced concrete deck using galvanized steel reinforcement are presented in Figure 4-1.

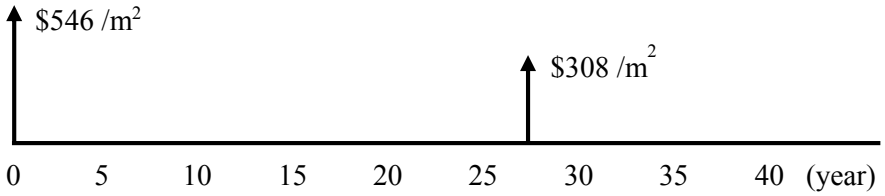

Figure 4-1 Cash flow of cost for reinforced concrete deck using galvanized steel

The present value of the total cost related to reinforced concrete is the summation of the initial cost, repair/replace cost; and maintenance and operation costs. To estimate the repair or replacement cost, Equation 4.1 is used:

$$P_r = F/(1+i)^n \tag{4.1}$$

where, P_r is the present value of the structure, F is cost of repair after n years, i is annual interest rate, and n is time to repair (here n = 25 years).

To calculate the present value of the annual Maintenance and Operation (M/O) costs Equation 4.2 is used:

$$P_{M/O} = A * \frac{(1+i)^n - 1}{i * (1+i)^n} \tag{4.2}$$

where, A is the uniform annual maintenance and operation cost and n the design life time of a structures (here n=40 years)

The present value of costs (P) for galvanized reinforced concrete can be estimated as follows:

$$P_r = 308/(1+0.04)^{25} = \$116/m^2 \tag{4.3}$$

$$P = P_0 + P_r = 546 + 116 = \$662/m^2 \tag{4.4}$$

The present values of the other methods have been determined by the same procedure. Only electrochemical prevention methods (Cathodic Protection) include maintenance and operational (M/O) cost. The estimated cost of methods for a 40-year time interval are presented as follows:

- Black Steel (as reference): \$546/m^2
- Epoxy-Coated Steel Reinforcement: \$521/m^2
- Galvanised Reinforcement: \$662/m^2
- Corrosion Inhibitor: \$573/m^2
- Silica Fume Concrete: \$695/m^2
- Cathodic Protection (SA): \$976/m^2
- Cathodic Protection (TI): \$853/m^2
- Cathodic Protection (ZI): \$843/m^2

The cost analysis revealed that the Cathodic Protection is the most expensive method of corrosion protection. Although, they have shown adequate performance.

To specify of a method, both technical and financial advantages and limitations of the method should be considered.

4.5 DATABASE ANALYSIS OF THE CHLORIDE DIFFUSION COEFFICINET IN CONCRETE

As mentioned earlier in Chapter 3, almost all proposed mathematical models have considered a constant value for the chloride diffusion coefficient (D) in their models. However, the experimental test results prove that the chloride diffusion coefficient is a time-dependent factor.

Mangat and Molloy (Mangat and Molloy, 1994a) have proposed the following mathematical relationship to determine the diffusion coefficient as a time-dependent parameter. In this model, the W/C ratio assumed to be the only influencing factor on the chloride diffusion coefficient.

$$D_i^* = D_i \times t^{\left[0.6-2.5\left(\frac{w}{c}\right)\right]} \tag{4.5}$$

In this study, the most significant available experimental test results in the literature were employed to compare with the data determined by Mangat and Molloy (1994b) proposed model. In this investigation, the chloride diffusion coefficient values extracted from literature for each specific W/C ratio were compared to the value determined by mathematical model predictions with the same input data. The experimental test results have been summarized in Table 4-3.

Table 4-3 Chloride diffusion coefficient database

Reference	W/C	Age	Mix Design			D
			Cement	Water	Aggregates	(m^2/s) *10^{-12}
(Polder, 1995)	0.4	1 w 4 w 14 w	420	168	NG	3 2 1
(Zhang and Gjørv, 1994)	0.5	2 m	330	165	2066 1894	3.26 1.56
(Luping and Nilsson, 1992)	0.7	1 d 3 d 7 d 28 d 90 d	270	189	1922	45.6 26.95 21.1 14.5 15.3
(Luping and Nilsson, 1992)	0.32	1 d 3 d 7 d 28 d 90 d 180 d	522	167	1750	7.39 6.22 4.93 3.22 1.79 1.74
(Kanaya et al., 1998)	0.6	1 y 3 y 5 y	275	165	1867	3.2 1.0 0.6
(Pedersen and Arntsen, 1998)	0.4	3 m 27 m	420	168	1853	5.5 1.7
(Pedersen and Arntsen, 1998)	0.45	3 m 27 m	420	189	1807	6.0 3.3
		3 m 27 m	360	162	1921	6.2 2.1
(Mangat and Molloy, 1994b)	0.58	28 d 90 d 270 d	530	307	1309	52.3 23.8 10.0
(Luping and Nilsson, 1993b)	0.54	1 w 4 w 14 w	300	162	NG	4.0 3.0 2.5
(Luping and Nilsson, 1993b)	0.4 0.6 0.8	3 m	690 605 540	276 363 432	1380 1210 1080	1.1 2.6 6.4

Reference	W/C	Age	Cement	Water	Aggregates	D $\times 10^{-12} m^2/s$
(Bamforth, 1993)	0.66	28 d	288	190	1900	2.07
	0.62		275	170.5	1940	1.49
	0.6		315	189	1835	1.77
(Collepardi et al., 1972)	0.5	3 m	400	200	1800	1.65
	0.6		384	230.4	1728	3.24
(Diab et al., 1988)	0.6	28 d	544	326.4	1360	8.0
	0.5		644	322	1288	5.5
	0.4		925	370	925	2.8
(Hooton et al., 1997)	0.35	28 d	380	133	1924	4.7
	0.4		374	149	1840	5.0
	0.45		369	165	1770	7.1
(Dhir et al., 1990)	0.825	28 d	200	165	2035	8.5
	0.822		225	185	1960	8.2
	0.830		235	195	1925	9.0
	0.579		285	165	1950	2.8
	0.578		320	185	1865	2.6
	0.574		340	195	1820	2.9
	0.377		385	145	1850	1.0
	0.384		430	165	1755	0.9
	0.429		455	195	1750	1.0

The output of database analysis are plotted and presented in Figure 4-2 to Figure 4-7.

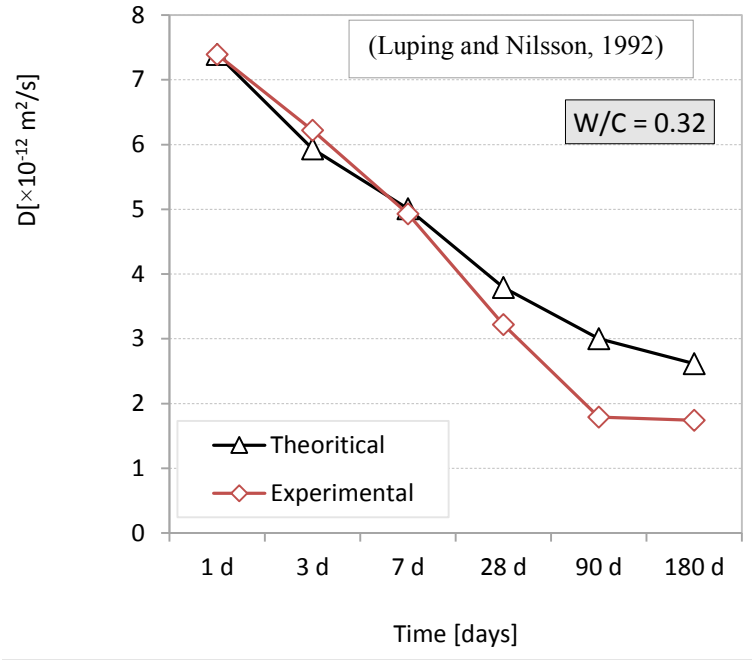

Figure 4-2 Chloride diffusion coefficient vs. time for concrete with W/C = 0.32

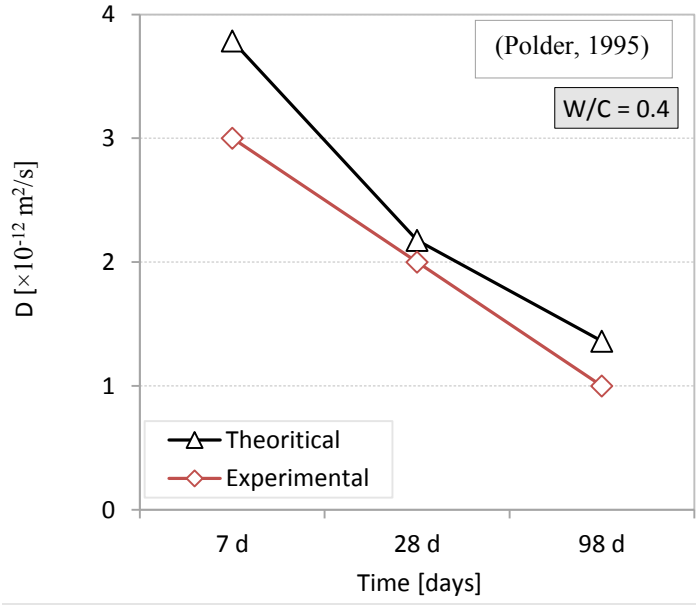

Figure 4-3 Chloride diffusion coefficient vs. time for concrete with W/C = 0.4

In Figures 4.2 and 4.3, in spite of the close trend between experimental results and theoretical prediction, the gap between two methods is observed. This gap for the W/C of 0.32 and 0.4 is approximately 1×10^{-12} m^2/s and $0.5\times10^{-12}m^2/s$, respectively. In two Figures

4.2 and 4.3, the value of chloride diffusion coefficient determined by mathematical model is greater than experimental one which shows a safer mode for service life determination.

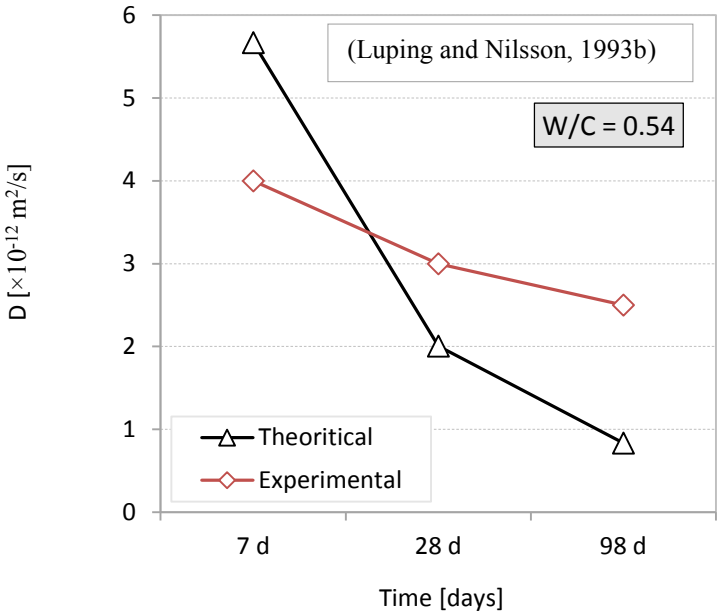

Figure 4-4 Chloride diffusion coefficient vs. time for concrete with W/C = 0.54

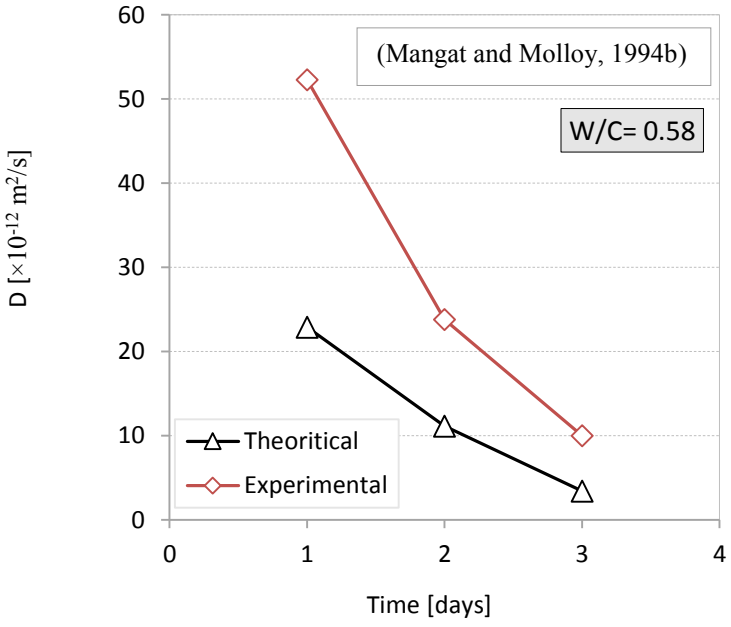

Figure 4-5 Chloride diffusion coefficient vs. time for concrete with W/C = 0.58

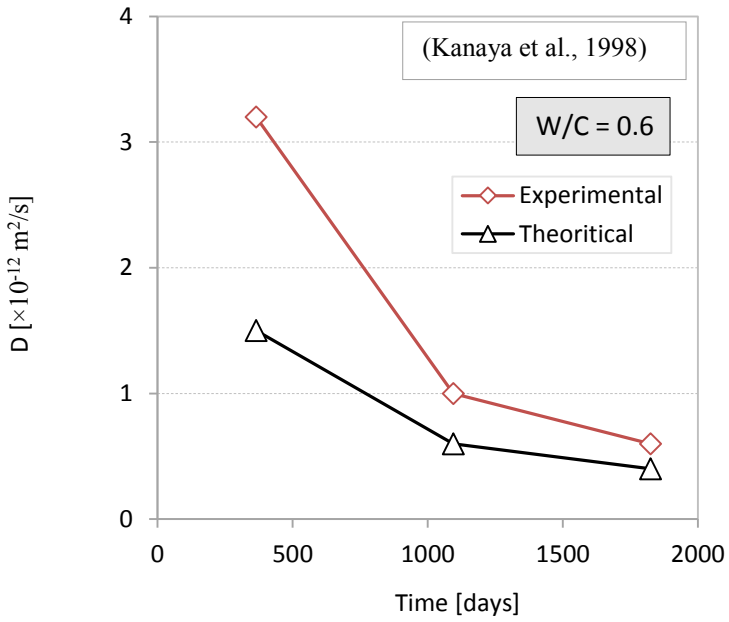

Figure 4-6 Chloride diffusion coefficient vs. time for concrete with W/C = 0.6

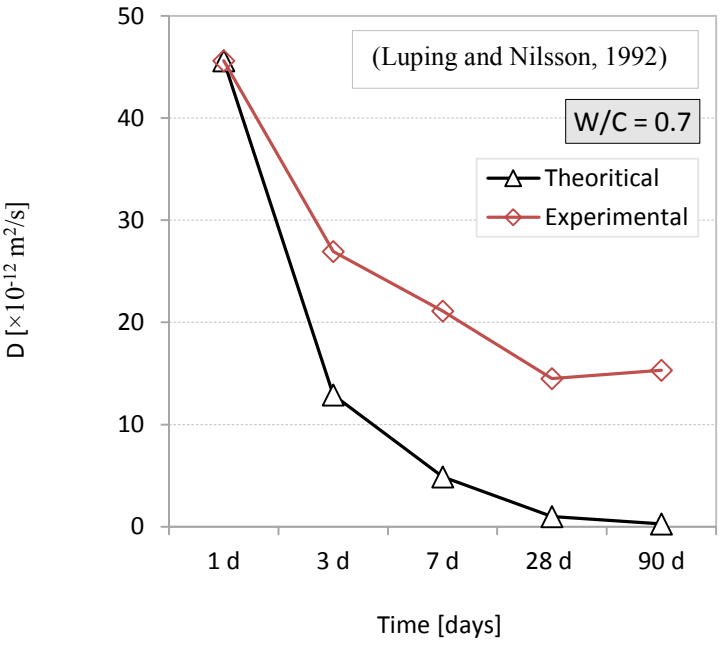

Figure 4-7 Chloride diffusion coefficient vs. time for concrete with W/C = 0.7

With increasing the W/C ratio, the gap between experimental and mathematical model increases. In addition, mathematical model results show a lower chloride diffusion coefficient values compared to experimental results. In this case, the predicted service life

based on mathematical output indicates longer service life than the actual service life of the structure.

Moreover, a review on the experimental results indicates that in some cases with reducing the W/C ratio, diffusion coefficient increases, e.g. in Figure 4-2 with W/C of 0.32 and Figure 4-3 with W/C of 0.4, D has been decreased which theoretically should be increased. This phenomenon proves that there are other influencing factors on diffusion coefficient which has to be taken into account such as proportion of coarse aggregate. In order to obtain a precise mathematical model these factors should be considered as well.

4.6 SUMMARY

4.6. 1 Assessment of the Corrosion Preventive Methods

Due to excessive impact of the premature deterioration of RC structures on environment, life-time cost of the structure, and safety issues; numerous studies and investigations have been conducted to extend the service life of RC structures.

It has been confirmed that the domain process in shortening the service life of RC structures is the chloride-induced corrosion of the steel reinforcement. So, many efforts have been focused to develop corrosion preventive methods of reinforced concrete. In this chapter, the most commonly used methods, in terms of technical performance and cost impact such as electrochemical protective techniques, epoxy-coated bars, galvanized steel bars, fibre reinforced polymer bars, and corrosion inhibitors were investigated.

Most of these methods such as epoxy coating, galvanized steel, fibre reinforced polymer, and electrochemical protections assume that aggressive liquids and gases can diffuse into the concrete. Based on this assumption, they have suggested the corrosion preventive methods by increasing the chloride threshold of steel bars, increasing the resistivity in adjacent bars, and electrochemical excitation.

Following the abovementioned techniques, the jeopardy and risk of sulfate attack still exists. In such cases, the chemical reactions between sulfate and concrete constituents

(C_3A) will result disruptive expansion by forming ettringite and gypsum leading to cracking and deterioration of concrete cover; consequently durability problems.

The technical assessment of the preventive methods in terms of difficulty, accuracy and possibility of the method, and disadvantages are presented in Table 4-4.

Table 4-4 The summary of technical assessment of the methods

Protection method	difficulty rate of execution	Possibility of service life prediction	Generated problems
EC	Moderate	Low	Pin holes, losing bond with bars
GR	Moderate	Moderate	High corrosion rate after the onset of corrosion
CP(SA)	Very high	High	Regularly monitoring and maintenance, insufficient protection if concrete resistivity is not uniform
CP(TI)	Very high	High	Regularly monitoring and maintenance, insufficient protection if concrete resistivity is not uniform
CP(ZI)	Very high	High	Regularly monitoring and maintenance, insufficient protection if concrete resistivity is not uniform
CI	Low	Low	Leaching out, acceleration in cement setting time
SFC*	Moderate	Moderate	High density of cracks and number of delamination

*SFC: Silica fume concrete

In economic evaluation of the cost implementation, maintenance and repair cost of the methods for a life span of 40 years have been determined and summarised in Table 4-5.

Table 4-5 Summary of the estimated cost of the methods for 40 years of life span

Protection Method	Initial Costs ($/m^2)	Repair Cost ($/m^2)	M/O Cost ($/Year/m^2)	Total Cost for 40 yrs ($/m^2)
BS	375	308	---	546
EC	405	308	---	521
GR	546	308	---	662
CP(SA)	650	662	1.2	976
CP(TI)	630	645	1.2	853
CP(ZI)	624	632	1.2	843
CI	435	762	---	573
SFC	600	308	---	695

Figure 4-8 Summary of cost analysis for various corrosion preventive methods illustrates the comparison of the cost of each corrosion preventive method for 40 years of life span.

Some of these methods such as corrosion inhibitor (calcium nitrate) and epoxy coated bars have shown a cost impact approximately similar to no protection reinforced concrete. However, these methods have not indicated sufficient performance to extend the service life of structures. Furthermore, these techniques are confronted to long-term physical and chemical degradation. Some of these preventive methods such as electrochemical techniques have an enormous cost effect and also difficulties in installation process although, they have shown adequate performance.

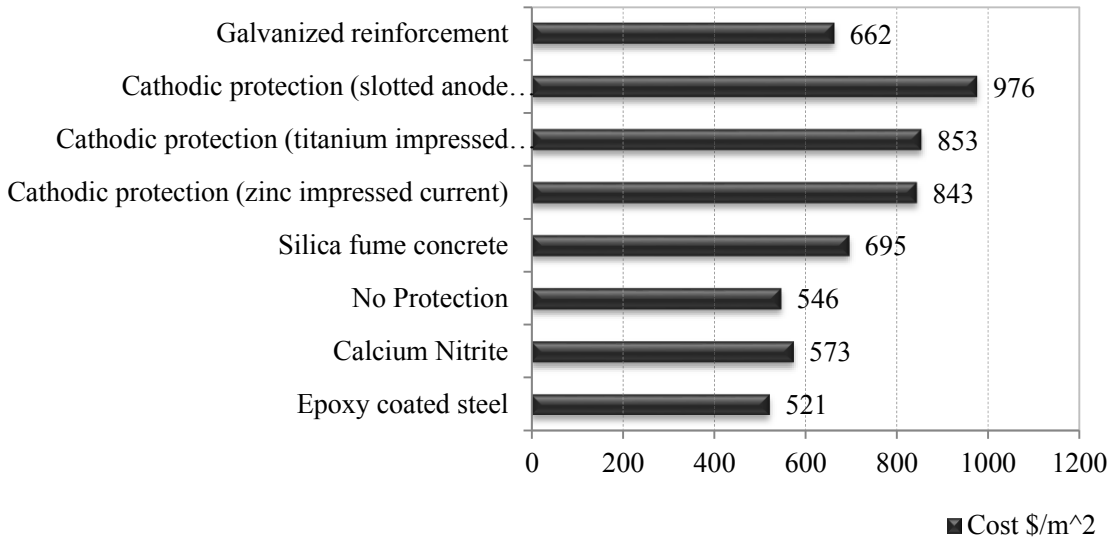

Figure 4-8 Summary of cost analysis for various corrosion preventive methods

As shown in Figure 4-8, it can be concluded that passive methods of corrosion protection are reasonably more cost effective than active methods.

From the foregoing it is apparent that the cost of repair and rehabilitation can be significantly higher than the cost of prevention during the design stage. Therefore, it is essential that every effort is made at the design stage to prevent corrosion occurring during the life of the structure. However, this is not easy to achieve. Surface treatments have shown good protection against chloride ingress and they are convenient to use and relatively inexpensive. However, they must be maintained and replaced, in some cases every 2 to 3 years, to remain effective. On the other hand, their effect prolongs only the period of corrosion initiation and once corrosion has begun, they cannot stop chloride-induced corrosion.

In the case of corrosion inhibitors, there are some concerns related to their effectiveness on chloride level and corrosion rate, the correct dosage level and their longevity. Published results are sometimes contradictory on the corrosion behaviour of steel in the presence of corrosion inhibitors. In addition, there are some doubts about the ability of migrating corrosion inhibitors to penetrate into concrete and reach the surface of the rebar, particularly in good quality concrete.

The poor performance of epoxy coated reinforcement has been reported in harsh environments such as bridge structures located in coastal enlivenments. The main concern is about the adhesion of the coating to the steel, either the poor initial adhesion or the loss of adhesion when the structure is exposed to wetting.

Stainless steels are more expensive and their use can have a significant effect on the cost of construction. In fact, their use has generally been limited to the more vulnerable parts of structures exposed to chloride environments such as joints of bridges or the splash zone of marine structures.

Cathodic prevention is a powerful way of stopping reinforcement corrosion provided the system remains active but it is relatively expensive to install and the cost of maintenance can also be high. Nevertheless, the cost of CP is significantly lower than the cost of repair and its early application is far more cost effective.

Concrete may be designed, in terms of quality and cover depth, in a way that provides protection against corrosion. However, the difficulty is firstly to estimate the required cover depth accurately and secondly to achieve that cover depth on site. In addition, concrete cover cannot exceed certain limits due to the risk of cracking. When the concrete cover does not provide sufficient protection, other protection methods such as cathodic protection may be adopted.

The recommendations in design codes for durable concrete (in terms of concrete grade and cover) have failed in some conditions of environmental exposure, leading to unacceptable levels of corrosion after a short period of time. A wet/dry environment coupled with high levels of chloride is one such case where this has occurred.

As a result, there is a need to determine the depth of chloride penetration appropriate to this exposure condition or propose alternative protection methods, if this is not possible. To estimate the depth of chloride penetration and thus the required cover depth, it is essential to understand how chlorides ions are transported through concrete.

4.6. 2 Analysis of the Chloride Diffusion Coefficient Database

One of the most important factors in predicting the service life of RC structures is chloride diffusion rate or chloride diffusion coefficient into the concrete. Accurate determination of chloride diffusion coefficient leads to precise estimation of the service life of the structures. As discussed in chapter 2, although it is proved that the chloride diffusion coefficient is a time-dependent parameter, there are limited mathematical models that express and predict the D. The most significant model has been proposed by Mangat and Molloy (Mangat and Molloy, 1994b).

In this chapter the most significant experimental results in regard with chloride diffusion coefficient from literature were compared to mathematical model prediction.

In Mangat and Molloy proposed model, only water cement ratio of the concrete mix has been considered as a variable because W/C is the most effective factor in formation of the micro-structure of the concrete. The data analysis conducted in this investigation showed that in spite of good correlation between values estimated by the Mangat and Molloy's model and the experimental data, still there is a gap between the analytical and experimental results.

Chloride diffusion coefficient is a micro-structural characteristic of the concrete. Therefore, the concrete mix proportions have a great influence in the value of this parameter. If the effects of other influencing factors, besides W/C ratio, such as proportion of coarse aggregate, cement content, and cement type are considered in the model, the analytical results can generate more accurate data to predict the service life of the structure.

CHAPTER 5

POLYMER-CONCRETE COMPOSITES

CHAPTER 5. POLYMER-CONCRETE COMPOSITES

5.1 INTRODUCTION

Although, conventional concrete has shown high compressive strength and modulus of elasticity, it has some imperfections such as low tensile strength, low ductility, and low strain capacity. In addition, concrete is a porous media which includes different types of pores and capillary tracts as well as micro and macro-cracks. To improve mechanical properties and durability performance of the concrete, polymer-concrete composites can be one of the effective methods. (Ohama, 1998).

Composite materials are produced by combining two or more distinct phases and materials to achieve properties far superior than each of the base materials. The properties of the composites not only depend on the properties of each individual material, but also on the interfacial zone properties of them (Li, 2003).

This chapter briefly reviews the properties of polymer-concrete composites through the available literature. This investigation concentrates on synthetic fibres and especially on polypropylene (PP) fibres and also, dispersion aqueous polymers especially styrene butadiene rubber (Latex). In addition, the microstructure and physical-mechanical properties of the polymer-concrete composites are studied.

5.2 SYNTHETIC FIBRES (POLYMER)

A synthetic fibre can be described as a flexible and macroscopically homogeneous body with a high length (l) to diameter (d) ratio (aspect ratio = l/d) which has a small cross-sectional area. (Brandt, 2008).

Synthetic fibres have become more attractive in recent years as secondary reinforcements for concrete structures materials. They can provide effective and relatively inexpensive reinforcement for the concrete. Fibres types that have been incorporated into the cement matrix are polyethylene (PE), polypropylene (PP), acrylics (PAN), poly vinyl alcohol (PVA), polyamides (PA), aramid, polyester (PES), and carbon. The properties of synthetic fibres vary widely with respect to the modulus of elasticity which is an important characteristic when fibres are used for producing structural composites materials (Zheng and Feldman, 1995).

Synthetic (polymer) fibres are increasingly being used to improve the mechanical properties of cementitious materials. Some fibres, such as polypropylene, are used very extensively, and many fibres are available that have been formulated and produced specifically for reinforcement of mortars and concrete (Brandt, 2008).

For cementitious materials, which the modulus of elasticity ranges from about 15 GPa to 40 GPa, this condition is difficult to meet with most synthetic fibres. Therefore, some high tenacity fibres have been developed for the concrete reinforcement, where the term “high tenacity” refers to fibres with a high modulus of elasticity, accompanied by high strength. However, both theoretical and applied research have confirmed that even with low modulus of fibres, considerable improvements can be obtained with respect to the strain capacity, toughness, impact resistance and crack control of the fibre reinforced concrete (FRC) composites (de LHONEUX et al., 2002).

The pioneering work on synthetic fibres emphasized the need to overcome disadvantages due to the low modulus of elasticity and poor bonding with the matrix. The latter was in particular a problem with many of the early synthetic fibres, due to their chemical composition and surface properties. Advances in this field, particularly with polypropylene

fibres, become feasible when it was recognized that fibres with special properties had to be developed for cement and concrete applications. (Bentur and Mindess, 2006).

In some applications, the poor tensile strength of concrete can be enhanced by combining concrete with small diameter fibres like synthetic fibres. Most of the current applications with fibre reinforced concrete involve the use of fibres ranging around 1% by volume of concrete. It is usually assumed that the fibres do not influence the tensile strength of the matrix, instead after the matrix has been cracked the fibres contribute by bridging the crack (Brandt, 2008).

Among the various kinds of composites, polypropylene fibres have become more and more important in engineering applications because of their relatively lower cost, light weight, and good corrosion resistance. Successful reinforcement of these composite materials is only achieved by obtaining sufficient load transfer between fibre and matrix (Kakooei et al., 2012).

Table 5-1 presents some physical and mechanical properties of the synthetic fibres.

Table 5-1 Physical and mechanical properties of several fibres

Fibre	Diameter (μm)	Specific gravity (g/cm^3)	Modulus of Elasticity (GPa)	Tensile Strength (GPa)	Elongation at Break (%)
Polypropylene	20-400	0.9-0.95	3.5-10	0.45-75	15-25
Aramid	10-12	1.44	63-120	2.3-3.5	2-4.5
Carbon	8-9	1.6-1.7	230-380	2.5-4.0	0.5-1.5
Nylon	23-400	1.14	4.1-5.2	0.75-1.0	16.0-20.0
Acrylic	18	1.18	14-19.5	0.4-1.0	3
Polyethylene	25-1000	0.92-0.96	5	0.08-0.6	3-100
Cement Matrix (to compare)	-	1.5-2.5	10-45	0.003-0.007	0.02

5.2. 1 Polypropylene Fibres

Polypropylene (PP) is a relatively modern product with a large molecule built up by a repetition of small simple chemical units until a polypropylene chain is formed. Monofilament PP fibres which have been used in this research are produced from 100% virgin homo-polymer polypropylene.

PP fibres are made of high molecular weight isotactic polypropylene. They can be made in three different geometries including monofilaments, film, and fibrillated. All three forms have been used successfully for mortars and concrete reinforcement. Monofilament polypropylene fibres are produced by an extrusion process, in which the polypropylene resin is hot drawn through a die of circular cross section. A number of continuous filaments are produced at one time, and are then cut to the appropriate lengths (Bentur and Mindess, 2006).

PP fibres as a secondary reinforcement are currently being used extensively throughout the world in all types of the concrete structures. Firstly, they have been proven as an effective method of controlling troublesome shrinkage in concrete. Secondly, after curing, the presence of fibres increases concrete long-term durability and toughness. PP fibres are true monofilament that totally disperses into the concrete mixing when added to the concrete (Brown et al., 2002).

PP fibers have several unique properties that make them especially suited for using in the concrete. They are chemically inert and stable in the alkaline environment of concrete with a relatively high melting point and low cost. They do not absorb water due to a hydrophobic surface which prevents any chemical adhesion with the concrete matrix; they are non-corrosive and compatible with all types of cements and admixtures. They do not affect concrete mix design, pumpability, placing, setting time and finishing surface characteristics (Geleji et al., 1977).

Polypropylene fibres are produced from homo-polymer polypropylene resin in a variety of shapes and sizes, and with differing properties. The main advantages of these fibers are their alkali resistance, relatively high melting point (165°C) and the low price of material. Their disadvantages are poor fire resistance, sensitivity to sun light, and a low modulus of elasticity (3GPa to 8 GPa). These apparent disadvantages are not necessarily critical. Embedment in the matrix provides a protective cover, helping to minimize sensitivity to fire and other environment effects (Larbi and Polder, 2007).

The modulus of elasticity of PP fibres is in the range of 3 GPa to 8 GPa, and the tensile strength as about 140 MPa to 690 MPa. The monofilament PP fibres can be produced in different diameters, ranging from about 25 μm to 0.5 mm. The chemical structure of PP fibre makes it “hydrophobic” with respect to the cementitious matrix reducing the

possibility of its chemical reaction either with the chemical compound produced in hydration process. PP fibres have some unique properties that make them suitable for incorporation into concrete matrices. They have a relatively high melting point with low cost raw materials (Alhozaimy et al., 1996).

5.2. 2 Effects of Polypropylene Fibres in FRC

The effectiveness of PP fibres in the cement matrix is to enhance the mechanical performance of the brittle matrix and it is dependent to a large extent on the fibre-matrix interactions.

The main role of short disperse fibres in the concrete is to control the surface crack opening and propagation. PP fibres at small amount of about 0.1% by volume of concrete are effective in suppressing most of the cracking and reducing its extent. Figure 5-1 represents the effect of PP fibres content (V_f) and length on plastic shrinkage cracking (Soroushian and Faiz Mirza, 1993).

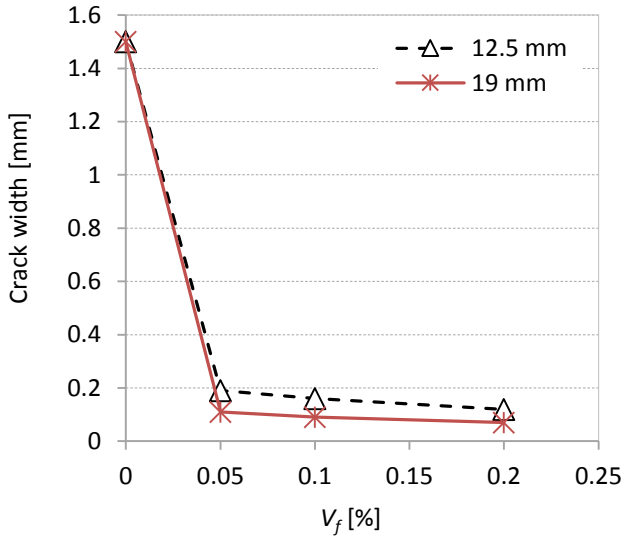

Figure 5-1 Effect of PP fibers content and length on plastic shrinkage cracking (Soroushian and Faiz Mirza, 1993)

Walton and Majumdar (Walton and Majumdar, 1975) determined the average bond values for monofilament fibers in the range of 0.34 MPa to 0.48 MPa after debonding, and 0.70

MPa to 1.23 MPa at the maximum. These values are not sensitive to environmental conditions or the W/C ratio of the matrix.

PP fibres have a significant effect on the rheological properties of fresh concrete. Workability tests showed that the slump of PP fibre-reinforced concrete decreased with the volume concentration of the fibre. Al-Tayyib et al. (Al-Tayyib et al., 1988) indicated that the addition of PP fibre at 0.5% by volume reduced the slump of 0.5 w/c ratio mix from 89 mm to 13 mm, although the mix flows satisfactorily and responded well to the vibration. The reduction in slump can be compensated for by using water-reducing admixtures or increasing the water content. Al-Tayyib et a1. (Al-Tayyib et al., 1988) also noted that PP fibres eliminated the plastic shrinkage cracking in slabs subjected to high temperature and wind effects. The influence of PP fibres on the drying shrinkage of concrete was not significant.

The investigation of PP fibre reinforced concrete indicated that there is no balling or tangling of fibres during mixing and placing. There was an appreciable increase in post-crack energy absorption capacity and ductility due to the addition of fibres. When compared to the corresponding plain concrete, there was a significant increase in both flexural fatigue strength and endurance limit (for two million cycles). Static flexural strength increased after being subjected to fatigue loading (Ramakrishnan et al., 1987).

The compressive strength of the concrete increased proportionally with the increase in volume ratio of PP fibres. The presence of PP fibres caused reduction of the concrete permeability, and amount of shrinkage (Kakooei et al., 2012).

5.2. 3 Durability of Polypropylene Fibre Reinforced Concrete

It is known that the tensile strength of concrete is relatively much lower than its compressive strength, therefore, crack propagation can be developed more quickly (Choi and Yuan, 2005). The tensile strength of concrete is only about 10% of its compressive strength, and concrete cracks when subjected to tensile stresses (Sanjuán and Moragues, 1997). Crack control plays a crucial role in the performance life of the concrete structure. This is because the settlement and plastic shrinkage cracks may pass through fresh

concrete, thus forming planes of weakness and lowering the integrity of the structure of concrete (Song et al., 2005). PP fibers mitigate plastic and early drying shrinkage by increasing the tensile property of concrete and bridging the forming cracks (Toutanji, 1999).

PP fiber has a low Young's modulus so they cannot prevent the formation and propagation of cracks at high stress level but they can bridge large cracks (Qian and Stroeven, 2000). Shrinkage especially the drying shrinkage influences the performance of structural concrete which could induce cracking and thus reduces the durability of the concrete and service life of the structure (Chindaprasirt et al., 2004).

PP fibre is introduced in the mix to minimize brittleness of the matrix thereby reducing the susceptibility to cracking of a concrete. It is also reported that PP fiber was effective in resisting the development of cracks caused by drying shrinkage (Toutanji et al., 1998, Huang, 2001).

An investigation conducted by Kakooei et al. (Kakooei et al., 2012) showed that the presence of polypropylene fibres reduced the permeability and volumetric expansion of the concrete which in turn had reduced the chance of the concrete cracking.

5.3 POLYMERS IN CONCRETE

Polymeric admixtures are defined as polymers used as a main ingredient effective at modifying or improving cement- based material properties. Such a polymeric compound can be a polymer latex, re-dispersible polymer powder, water-soluble polymer or liquid polymer (Diab et al., 2013).

Polymers in concrete have received significant notice in recent years. Polymers are weak in compression but can have higher tensile capacities and provide excellent adhesion to other materials. They are also resistant to physical (i.e., abrasion, erosion, impact) and chemical attack. Combinations of polymers and concrete therefore can exploit the useful properties of both and yield composites with excellent strength and durability properties. There are three types of polymer-concrete composites with polymeric compound including

polymer impregnated concrete (PIC), polymer concrete (PC), and polymer modified concrete (PMC) (Hollaway, 1993, Zhong and Chen, 2002).

5.3. 1 Polymer Impregnated Concrete (PIC)

PIC is produced by impregnating hydrated Portland cement concrete with a low viscosity monomer, usually methyl methacrylate, which is subsequently polymerised by radiation or thermal catalytic techniques. Since the polymer ideally fills the voids and binds with the cement matrix and aggregates, there is no need to have high quality concrete for PIC (Balázs and Kovács, 1982).

PIC typically develops compressive strength of the corresponding conventional concrete by three to four times and increases tensile and flexural strength. Furthermore, PIC has excellent durability, particularly freezing and thawing and acid resistance, due to its extremely low permeability. Although the modulus of elasticity of the polymer is no more than 10% of the concrete elastic modulus, PIC shows the considerable increase (between 50% and 100%) in the modulus of elasticity of the normal concrete (Fowler, 1999).

With such outstanding properties, many applications for PIC are predictable including bridge decks, wharves, hazardous waste containment, post-tensioned beams and slabs and so on. However, because of the necessity to the special equipment and technology, manufacturing of PIC cannot be commercialised with current level of technology and cost (Tazawa and Kobayashi, 1973).

5.3. 2 Polymer Concrete (PC)

Polymer concrete (PC) consists of aggregate with a polymeric binder without Portland cement and water. Polyester-styrene, acrylics and epoxies have been the most widely used monomers, but vinyl ester, furan, and urethane have also been used. The polymer matrix binds very well to the aggregate particles with no transition zone (Fowler, 1999).

Considerable efforts have been made to develop and use PC as a repair material. Its rapid setting, excellent bond with the old concrete and steel reinforcement as well as high strength and durability performance make it very attractive and effective repair material.

Setting time and time for development of maximum strength can be readily varied from a few minutes to several hours by adjusting the temperature and catalyst system. The properties of PC include rapid curing at ambient temperature, high tensile, flexural and compressive strengths, good adhesion to most surfaces, good long-term freeze–thaw durability, low permeability to water and aggressive media, and good chemical resistance (Muthukumar and Mohan, 2004).

Some failures have occurred because of incompatibility between PC and the concrete substrate as a result of the difference in coefficients of thermal expansion coupled. A possible problem with some PC is its sensitivity to high temperature and to cyclical temperature changes (O'Connor and Saiidi, 1993).

PC in precast elements represents an excellent use of the material due to its rapid curing, ability to form complex shapes, and excellent vibration damping (Rebeiz, 1996).

5.3. 3 Polymer Modified Concrete (PMC)

Polymer modified concrete is normal Portland cement concrete with a polymer as an admixture. The polymer and the cement hydration products comingle and create two interpenetrating matrices working together which results the improvement of the material properties of conventional concrete (Knapen and Van Gemert, 2009).

Polymers are materials with long chain molecules made up of many individual monomers connected end to end. Polymers are classified as elastomers, thermosetting, and thermoplastics. Each of these polymers is characterised by the type and relative amount of crosslinking of the polymer chains. Polymers used in PMC are the thermosetting and thermoplastic types. The physical characteristics of the polymers used in PMC affect the properties of the hardened PMC (Kardon, 1997).

The atomic composition of the monomers affects the amount and type of crosslinking and the chemical properties of the polymer and influences the properties of the fresh PMC. Polymerisation can occur with little energy input or only in the presence of a chemical catalyst. Polymers can be ionic or nonionic depending on the atomic charge of the side chains. Ionic polymers tend to orient themselves around other particles, such as cement

grains. Polymerisation of the monomers can take place prior to combination with Portland cement mortar or concrete or can be initiated after mixing (Ohama, 1998).

The polymer dispersions widely used are styrene-butadiene rubber (SBR) latex, ethylene-vinyl acetate (EVA), and polyacrylic ester (PAE) emulsion in Japan and Europe, and the styrene- butadiene rubber latex, polyacrylic ester emulsion, and epoxy (EP) resin in the United States. SBR has been widely used for floor and bridge overlays, although the minimum thickness is usually about 30 mm, they have shown excellent bond strength to concrete, higher flexural strength, and lower permeability (Hollaway, 1993).

When polymers are incorporated in PMC as latex, the composite is referred to latex modified concrete (LMC). LMC is the most common type of PMC because latex is relatively simple to incorporate in mortar or concrete. It is added with the other ingredients during the mixing of the fresh concrete. The water portion of the latex must be considered in the overall mix design of the concrete. Latexes are suspensions in the water of solid monomers or polymers (Zhong and Chen, 2002).

Due to this improved performance, LMCs are being used increasingly in bridge-deck overlays, in repair and rehabilitation operations, patch applications and in the construction of new pavements, garages, marine structures, tunnels, and pipe linings. LMCs are more widely used than the other polymer concrete systems due to their less complicated production method and lower cost (Kuhlmann, 1985).

5.3. 4 Latexes and Their Properties

Latex is a stable dispersion of organic polymer particles in an aqueous surfactant solution giving a milky fluid that is generally white in colour. On drying, these particles coalesce to form a continuous film. An organic polymer is a substance composed of giant molecules formed by union of a number of simple molecules known as monomers. Latex modified concretes were developed to minimise or to completely eliminate the weaknesses of Portland cement concretes. These weaknesses include low tensile and flexural strength, low ductility, low abrasion resistance, relatively high porous system, and cracks. Polymer

modified concretes have higher tensile and flexural strengths, frost action resistance, and considerable lower permeability (Ohama, 1995).

Many types and formulation of latexes are manufactured however, only those specifically developed for use in hydraulic cement can be used in mortar or concrete applications. Various latexes that have been for modification of Portland cement mixtures are listed as follows (Ohama, 1995):

Elastomeric:

- Natural Rubber (NR)
- Styrene-Butadiene (SB)
- Styrene-Butadiene Rubber (SBR)
- Acrylonitrile-Butadiene Rubber (ABR)

Thermoplastic:

- Polyacrylic Ester (PAE)
- Styrene-Acrylic (SA)
- Ethylene Vinyl Acetate (EVA)
- Polyvinyl Acetate (PVAC)
- Polyvinylidene Chloride (PVDC)
- Vinyl Acetate-acrylic Copolymer (VAC)

Occasionally, blends of different types of latexes such as elastomeric latex with a thermoplastic one may be used. These are known as mixed latexes.

The properties of LMC depend on the type of latex used; within each type of latex there are many variations that result in different properties in modified concretes. Viscoelasticity is a characteristic of certain materials that exhibit both viscosity and elasticity. Viscoelastic polymers are generally made up of long-chain molecules that tend to intertwine and tangle. At low temperatures, the chains are close together and interlocked, causing the material to

behave as an elastic solid. At high temperatures, the chain move apart, so that they can stretch a long way and become more flexible. (Ramakrishnan, 1992).

Walters (Walters, 1987) has reported that Portland cement concrete modified with a vinyl acetate homo-polymer latex usually has poorer water resistance that that of a similar unmodified concrete. A latex modified Portland cement concrete using an SBR with lower molecule weight will not have the same strength, adhesion, and water resistance properties as that using a latex with higher molecular weight, even if the monomer composition and other ingredients are the same.

Latexes, most notably those based on liquid rubber such as SBR, have been employed to dramatically increase the tensile and flexural strengths of the concrete (Ohama, 1987). However, latexes frequently provide improvements in these strength parameters when incorporated in a concentration more than a critical value. On the other hand, an increase in latex concentration can substantially diminish the compressive strength by reducing the quantity of Portland cement in the mixture. This phenomenon together with an increase in viscosity, which is likely to influence the workability of the paste, obviously requires serious consideration (Beaudoin and Ramachandran, 1989).

The results of research study conducted by Barluenga and Henandez-Olivares (Barluenga and Hernández-Olivares, 2004) indicated that the consistency of LMC depends on both water-to-cement ratio (W/C) and polymer-to-cement ratio (P/C). Also, compressive strength decreased as P/C ratio increased and flexural strength does not depend on P/C ratio. In general, the properties of polymer modified mortar and concrete depend strongly on the polymer content or polymer cement ratio (P/C). P/C defined as the mass ratio of polymer solids in a polymer-based admixture to the amount of cement/cementitious materials in a polymer modified mortar or concrete.

An experimental investigation conducted by Lewis and Lewis (Lewis and Lewis, 1990) showed that regardless of the concentration of polymer, both SBR and Acrylic modified concretes suffer significant reduction of compressive strength. At the same time there is some indication of improved tensile strength. The fracture surface indicates that in polymer-modified concrete, the fracture propagates preferentially through the cement matrix, with fewer fractures in large aggregate than in the conventional concrete samples as controls. Moreover, they observed that the workability of latex modified concrete is

much higher than the normal concrete, and rapidly increases with the higher concentration of polymer.

In addition, for a constant ratio of polymer to cement, the workability increases remarkably with a small variation in water content. Whereas, experimental study conducted by Çolak (Çolak, 2005) showed that the workability of the latex modified concrete decreases by increasing latex concentration. But, this depends on the W/C ratio of the mixture and can be greatly compensated by using a suitable superplasticizer. Also, Çolak concluded that addition of latex to the Portland cement concrete decreases compressive strength.

Bentur (Bentur, 1982) in his journal article under the topic of "properties of polymer latex-cement composites" stated that addition of latex improves the rheological properties of the fresh paste and enables reduction of W/C ratio. SB latexes enhance only modulus of rupture (improves the ductility of the composite) and do not give increase in compressive strength.

Styrene butadiene rubber (SBR) latex has been widely used as one of the most suitable polymeric admixture in the concrete (Ohama, 1987). The molecular structure of SBR comprises both the flexible butadiene chains and the rigid styrene chains. The combination of those chains offers the SBR-modified concrete many desirable characteristics properties such as good mechanical properties, water tightness and abrasion resistance (Yang et al., 2009).

A very recently published experimental investigation conducted Diab et al. (Diab et al., 2014) illustrates that the latex participation ratio in co-matrix strength is influenced by type of cement matrix, type of curing (dry, wet), latex type, latex solid to water ratio, and age. Moreover, they concluded that SBR solid to water ratio increases the flexural strength and pull out bond strength.

Ramli et al. (Ramli et al., 2013) concluded that by modifying Portland cement concrete with 15% polymer latex, the characteristics of the resulting mix were greatly enhanced. The PMCs had a porosity value of at least 5 times smaller than that of the unmodified concrete.

In a significant experimental study performed by Wang et al. (Wang et al., 2006), the content of $Ca(OH)_2$ in wet-cured SBR modified cement pastes increases with P/C ratio firstly and then declines after reaching a maximum, and in the longer hydration time the variation is more obvious. Appropriate addition of SBR accelerates the cement hydration reaction, and the degree of cement hydration is maximal when P/C ratio is 10%. They interpreted this process as the variation of the degree of cement hydration with P/C ratio is dependent on the formation of polymer film in the pastes. When P/C ratio is below 10%, the latex and cement can mix perfectly and there is no polymer accumulation. This phenomenon allows free transfer of ions in the system. Meantime, polymer phase maintains some water in its structure and provides water for cement hydration successively, which results in the maximum of the degree of cement hydration change to higher P/C ratio with curing time. However, when P/C ratio is higher than 10%, the formed polymer film in the paste becomes thicker, which limits the transfer of ions, and thus prevents further cement hydration.

All polymers act as water reducers to some extent. (A water reducer increases the workability of the concrete, in some cases allowing reduction of the ratio of water to cement, which increases strength.) SBR is the most powerful water reducer of the others, and leads to increase in strength (Lewis and Lewis, 1990).

5.3. 5 Concept of Latex Modification

Any form of cement-compatible latex has a somewhat symbiotic relationship with the traditional concrete components of cement and aggregate. For solidification of latex, it must be suspended in water, and then give up that water. As the proportion of water in the latex drops below a critical fraction, the polymer particles suspended in the water begin to coalesce into a solid. On the other hand, cement requires water in order to carry out the hydration process. When an aqueous latex and cement are mixed together, the water in the latex is taken up by the cement hydration process. In this case, two materials tend to form solids in an interlacing skeleton (Su et al., 1991, Silva and Monteiro, 2006).

Emulsion polymerisation is the interesting process in modifying Portland cement. An excellent hypothesis supported by electron microscope and other studies has been put forward by Ohama (Ohama, 1987) to explain the latex modification process for SBR

latexes. Latex modification occurs in two processes: cement hydration and latex film formation. Normally, the latex film formation occurs after the cement hydration. In surfaces where there is loss of water due to evaporation, the film formation will be faster than the cement hydration.

When polymer latexes are mixed with fresh cement systems, the polymer particles are uniformly disperse in the system. In an emulsion polymer system, as the water evaporates, the discrete polymer spheres approach each other and eventually touch and fuse into a continuous film. The hydrated cement phase and polymer phase interpenetrate, and aggregates are bound by this co-matrix phase. Scanning electron microscope images (Ma et al., 2011) show the solidification of the polymers and film formation of polymer in the concrete (Figure 5-2 and Figure 5-3).

In the latex system, the cement gel is gradually formed by hydration of cement. Water is saturated with calcium hydroxide formed during the hydration. It is possible that the $Ca(OH)_2$ in the water reacts with the silica surface of the aggregate and forms a calcium silicate layer. According to recent studies, the formation of $Ca(OH)_2$ and ettringite in the contact zone between cement hydrates and aggregates contributes to the bond between them (Ribeiro et al., 2008).

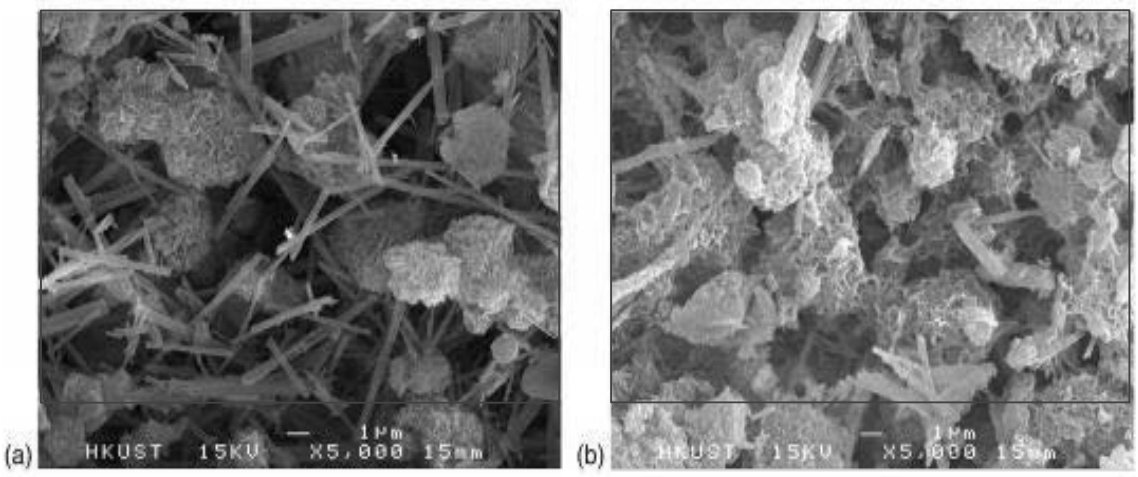

Figure 5-2 Microstructure of: Cement hydration products in conventional concrete (a), Formation of polymer films and reducing the concrete pores in polymer-modified concrete (b) (Ma et al., 2011)

With loss of water due to evaporation and cement hydration, polymer particles are gradually confined the capillary pores. As cement hydration proceeds, and the capillary

water is reduced, the polymer particles coalesce to form a continuous close-packed layer on the surfaces of the cement gel and unhydrated cement particle mixtures, and simultaneously adhere to the mixtures and the silicate layer over the aggregate surfaces. Latex particles are spherically shaped with size range variety from 0.05 to 0.50 μm in diameter. Solid content of the latex is approximately 50% which is an important fact when adjusting the water content of the mix design(Ray et al., 1994a).

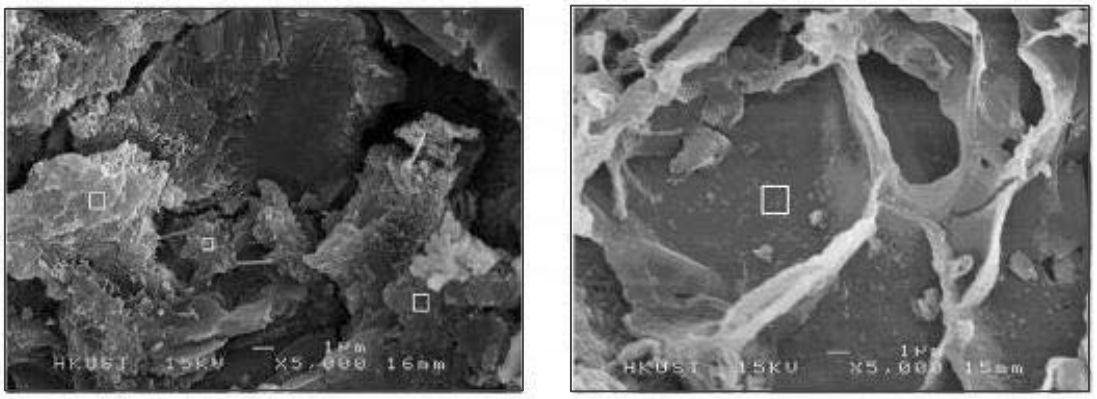

(a) (b)

Figure 5-3 Microstructure of unmodified concrete (a) and modified concrete (b) (Ma et al., 2011)

5.3. 6 Mechanical Properties of Polymer (Latex) Modified Concrete

The consistency of PMC depends on both water cement ratio and percentage of latex in the concrete mix. The parametric study conducted by Barluenga and Hernandez-Olivares (Barluenga and Hernández-Olivares, 2004) confirmed the effect of the both parameters on the mechanical properties of the concrete. Their test results showed that by increasing the proportion of the latex in the concrete mix, compressive strength decreased. Moreover, flexural strength increased by increasing the latex percentage. The tests performed by Bentur (Bentur, 1982) and Çolak (Çolak, 2005) showed similar results.

Diab et al. (Diab et al., 2014) concluded that the strength of modified cement paste divides into latex network strength and cement matrix strength. These strengths depend on unmodified cement paste degree of hydration and modified cement paste degree of hydration. In addition, the cement degree of hydration decreases as latex solid to water ratio increases.

The shrinkage stress-induced micro-cracks in latex modified concrete are bridged by the formation of polymer films or membranes and prevent crack propagation. The test results of experimental investigation conducted by Van Gemert (Van Gemert, 2007) clearly confirmed the process.

The latex particles also reduce the rate and extent of moisture movement by blocking the water passages and reducing evaporation of excess mixing water. This results in increased tensile strength and fracture toughness. The tensile strength of the PMC showed nearly linear relation with the mass fraction of the polymer (Zhong and Chen, 2002).

During the initial stages, latex modified concrete are more sensitive to plastic shrinkage cracking than plain concrete because of the water reducing influence of latex in the mixture (Beaudoin and Ramachandran, 1989).

Water evaporation takes place at the surface of the mixture. When the latex solids coalesce before adequate cement hydration occurs, the cement paste may shrink before sufficient tensile strength develops to restrain crack formation. Therefore, surface evaporation should be prevented or minimized by adequate curing systems (Wang et al., 2005).

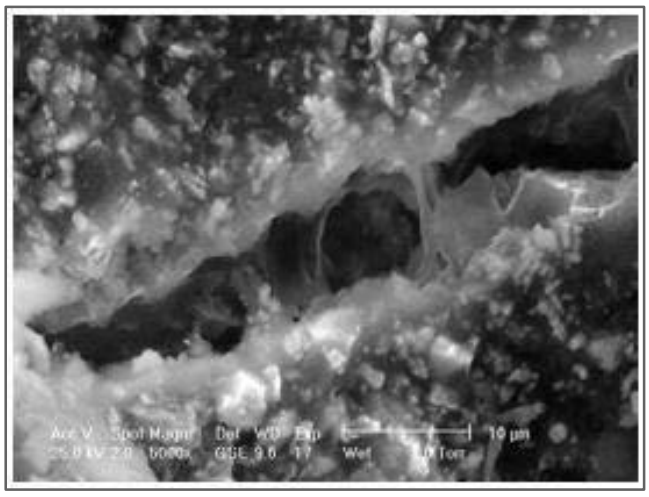

Figure 5-4 Crack bridging/healing by the formation of polymer films in the concrete (Van Gemert, 2007)

Reberio et al. (Ribeiro et al., 2008) conducted a comprehensive experimental investigation on the mechanical properties of Styrene-Butadiene polymer modified concrete. They

concluded that the compressive strength of PMC decreases by increasing the amount of the polymer but flexural and tensile strengths increase. They considered that the reason for this mechanical behaviour of PMC is the simultaneous polymer action on the atrophy of the growth in hydrated calcium hydroxide crystals and the reduction in the density of the micro-cracks in the paste-aggregate interface (ITZ). This process associated with the delay in the cement hydration and with the increase in the air content of PMC, leading to a significant increase in flexural and tensile strengths of PMC without improvement in compressive strength. Furthermore, the influence of polymer on the cement hydration reactions proved by Knapen and Van Gemert (Knapen and Van Gemert, 2009).

5.3. 7 Durability Performance of Polymer (Latex) Modified Concrete

The available literature in relation with durability performance of the PMC incorporating SBR (latex) is reviewed in terms of water permeability, chloride diffusion, and chemical attacks.

The durability of the concrete depends on the mass transfer properties of the concrete and mass transfer property in PMC has direct correlation with the polymer film formation technology. Muhammad and Ismail (Muhammad and Ismail, 2012) observed that in SBR latex proportion less than 5%, the continuous polymer film may not been formed, rather a cluster of the isoprene particles may be present in capillary pores and voids (Figure 5-5).

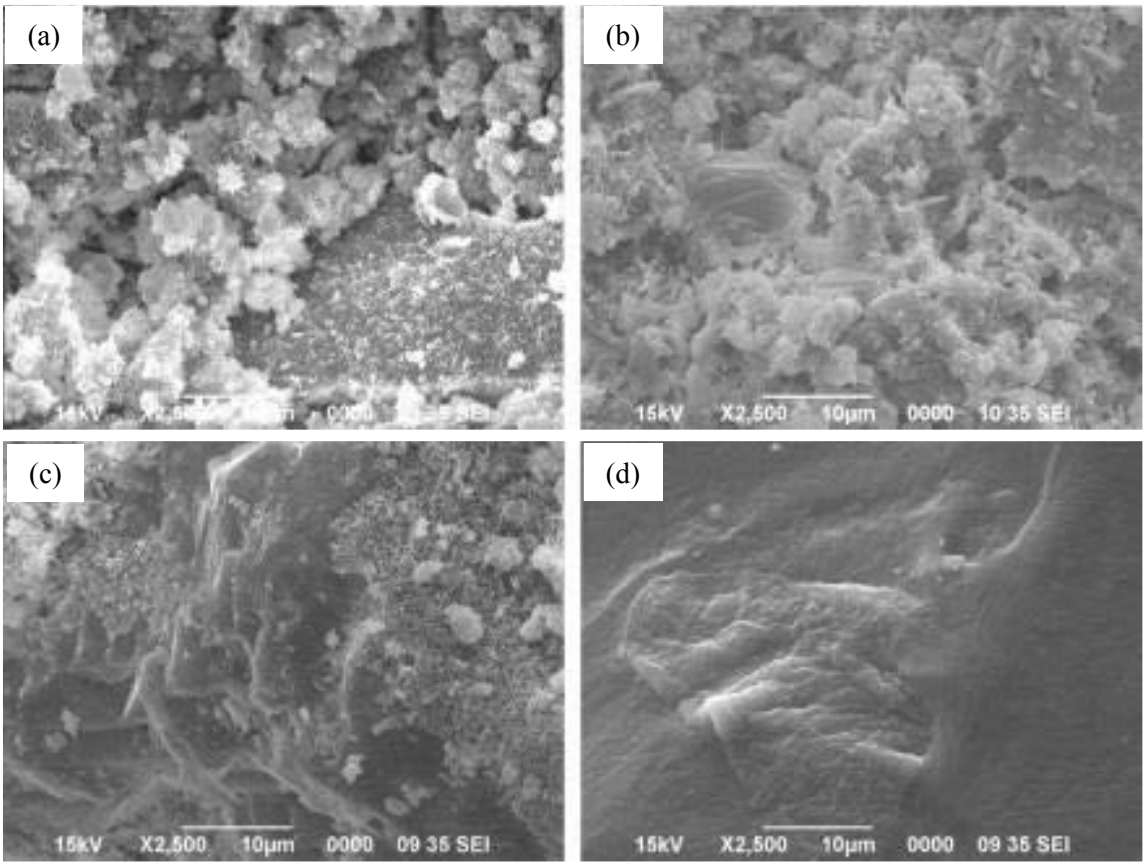

Figure 5-5 Morphologies: mortar with 5% latex (a), mortar with 10% latex (b), mortar with 20% latex (c), and latex film (d) (Muhammad and Ismail, 2012)

Shaker et al. (Shaker et al., 1997) found out that the water penetration depth of latex modified concrete (LMC) was 75% lower than the conventional concrete. Also, LMC shows 50% reduction in water absorption (sorptivity).

In an experimental study conducted by Sukontasukkul and Nitipon (Sukontasukkul and Boonpradit, 2006), they observed that the polymer film successfully provided internal barrier inside the concrete to prevent the moisture loss in the concrete. In addition, they concluded that the resistance to water penetration of the concrete can be improved by forming the polymer film inside the concrete microstructure and pores.

Yang et al. (Yang et al., 2009) conducted an experimental study to evaluate the microstructure and chloride permeability of the SBR latex modified cement mortars which prepared with various polymer to cement (P/C) mass ratios, a constant water to cement ratio of 0.45 and constant sand to cement ratio of 2. The FESEM images proved that the mixing SBR latex in fresh mortar altered the morphology and microstructure of the

hardened mortar. Through the cement hydration matrix, a continuous polymer film became more and more visible with the increasing P/C ratio in the mortar. At a P/C ratio more than 10%, the interpenetrating network structure of SBR and cement hydrates was found to bind sand particles together. The SBR latex reduced the general ionic permeability of the mortar, as indicated by reduced electric charge (Q) passing through the sample. Electro-migration tests demonstrated that the incorporation of SBR latex improved the chloride penetration resistance of the mortar by reducing the apparent diffusion coefficients of chloride ions.

Another significant published investigation performed by Ramli et al. (Ramli et al., 2013) revealed the following conclusions:

- The porosity of modified and unmodified of the mortar samples was comparable at ages of 28 and 6 months. However, at the ages of 12 and 18 months, there was a pronounced reduction in total porosity in modified cement samples by SBR latex.
- With 15% polymer latex, the porosity value for modified cement samples was 5 times smaller than unmodified samples and showed approximately 60% reduction in water absorption.
- The maximum average of interconnected pores diameters for unmodified cement mortars were significantly more than modified samples.

There are quite a few significant literatures in connection with the diffusion of chloride into SBR latex modified concrete. One of them is an experimental study conducted by Rossignolo and Agnesini (Rossignolo and Agnesini, 2004). They investigated the effects of SBR modification on the durability of lightweight aggregate concrete. Test results indicated that modified concrete had better durability performance than unmodified concrete in terms of chloride diffusion and corrosion resistance. The increase in the time to corrosion-induced crack for modified concrete with P/C ratio of 5% and 10% reported as 45% and 85%, respectively.

5.4 SUMMARY

This chapter investigated the mechanical properties and durability characteristics of synthetic fibres (polymeric fibres) and polymers as admixtures in the concrete. The reason of investigation and study of both synthetic fibres and polymers is expressed as follows:

- By extensive investigation and reviewing the significant literature regarding to the durability and service life of the RC structures, author has reached to this conclusion that there are two main sources of the diffusion and/or penetration of liquids and gases into the concrete. One of these sources are cracks (especially surface cracks) generated by different process and phenomena such as plastic shrinkage, plastic settlement, drying shrinkage, and thermal cracks. The other way of the mass transfer into the concrete is the interconnected pores system inside the concrete mostly generated by capillary process and air voids.

- Synthetic fibres are able to reduce the number and the size of the surface cracks efficiently and polymers are able to block the pores and capillary tracts by formation impermeable film in the microstructure of the concrete. By combining the properties of these materials (reducing the cracks and blocking the pores) in the polymer-concrete composites, it is anticipated that the rate of the diffusion of aggressive ions into the concrete will be decreased remarkably. This is the hypothesis behind the use of the synthetic fibres and polymers in the concrete in this research.

In this chapter, the physical and mechanical properties of synthetic fibres were investigated. Based on the results revealed in the literature, to conduct the experimental program and investigation of this research, polypropylene (PP) fibres were selected to make fibre reinforced concrete (FRC) as polymer-concrete composite due to good physical-mechanical properties, good bond with cement matrix, high modulus of elasticity, and non-corrosive properties.

PP fibres incorporating in the concrete improves the resistance of impact, shatter, and abrasion; shear strength, flexural strength, tensile strength, and concrete toughness. Furthermore, adding PP fibres to the concrete mix reduces the shrinkage.

In addition, some significant available literature regarding to durability of PP fibre reinforced concrete were investigated. But, there is not any comprehensive experimental investigation in this area to cover all factors regarding to durability performance of the reinforced concrete incorporating PP fibres.

Various categories of polymeric concrete and their properties were studied. Due to very easily to produce and cost efficiency, polymer modified concrete (PMC) were chosen to work on it in this research. Among the different appropriate type of polymers to make PMC, due to excellent compatibility with the Portland cement, styrene butadiene rubber (SBR) which is a type of latex was selected to incorporate in the concrete mix.

Physical and mechanical properties of SBR were investigated. Latex decreases the compressive strength of the concrete considerably even in low proportion (<10%). Due to this side effect, PMC incorporating SBR has not been considered as a structural material.

SEM images proved that the SBR film formation inside the microstructure of the concrete potentially can improve the durability performance of the concrete. But, there is no extensive experimental investigation to confirm how PMC incorporating SBR can improve the durability of the concrete which consequently can extend the service life of the structure.

Polymer-concrete composites are multi-phase materials produced by combining aqueous or powder state polymers and/or reinforcing fibres in order to enhance the mechanical and durability performance of the plain concrete.

CHAPTER 6

EXPERIMENTAL PROGRAM

CHAPTER 6. EXPERIMENTAL PROGRAM

6.1 INTRODUCTION

In maritime structures, the effect of local environment and geographical configurations has a significant bearing on performance of the structures. As discussed in the literature review, diffusion of chloride ions through concrete pores in saturation and absorption states are two involved domain transport mechanisms. Diffusion is a slow and quite well understood process, although the effect of time on the chloride diffusion coefficient and surface chloride concentration is not completely established.

In the state of absorption, there are complications interpreting sorptivity values and the role of this process in chloride ingress is not well understood yet. The use of different methods makes it difficult to interpret the results and compare them to one another. In addition, the majority of the test methods including those suggested in codes and standards are not representative of conditions found on site. There are only a few studies on chloride diffusion into concrete exposed to wetting and drying cycles and majority do not measure the sorptivity of the concrete. Therefore, the relationship between sorptivity and depth of chloride penetration due to wetting and drying cycles is not clear enough.

The literature review also revealed that the most widely used chloride penetration prediction models are based on Fick's second law of diffusion due to their relative simplicity and the fact that they provide a good fit to the field data. However, these models are not realistic and ignore the time dependent nature of chloride diffusion coefficient and surface chloride concentration. On the other hand, there is no universal agreement on the

variation of chloride diffusion coefficient (D_c) and surface chloride concentration (C_s) together with different variables such as exposure time, concrete composition, and wetting and drying cycles.

6.2 METHODOLOGY

The investigation of experimental program methods can be divided into two categories including, investigation on the mechanical properties and durability characteristics of conventional Portland cement concrete and polymer-concrete composites. In this study an extensive experimental program has been conducted to compare the data and results of each test for different categories of concrete.

Investigated mechanical properties are compressive, tensile, and flexural strengths. In addition, the durability characteristics of the each concrete category have been assessed and analysed based on two different approaches including (a) chloride profile and (b) time to corrosion-induced crack.

Due to the lack of extensive experimental investigations in relation to the durability performance of polymer-concrete composites in the literature, the experimental program of this research was planned to study the effect of PP fibres reinforced concrete (FRC), polymer (latex) modified concrete (PMC), and combination of these two polymeric materials as fibre reinforced polymer modified concrete (FRPMC), with different proportions, on the durability performance of the concrete exposed to severe environmental conditions.

Firstly, to produce high quality Conventional Concrete (CC) all significant influencing parameters such as cement content, water cement ratio, and aggregate proportion were considered along with proper mixing procedure, consolidation, and curing method.

Secondly, based on the available literature, it has been revealed that by increasing the polymer proportion in the concrete mix, compressive strength of the concrete decreases considerably. Due to this phenomenon, PMC has been already applied just as a repair mortar or concrete in rehabilitation programs or as a protective layer for concrete bridge decks. In order to be able to use latex modified concrete as a structural material, producing

PMC with desired mechanical properties similar to the conventional concrete was a challenge and target of this study.

The objectives of this extensive experimental program can be expressed as follows:

- An optimum mix design to obtain high quality conventional concrete with certain strength.
- Obtaining optimum mix design and mechanical properties of polymer modified concrete as a structural material.
- Investigation on the best curing method for PMCs.
- In order to use Fick's second law, determining chloride profiles for conventional concrete (CC), PMC, FRC, and FRPMC specimens has been accomplished based on pure diffusion environment (continuously immersed in chloride solution).
- Calculating the chloride diffusion coefficient for each concrete type to verify proposed mathematical model for predicting the chloride diffusion coefficient as a time-dependent parameter.
- Estimating corrosion-free service life (conservative assumption) of the RC structure based on the chloride profiles for all concrete types.
- Monitoring and determining the time to corrosion-induced crack by conducting accelerate chloride-induced corrosion (ACIC) test.

The materials, equipment, sample preparation, and test procedures are illustrated and discussed in this section.

6.2.1 Structural Concrete

Phase (I) was carried out to obtain an appropriate concrete mix design to produce high quality structural concrete for all types of the concrete categories including CC and polymer-concrete composites used in this research study. Compressive strength of concrete is related to the pore structure of the concrete. Concrete with higher dense microstructure generally shows a higher compressive strength. Besides compressive

strength, tensile strength, and flexural strength tests were also conducted in order to monitor the effect of polymer-concrete composites on these mechanical properties.

The following guidelines are recommended in AS 4997-2005 for structural concrete in a maritime structure:

- Specifying special-class concrete.
- A minimum characteristic compressive strength (f_c') of 40 MPa.
- General purpose Portland cement alone as the binder, or blended cement in accordance with AS 3972.
- Cementitious content should not be less than 400 kg/m^3.
- A maximum water to binder material ratio not more than 0.40. Super-plasticizers should be used, to reduce water content whilst maintaining adequate workability.
- Concrete should be placed in watertight forms, thoroughly compacted and protected from excessive temperature and wind evaporation during the curing period.

6.2.2 Durability Performance

Phase (II) was performed to investigate and evaluate the durability performance of polymer-concrete composites exposed to severe exposure conditions. To have a platform to produce a durable concrete the provided recommendations in Australian Standards, AS 4997-2005, The "Guidelines for Design of Maritime Structures" was considered as the criteria for the design of the concrete mix. Reducing the opportunity for chloride diffusion into the concrete is the objective of durability design of the concrete.

The measurement of the chloride content in various time intervals within different depth from the concrete surface is used to calculate the chloride diffusion coefficient. Consequently, the corrosion-free service life of each concrete type will be estimated.

To be able to obtain the service life, including corrosion propagation time, till generation of the first visible corrosion-induced crack, the accelerated chloride-induced corrosion

(ACIC) test was carried out. Time to cracking results can be used to compare the service life of the different concrete types, reliably.

6.2.3 Exposure Conditions

Reinforcing steel in concrete structures permanently submerged in sea water suffers only limited corrosion due to the oxygen availability in the water (A2 classification in AS 3600-2009). However, in the tidal and splash zone (C2, AS 3600-2009) due to alternatively wetting and drying of the concrete, rapid and severe corrosion is the consequence of increasing surface chloride concentration and chloride diffusion rate, together with the high availability of oxygen and moisture in the concrete.

In this experimental study, specimens were exposed to high concentration of sodium chloride solution and periodic wetting-drying cycles as simulation of severe environmental exposure conditions. Concrete exposed to wetting-drying cycles may become saturated depending on the exposure condition (e.g. frequency of wetting/drying periods). Saturation is a moisture state which concrete experiences on site and thus, it should be included in modelling.

The summary of methodology of the experimental phase is presented in Figure 6-1.

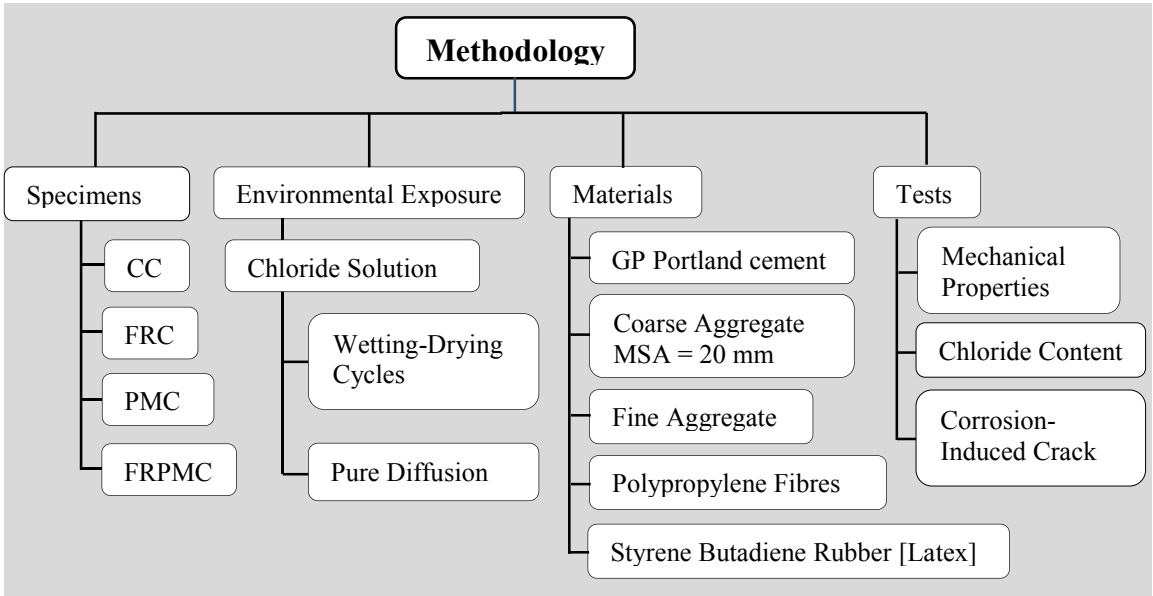

Figure 6-1 Methodology of the experimental phase

6.3 MATERIAL PROPERTIES

In this section the physical and/or mechanical properties of each material are described. In this section, the properties of the aggregates, polypropylene (PP) fibres, and Styrene Butadiene Latex as aqueous polymer are investigated. Since generally 65% to 75% of the concrete volume has been occupied by aggregates, the mechanical and physical properties of the aggregates such as strength, water absorption, and specific gravity have a great influence on the quality and performance of the concrete.

6.3.1 Aggregate

Coarse aggregates with the maximum size of 20 mm (Maximum Size of Aggregate, MSA) and two types of fine aggregates including coarse and fine sand were used in the concrete mixes. To achieve high quality concrete, sieve analysis and aggregate grading had to be carried out. Well graded aggregate is one of the most important factors to produce less porous and more durable concrete. Since different standards have recommended different limits for aggregate grading, in this study, sieve analysis for concrete aggregates was conducted based on Australian Standards AS 2758.1. The grading curve of the aggregate was located between the upper limit curve and lower limit curve recommended by AS 2758.1. The aggregate type used in this study is presented in Figure 6-2

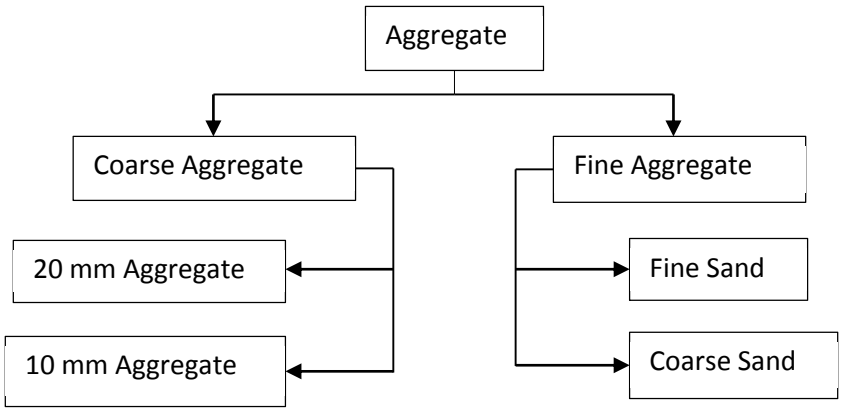

Figure 6-2 Aggregate grading type used in this study

Sieve Analysis of Coarse Aggregates:

Sieve analysis was conducted with 15,000 g of the coarse aggregate with MSA 20 mm. Results showed that in a certain point (19mm, 83.95%) the curve has passed the upper limit of the standard grading curve. To modify the grading curve, 25% of coarse aggregate (MSA=20mm) was replaced by coarse aggregate with MSA of 10 mm. The results of the initial and modified sieve analysis are presented in Table 6-1. In addition, grading curve of coarse aggregate is shown in Figure 6-3.

Table 6-1 Sieve analysis of coarse aggregate

	Initial Sieve Analysis			Modified Aggregate Sieve Analysis				
Sieve Size (mm)	Retained (g)	Passing (gr)	Passing (%)	Retained (g)	Passing (g)	Passing (%)	AS2758.1	
26.5	0	15000	100	0	15000	100	100	100
19	2407.5	12592.5	83.95	1945.4	13054.6	87.03	85	100
9.5	11211.5	1381	9.21	11648.6	1406	9.37	0	20
4.75	1330	51	0.34	1344.4	61.6	0.41	0	5
< 4.75	51	0		61.6	0			
Sum	15000			15000				

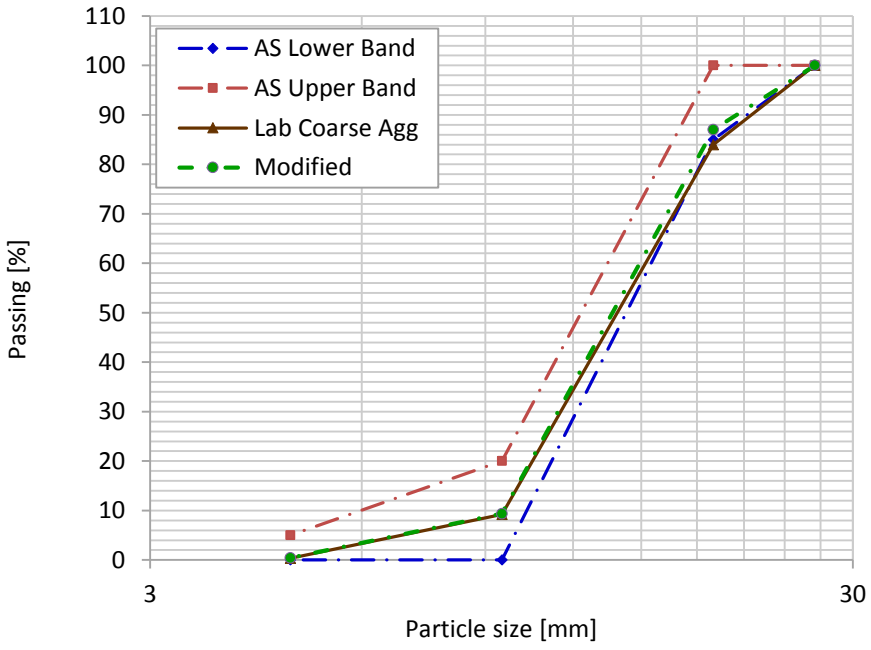

Figure 6-3 Grading curve of coarse aggregate

The sieve analysis illustrates that the coarse aggregate in the concrete mix design should consist 80% of coarse aggregate with MSA 20 mm and 20% of aggregate with MSA 10 mm.

To design the concrete mix, we also have to determine the water absorption capacity and density of the aggregates.

Sieve Analysis of Fine Aggregates:

Sieve analysis, based on AS 2758.1, was carried out for 5,000 g of coarse sand in order to achieve grading curve. The summary of this analysis has been presented in Table 6-2.

Table 6-2 Sieve analysis of fine aggregate

	Initial Sieve Analysis			Modified Aggregate Sieve Analysis				
Sieve Size	Retained (g)	Passing (g)	Passing (%)	Retained (g)	Passing (g)	Passing (%)	AS 2758.1	
9.5mm	13	4987	99.74	13	4987	99.74	100	100
4.75mm	305.1	4681.9	93.64	288.1	4698.9	93.98	90	100
2.36mm	1912.5	2769.4	55.39	1501	3197.6	63.95	60	100
1.18mm	1209.7	1559.7	31.19	1282	1915.4	38.31	30	100
600µm	566.6	993.1	19.86	788.2	1127.2	22.54	15	80
300µm	388.6	604.5	12.09	484.3	642.9	12.86	5	40
150µm	267.7	336.8	6.74	300.6	342.3	6.85	0	25
<150µm	336.8			342.3				
Sum	5000			5000				

The sieve analysis results revealed that the grading curve of coarse sand is close to the upper limit of the standard and even in the point (2.36mm, 55.39%) is out of limit. With adding approximately 25% of fine sand to the coarse sand the grading curve was modified. It means that the total weight of fine aggregate, estimated in the concrete mix design, consists of 75% of coarse sand and 25% of fine sand. The initial and modified grading curves of fine aggregates are shown in Figure 6-4.

By obtaining a well-graded aggregate, the quality of the concrete can be definitely improved due to higher density. The quality of the aggregates plays a fundamental role in

the quality of concrete. This is a reflection of the size, physical and chemical properties of the aggregates.

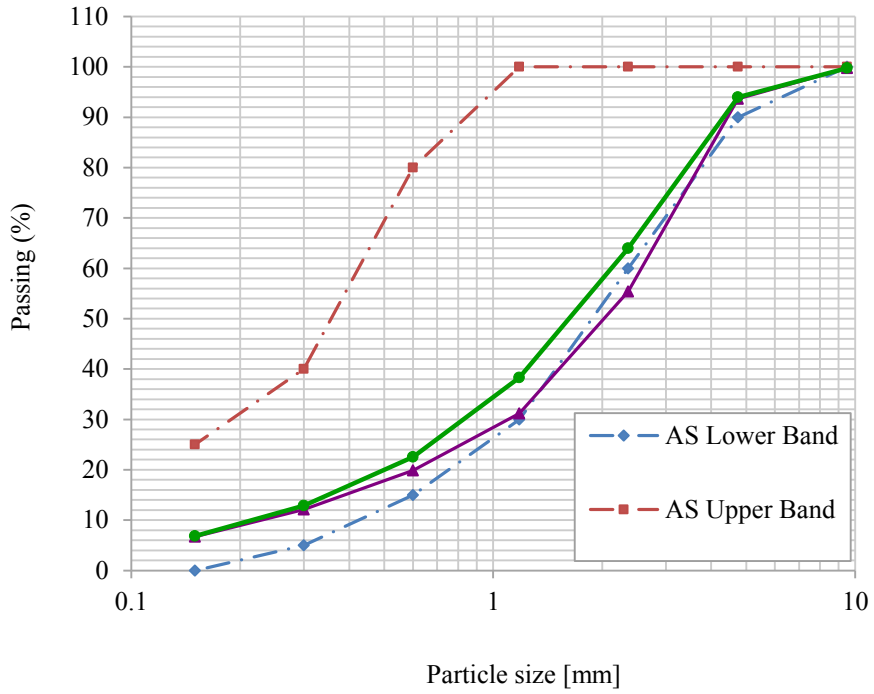

Figure 6-4 Grading curves of fine aggregates

Density (Specific Gravity) and Water Absorption Capacity of Coarse Aggregate

Water Absorption (WA) capacity and specific gravity, ρ_s, are two important physical properties of the aggregate. If aggregates have high water absorption capacity, they may absorb the mixing water of the concrete which has been estimated to be enough to hydrate cement grains. In this case the unhydrated cement particles cannot contribute to the strength gain of the concrete. Consequently, the strength of the concrete decreases dramatically. Moreover, coarse aggregates are affective component to concrete strength characteristics. Light weight aggregate or porous aggregate with relatively low specific gravity can reduce the strength and other mechanical properties of the concrete considerably. These two parameters, WA and ρ_s, were estimated according to AS 1141.6.1-2000 and results are presented in Table 6-3

Table 6-3 Water absorption and density of coarse aggregate

Item	Weight (g)	Density in SSD* (ρs) (t/m3)	WA (%)	Dry (t/m3)
Basket + Material (W1)	5987.00			
Empty Basket (W2)	2188.00			
Surface Dry Material (m2)	6016.00	2.71	1.48	2.67
Oven Dry Material (m1)	5928.00			
Water density	0.998			

*Saturated surface dry

6.3.2 Portland Cement

According to recommendation in AS 4997-2005, General Purpose (GP) cement was selected to be used in this research program. GP cement is a cost effective, high quality building material. In addition, the level of consistency and versatility of GP cement makes it an ideal choice in virtually all construction applications.

The benefits of GP cement can be summarised as follows:

- High versatility allowing use in a wide variety of concrete applications
- Compatible with most admixtures and supplementary cementitious materials

Table 6-4 illustrates the relevant specified requirements of AS 3972 and the indicative values achieved.

Table 6-4 GP cement properties based on AS 3972

Property		AS 3972-2010 Type GP	Indicative GP
Setting Time	Min.	45 min	60-150 min
	Max.	6 hrs	2.0-3.5 hrs
Soundness	Max	5 mm	< 3 mm
SO_3	Max	3.5%	< 2.9%
ISO Mortar	3 Day (min)	-	30-42 MPa
Compressive	7 Day (min)	35 MPa	43-54 MPa
Strength	28 Day (min)	45 MPa	54-65 MPa

6.3.3 Polypropylene (PP) Fibres

In this study for reducing the number and size of the cracks, the composite of Polypropylene (PP) fibres and concrete were selected to make Fibre Reinforced Concrete (FRC). PP fibres have become more and more important in engineering applications due to their good bond strength with cementitious matrix, low cost, light weight, low impact on concrete workability, proper finishing surface, and excellent corrosion resistance.

Monofilament PP fibres with the length of 19 mm were incorporated in the concrete mix to produce fibre reinforced concrete (FRC). The properties of the PP fibres used in this study are expressed in Table 6-5. Figure 6-5 shows the monofilament propylene fibres which used in the experimental program.

Table 6-5 Properties of PP fibres

Technical Data	PP fibre
Nominal Diameter (μm)	24
Elongation at Break (%)	63
Softening (melting) point (℃)	160
Density (g/ml)	0.91
Young's Modulus (GPa)	3.5

Figure 6-5 Monofilament Polypropylene Fibres used in this study

The experimental investigations conducted on mechanical properties of PP FRC have reported various and divergent outcomes. For instance, Mindness and Vondran reported a 25% increase in compressive strength at 0.5% volume percentage of the polypropylene fibres (Mindess and Vondran, 1988). Whereas, Massoud et al. revealed that the role of polypropylene fibers is insignificant in differentiating compressive strength using the same fibre volume fraction (0.5%) in the concrete mix (Massoud et al., 2003).

The results of test conducted by Nanni et al. indicated that typical proportion of polypropylene between 0.1% and 0.3% by volume of the concrete has the optimum effect on both shrinkage and temperature cracking control, and mechanical characteristics as the secondary reinforcement. (Nanni and Meamarian, 1991).

In order to have a more uniform mix and make sure that fibres are dispersed evenly in the mix, researchers have tried different mixing sequences. For instance, Manolis et al. have

allowed a 3 to 5 minutes mixing time after the fibres were added to the prepared concrete mix to achieve good fibre dispersion (Manolis et al., 1997).

In this experimental program, the concrete mixing procedure was conducted based on the Australian Standard AS 1012 requirement and then PP fibres were added to the ready mix concrete. Several trials of mixing time showed that four minutes, as the duration of the mixing process of PP fibres, would satisfy uniform distribution of the PP fibres in the concrete mix. With this process, full fibre dispersion was achieved and no segregation was observed.

Bayasi and Zeng reported that incorporation of PP fibres in the concrete reduces the workability of the fresh concrete. With 0.5% of 12.7 mm and 19 mm PP fibres, slump test results showed the reduction of 11.6% and 88.5%, respectively (Bayasi and Zeng, 1993). Other research works have also reported that the proportion of PP fibres more than 0.3% affects concrete slump noticeably (Pantazopoulou and Zanganeh, 2001, Al-Tayyib et al., 1988).

As a conclusion, according to the conducted investigations on the optimum proportion of the PP fibres in the concrete to comply with the fresh and hardened concrete properties, PP fibres volume fraction (V_f) were considered as 0.1%, 0.2%, and 0.3% by volume of the concrete. The reason behind this selection was related to the objective of this research which intended to investigate the durability performance instead of improving PP FRC mechanical properties.

6.3.4 Styrene Butadiene Rubber (Latex)

Latex, which may be natural or synthetic, is an emulsion consisting of proteins, alkaloids, starches, sugars, oils, tannins, resins, and gums that thickens when exposed to air. There are different types of latex used in construction industry. Latex, which is considered as thermoplastic polymer and elastomer, forms continuous layers of polymeric film when dried. SBR latex is one of the most widely used of the polymers which is compatible with cementitious materials.

The specific latex type that is used in this project (see Figure 6-6) is carboxylate styrene butadiene copolymer latex, which is designed to be added to the concrete, to improve the

bond strength of fibre and cementitious material and provide chemical resistance. Therefore, by adding latex to the concrete mix, it is proposed that the bond strength of cementitious materials with aggregates and fibres will be increased.

The presence of the carboxyl in the SBR latex can improve the solidification behaviour, which in turn improves the elastic properties of the polymeric film used in the concrete matrix (De Sarkar et al., 2000).

The SBR latex was determined to have a relative density of 1.0 and a solids content of 48%. In addition, the air content of the PMC mixes may possibly be affected by the presence of surfactants in this admixture (Ray et al., 1994b). The polymer particles in the latex are spherically shaped with size ranging from 0.05 μm to 0.50 μm in diameter. Solid content of the latex is approximately 50% which is an important phenomenon when adjusting the water content of the mix design.

Figure 6-6 Styrene Butadiene Rubber (latex)

6.3.5 Superplasticizer

Based on Australian Standard AS 4997-2005, the maximum water cement ratio (W/C) for maritime structures should be 0.4. The fresh concrete mix with such a low water cement ratio cannot be a workable concrete. Therefore, superplasticiser as a chemical admixture has to be added to the concrete mix in order to achieve a slump of 60mm to 80mm. The superplasticiser used in this project is categorised as polycarboxylate-based

high range water reducer admixture. ViscoCrete 5-500 a SIKA product has been used as a superplasticiser in this study (see Figure 6-7).

Figure 6-7 Superplasticiser used in this study

6.4 TEST METHODS AND PROCEDURES

So far, there has not been any significant investigation in literature covering the characteristics of both forms of the polymer-concrete composites (FRC and PMC) as fibre reinforced polymer modified concrete (FRPMC). Therefore, this extensive research study is a benchmark field research in this regard. To fulfill requirement, a precise extensive experimental program has been conducted for more than three and half years in order to investigate all properties of the polymer-concrete composites.

In this section, test methods and experimental procedures in order to investigate the mechanical properties and durability performance of the polymer-concrete composites are described.

6.4.1 Concrete Categories

In the experimental program, four concrete categories including Conventional concrete (CC), polypropylene fibre reinforced concrete (FRC), SBR latex modified concrete (PMC), and polypropylene fibre reinforced polymer modified concrete (FRPMC) have been investigated.

The different concrete types which have been used in this study are illustrated schematically in Figure 6-8. The mechanical properties and durability characteristics of all concrete categories have been monitored and measured.

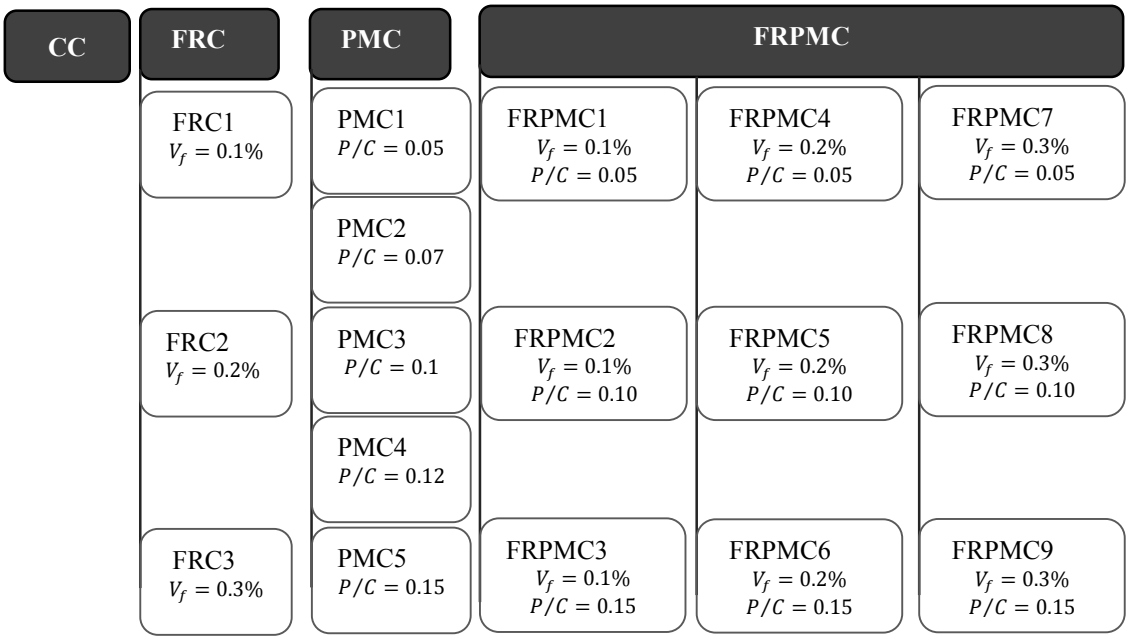

Figure 6-8 Concrete categories in this research study

6.4.2 Concrete Mix Design

Concrete mix design is one of the most determinant parameters to achieve durable concrete. An appropriate concrete mix design will result in high quality concrete. Concrete mix for conventional concrete was designed according to the recommendations of AS 4997-2000. To fix an optimum mix design in order to obtain desired both fresh and hardened concrete properties, several trial mixes were prepared and tested.

According to AS 3600-2009, clause 4.5, for a concrete structure with exposure classification "C", characteristic compressive strength (f_c') should not be less than 50 MPa. If obtaining the strength of 50 MPa is not possible, can be at least 40 MPa but, the minimum cement content should not be less than 470 kg/m3.

According to AS 4997-2005 clause 6.3.3, the following recommendations for structural concrete, have been suggested:

- A minimum characteristic compressive strength of 40 MPa

- Minimum Portland cement (GP) content of 400 kg/m^3
- Maximum water cement ratio of 0.4

Based on the Australian Standards recommendations and in order to make high quality concrete, following assumptions were selected to design the concrete mix.

- Characteristic compressive strength of 50 MPa
- Cement (GP) content of 400 kg/m^3
- Water cement ratio of 0.35

Since water cement ratio less than 0.4 decreases the concrete workability noticeably, superplasticiser has been added to the concrete mix at the time of batching to achieve desired concrete workability. The range of the slump was considered between 60 mm and 80 mm.

Based on the characteristic compressive strength, mean strength which will be used for designing of the concrete mix can be estimated as follows:

$$f_c' = f_m - k \cdot s \tag{6.1}$$

$$f_m = f_c' + 1.65\sigma \tag{6.2}$$

where f_m is the target mean strength, f_c' is the characteristic compressive strength, and s is the standard deviation of the normal distribution.

$$f_m = 50 + 1.65 * 5 = 58.25\ MPa \tag{6.3}$$

The final mix design of conventional concrete is presented in Table 6-6. In addition, the proportion of the materials in the concrete mix is illustrated in Figure 6-9.

Table 6-6 Mix design of the conventional concrete

Material	Magnitude (kg/m3)
Cement (GP)	400
Water	140
Coarse aggregate (20mm)	880
Coarse aggregate (10mm)	293
Coarse Sand	586
Fine Sand	195
Superplasticiser	4100 (ml/m^3)

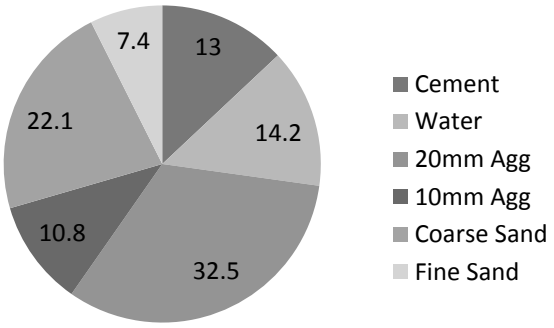

Figure 6-9 Proportion (%) of the materials in the final concrete mix

6.4.3 Sample Preparation

The mixing process for the conventional concrete was conducted in accordance with Australian Standard AS 1012.2. The same procedure was applied for mixing and casting FRC and PMC specimens with some additional considerations as follows:

- After completing the mixing procedure based on AS 1012.2, PP fibres were added to the freshly mixed concrete. Since the monofilament PP fibres must be uniformly dispersed and distributed throughout the whole matrix, four minutes time was considered as an additional mixing time for FRC specimens. As discussed earlier,

increasing the proportion of fibres causes the reduction of workability of freshly mixed concrete leading to usage of more Superplasticiser.

- For casting PMC specimens, the latex was added to the mixing water. Moreover, the amount of the mixing water had to be reduced in accordance of the amount of water in the latex. It was observed that increasing SBR latex proportion increases the workability of the fresh concrete mix.

The prepared samples for obtaining mechanical properties of the concrete are shown in Figure 6-10.

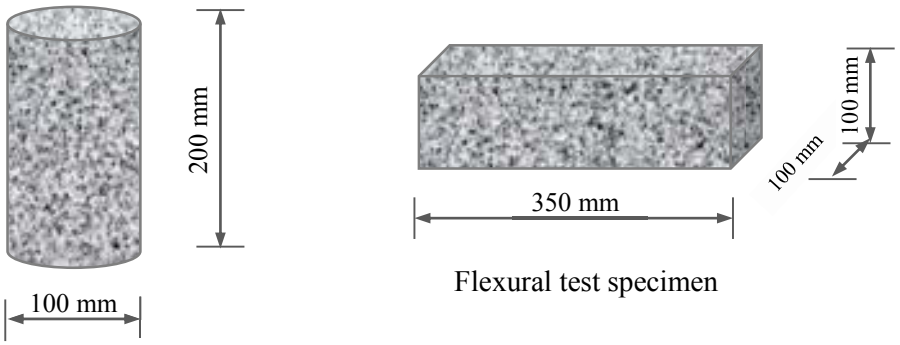

Compressive and tensile test specimen

Flexural test specimen

Figure 6-10 Samples for mechanical properties tests

Since chloride diffusion into the concrete is the dominant factor in concrete structures deterioration, chloride profile can be used to estimate the residual corrosion-free service life of the structure. The chloride profile is attained by measuring the concentration of chloride in different depth of the concrete cover in a certain time. By using the chloride profile, initiation time of corrosion can be predicted. Chloride profile can be used as a criterion to assess the durability of the concrete.

Assuming the initiation time of steel corrosion in the concrete, as the end of the service life, is a conservative method to estimate the structure service life. Therefore, it is optimised to consider the time corresponding to the crack formation on the concrete cover as the end of the service life. This assumption means considering corrosion initiation time plus corrosion propagation time till the generation of the first crack on the concrete cover.

Both chloride content measurement and corrosion-induced crack have been monitored and measured as durability assessment of different type of concretes in the experimental program of this study.

The samples size used for chloride content measurement (a) and for corrosion-induced crack (b) are presented in Figure 6-11. To obtain more accurate and reliable results and also to be able to conduct error analysis, for any particular test three specimens were tested.

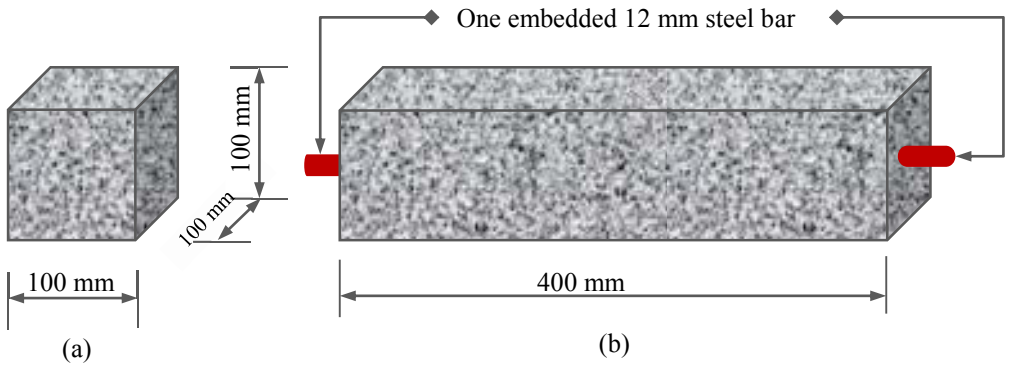

Figure 6-11 Samples characteristics for chloride content measurement (a) and corrosion-induced crack (b)

Mixing the concrete and sample preparation at UTS concrete laboratory are presented in Figure 6-12.

Figure 6-12 Research samples preparation

6.4.4 Mechanical Properties of Polymer Modified Concrete

As discussed in Chapter 5, studies have revealed that adding Styrene Butadiene Rubber (Latex) to the concrete mix, compressive strength is decreased. The reduction of compressive strength is directly related to polymer cement ratio (P/C). The initial test results, in this study, also confirm the same trend. The cause of this process is the generation of bubbles due to chemical reactions in the concrete mix which is called foaming phenomenon. This foaming phenomenon reduces the density and consequently, compressive strength of the concrete. Due to low compressive strength of the PMC incorporating latex, this material has not been used as a structural material. So far, PMC has been employed as repair mortar or as an over layer in horizontal elements such as bridge decks. One of the efforts and tasks in this research study is to increase mechanical properties of PMC in order to be used as a structural concrete.

Since PMC is highly sensitive to the polymer proportion in the concrete mix (polymer cement ratio, P/C) and W/C ratio, the effect of these parameters are investigated. The effect of P/C on compressive strength of the PMC with W/C ratio of 0.35 is presented in Figure 6-13. This graph shows that by increasing P/C ratio, compressive strength deceases dramatically which confirms the generation of bubbles (foaming phenomenon) in the mix.

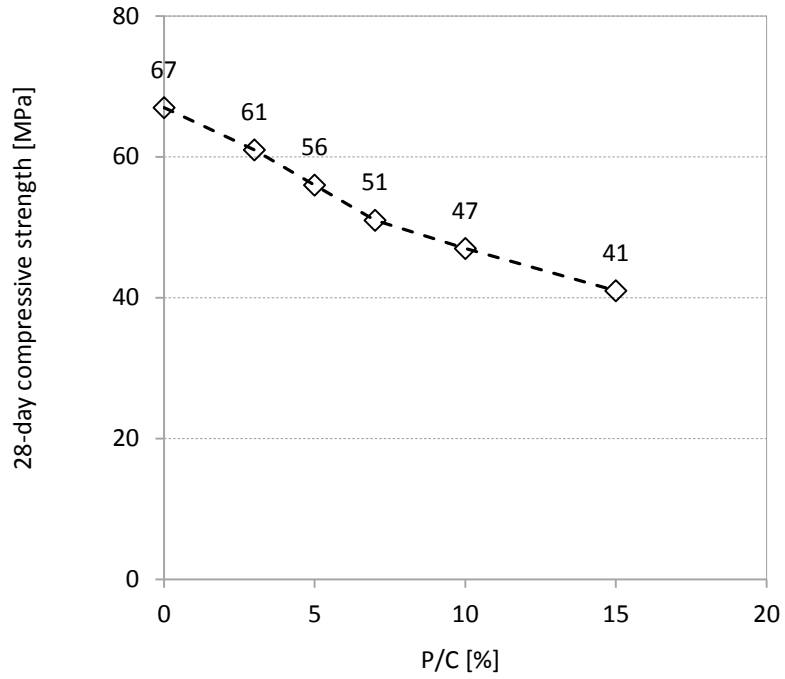

Figure 6-13 Effect of P/C ratio on PMC compressive strength

The experimental results depicted that with P/C of 10% and 15%, PMC compressive strength decreased by approximately 30% and 40%, respectively.

The influence of water cement ratio on compressive strength of PMC is presented in Figure 6-14. C ratio of/This investigation was conducted on a constant P 0.05 (5%)The . test results indicated that PMC is highly sensitive to water content in the concrete mix. Similar to CC, increasing w/c ratio decreases PMC compressive strength but the rate of strength reduction in PMC is much greater than CC. For instance, by increasing w/c ratio from 0.3 to 0.4, compressive strength of PMC decreases by approximately 25% which is considerable strength reduction.

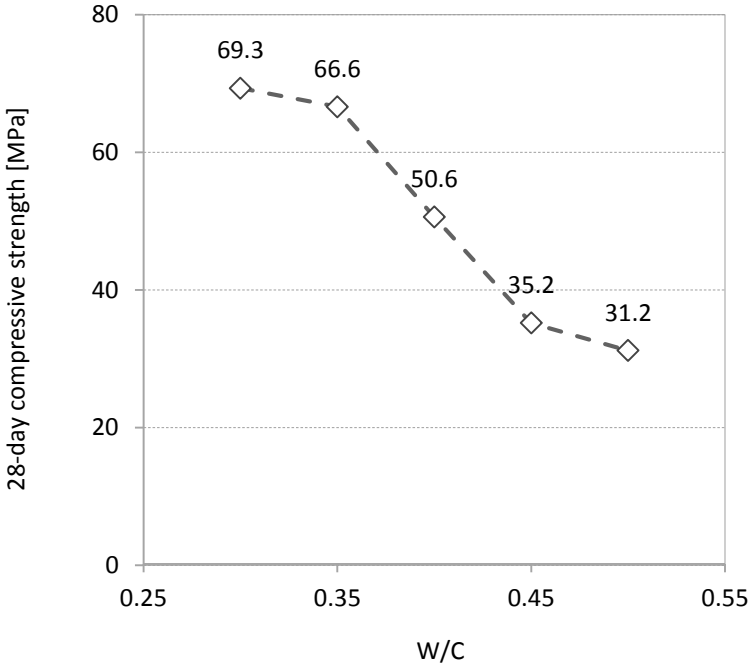

Figure 6-14 Effect of W/C ratio on PMC compressive strength

In order to improve mechanical properties of PMC, the amount of generated bubbles have to be reduced significantly. If polymer (latex) modified concrete is going to be used as a structural concrete, the air entrainment in the mix should be reduced to about 1.5 to 2 per cent. To solve this problem, antifoaming agent (defoamer) is added to the concrete mix during the mix process. The most powerful antifoaming agents are silicon-based chemicals and have been used in this research.

The first challenge in this regard was to find the most effective antifoaming (AF) agent available in the market which would be chemically compatible with the cement hydration chemical reactions and would not have any negative effect on the concrete properties. After conducting comprehensive research about the chemical supplier companies and their relevant products and studying the products datasheet, six silicon-based AF agents were selected to be examined. In order to be able to select the most effective defoamer, several trial mixes of PMC with a constant P/C ratio and AF agents were performed. In all concrete mixes, the proportion of all kind of AF agents was exactly the same.

The effect of the each AF agent on fresh and hardened concrete properties such as slump, air content, density, and compressive strength were measured and examined. Test results

revealed that the PES-4B, which is a silicon oil type AF agent, showed better effect and performance comparing to the other products.

The specifications of the six initial selected AF agents are illustrated in Table 6-7.

Table 6-7 Specifications of used antifoaming agents

Antifoam	Type	State	Colour	pH	Density(g/m^3)
N-1000	Oil Based	Liquid	Hazy Amber	8	0.91
DPC	Blend Glycol	Liquid	White Milky	N/A	0.99
D3	Silicon Oil	Liquid	White Milky	8	1
D5100	Alcoxy derivative copolymers	Liquid	Light Yellow-Tan	N/A	0.9
D5002	blend of anionic & non-ionic surfactants	Liquid	Yellow-Tan	N/A	0.9
PES-4B	Silicon Oil	Liquid	light yellow	10	0.97

Six selected AF are presented in Figure 6-15. By selecting the most effective A/F agent, the second challenge began. The next step was to obtain and fix the most effective proportion of selected AF agent. To perform this, the AF agent proportions of 5%, 8%, 10%, and 15% by weight of the latex, were chosen to be investigated. The best results were related to the 10% proportion of AF agent in the mix. The average results of compressive strength for PMC with (10%AF) and without AF agent are presented in Figure 6-16. Improving compressive strength up to 42% was a fantastic result because this concrete gained approximately similar compressive strength as conventional concrete and can be classified as structural concrete.

Figure 6-15 Used antifoaming agents in this study

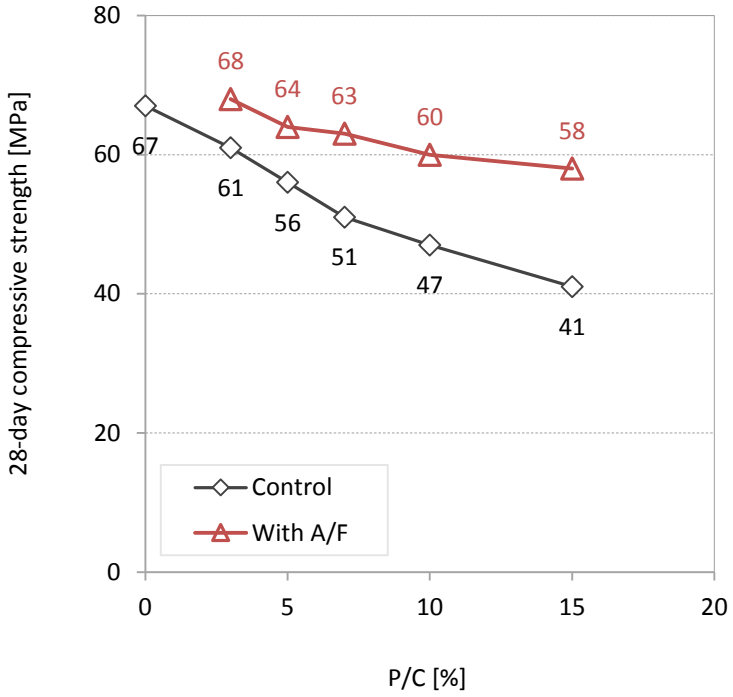

Figure 6-16 Effect of antifoaming agent on PMC compressive strength

6.4.5 Curing System

Wet curing system was performed for CC and FRC specimens (immersed in saturated water with lime) as can be seen in Figure 6-17.

Figure 6-17 Curing method for CC and FRC specimens

There is no guideline about the best curing system for PMC incorporating latex in the literature or standards. A comprehensive investigation was carried out and different curing regimes were examined to find out the best and the most effective curing method for PMC.

As a result of this investigation, it is found out that curing method for PMC is completely different with the curing regime for CC. Polymer (latex) modified concrete is very sensitive to moisture especially in the early ages. The type and duration of curing system have significant influence on the strength gain development rate and 28-day compressive strength as the final compressive strength. The polymer is in liquid form and it needs some time to lose the water in order to be solidified. During this period, PMC should not be exposed to moisture; otherwise solidification of polymer will never take place.

Different curing methods were applied to the specimens and 7-day and 28-day compressive strength test were conducted to compare the efficiency of the different methods. The experimental results of this study showed that the best curing regime is maintaining the specimens in an environment with 100% of relative humidity for the first 48 hours (see Figure 6-18). After that, specimens should be immersed as wet curing for five (5) days. In this stage, 7-day compressive strength was performed. Then, specimens should be air cured for 21 days to allow the excess water to evaporate and this allows the latex film to be formed. After this period, 28-day compressive test was conducted.

The experimental results illustrate that the first 48 hours 100% of relative humidity cause the basic strength of PMC to be achieved, because the latex is allowed to undergo film

formation. After film formation, standard wet curing will not adversely affect strength development. Five days of wet curing is undertaken to prevent the evaporation of mixing water which is needed for hydration process. After this period, the formation of polymer film will not allow the mixing water inside the concrete to be evaporated and 21 days air-cured period does not affect the cement hydration process. Figure 6-19 presents the average of compressive strength test results of both CC and PMC exposed to different curing procedures.

Figure 6-18 Moisture curing of PMC and FRPMC specimens for 48 hours

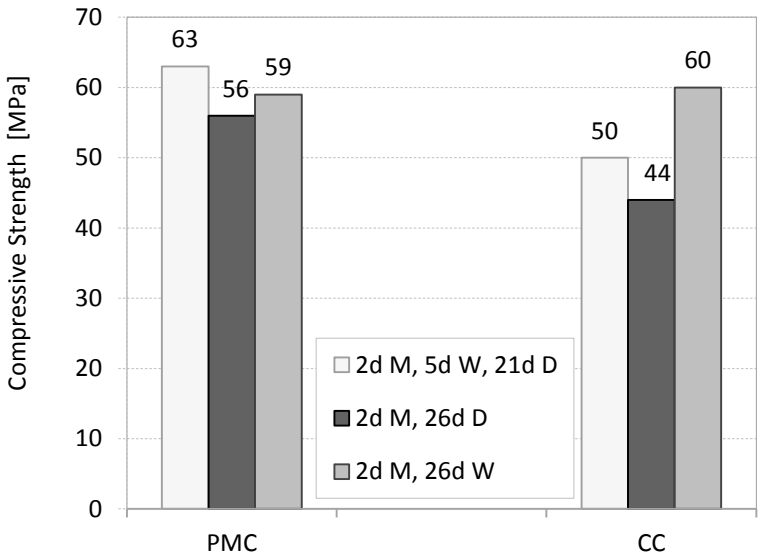

Figure 6-19 Effect of different curing methods on compressive strength of CC and PMC

6.4.6 Concrete Trial Mixes

To achieve an optimum concrete mix design, trial mixes were prepared and fresh and hardened concrete properties were measured and determined. The first trial mixes were conducted to find out the effect of clay and other impurities stuck to the coarse aggregate on the compressive strength of the concrete. To investigate this effect, some specimens with unwashed and some with washed coarse aggregate shown in Figure 6-20 were prepared and tested.

Figure 6-20 Washed coarse aggregate

Concrete mix characteristics are presented in Table 6-8. The summary of test results of trial mixes compressive strength for washed and unwashed coarse aggregate are presented in Table 6-9. The results show that using unwashed aggregate decreases the compressive strength up to 12%. Consequently, the coarse aggregate for making main specimens were washed and dried to saturated surface dry (SSD) condition.

Table 6-8 Trial concrete mix to investigate the effect of unwashed aggregate on concrete properties

Specimen Code	Sub	Aggregate condition	Cement Kg/m^3	20mm Kg/m^3	10mm Kg/m^3	CS Kg/m^3	FS Kg/m^3	Water Kg/m^3	w/c Kg/m^3	S/P ml/m^3
F1	F1-1	U*	400	880	293	586	195	160	0.4	2350
	F1-2		400	880	293	586	195	160	0.4	2350
	F1-3		400	880	293	586	195	160	0.4	2350
F2	F2-1	W**	400	880	293	586	195	160	0.4	2270
	F2-2		400	880	293	586	195	160	0.4	2270
	F2-3		400	880	293	586	195	160	0.4	2270
F3	F3-1	U	400	880	293	586	195	140	0.35	2520
	F3-2		400	880	293	586	195	140	0.35	2520
	F3-3		400	880	283	586	195	140	0.35	2520
F4	F4-1	W	400	880	293	586	195	140	0.35	2460
	F4-2		400	880	293	586	195	140	0.35	2460
	F4-3		400	880	293	586	195	140	0.35	2460

*Unwashed Coarse Aggregate
** Washed Aggregate

Table 6-9 Effect of washed and unwashed coarse aggregate on concrete compressive strength

Specimen Code	Mean 28-day Compressive Strength (MPa)
F1	51
F2	56
F3	60
F4	67

In this study some fresh properties of the concretes such as slump, air entrapped, and density have been monitored and measured. The summary of the test results is presented in Table 6-10.

Table 6-10 Fresh properties of different concrete categories

Specimen Code	Superplasticizer (ml)	Slump (mm)	Air entrapped (%)	Density (kg/m^3)
CC	2970	65	1.5	2510.24
FRC1	3145	62	2.0	2500.84
FRC2	3210	55	2.1	2506.59
FRC3	3280	51	2.3	2545.93
PMC1	1800	67	1.6	2558.21
PMC2	1720	72	-	-
PMC3	1650	75	1.8	2503.24
PMC4	1610	77	-	-
PMC5	1585	82	2.1	2499.93
FRPMC1	2885	65	1.7	2505.1
FRPMC2	2820	67	1.9	2483.2
FRPMC3	2795	73	2.2	2473.75
FRPMC4	2985	63	2.3	2494.18
FRPMC5	2935	68	2.2	2480.79
FRPMC6	2880	70	2.3	2455.16
FRPMC7	3010	58	2.2	2442.94
FRPMC8	2975	66	2.4	2430.96
FRPMC9	2915	73	2.4	2429.24

Since the fresh concrete properties affect the hardened concrete properties, some fresh concrete properties such as slump, density, and air content were measured and controlled (as a part of concrete quality control) for all concrete batches. The measurement of these properties is shown in Figure 6-21 and Figure 6-22, respectively.

Figure 6-21 Slump test

Figure 6-22 Air entrapped measurement

6.4.7 Compressive Strength

The most commonly used hardened concrete property is compressive strength. This is partly because it is an easy test to perform. Moreover, many of desirable characteristics of concrete are qualitatively related to its compressive strength. However, the main reason for compressive test popularity is the intrinsic importance of the compressive strength in concrete structural design (Neville, 1991). In the Australian Standards, method of testing concrete, only cylindrical specimens which are prepared in accordance with AS 1012.8 are satisfactory to be tested to determine the concrete compressive strength. Specimens for compressive test are shown in Figure 6-23.

Figure 6-23 Specimens for compressive strength test

Therefore, all compressive tests are performed on standard cylinders (100 mm × 200 mm) following AS 1012.9-1999 procedural requirements. Compressive strength test was conducted according to Australian Standard AS1012.14. Universal compressive test machine is shown in Figure 6-24.


Figure 6-24 Compressive test machine

6.4.8 Indirect Tensile Strength

The indirect tensile test ('Brazilian' or splitting test) is an indirect way of determining the tensile strength of concrete. The tensile strength measured in the splitting test is believed to be close to the direct tensile strength of concrete (Neville 1991).

In this study, the indirect tensile test is conducted in accordance with AS 1012.10 -2000 on standard cylinders. The concrete cylinder is loaded until the failure takes place by indirect tension in the form of splitting along the vertical diameter. For each concrete type, indirect tensile test is performed at 7 and 28 days of age and for each age, 3 cylindrical samples are tested. The test is conducted under a load scale of 1800 kN universal testing machine with load rate equivalent to 1.5 ± 0.15 MPa per minute. The indirect tensile strength of the specimen is calculated by Equation 6.4.

$$f_{ct.sp} = \frac{2000\,P}{\pi LD} \tag{6.4}$$

where $f_{ct.sp}$ is the indirect tensile strength in MPa, P is the maximum applied force in kN, L is the length of specimen in mm and D is the diameter in mm.

6.4.9 Flexural Tensile Strength, Modulus of Rupture (MOR)

The cast specimens for flexural test are shown in Figure 6-25.

Figure 6-25 Specimens for flexural test

Flexural tests for CC and PMC specimens were performed based on AS 1012.11-2000 and modulus of ruptures were calculated from the Equation (6.5).

$$f_{ct.f} = \frac{PL1000}{BD^2} \tag{6.5}$$

where $f_{ct.f}$ is the modulus of rupture in MPa, P is the maximum applied force in kN, L is span length in mm, B is the average width of the specimen at the section of failure in mm and D is the average depth of specimen at the failure section in mm.

Flexural tests for FRC and FRPMC specimens were performed according to ASTM C1609 which has been specially specified for FRC.

Flexural test set up is presented in Figure 6-26.

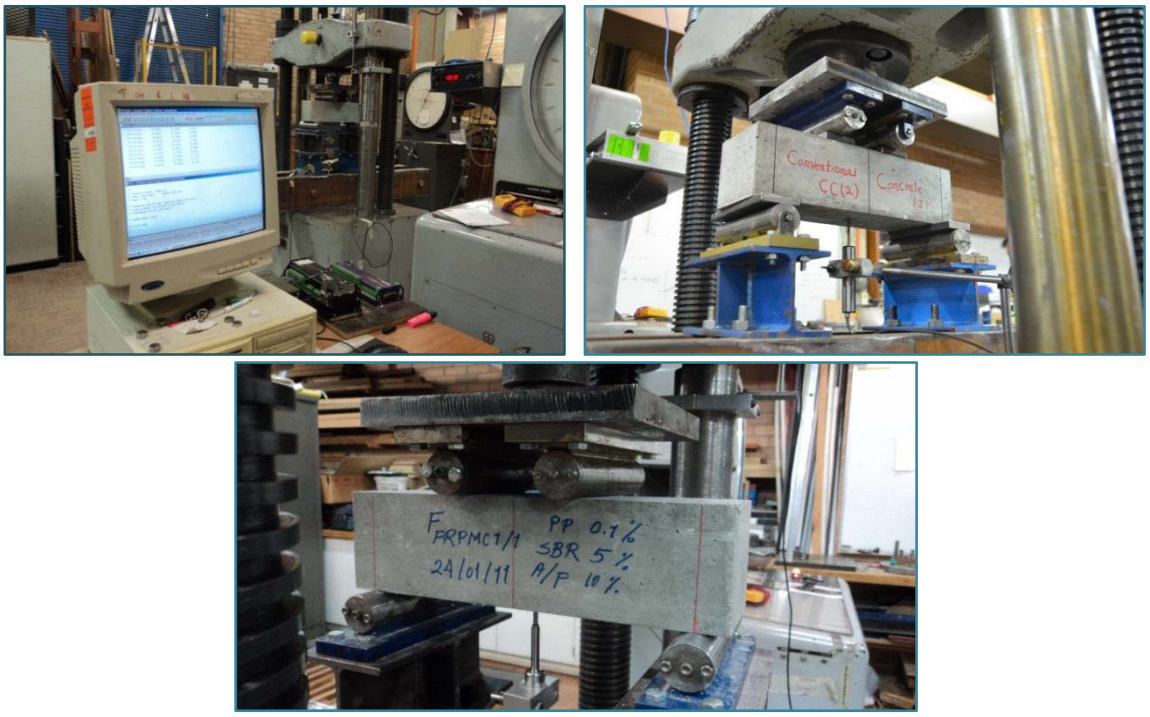

Figure 6-26 Flexural test machine and set up

6.5 DURABILITY ASSESSMENT TESTS

As discussed earlier in Chapter 2, chloride diffusion into the concrete is the dominant factor in deterioration of RC structures. By measuring the chloride ions concentration in different depths of the concrete cover at certain times, it will be possible to predict the time when chloride content near steel reinforcement will reach to critical chloride level. The time from construction of the structure to reaching chloride content to a critical level at the steel reinforcement surface is called corrosion-free service life. Therefore, preparing chloride profile from the laboratory specimens or field core samples can be used to predict the corrosion-free service life of the structure.

Assuming the initiation time of steel corrosion in the concrete, as the end of the service life, is a conservative method to estimate the structure service life. Therefore, it is optimised to consider the time corresponding to the crack formation on the concrete cover as the end of the service life. This assumption means considering corrosion initiation time plus corrosion propagation time till the generation of the first crack on the concrete cover.

Therefore, to assess the chloride diffusion resistance of different concrete types, the chloride profile of the concrete exposed to long-term pure diffusion test and also time to corrosion-induced cracking utilizing accelerated chloride-induced corrosion were monitored and measured.

Diffusion and absorption are two major transport mechanisms involved in chloride ingress into the concrete.

Diffusion occurs due to the chloride concentration gradient and is a relatively slow and continuous process. This mechanism is quite well understood, although the following factors complicate the process:

- Chloride diffusion coefficient decreases with time due to the enhancement of concrete pore structure. Whereas, most diffusion equations assume a constant coefficient.
- Periodic wetting and drying cycles causes the increase of surface chloride concentration with age (time) instead of being constant as it is commonly assumed.

Absorption occurs due to surface tension (capillary action) and involves a liquid being sucked into originally empty or partially filled pores in the concrete by capillary forces. There will be no absorption if the pores are full. Thus, absorption continues until saturation or until there is no more reservoir of solution (Hong and Hooton, 1999). It can therefore be seen that absorption is a discontinuous process.

Although, during the last decade, considerable attention has been paid to absorption, there is still lack of understanding of the mechanism of chloride ingress in concrete exposed to cyclic wetting and drying. The relationship between absorption and depth of chloride penetration in concrete has not been established accurately yet. Chloride penetration prediction models are based on diffusion and ignore the effect of absorption phenomenon.

There are also complications interpreting sorptivity values as a measure of capacity of concrete absorption. Absorption of concrete is very sensitive to the moisture state of the concrete and therefore specimens should be conditioned to a defined initial state of moisture, before taking any measurements. This sensitivity to the initial moisture content causes problems and difficulties in measuring the absorption properties of concrete and comparing the values of sorptivity reported in different works.

As a result of both diffusion and absorption mechanisms, chloride ions penetrate into the concrete and after reaching chloride threshold level at the steel surface, the corrosion process can be initiated.

Some scholars believe that service life of a RC structure is ended with the initiation of steel corrosion. This service life, which is equal to the initiation time of corrosion, is called corrosion-free service life and relatively is a conservative value of service life. The base of this assumption is the corrosion initiation time is much longer than the time from corrosion initiation to cover cracking (Funahashi, 1990, Maage et al., 1996, Liang et al., 1999, Khatri and Sirivivatnanon, 2004).

It is widely accepted that the state of cover cracking induced by corrosion is identified as serviceability limit state of reinforced concrete structures. (Bhargava et al., 2006, Angst et al., 2012, Chen and Mahadevan, 2008, Guzmán et al., 2011). In this case, the total service life of the structure is equal to initiation plus propagation time of corrosion till the initiation of the crack.

In the experimental phase of this research, for all polymer-concrete composites and conventional concrete specimens, service life has been investigated, estimated, and compared by utilizing initiation time of corrosion.

For estimation of corrosion-free service life, the chloride content has been measured and prepared by providing pure diffusion mechanism. For estimation of time to corrosion-induced crack, coupled diffusion and absorption mechanisms by providing wetting and drying cycles along with the high concentration of chloride solution as environmental exposure conditions were performed. After 18 months of the simulated environmental exposure, to obtain the time to cover cracking, an accelerated electrochemical method was deployed.

By obtaining the results of these tests, comparing the durability performance of different concrete types can be carried out more accurately and reliably.

6.5.1 Pure Diffusion Test Method (Chloride Profile)

Diffusion measurement test can be divided into three categories of steady state, non-steady state and electrical tests. The electrical tests can also be subdivided into two groups of steady state or non-steady state electrical tests. Each method has advantages and weaknesses and, therefore depending on the situation, suitable test should be selected and applied.

The advantage of electric methods is that that they can achieve the results rapidly and the limitation is that they measure directly the conductivity of concrete not its chloride diffusivity. Although, some attempts at correlating the electrical tests results and chloride diffusivity tests results have been carried out, still there is a lack of understanding the fundamental involved processes. This uncertainty makes the interpretation of the results complicated and doubtful. Hence, it is better to avoid using electrical test method if there is sufficient time to perform chloride diffusivity testing.

All steady-state and non-steady-state diffusion tests are time consuming and therefore not suitable for use in quality control. However, they can be used in laboratory experiments and they also have the advantage of yielding a meaningful value of chloride ion diffusivity.

Among the long-term diffusion tests like Diffusion Cell, Ponding Test and Bulk Diffusion Test, Bulk Diffusion Test (NT Build 443) is claimed to be the most accurate as it measures pure diffusion (Stanish and Thomas, 2003).

In the Diffusion cell test the condition of specimens is not consistent with the condition of the concrete in practice (Page et al., 1981, Basheer et al., 2001). In the Ponding test diffusion is not the only mechanism involved in the transport of chloride into concrete and other mechanisms such as absorption or wicking action are also associated with chloride penetration (Stanish et al., 1997).

To conduct the Bulk Diffusion test, cube specimens (100mm×100mm×100mm) were cured for 28 days. After curing period, they were coated on five sides with epoxy resin and left for 24 hours for the epoxy to cure. Then, they were immersed in water and weight gain of each cube was recorded every day. The immersion in water was continued until the weight gain was less than 0.01% of the sample weight per day to make sure that the

concrete was fully saturated. They were then immersed in salt solution (NaCl) with concentration of 16.5% for diffusion test as shown in Figure 6-27 and Figure 6-28.

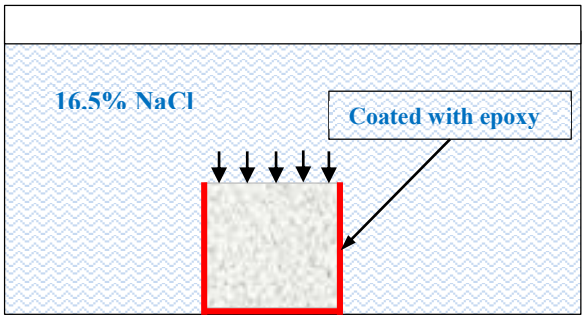

Figure 6-27 Exposure conditions and duration based on Volhard Method

Figure 6-28 Exposure condition

The test method to obtain chloride content in the sample was conducted based on RILEM TC178-TMC, 'Analysis of Total Chloride Content in Concrete', analysis of total chloride content in concrete (Rilem).

The procedure of ground concrete sample preparation can be seen in Figure 6-29 and Figure 6-30. In this procedure, concrete sample is cut into slices with 10 mm of thickness with dry saw.

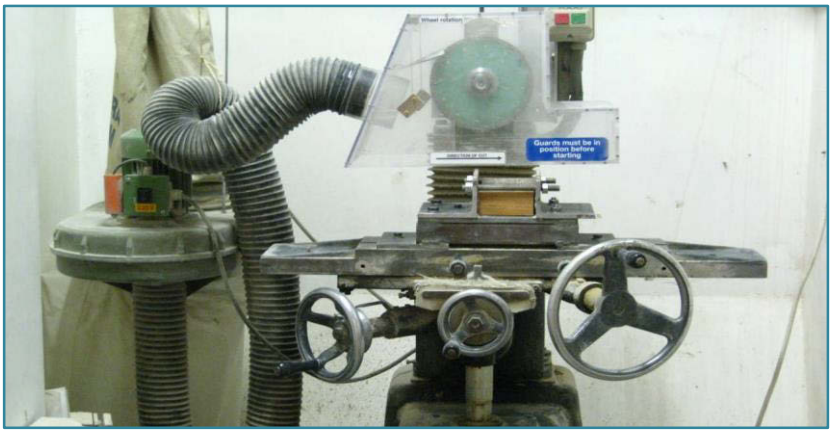

Figure 6-29 Concrete grinding machine

Figure 6-30 Concrete powder samples

This method is called Volhard Method of analysis (extraction and quantification) of total chloride content in hardened concrete. In this method, the sample must be ground to pass through a 0.16 mm sieve, carefully homogenised and dried at 105-110°C for 24 hours. At least two sample portions must be weighted to the nearest 0.0001g and be tested. In the Volhard method, chlorides are first precipitated with excess silver nitrate, then excess silver is titrated with potassium (or sodium) thiocyanate. To detect end point we use Fe3+ cations, which easily react with the thiocyanate, creating distinct wine red complex.

There are two reactions, as this is a back titration. First, we precipitate chlorides from the solution:

$$Ag^+ + Cl^- \rightarrow AgCl\ (s)$$

Then, during titration, reaction taking place is:

$$Ag^+ + SCN^- \rightarrow AgSCN\ (s)$$

In back titrations sample size is more difficult to calculate than during normal, direct titrations. For best accuracy excess of silver should be titrated with about 40-45 mL of titrant (we used 50 mL burette). We start with 50 mL of pipetted silver nitrate and we will titrate excess with about 25 mL of thiocyanate solution, and finally assuming both solutions used are 0.1 M, aliquot taken for titration should contain about 0.09 g chloride anion (2.5 millimoles).

Note, that silver nitrate can be added not using single volume pipette, but from burette. If the amount of chlorides is approximately known, this way it is possible to control excess of silver nitrate and volume of the thiocyanate titrant.

End point is detected with the use of iron (III) thiocyanate complex, which have very distinct and strong wine colour.

As in every back titration, to calculate amount of substance we have to subtract amount of titrated excess from the initial amount of reactant used. In the case of argentometric calculations are easy, as all substances used react on the 1:1 basis.

First we have to calculate number of moles of silver nitrate initially added to the chlorides sample. Assuming it was 50 mL of 0.1 M solution, it contained 5 millimole of silver. Then, excess was titrated according to the reaction equation:

$$Ag^+ + Cl^- \rightarrow AgSCN\ (s)$$

Thus amount of excess silver is C×V, and amount of Cl is 0.005-C×V moles.

The procedure of the test is expressed as follows:

- Pipette aliquot of chlorides solution into 250mL Erlenmeyer flask
- Add 5 mL of 1+1 nitric acid
- Dilute with distilled water to about 100 mL
- Add 50 mL of 0.1M silver nitrate solution
- Add 3 mL of nitrobenzene
- Add 1 mL of iron alum solution
- Shake the content for about 1 minute to flocculate the precipitate

- Titrate with thiocyanate solution till the first colour change

By obtaining chloride profile, the Crank's error function solution to Fick's second law discussed earlier (Equation 2.17) is fitted to the chloride curve to estimate chloride diffusion coefficient (Stanish et al., 1997).

The used chemical substances and deployed equipment to carry out the measurement of the chloride content are shown in Figure 6-31 and Figure 6-32, respectively.

Figure 6-31 Potassium chromate and silver nitrate solutions for identifying concentration of chloride ions in salt solution

Figure 6-32 Equipment used for chemical tests

6.5.2 Time to Corrosion-Induced Crack

Since the corrosion of reinforcing steel bars is a long term electrochemical process, the electrochemical accelerated methods can help to obtain the results in relatively shorter time for laboratory investigations (Saetta, 2005, Ha et al., 2007). Accelerated Chloride-Induced Corrosion (ACIC) Test method, which have been used with various scholars, with constant impressed voltage was performed to identify the time to crack initiation in the concrete cover for all categories of concrete (Rossignolo and Agnesini, 2004, Okba et al., 1997, Shaker et al., 1997).

Time to corrosion-induced crack was considered as a criterion for chloride diffusion resistance of the concrete. The specimen with longer time to cracking is considered higher resistant to chloride diffusion

In this electrochemical test, the embedded steel in concrete acts as an anode and steel bar performs as a cathode and the electrolyte is Sodium Chloride solution with 15% concentration. During the test a 30 V constant voltage is applied from the external DC source between anode and cathode. The intensity of electrical current versus time is continuously recorded by using high resolution digital data logger (see Figure 6-33).

Figure 6-33 High resolution data logger

According to the concept of this method, any impulsive raise in electrical current indicates corrosion-induced cracking in concrete cover. The time correspond to this raise of current is considered as corrosion time. The schematic of the test arrangement is shown in Figure 6-34.

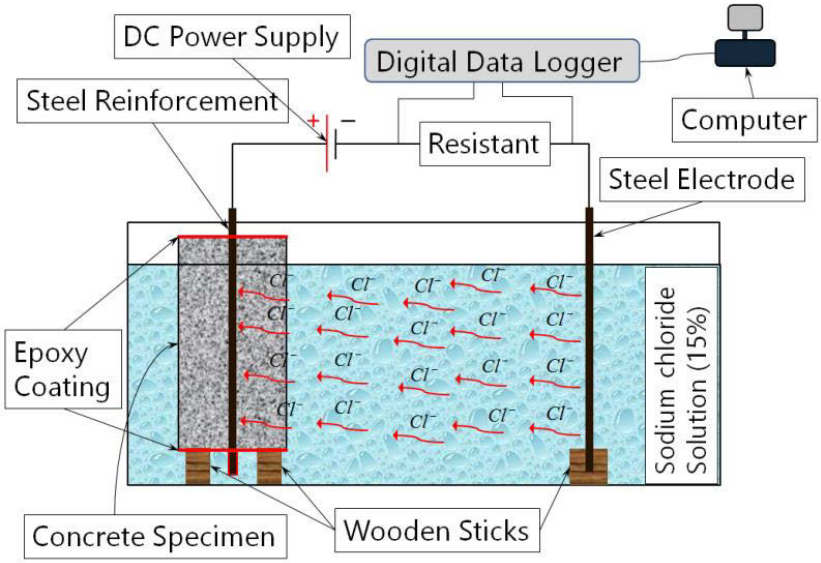

Figure 6-34 Schematic arrangement of accelerated chloride-induced corrosion test

Selection of the constant voltage of 30 V was carried out based on the test results performed by McGrath and Hooton (McGrath and Hooton, 1996). According to their

investigation on influence of voltage on chloride diffusion coefficient, 30 Volts applied potential showed the least error in calculating chloride diffusion coefficient utilizing both non-steady-state and steady-state approach. They concluded that the resulting error increases as applied potential decreases.

Some equipment and laboratory test set up for the measurement of time to cracking is presented in Figure 6-35. In order to determine the time at which the specimen cracked (referred to as corrosion time), the intensity of the electric current was recorded at different time intervals by high resolution digital data logger and the specimens were monitored periodically by visual inspection.

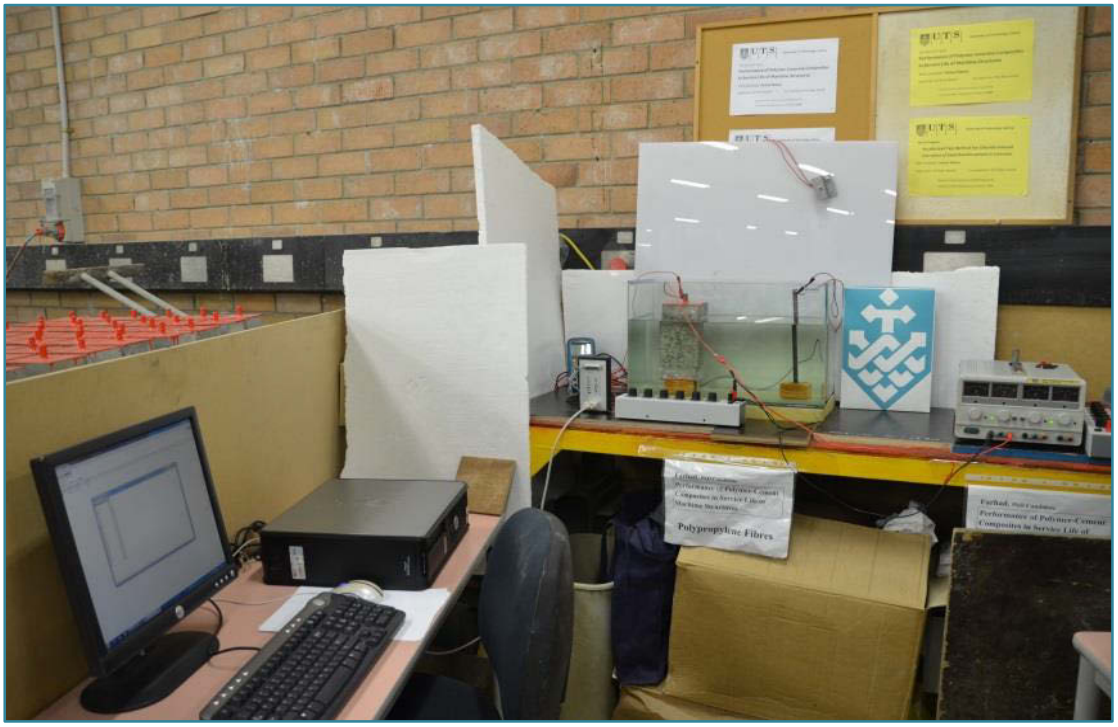

Figure 6-35 Time to corrosion-induced crack laboratory test set up

To prepare the specimens for estimation of time to corrosion-induced crack, they were exposed to one week of wetting in high concentration of chloride solution following by two weeks of drying by powerful fan in ambient environment. The prepared samples for ACIC test are shown in Figure 6-36. The wetting and drying cycle conditions are shown in Figure 6-37 and Figure 6-38, respectively.

Figure 6-36 Samples for ACIC test

Figure 6-37 Wetting cycle conditions

Figure 6-38 Drying cycle conditions

6.6 SUMMARY

In this chapter experimental phase has been presented extensively. To produce high quality of conventional concrete, firstly an accurate aggregate sieve analysis was accomplished and relatively uniform aggregate grading to make a dense concrete with the porosity as low as possible was obtained. Secondly, several trial concrete mixes were prepared and controlled to obtain the optimum mix proportions. Mix design assumptions were considered based on "Durability Design of Maritime Structure" AS 4997-2005.

According to literature review results, the mechanical properties of PMC are not in the acceptable range and cannot be deployed as a structural concrete. Compressive strength of PMC was dramatically decreased by increasing P/C ratio. A comprehensive experimental investigation was carried out to overcome this malfunction and improve mechanical properties of PMC. The problem was associated to the generation of the large amount of air bubbles in concrete (foaming phenomenon) mix after mixing latex with the cement which could reduce the density as well as compressive strength of the concrete remarkably. This problem was solved by searching for suitable antifoaming agents, testing the performance of all antifoaming agents, selecting the most effective one, and investigating the best proportion of the selected antifoaming agent.

As chloride diffusion into the concrete is the dominant factor in deterioration of the concrete structures, chloride diffusion resistance is considered as the most important criteria for assessment of concrete durability.

To assess the durability of the different concrete types, two methods including providing chloride profile in pure diffusion test condition (according to NordTest: NT Build 443) and time to corrosion-induced crack by deploying accelerated chloride-induced corrosion test method, were applied.

With chloride content results, time-dependency of chloride diffusion coefficient can be investigated by the proposed mathematical model can be calibrated by experimental results.

Reinforced concrete specimens were exposed to high concentration chloride solution (15%) and wetting and drying cycles for 12 months. After this period, accelerated

chloride-induced corrosion test were conducted to obtain time to cracking of the specimens which can be considered as resistance of concrete to chloride diffusion.

CHAPTER 7

EXPERIMENTAL RESULTS AND DISCUSSION

CHAPTER 7. EXPERIMENTAL RESULTS AND DISCUSSION

7.1 INTRODUCTION

In this chapter the results of experimental program are presented and discussed. The experimental results can be divided into two major groups including the results related to physical and mechanical properties; and the results regarding to durability performance of the different type of concretes exposed to severe environmental exposure.

Physical and mechanical properties results include (1) fresh concrete properties such as density, air entrapped, and slump; and (2) hardened concrete properties such as compressive strength, tensile strength and flexural strength. These tests have been conducted to insure that all types of concrete have desired/acceptable mechanical properties in order to be used as structural materials. Also, these properties can be compared to find out the effect of polymer-concrete composites on mechanical properties of the concrete.

Durability assessment can be divided to two separate experimental procedures. One group of results is the durability performance of the concretes in terms of chloride diffusion process by measuring the chloride content within different depths over the time. The chloride content is a common used criterion to compare and assess the chloride resistance of the concrete samples. Chloride concentration at the steel reinforcement surface identifies the risk of the steel corrosion in concrete by comparing to the chloride threshold

level. The results of these tests can be used to predict the corrosion-free service life or in another word, to estimate corrosion initiation time.

The second group of the tests is the measurement of time to corrosion-induced crack by conducting accelerated electrochemical method. In this test, the concrete specimen, which has been reinforced with one embedded 12 mm steel bar, is subjected to external constant potential and high concentration of chloride solution till the generation of the first crack. The time corresponding to cracking can be considered as the end of the service life of the structure. This method indicates the service life as the time up to cover cracking which includes both initiation corrosion time and corrosion propagation time.

Figure 7-1 shows the experimental results classification of this study.

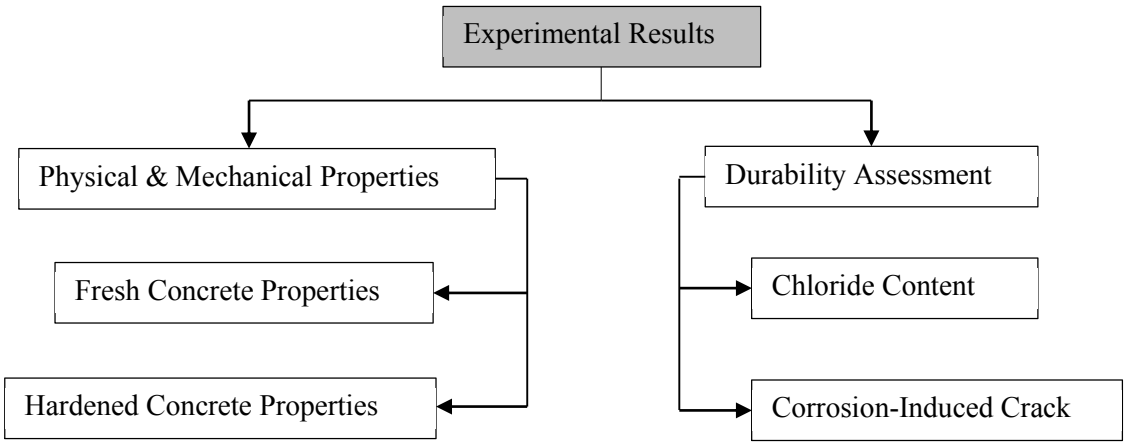

Figure 7-1 Experimental results classification

In this chapter the following contractions are used:

- Conventional Concrete: CC
- Fibre Reinforced Concrete: FRC
- Polymer Modified Concrete: PMC
- Fibre Reinforced Polymer Modified concrete: FRPMC
- Polypropylene Fibres: PP Fibres
- V_f: Ratio of PP Fibres volume to concrete volume

- Polymer Cement Ratio: P/C

7.2 FRESH CONCRETE PROPERTIES

In this section the discussion related to the plastic state results of the conventional concrete and polymer-concrete composites are presented. Measurable quantities of fresh concrete including air content, slump, and density are presented and discussed. The averages of the results related to fresh concrete properties are illustrated in Table 7-1.

Table 7-1 Average of fresh concrete properties

Concrete Type	Code of Samples	PP Fibers V_f, [%]	Latex P/C, [%]	Air Content [%]	Slump [mm]	Density [kg/m^3]
CC	CC	0	0	1.8	50	2521
FRC	FRC1	0.1	0	1.9	50	2510
	FRC2	0.2	0	2.0	65	2499
	FRC3	0.3	0	2.1	60	2487
PMC	PMC1	0	5	2	65	2496
	PMC2	0	10	2.1	70	2474
	PMC3	0	15	2.3	65	2458
FRPMC	FRPMC1	0.1	5	1.7	65	2496
	FRPMC2	0.1	10	1.9	60	2485
	FRPMC3	0.1	15	2.2	60	2467
	FRPMC4	0.2	5	2.3	50	2492
	FRPMC5	0.2	10	2.4	60	2481
	FRPMC6	0.2	15	2.2	65	2465
	FRPMC7	0.3	5	2.1	50	2477
	FRPMC8	0.3	10	2.3	50	2473
	FRPMC9	0.3	15	2.3	55	2460

7.3 COMPRESSIVE STRENGTH

As specified in AS 1012.9, all cylinder test specimens are prepared to be capped by gypsum as shown in Figure 7-2, which is to be contact with the platens of a testing machine, to achieve a plane surface in order to provide uniform loading.

Figure 7-2 Capped specimens by gypsum for compressive strength test

For both 7-day and 28-day compressive test three specimens were examined. The average of the compressive strength test results, accompany with the error analysis, are presented in Table 7-2.

Figure 7-3 shows the rate of compressive strength development for FRC (a) and PMC (b) samples which are compared to the behaviour of CC sample. The rate of strength improvement of FRCs from 7-day to 28-day was clearly higher than CC. The reason can be expressed as the improvement of bond strength between fibres and cement matrix. Increasing bond strength causes the higher contribution of fibres in bearing the load after crack generation (bridging effect). Figure 7-4 illustrates the strength development of FRPMCs specimens against CC. Using PP fibres in PMC increased the compressive strength of PMCs considerably.

Table 7-2 Average of compressive strength test results

Concrete Type	7-day Compressive Strength (MPa ± SD*)	28-day Compressive strength (MPa ± SD)
CC	47.0 ± 2.38	67.0± 2.00
FRC1	49.0 ± 1.48	72.0 ± 1.22
FRC2	51.0 ± 1.43	75.0± 1.14
FRC3	53.0 ± 1.15	76.0 ± 1.64
PMC1	47.0 ± 2.42	66.0 ± 1.28
PMC2	44.0 ± 2.03	64.0 ± 1.34
PMC3	43.0 ± 2.09	63.0 ± 1.47
FRPMC1	48.0 ± 1.43	70.0 ± 1.74
FRPMC2	47.0 ± 1.30	68.0 ± 1.25
FRPMC3	46.0 ± 1.85	66.0 ± 1.44
FRPMC4	50.0 ± 1.17	74.0 ± 1.99
FRPMC5	47.0 ± 1.45	72.0 ± 1.21
FRPMC6	45.5 ± 1.91	68.0 ± 1.61
FRPMC7	48.0 ± 1.26	77.0 ± 1.54
FRPMC8	46.0 ± 1.69	74.0 ± 1.77
FRPMC9	45.0 ± 1.44	71.0 ± 1.86

Average of compressive strength test results was calculated to the nearest 0.5 MPa in accordance to AS 1012.9.
*Statistical Deviation

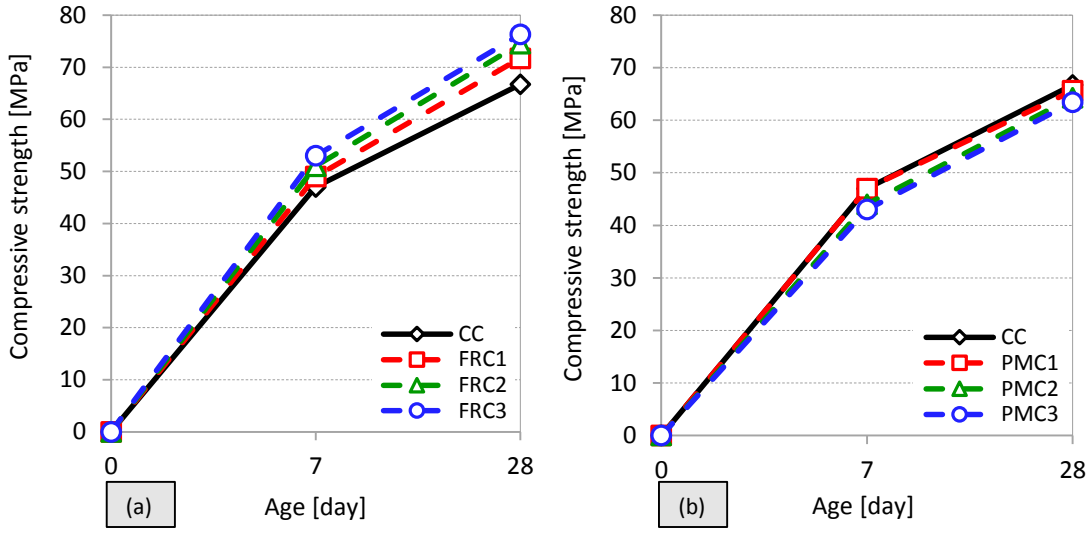

Figure 7-3 Compressive strength development of FRCs (a) and PMCs (b)

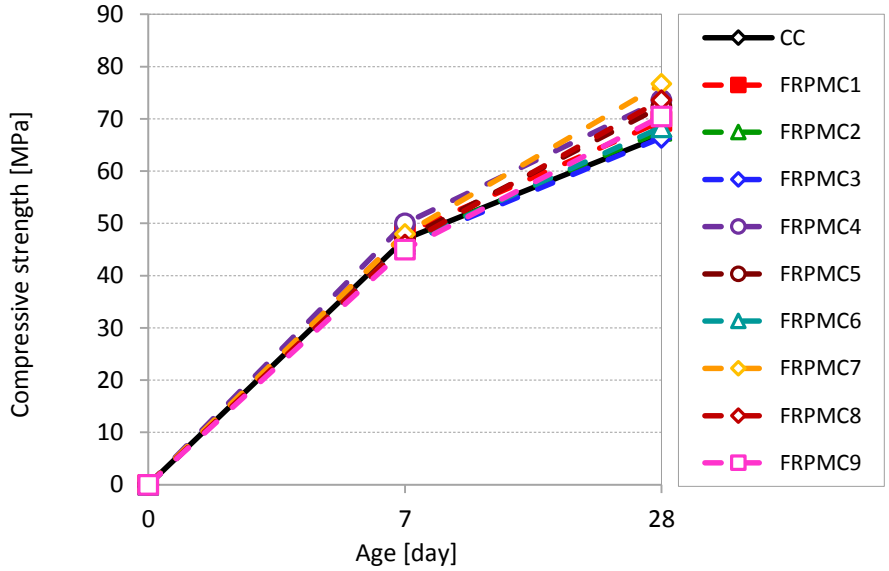

Figure 7-4 Compressive strength development of FRPMCs

As a general trend, FRCs showed slightly higher compressive strength than CC. FRCs compressive strength increases by increasing the proportion of PP fibres (see Figure 7-5 a). PMCs indicated lower compressive strength than CC. The strength reduction was correspondence with polymer cement ratio increment (see Figure 7-5 b). Although, the compressive strength test results of PMCs are less than CC strength they are still in acceptable range of target strength which was assumed as 60 MPa and can be categorised

as a structural concrete. The strength gain of PMC was one of the achievements of this study.

Figure 7-5 (a, and b) presents the effects of PP fibres and latex proportions on concrete compressive strength, respectively. The graphs show that flexural strength changes linearly with proportions of PP fibres and latex in the concrete. Two empirical models to predict compressive strength of FRCs and PMCs regarding the proportion of polymers are suggested as follows:

For FRCs: $f_{cm} = 31.6\,(V_f) + 67.56$ (7.1)

For PMCs: $f_{cm} = -0.22\,(P/C) + 66.68$ (7.2)

where f_{cm} is compressive strength, V_f is the volume fraction of PP fibres [%], and P/C is the polymer cement ratio [%].

Figure 7-6 confirms that using PP fibres improves compressive strength of PMC. For instance; Compressive strength of PMC3 incorporating latex, with P/C of 0.15, is 63.4 MPa. Concrete types corresponding PMC3 are FRPMC3 (0.1% of PP fibres), FRPMC6 (0.2% of PP fibres), and FRPMC9 (0.3% of PP fibres) with the same proportion of latex gaining 66.4 MPa, 68.4 MPa, and 70.5 MPa of strength, respectively. The strength improvements are 4.73% for FRPMC3, 7.89% for FRPMC6, and 11.2% for FRPMC9.

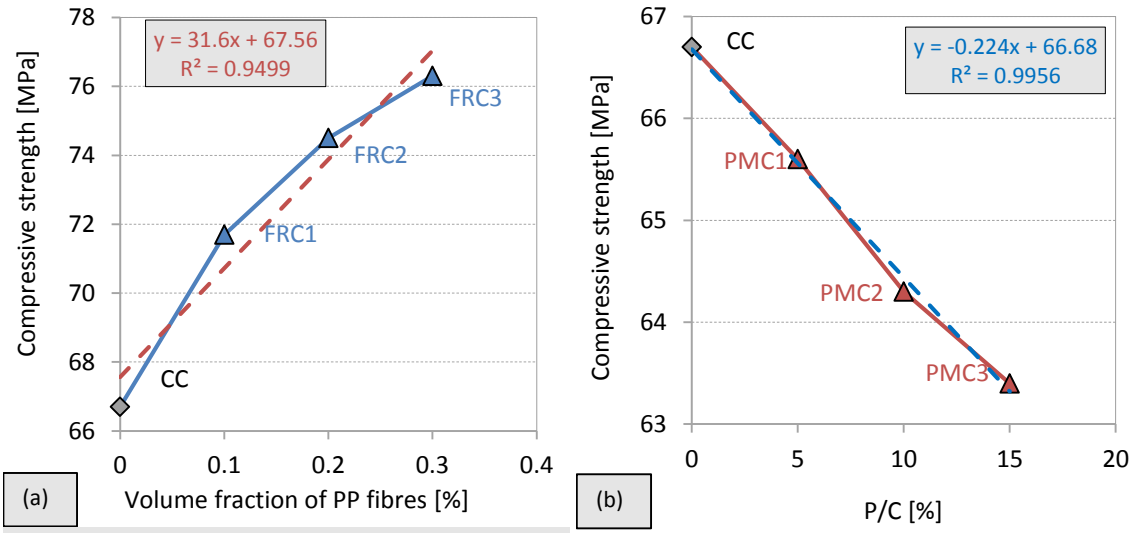

Figure 7-5 Compressive strength of FRCs (a) and PMCs (b)

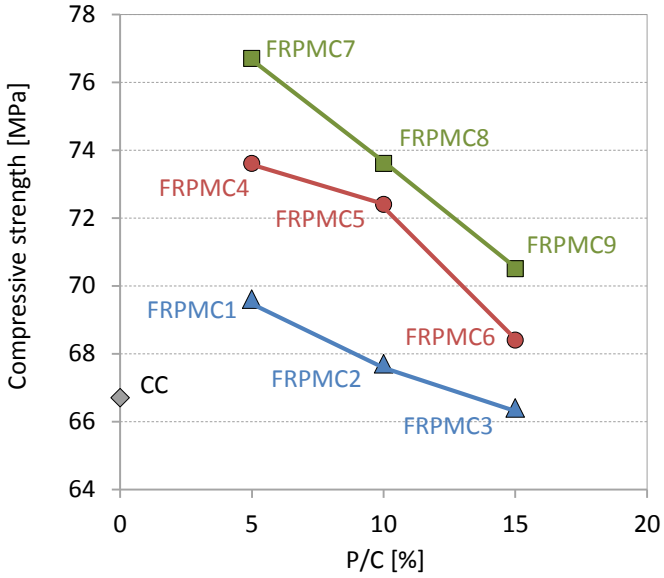

Figure 7-6 Compressive strength of FRPMCs

Figure 7-7 specifies the effect of polymers on compressive strength of the concrete. As can be seen, PP fibres increased the compressive strength up to 14% by using volume fraction of 0.3% of PP fibres. Whereas, latex polymer reduced the compressive strength up to 5% compared to CC which was not a significant reduction.

Applying both PP fibres and latex in concrete, to make a complete polymer-concrete composite structure, definitely improved the compressive strength up to 16% in FRPMC7. Conjunction of latex with PP fibres in concrete increased the bond strength by modifying the interfacial transition zone between fibres and cement matrix. Bond strength improvement has been achieved by reducing the porosity of the interfacial zone.

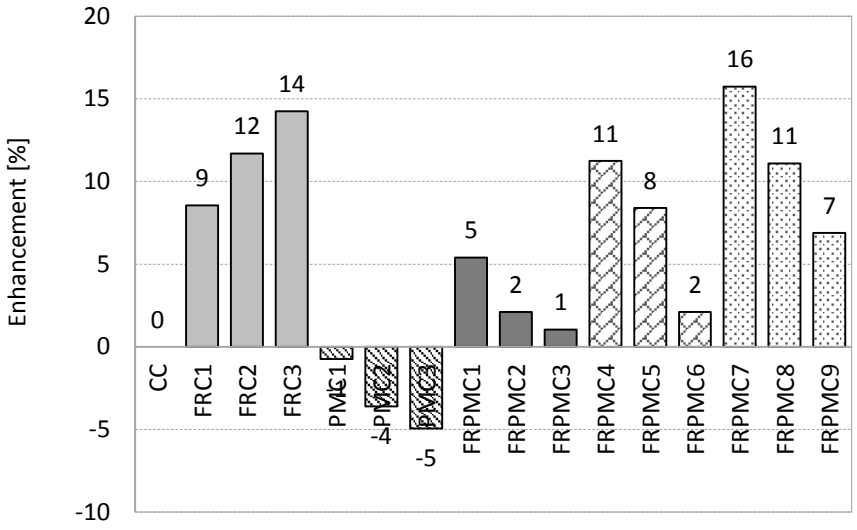

Figure 7-7 Effect of polymer-concrete composites on compressive strength

7.4 FLEXURAL STRENGTH

Flexural tests were conducted in accordance with two standards AS 1012.11-2000 for CC and PMC specimens and ASTM C1609 for FRC and FRPMC specimens. Some specimens after test are shown in Figure 7-8.

Figure 7-8 Specimens after flexural test

The average results of maximum load, maximum deflection, and modulus of rupture for each concrete category are presented in Table 7-3.

Table 7-3 Average results of flexural test

Concrete Type	Max. Load [kN]	Max. Deflection [mm]	$f_{ct,f}$ [MPa]
CC	22.554	0.527	6.76
FRC1	23.965	0.545	6.96
FRC2	24.159	0.792	7.09
FRC3	24.317	0.634	7.31
PMC1	22.249	0.553	6.67
PMC2	22.013	0.344	6.56
PMC3	21.507	0.378	6.42
FRPMC1	22.481	0.290	6.81
FRPMC2	22.781	0.5485	6.74
FRPMC3	21.722	0.803	6.42
FRPMC4	23.900	0.600	7.10
FRPMC5	23.362	0.876	6.91
FRPMC6	22.158	0.580	6.57
FRPMC7	25.730	0.719	7.57
FRPMC8	25.046	0.639	7.46
FRPMC9	23.592	0.614	6.87

Figure 7-9 shows the effect of polymers on load bearing capacity in flexural test. PMCs showed lower failure loads compared to CC. Whereas, FRCs indicated higher load bearing capacity than CC. Combination of PP fibres, volume fraction of 0.3%, with latex notably improved maximum load failure by 14%. Increase of the bond strength between PP fibres and cement matrix by latex, increases bridging effect of the fibres. On the other hand, most of fibres will contribute in load bearing till breaking and not pulling out. This process consequently increases the maximum load of failure in FRCs.

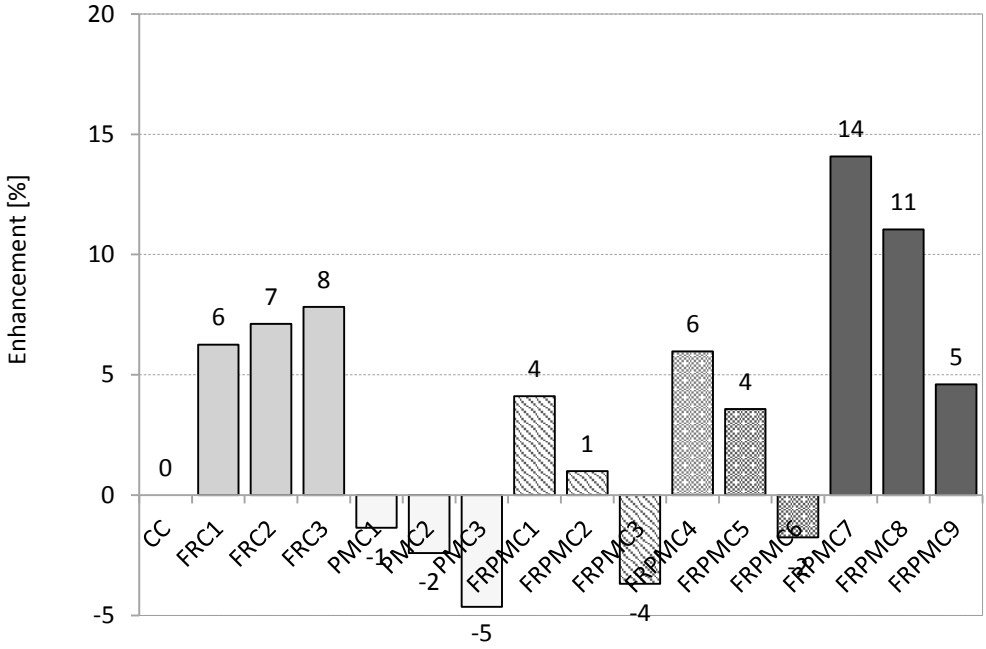

Figure 7-9 Comparison of maximum load of failure in flexural test

The average results of modulus of rupture for all types of concrete are presented in Figure 7-10.

The results of flexural tests have similar trend to compressive strength test results. PMCs showed lower flexural strength than CC. FRCs improved modulus of rupture by 8%.

Figure 7-11 (a, and b) presents the effects of PP fibres and latex proportions on flexural strength, respectively. The graphs show that flexural strength changes linearly with proportions of PP fibres and latex in the concrete as follows:

For FRCs: $f_{ct.f} = 1.76\,(V_f) + 6.76$ (7.3)

For PMC: $f_{ct.f} = -0.023(P/C) + 6.77$ (7.4)

where $f_{ct.f}$ is flexural strength, V_f is the volume fraction of PP fibres [%], and P/C is the polymer cement ratio [%].

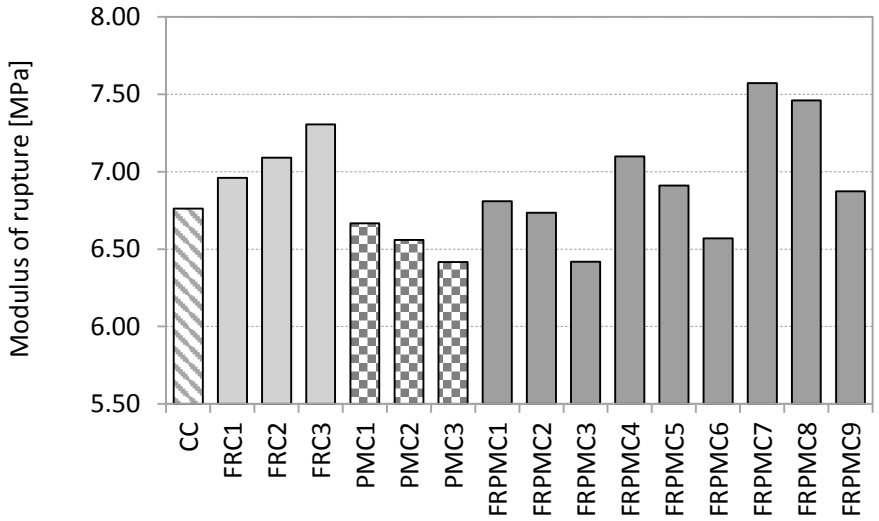

Figure 7-10 Average results of flexural strength for all categories of concrete

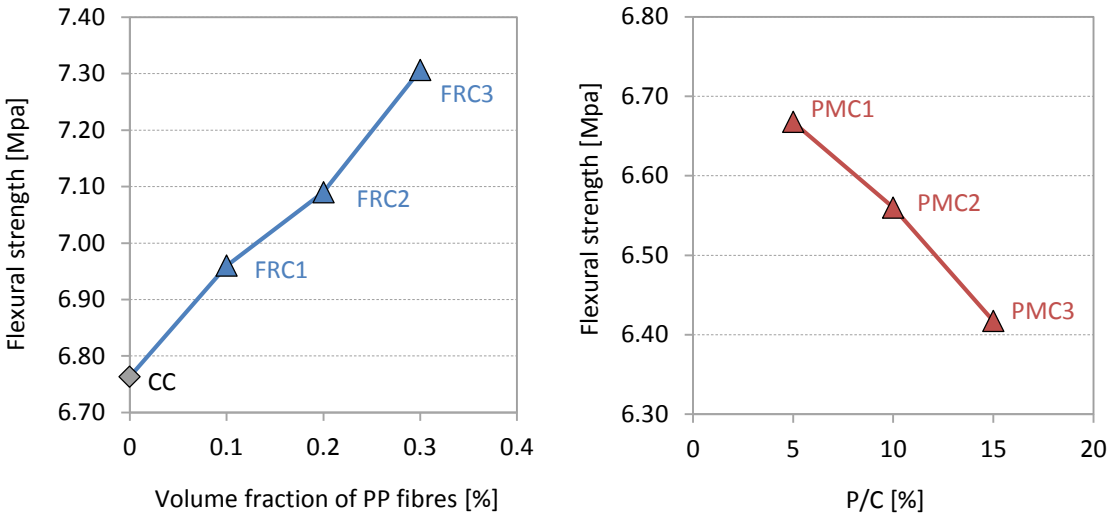

Figure 7-11 Flexural strength of FRCs (a) and PMCs (b)

Figure 7-12 presents the effect of the mixed structure of PP fibres and latex on flexural strength of the concrete. The graph clearly shows that by increasing the proportion of fibres in PMCs, flexural strength improves.

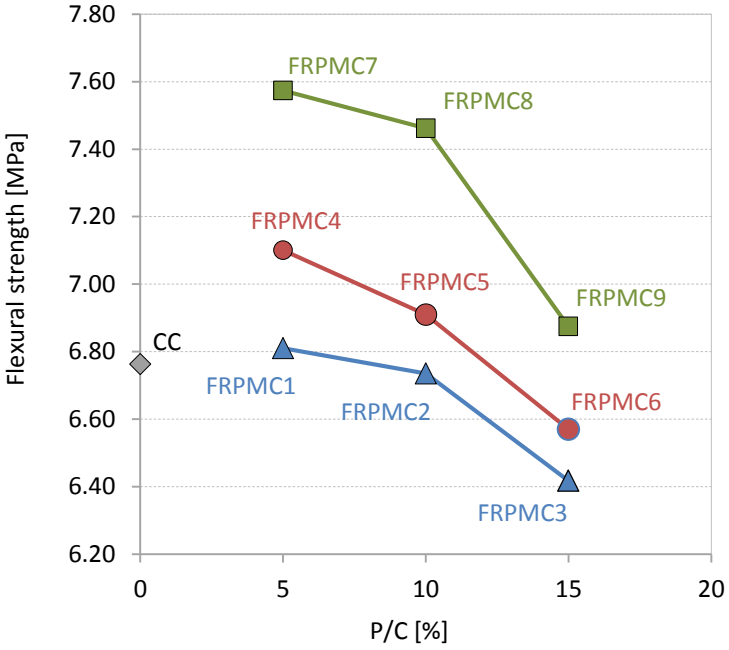

Figure 7-12 Flexural strength of FRPMCs

7.5 TENSILE STRENGTH

In this study, the indirect tensile test is conducted in accordance with AS 1012.10 -2000 on standard cylinders. The averages of 7-day and 28-day tensile strength of all concrete types are presented in Table 7-4.

Results expressed that latex-concrete composites do not affect the tensile strength of concrete. PP fibres-concrete composites increased the tensile strength by approximately 9%. FRPMCs showed better results in tensile test. For example; FRPMC5 showed 10% increment in tensile strength compared to CC.

Figure 7-13 (a, and b) presents the effect of PP fibres and latex proportions on tensile strength of the concrete. Tensile strength of FRCs is increased by increasing volume fraction of PP fibres. PMC showed a different tensile behaviour corresponding to the proportion of latex in the concrete. With P/C of 5%, tensile strength decreased by 2.9%. Nevertheless, by increasing latex proportion tensile strength increased.

Table 7-4 Average of 7-day and 28-day tensile strength test results

Concrete Type	Tensile Strength [MPa]		Enhancement [%]
	7-day	28-day	
CC	4.9	5.80	0.0
FRC1	5.2	6.06	4.6
FRC2	5.4	6.19	6.7
FRC3	5.6	6.31	8.8
PMC1	4.8	5.63	-2.9
PMC2	5.0	5.81	0.2
PMC3	5.1	5.86	1.0
FRPMC1	5.3	6.22	7.2
FRPMC2	5.4	6.24	7.6
FRPMC3	5.5	6.32	8.9
FRPMC4	5.5	6.33	9.2
FRPMC5	5.6	6.37	9.8
FRPMC6	5.6	6.33	9.2
FRPMC7	5.6	6.34	9.4
FRPMC8	5.5	6.29	8.4
FRPMC9	5.6	6.33	9.1

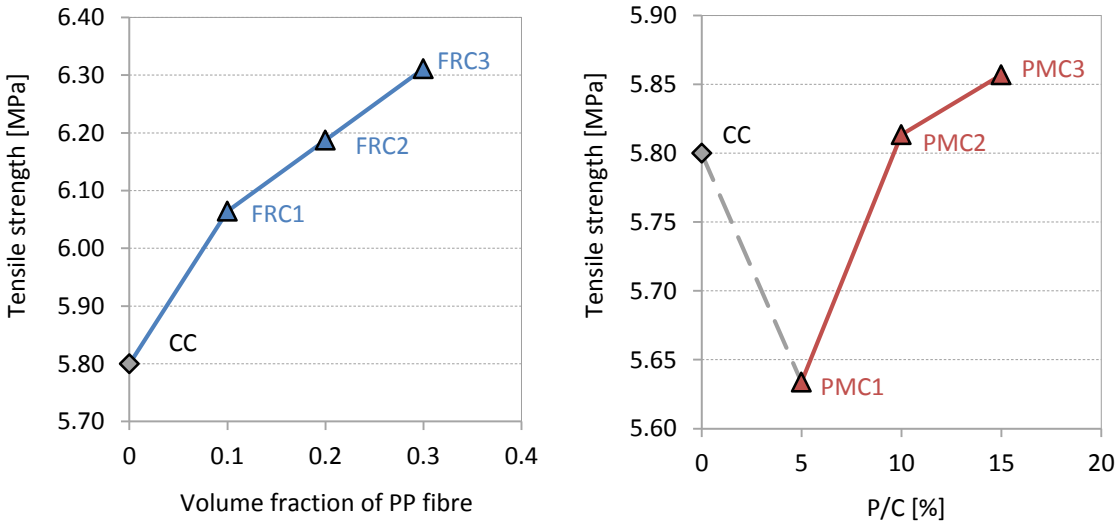

Figure 7-13 Tensile strength of FRCs (a) and PMCs (b)

Combination of PP fibres and latex polymer improved tensile strength of the concrete as shown in Figure 7-14. Similar conclusion to flexural strength can be stated for tensile strength results, too. Bond strength of fibres and cement matrix is improved by latex influence. Bond strength development will cause more efficient bridging effect provided by fibres.

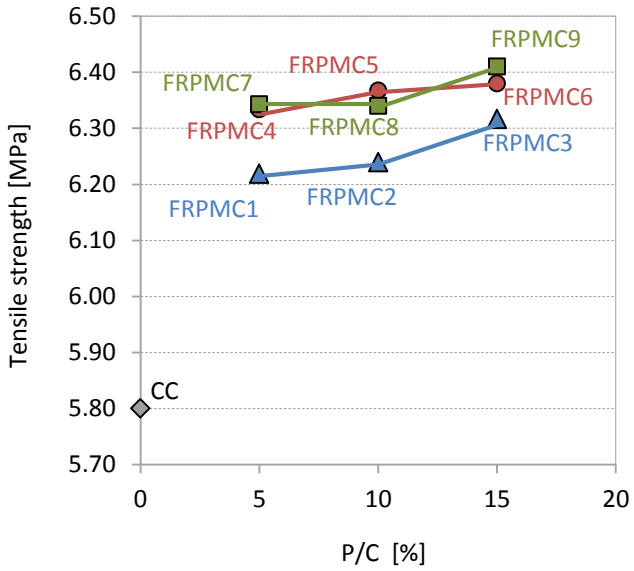

Figure 7-14 Tensile strength of FRPMCs

7.6 DURABILITY EVALUATION

In this section two series of test results are presented as follows:

- The results and discussion of chloride content measurements
- The results and discussion of time to corrosion-induced cracking

7.6.1 Results and Discussion of Chloride Content Measurement

As discussed earlier in Chapter 6, specimens were maintained in pure diffusion conditions (always submerged) and subjected to high concentrated chloride solution (16.5%) for 24 months. In time intervals of 1, 5, 9, 13, 17, 21, and 24 months, chloride measurement in different depths of 5 to 15 mm, 15 to 25 mm, 25 to 35 mm, 35 to 45 mm, and 45 to 55 mm was performed. In following presented tables and graphs the average depth has been used

as 10 mm, 20 mm, 30 mm, 40 mm, and 50 mm. For each concrete type two measurements were carried out and average value has been reported. Chloride content is reported in percent by weight of cement (%bwc).

Chloride measurement was taken place according to NT Build 443.

The first 5 mm of the depth of each specimen was removed to reduce the skin effect factor on the chloride content which consequently decreases the error in estimations. Chloride content up to depth of 5 mm was measured in abovementioned time intervals and considered as surface chloride concentration (C_s).

The change in chloride content over time and chloride content in different depths from concrete surface (chloride profile) are indicated from Figure 7-15 to Figure 7-30. All results show similar trend of chloride content over time which is close to logarithmic curve.

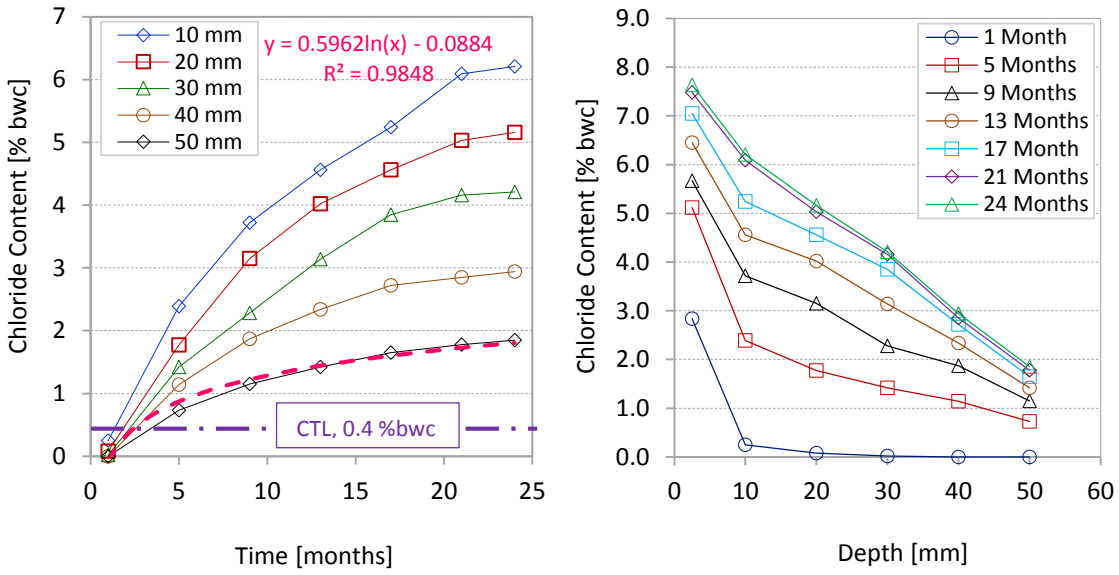

Figure 7-15 Chloride content measurement results for CC

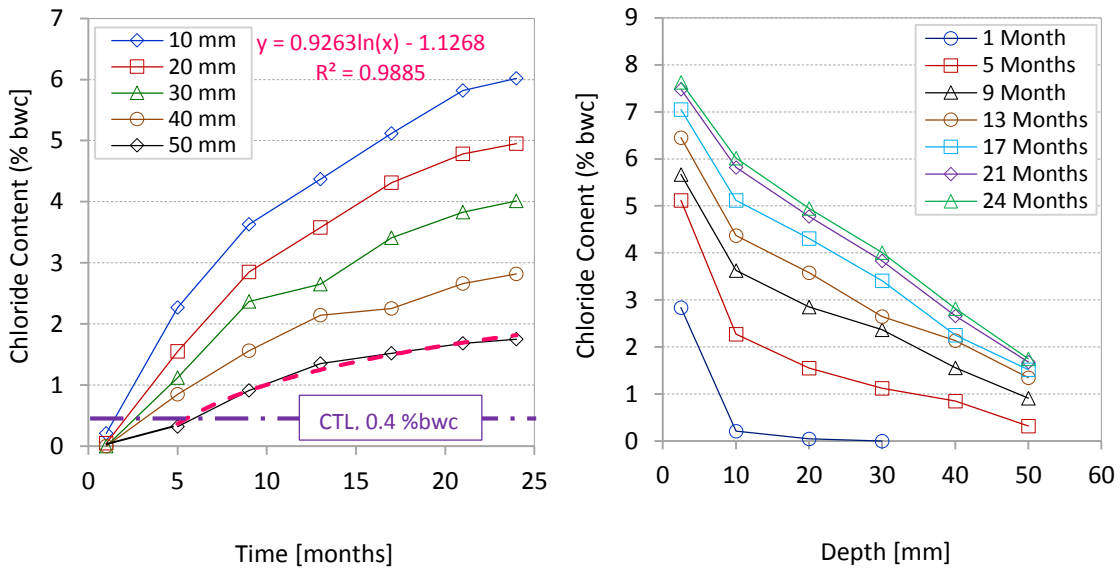

Figure 7-16 Chloride content measurement results for FRC1

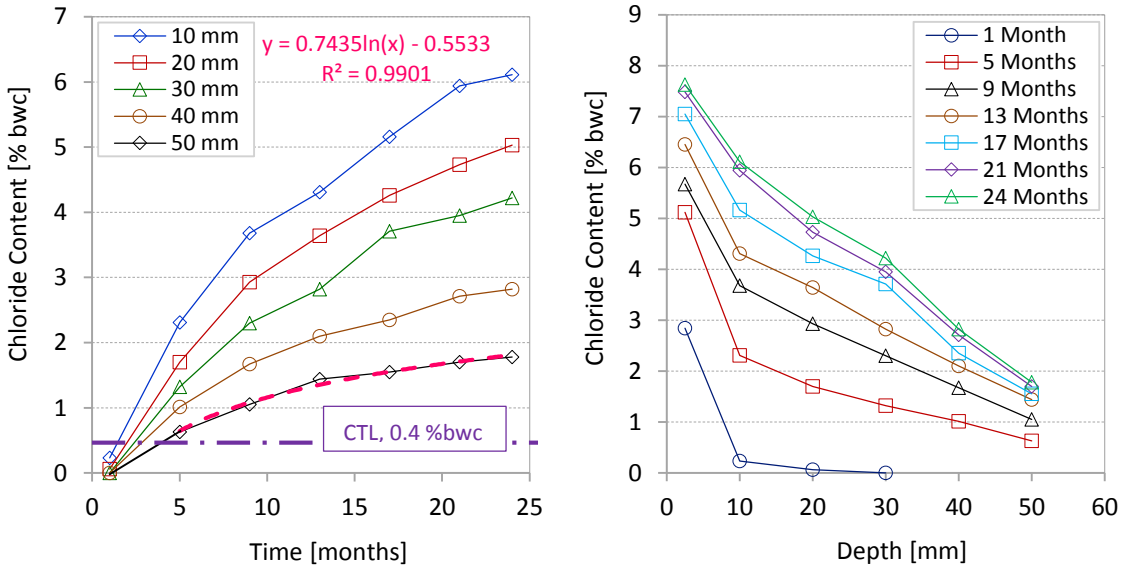

Figure 7-17 Chloride content measurement results for FRC2

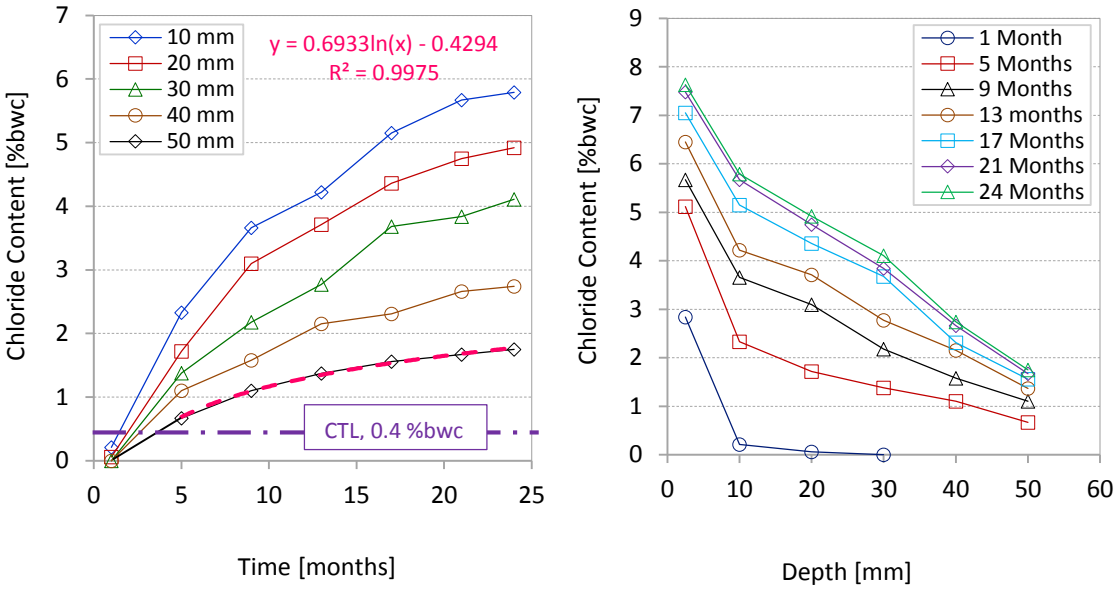

Figure 7-18 Chloride content measurement results for FRC3

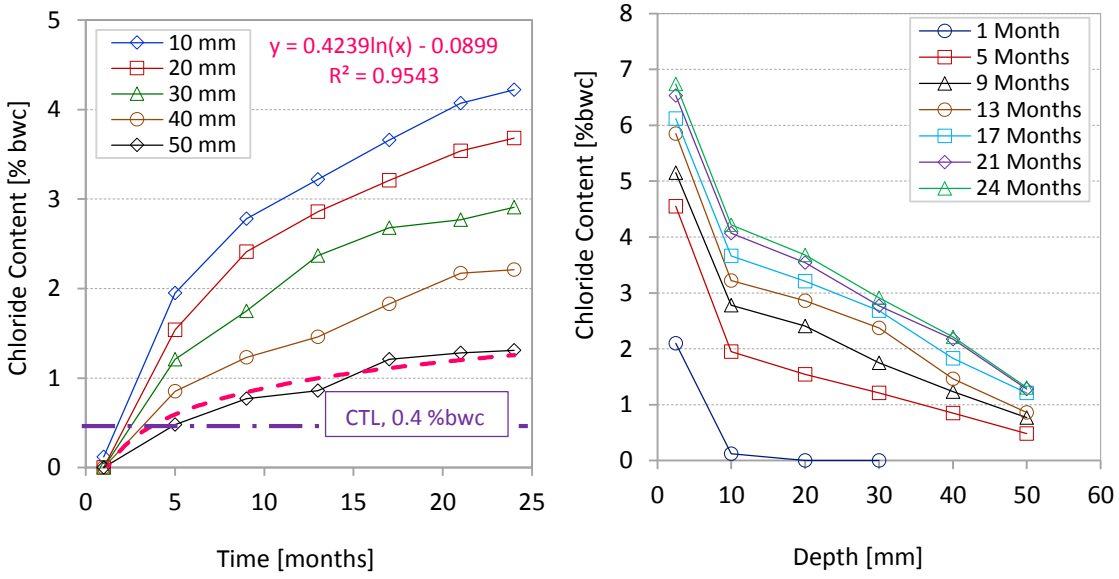

Figure 7-19 Chloride content measurement results for PMC1

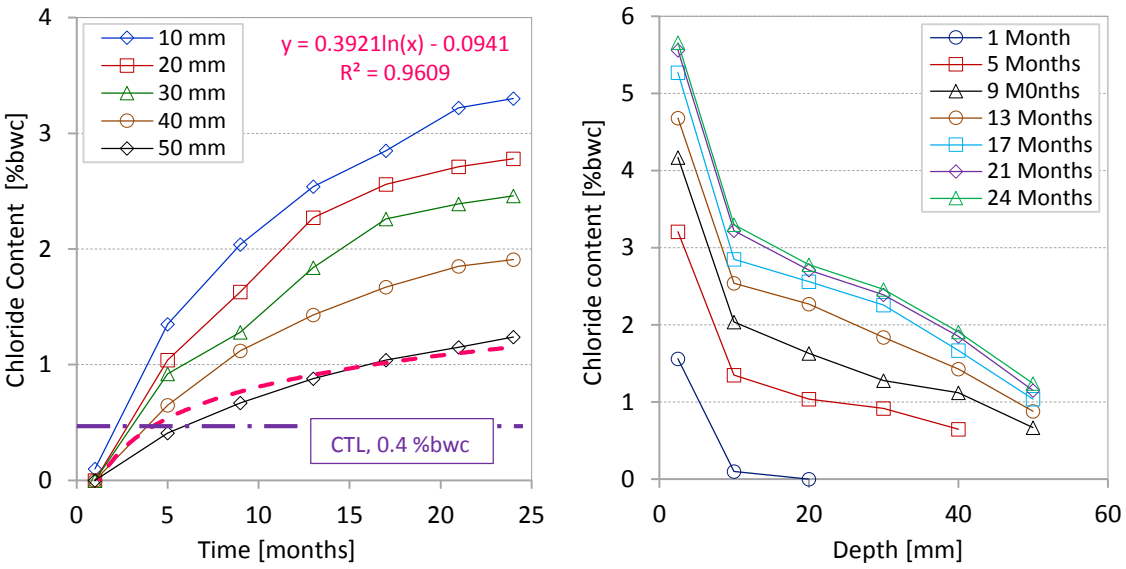

Figure 7-20 Chloride content measurement results for PMC2

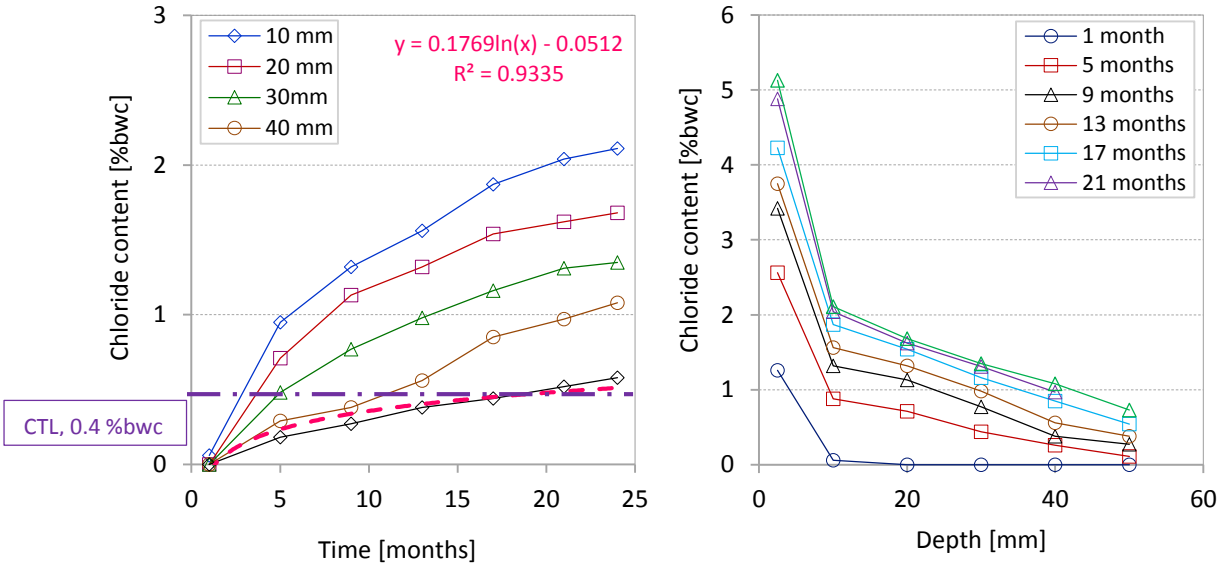

Figure 7-21 Chloride content measurement results for PMC3

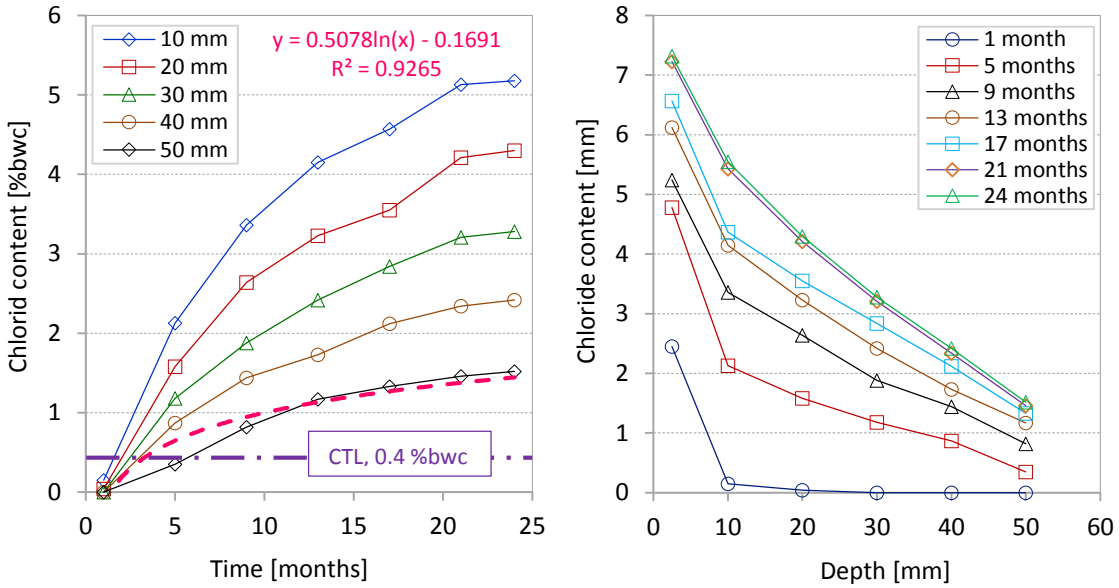

Figure 7-22 Chloride content measurement results for FRPMC1

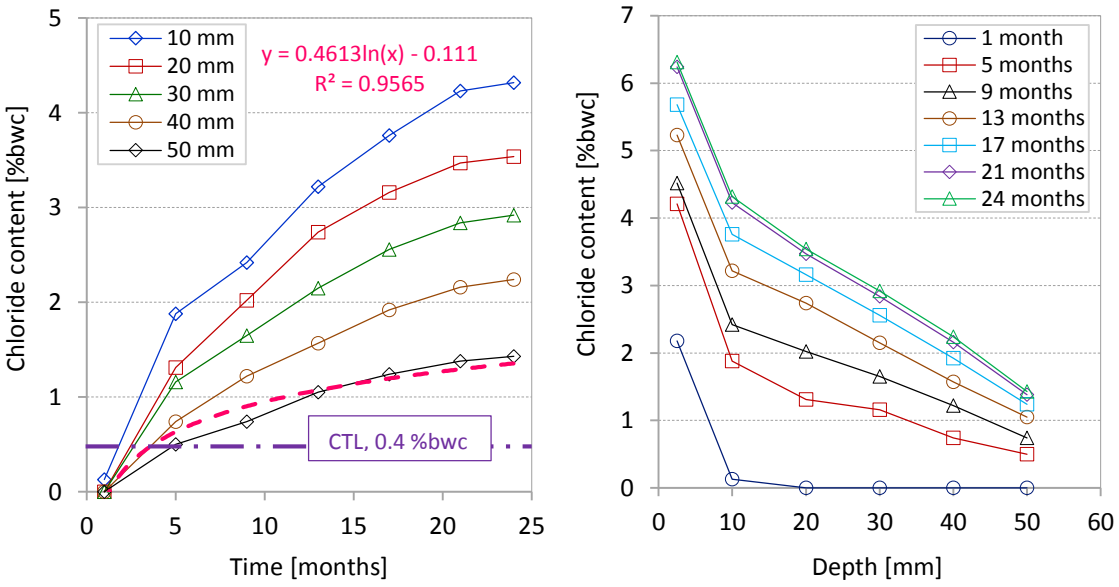

Figure 7-23 Chloride content measurement results for FRPMC2

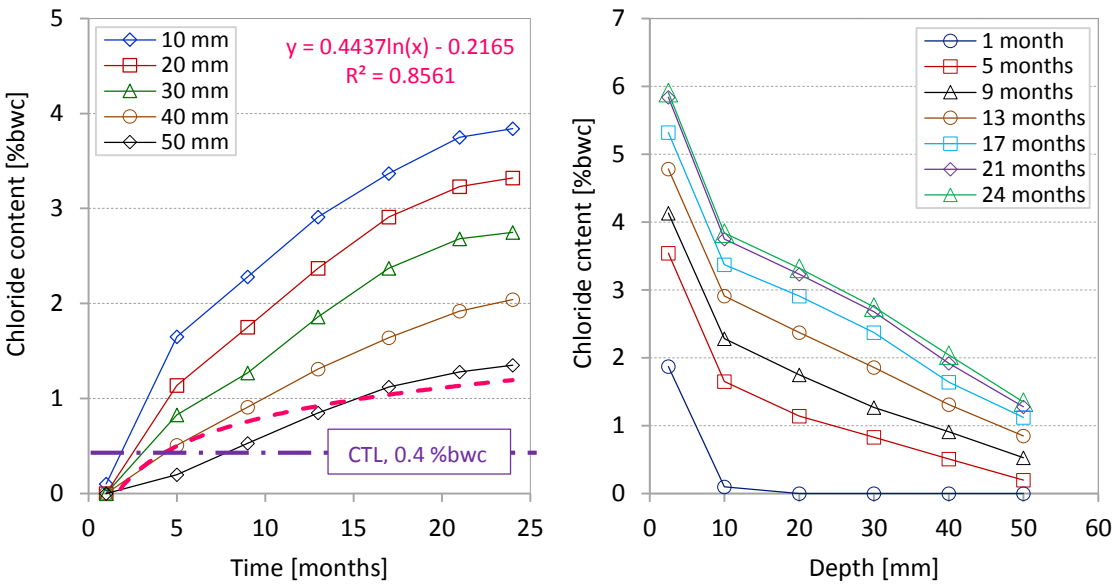

Figure 7-24 Chloride content measurement results for FRPMC3

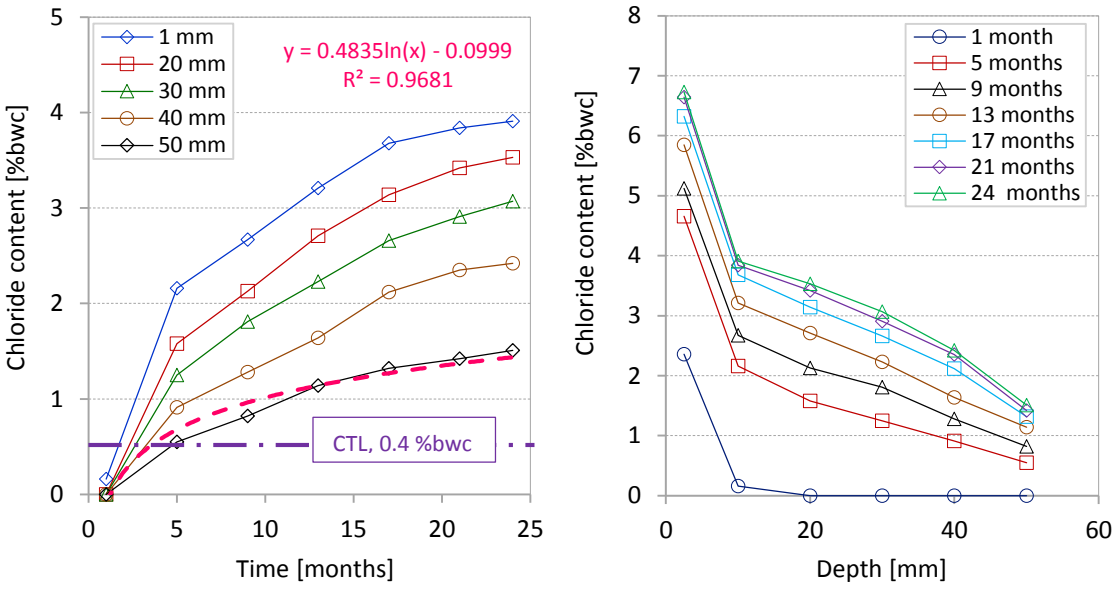

Figure 7-25 Chloride content measurement results for FRPMC4

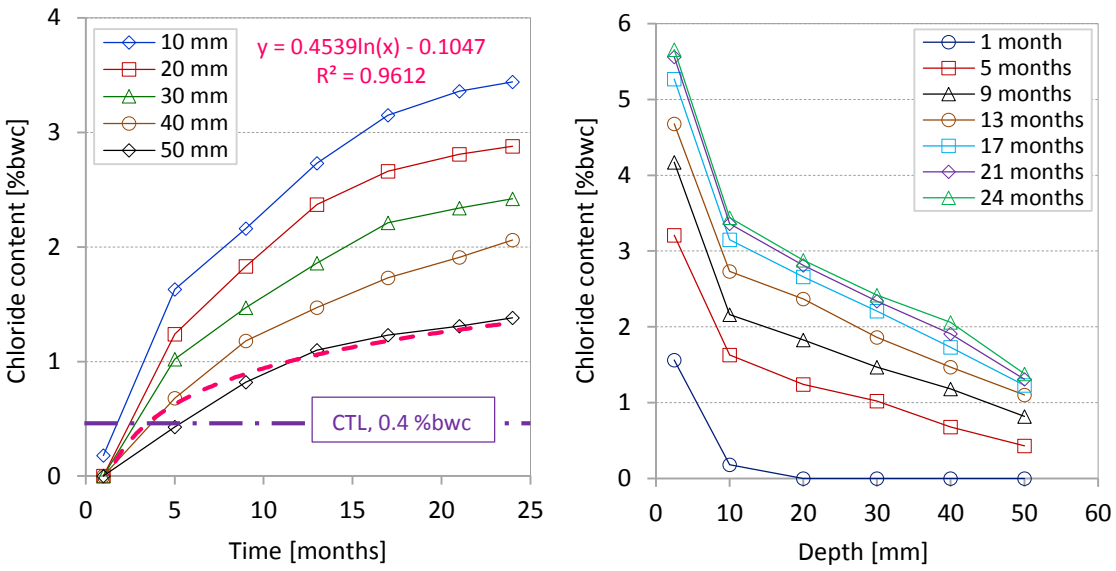

Figure 7-26 Chloride content measurement results for FRPMC5

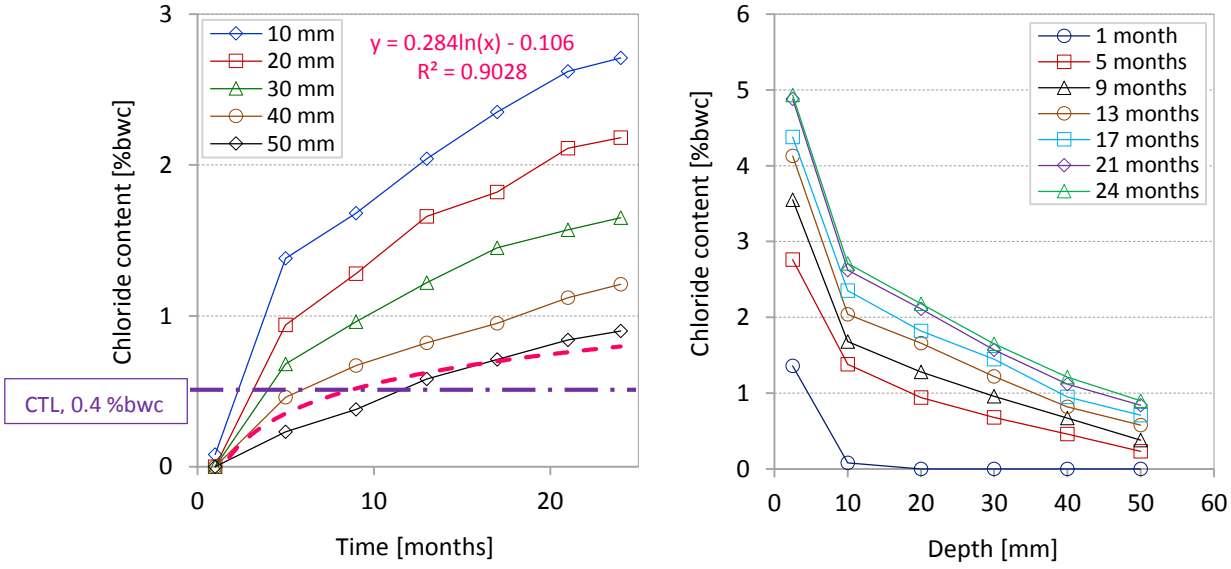

Figure 7-27 Chloride content measurement results for FRPMC6

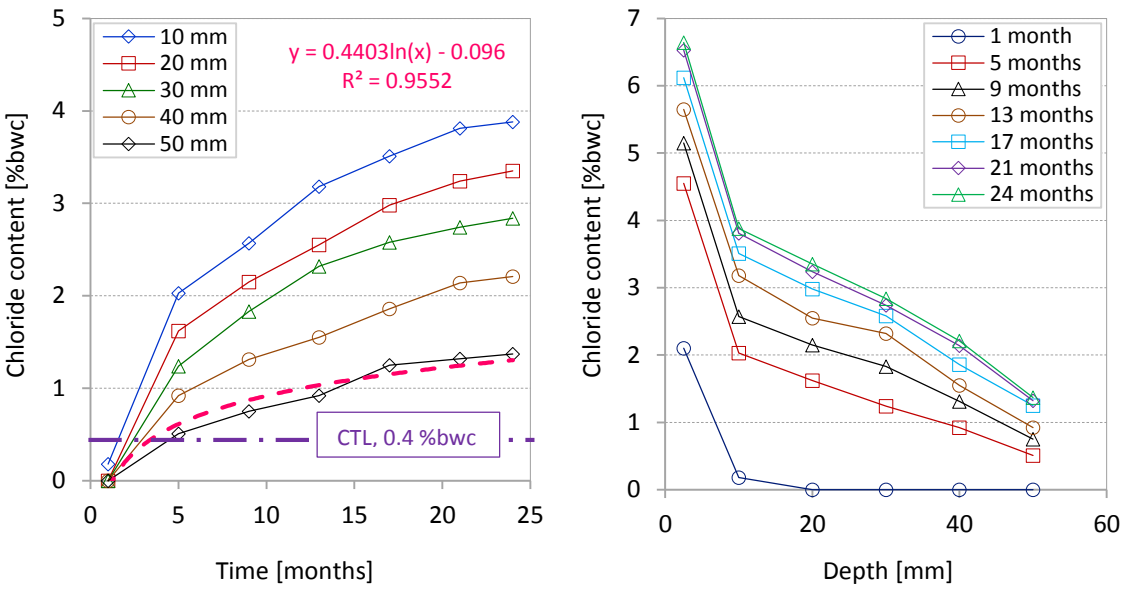

Figure 7-28 Chloride content measurement results for FRPMC7

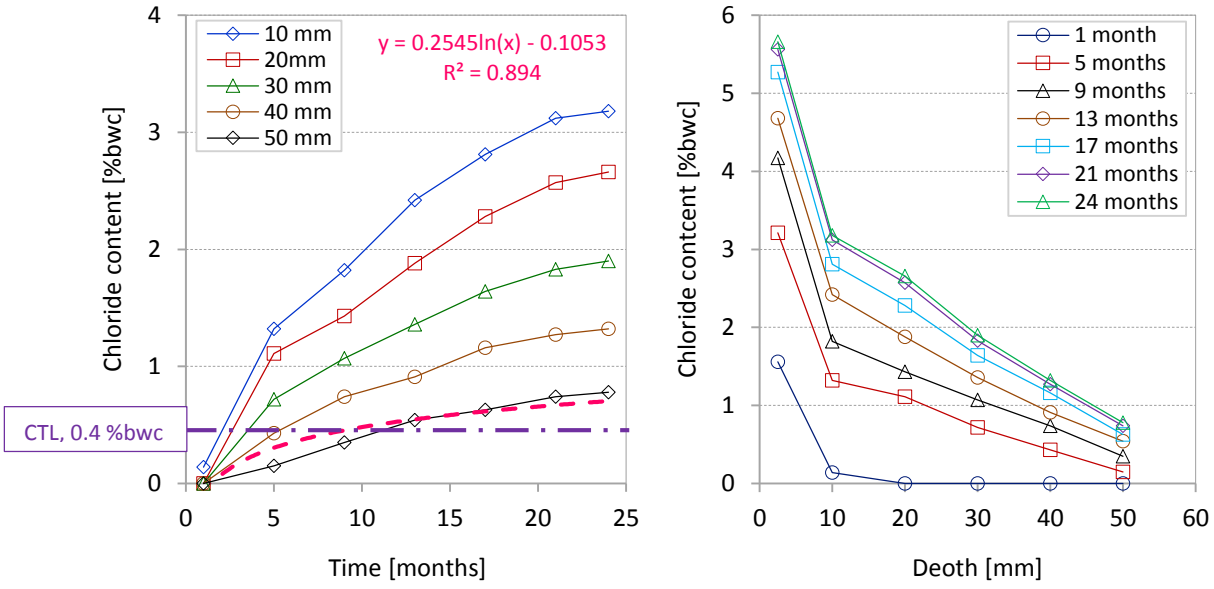

Figure 7-29 Chloride content measurement results for FRPMC8

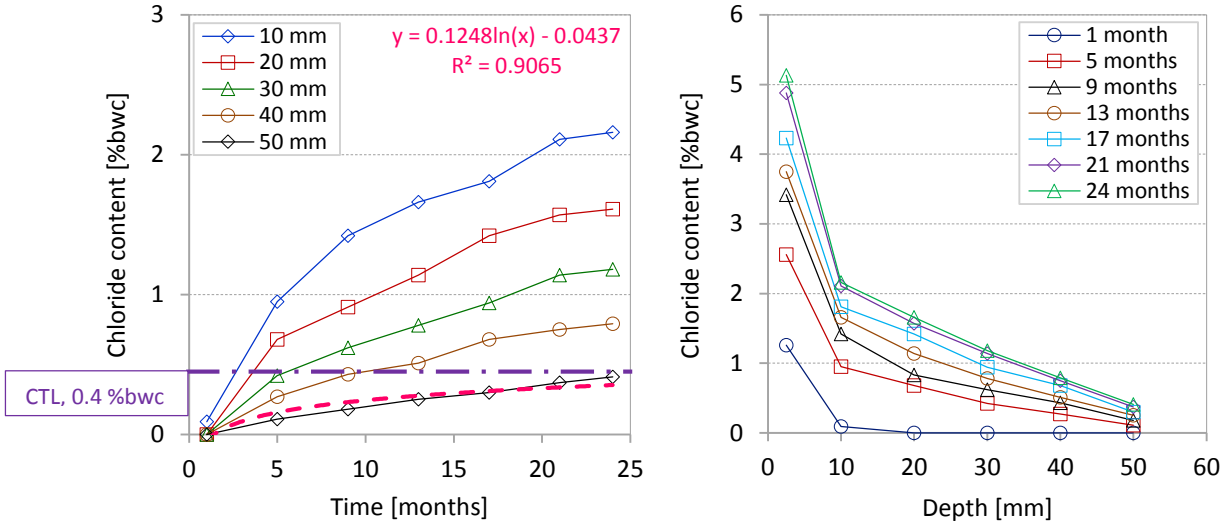

Figure 7-30 Chloride content measurement results for FRPMC9

Results revealed that the relationship between chloride content and time is a logarithmic equation. Based on the results, empirical models to determine chloride content for different types of concrete are proposed as follows:

For CC

$$C_c = 0.596\ ln(t) - 0.088 \tag{7.5}$$

For FRCs

$$C_c = \left[1 - \frac{V_f}{\propto}\right] ln(t) - 0.703 \tag{7.6}$$

For PMCs

$$C_c = \left[1 - \left(\beta\ (P/C)\right)\right] ln(t) - 0.09 \tag{7.7}$$

where C_c is the chloride content [%bwc], V_f is the volume fraction of PP fibres [%], P/C is the polymer cement ratio [%], $\propto = 0.926, and\ \beta = 7.09$ are empirical constants.

To investigate the effect of polymer-concrete composites on chloride diffusion in concrete, the maximum chloride content in different depths for all concrete types are presented in Figure 7-31 to Figure 7-35.

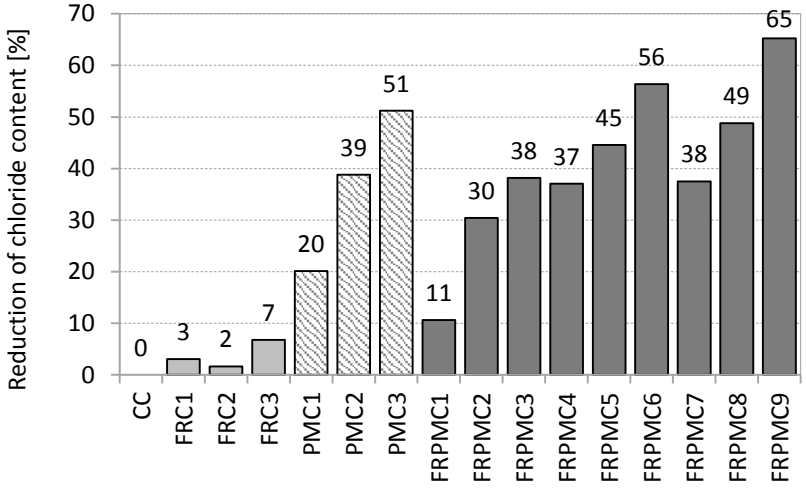

Figure 7-31 Reduction of chloride content at depth of 10 mm

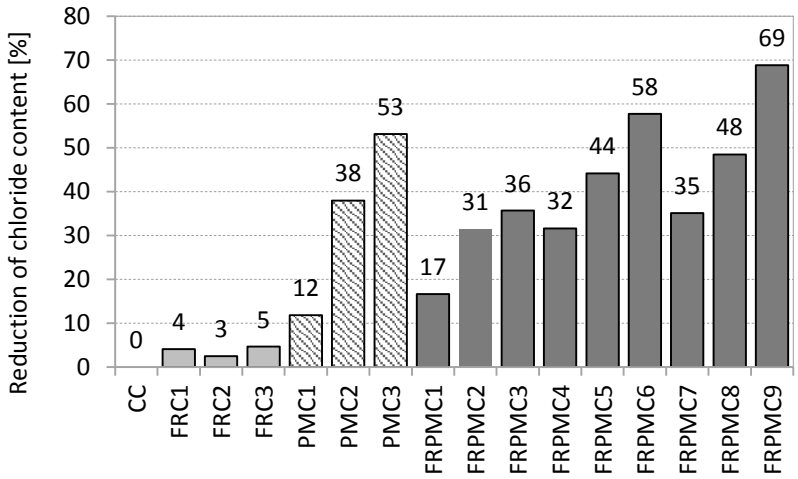

Figure 7-32 Reduction of chloride content at depth of 20 mm

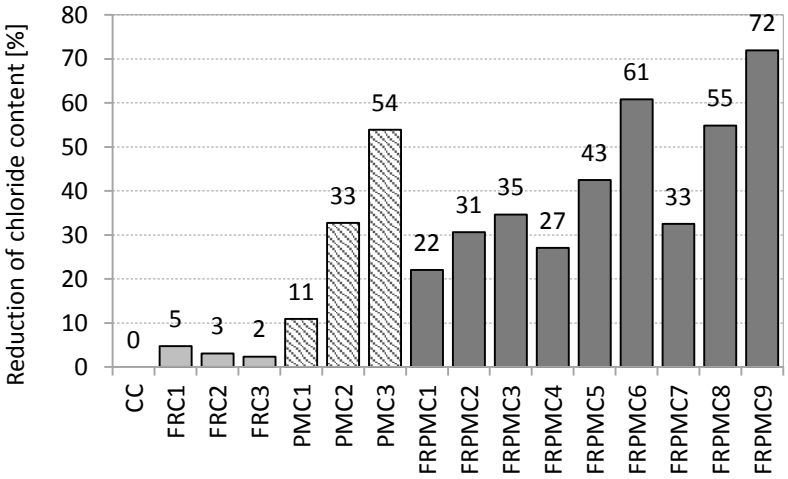

Figure 7-33 Reduction of chloride content at depth of 30 mm

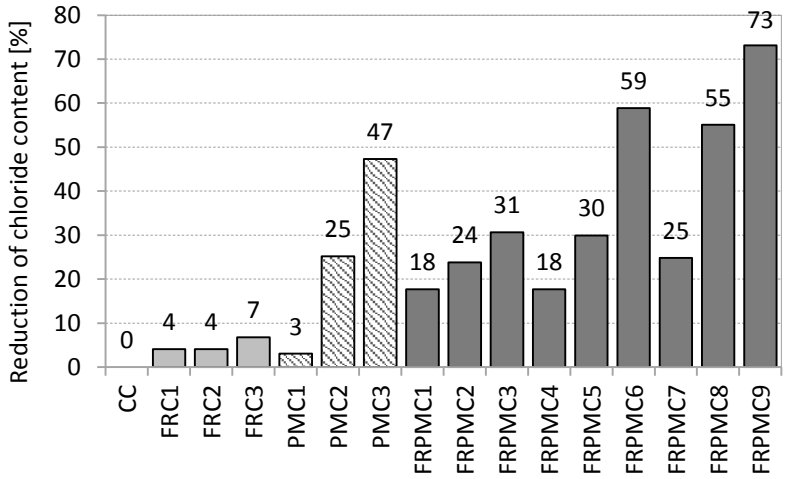

Figure 7-34 Reduction of chloride content at depth of 40 mm

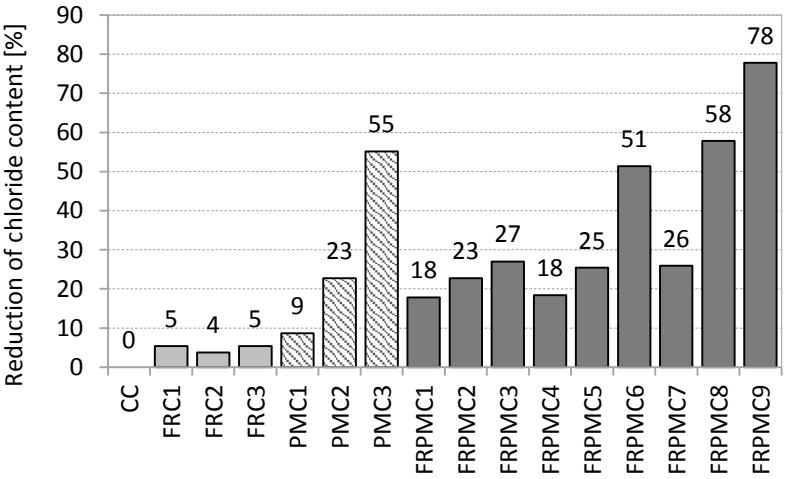

Figure 7-35 Reduction of chloride content at depth of 50 mm

The results show that all types of polymer-concrete composites can reduce the rate of chloride diffusion into concrete. Among all polymer-concrete composites PMC3, FRPMC6, FRPMC8, and FRPMC9 have consistently shown the most chloride resistance compared to the other type of polymer-concrete composites investigated in this study. FRPMC9 has the minimum chloride diffusion rate among the other types of concrete and shows approximately 75% reduction of chloride content in various depths compared to CC.

In conclusion, it can be expressed that polymer-concrete composites can significantly reduce the diffusion rate of chloride into concrete especially in combination of PP fibres with latex.

7.6.2 Results and Discussion of Time to Corrosion-Induced Cracking Test

To obtain the time to first repair, the time required to crack must be determined. For diffusion controlled chloride transport, limited work has been performed in determining the time required to crack the concrete cover as a result of steel corrosion. Pfeifer (Pfeifer, 2000) reported that concrete would crack after 25 μm of the steel reinforcement surface has corroded. The time to cracking is determined using the relationship proposed by Pfeifer as follows:

$$Time\ to\ Cracking\ (years) = \frac{25\ \mu m}{corrosion\ rate\ \left(\frac{\mu m}{year}\right)}$$

Steel corrosion in concrete is an electrochemical process. In this process, concrete acts as an electrolyte therefore, concrete resistivity is an important parameter in corrosion propagation. A concrete with higher electrical resistivity will cause a longer corrosion propagation time. Corrosion propagation time depends on the corrosion rate, oxygen flow, temperature, concrete resistivity, depth of cover and its quality, diameter and spacing of reinforcing steel, moisture content, and tensile strength of concrete.

The associated deterioration leads to a variety of negative effects with respect to both structural and durability performance of the RC structures. The prediction of corrosion propagation is therefore a complex process mainly due to the difficulty in incorporating

all the relevant factors affecting the process and the associated damage in a prediction model (Otieno et al., 2011).

Since corrosion of reinforcing steel in concrete is a long-term electrochemical process, the accelerated electrochemical methods can help to obtain the results in relatively shorter time for laboratory investigation. In this investigation, the Accelerated Chloride-Induced Corrosion Test (constant impressed voltage technique) was performed to compare the corrosion time of embedded steel bar in different categories of concrete.

In this method, the current intensity showed a sudden rise indicating the cracking of the concrete cover of specimen by corrosion (referred to as corrosion time). The relationship between corrosion current intensity (mA) and time (hours) was plotted every one hour by a digital data logger in order to determine the time to cracking of the each specimen. Therefore, the corrosion time can be defined as the time from the start of the experiment to the instant rise of the current.

As explained in Chapter 6 in detail, the results of this test indicate time to first visible cracking due to corrosion of the steel reinforcement in concrete. The cracking begins at the steel–concrete interface and propagates outwards and eventually results in the thorough cracking of the concrete cover and this would indicate the loss of service life for the corrosion affected structures.

The results of time to corrosion-induced cracking for FRCs are presented in Table 7-5.

Table 7-5 Time to corrosion-induced cracking of FRCs compared to CC

Concrete Type	Specimens' Code	Time to Cracking [hours]	Average [hours]	Enhancement [%]
CC	CC1	405	398	0
	CC2	391		
FRC1	FRC1-1	429	434	9
	FRC1-2	438		
FRC2	FRC2-1	464	461	16
	FRC2-2	457		
FRC3	FRC3-1	517	544	27
	FRC3-2	492		

Figure 7-36 illustrates the improvement in corrosion time from 398 hours to 544 hours by polymer-concrete composite incorporating PP fibres. Although, PP fibres-concrete

composites could enhance the service life of the structure only up to 27%, this improvement means adding15 years to service life if we assume a design service life of 50 years for the structure.

An empirical model is suggested to predict the corrosion time in FRCs regarding the volume fraction of PP fibres.

$$t_{corr} = 346.5(V_f) + 397.15 \quad (7.5)$$

where t_{corr} is the corrosion time [hours], and V_f is the volume fraction of PP fibres [%].

Latex-concrete composites showed an extraordinary improvement of corrosion time up to 130%. The results of time to corrosion-induced cracking for PMCs are presented in Table 7-6.

The increment rate in corrosion time of PMCs can be observed in Figure 7-37. This graph illustrates that service life of a concrete structure using polymer-concrete composites can be increased by 2.30 times. For instance, the design service life of 50 years for a marine structure can be increased up to 115 years.

An empirical model is suggested to predict the corrosion time in PMCs regarding the polymer cement ratio (P/C).

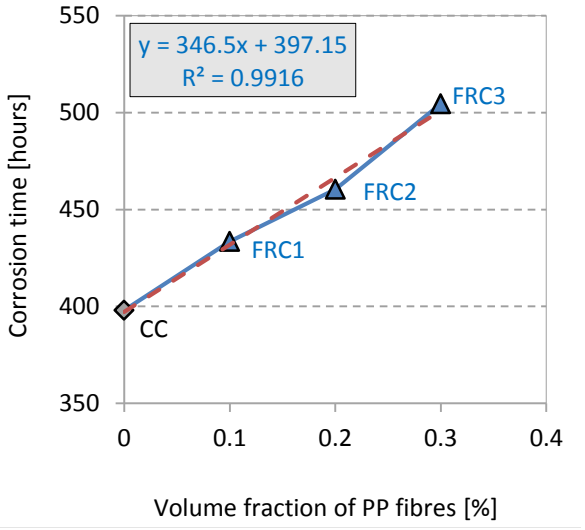

Figure 7-36 Corrosion time for FRCs

Table 7-6 Time to corrosion-induced cracking of PMCs compared to CC

Concrete Type	Specimen's Code	Time to Cracking [hours]	Average [hours]	Enhancement [%]
CC	CC1	405	398	0
	CC2	391		
PMC1	PMC1-1	545	541	36
	PMC1-2	537		
PMC2	PMC2-1	732	731	84
	PMC2-2	729		
PMC3	PMC3-1	919	915	130
	PMC3-2	911		

$$t_{corr} = 34.82(P/C) + 385.1 \tag{7.6}$$

where t_{corr} is the corrosion time [hours], and P/C is the polymer cement ratio [%].

After investigating the effects of FRC and PMC as polymer-concrete composites on corrosion time and service life of a concrete structure, the effects of combining PP fibres and latex polymer on corrosion time will be discussed. As it has been discussed in Chapter 6, this polymer-concrete composite is called Fibre Reinforced Polymer Modified Concrete or FRPMC (this nomenclature has been specified by the author for the first time in polymer-concrete composite investigations).

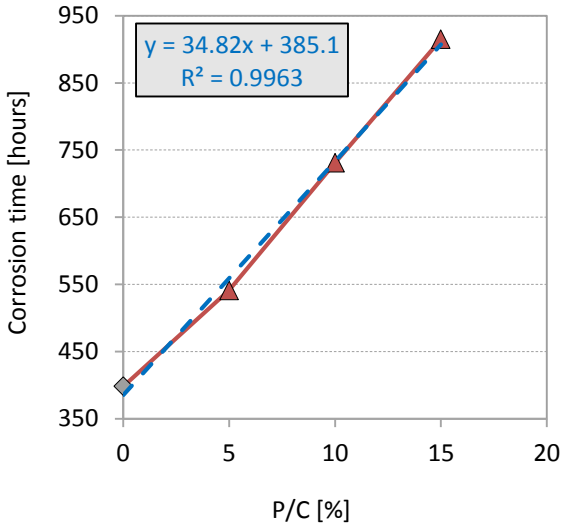

Figure 7-37 Corrosion time for PMCs

The results of time to corrosion-induced cracking of FRPMCs are presented in Table 7-7.

Table 7-7 Time to corrosion-induced cracking of FRPMCs compared to CC

Concrete Type	Specimen's Code	Time to Cracking [hours]	Average [hours]	Enhancement [%]
CC	CC1	405	398	0
	CC2	391		
FRPMC1	FRPMC1-1	571	527	32
	FRPMC1-2	482		
FRPMC2	FRPMC2-1	722	729	83
	FRPMC2-2	735		
FRPMC3	FRPMC3-1	927	923	132
	FRPMC3-2	918		
FRPMC4	FRPMC4-1	581	578	45
	FRPMC4-2	575		
FRPMC5	FRPMC5-1	765	759	91
	FRPMC5-2	752		
FRPMC6	FRPMC6-1	948	956	140
	FRPMC6-2	964		
FRPMC7	FRPMC7-1	661	665	67
	FRPMC7-2	561		
FRPMC8	FRPMC8-1	785	782	96
	FRPMC8-2	778		
FRPMC9	FRPMC9-1	981	983	147
	FRPMC9-2	985		

As can be observed in Figure 7-38, the combination structure of PP fibres and latex polymer in concrete improves service life of the structure significantly. This improvement is a function of PP fibre and latex proportions in the concrete and results showed approximately a linear dependency of corrosion time to proportions of PP fibres and latex. Increasing the proportions of the PP fibres and latex increases the corrosion time.

Figure 7-39 compares the effect of polymer-concrete composite on corrosion time to CC in percentage. All of polymer-concrete composites structures (fibres, latex and combination of them) enhanced corrosion time of conventional concrete. Latex modified concrete showed a significant improvement from 36% for P/C of 5% to 130% for P/C of 15% in corrosion time. Moreover, results confirmed that the combination of PP fibres and latex in concrete improved corrosion time extraordinary up to 147%. This enhancement can be described as follows:

If we assume a design service life of 50 years for marine concrete structure, this service life can be increased up to 124 years by using a combined structure of PP fibres and latex polymer.

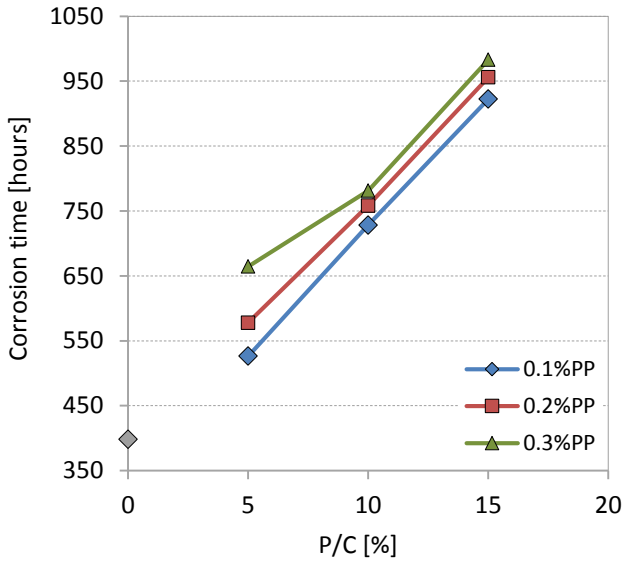

Figure 7-38 Corrosion time for FRPMCs

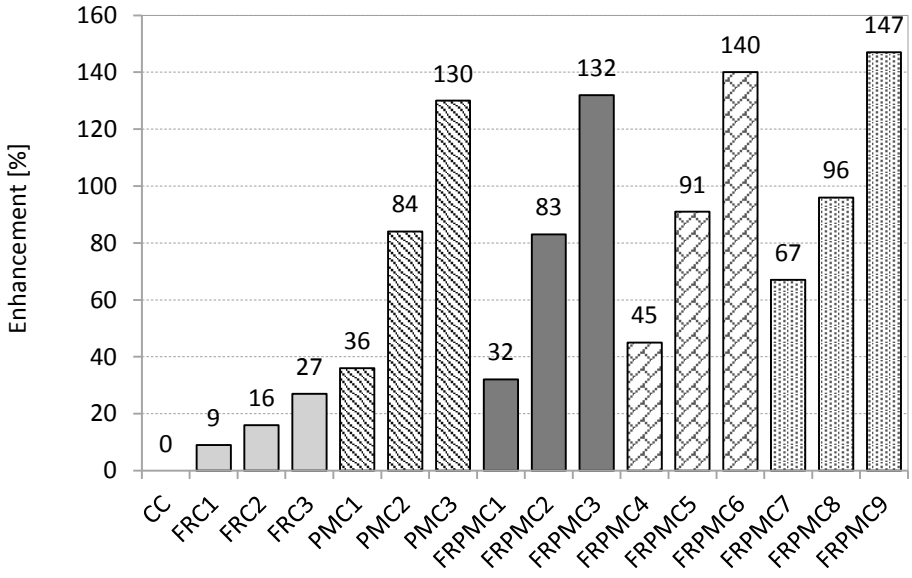

Figure 7-39 Effect of polymer-concrete composites on corrosion time

7.7 SUMMARY

In this chapter, experimental results of different tests were presented and discussed. Utilising comparative method, the effects of polymer-concrete composites on both mechanical properties and durability performance of concrete were investigated. Referring to the test results, it can be strongly expressed that polymer-concrete composites enhance the concrete properties in terms of strength and durability.

7.7.1 Fresh Concrete Properties

Fresh concrete properties measured and the following conclusion can be expressed:

- Latex polymer increases workability of the concrete and also decreases the possibility of segregation. By using latex in the mix the amount of superplasticiser can be decreased maintaining similar workability.
- Latex increases the air content in the mix as well. This phenomenon increases workability of the concrete. Mixing antifoaming agent can reduce the air content considerably and bring it to the acceptable range.
- PP fibres reduce workability of the concrete slightly. This can be compensated by adding superplasticiser to the mix. Air content in FRCs is in the acceptable rage, although it is higher than CC.

7.7.2 Hardened Concrete Properties

In order to examine the effects of polymers on mechanical properties of concrete, compressive strength, flexural strength, and tensile strength were investigated.

Results showed that all polymer-concrete composites obtained compressive strength higher than the minimum design compressive strength of 60 MPa. Test results showed improvement of compressive strength for all polymer-concrete composites except PMCs. Compressive strength of PMCs was enhanced by adding an appropriate antifoaming agent. FRCs and FRPMCs increased compressive strength up to 14% and 16%, respectively.

Test results showed enhancement of flexural strength of FRCs and FRPMCs by 8% and 14%, respectively. PMCs indicated a reduction of 5% in flexural strength. Two empirical models were proposed to determine flexural strength of FRCs and PMCs.

Test results revealed that PMCs do not influence on tensile strength. Whereas, FRCs and FRPMCs increased tensile strength approximately up to 9% and 10%.

7.7.3 Durability Performance

Since chloride ion diffusion is dominant factor in deterioration of the RC structures, the measurement chloride diffusion rate in concrete can be applied to investigate the durability of the concrete exposed to severe environment such as marine environment. In this study, 16 types of concretes including CC, FRC, PMC, and FRPMC were exposed to high concentration of chloride solution and chloride content in different depths over time were measured.

Results revealed that all types of polymer-concrete composites showed high resistance to chloride diffusion especially PMCs and FRPMCs. As an average, PMCs and FRPMCs, compared to chloride content of CC, could reduce the chloride content by approximately 50% and 75%, respectively. Chloride content measurement can be used to determine the corrosion-free service life of the structure.

Results related to corrosion time revealed that all polymer-concrete composites (fibres, latex and combination of them) enhanced corrosion time of conventional concrete. Latex modified concrete showed a significant improvement from 36% for P/C of 5% to 130% for P/C of 15% in corrosion time. Moreover, results confirmed that the combination of PP fibres and latex in concrete improved corrosion time extraordinary up to 147%. This enhancement can be described as follows:

If we assume a design service life of 50 years for marine concrete structure, this service life can be increased up to 124 years by using a combined structure of PP fibres and latex polymer.

CHAPTER 8

ANALYTICAL MODEL FOR CHLORIDE DIFUSSION COEFFICIENT

CHAPTER 8. NEW ANALYTICAL MODEL FOR CHLORIDE DIFFUSION COEFFICIENT

8.1 INTRODUCTION

The main scope of this chapter is to develop an analytical model for chloride diffusion coefficient (D) as a time-dependent parameter in order to calculate the amount of chloride ingress into concrete accurately. The precise approach to measure the chloride content over time causes precise estimation of service life of the structure exposed to severe environment such as marine environment.

Many parameters, including material characteristics, climatic environment, and construction method affect the chloride ingress in concrete. At present, it is difficult to specify these parameters with sufficient precision to be used in a mathematical model. Nevertheless, the objective of this study is to establish a practical and reliable mathematical model that can accommodate the abovementioned parameters.

Penetration of chloride ions into concrete through the interconnected pores and surface cracks reduces the pH of the concrete. If the concentration of the chloride ions at the surface of the steel reinforcement reaches a critical value (chloride threshold level, CTL), due to depassivation the corrosion of steel in concrete initiates (initiation period). After some time (corrosion propagation time), corrosion-induced cracks propagate into the concrete cover surface and cause the acceleration of the diffusion rate of the chloride into concrete, and consequently high rate of deterioration of the structure.

In this study, service life is defined as the initiation period which is the time taken for chlorides to reach to CTL at the steel surface.

As described in Chapter 6, transport mechanisms relevant to chloride ingress in reinforced concrete structures exposed to chloride environment include (1) ionic diffusion in saturated concrete; and (2) water surface absorption in partially-saturated concrete (capillary sorption). Fick's second law is the governing equation in the diffusion process. Therefore, corrosion-free service life is determined by applying Fick's second law. One of the important parameters in Fick's law is the chloride diffusion coefficient (D). In this study, the diffusion of chloride ions into saturated concrete is investigated and a mathematical model for chloride diffusion coefficient is developed.

Based on the described processes including (1) chloride diffusion into the concrete and; (2) corrosion of steel in concrete, mathematical models have been proposed for both of them. In Chapter 3, an extensive investigation of mathematical models for predicting the service life of Reinforced Concrete (RC) structures was accomplished. Proposed mathematical models can be classified into three different categories as follows:

- Chloride diffusion models
- Steel reinforcement corrosion models
- Service life prediction models

In all modelling categories, chloride diffusion coefficient (diffusivity, D) has an important and effective role in chloride ingress using Fick's second law. Most of these models have considered the diffusivity (D) as a constant parameter over the service life of the structures. The most significant relevant models have been described in Chapter 3 and summarised in Table 8-1.

Table 8-1 Database for the chloride ingress mathematical models

	Mathematical Model	Presented by
1	$\frac{\partial \emptyset}{\partial t} = D\frac{\partial^2 \emptyset}{\partial x^2}$ D is constant	Fick's Second Law
2	$t = \frac{1}{12D}\left(\frac{d_c}{1-\sqrt{\frac{C_{th}}{C_s}}}\right)^2$ D is constant	Bazant (1979b)
3	$C_{(x,t)} = C_s\left[1 - erf\left[\frac{x}{2(Dt)^{\frac{1}{2}}}\right]\right]$ D is constant	RILEM Report 14, (1996)
4	$C_{(x,t)} = S\sqrt{t}\left[1 - erf\left(\frac{x}{2\sqrt{Dt}}\right)\right]$ D is constant	Weyers (1998)
5	$J_{ix} = -D_e\left[\frac{\partial C_f}{\partial x} - \frac{eFE}{RT}C_f\right]$	Liang et al. (1999)
6	$D_i = \frac{RT\sigma_i}{{Z_i}^2F^2C_i}$ D, depends on partial conductivity of species	Nernst-Einstein (1975),
7	$\frac{\partial C}{\partial t} = div[D_i\nabla(C)] - \frac{1}{\omega}\cdot\frac{\partial S}{\partial t}$ Effect of chloride binding capacity (free chloride)	Basheer et al. (1996)
8	$T_i = f(C_s, C_{th}, D, d_c) = \frac{{d_c}^2}{4D\left[erf^{-1}\left(1-\frac{C_{th}}{C_s}\right)\right]^2}$ D is constant	Zhang and Lounis, (2009)
9	$L_i = \frac{d^2}{(A\cdot D_{Cl})}$ D is constant	Siemes and Polder, (1998)

Song et al. (Song et al., 2008) proposed their mathematical model for time-dependent diffusion coefficient as shown in Equation 8.1.

$$D_{(t)} = D_0 \left(\frac{t_0}{t}\right)^m \tag{8.1}$$

where $D_{(t)}$ is the diffusion coefficient at time t (m^2/s), D_0 is the diffusion coefficient at time t_0 (m^2/s), t_0 is the standard time (one year or 28 days) (s), t is the time (s), and m is the age factor.

As the cement particles are hydrated, capillary pores are partially blocked. This blocking of pores process consequently reduces the paths for diffusing of chloride ions into the concrete (Winslow et al., 1994).

According to the Crank's solution (Equation 8.2), chloride diffusion coefficient (D) and surface chloride concentration (C_s) are two important factors to determine the chloride content.

$$C_{(x,t)} = C_s \left[1 - erf\left[\frac{x}{2(Dt)^{\frac{1}{2}}}\right]\right] \tag{8.2}$$

Both parameters (D and C_s) have been extensively used as constant values to predict the chloride content in the concrete. Both surface chloride concentration and chloride diffusion coefficient are time-dependent parameters as discussed in Chapter 2. Chloride diffusivity can be changed when the concrete pore structure changes due to development of cement hydration process over time.

Therefore, if the parameters D and C_s are used as constant values, gross error can be made by using Equation 8.2. Thus, time dependency of those parameters should be monitored and simulated in real situations over a long period of time to determine and calibrate the real values of D and C_s.

In this chapter by employing the available database and models (Table 8-1), a refined mathematical model for chloride diffusion based on Song et al.'s model (Equation 8.1) is proposed.

The values of chloride diffusion coefficient, determined by the model proposed in this study, will be subsequently used as input data in the computer model by utilising ABAQUS/CAE software to estimate the chloride content in different time slots.

8.2 TIME DEPENDENCY APPROACHES OF THE CHLORIDE DIFFUSIVITY

In this section the database of chloride diffusion coefficient are investigated to propose and develop a new mathematical model for D as a time-dependent parameter.

8.2.1 A. Costa and J. Appleton Approach (1999)

In Costa and Appleton's (1999) experimental study, it has been confirmed that chloride diffusion coefficient value changes over time.

They cast three different concrete slab samples with different mix designs. The slabs were then exposed to a marine environment for three to four years to investigate the chloride diffusion coefficient. Mix designs of the slabs are presented in Table 8-2.

Table 8-2 Mix design and concrete properties for slabs, Costa & Appleton (1999)

Material [kg/m^3] & Concrete Properties	Samples C1	C2	C3
Portland Cement	300	425	500
Sand (4.76 mm)	822	677	-
Coarse Aggregate I (19.1 mm)	500	481	-
Coarse Aggregate II (9.5 mm)	631	750	-
W/C	0.5	0.3	0.35
Slump [mm]	70	170	-
Dry Density [kg/m^3]	2330	2410	2320
Compressive Strength (MPa)	34	54	66

To determine the chloride penetration rate (diffusivity, D), chloride content in samples was measured at various depths in equal time intervals. For each time period, ground concrete samples at each 5 mm depth increment were taken from two adjacent holes using a 20 mm

diameter drilling tool. The samples were analysed to measure the total chloride (acid soluble chloride).

During their experimental study numerous chloride profiles were obtained. The average of the test results are presented in Table 8-3.

Table 8-3 Test results of diffusivity and surface chloride concentration, Costa & Appleton (1999)

	C1		C2		C3	
Time [months]	D $\times 10^{-12}$ m^2/s	Cs %bwcon	D $\times 10^{-12}$ m^2/s	Cs %bwcon	D $\times 10^{-12}$ m^2/s	Cs %bwcon
6	4.83	0.17	2.34	0.15	2.08	0.15
9	3.65	0.21	1.7	0.17	1.52	0.22
12	2.75	0.26	1.48	0.19	1.24	0.19
15	2.63	0.25	1.45	0.23	1.33	0.21
18	2.66	0.3	1.42	0.23	1.01	0.3
24	2.3	0.32	1.2	0.27	1.15	0.29
30	1.92	0.35	1.02	0.35	0.92	0.37
36	1.87	0.42	1.05	0.36	0.88	0.34

In the present investigation, all output data from the Costa & Appleton (1999) study has been examined and analysed in order to obtain a mathematical correlation between chloride diffusivity and time. Values of chloride diffusion coefficient for all concrete samples are shown in Figure 8-1.

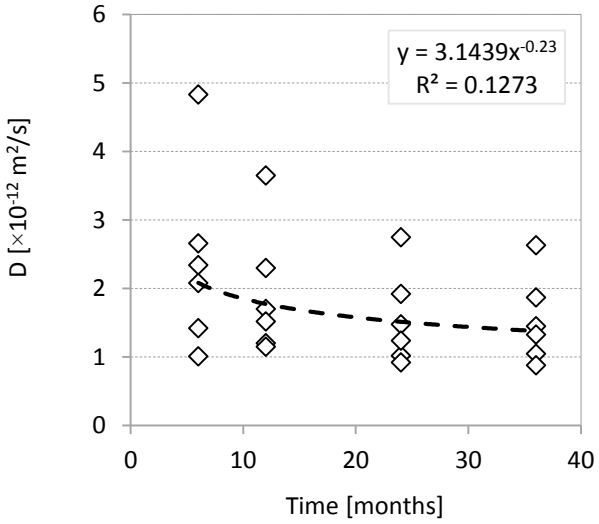

Figure 8-1 Diffusivity vs. time, (Costa and Appleton, 1999)

According to Figure 8-1, the best fit curve to express the relationship between D and t can be presented in Equation 8.3.

$$D = 3.1439(t)^{-0.23} \tag{8.3}$$

8.2.2 Luping and Nilsson Approach (1992)

Luping and Nilsson (1992) investigated the quantitative relationship between chloride diffusivity and concrete age. They prepared three types of concrete samples with different water cement ratio of 0.32, 0.54, and 0.7. Mix designs of the samples are illustrated in Table 8-4.

Table 8-4 Concrete mix design, Luping & Nilsson (1992)

Sample	W/C	Cement [kg/m^3]	Aggregates [kg/m^3]	Water [kg/m^3]
1	0.32	522	1750	167
2	0.54	300	-	162
3	0.7	270	1922	189

They used the colorimetric method to measure the chloride content. The total chloride content of the powder was determined by using Berman's method. Their test results are presented in Table 8-5.

Table 8-5 Chloride diffusivity vs. time, Luping & Nilsson (1992)

Time [day]	1	3	7	14	28	90	180
D [$\times 10^{-12}$m^2/s] Sample 1	7.39	6.22	4.93	-	3.22	1.79	1.74
D [$\times 10^{-12}$m^2/s] Sample 2	4	3	-	2.5	-	-	-
D [$\times 10^{-12}$m^2/s] Sample 3	45.6	26.95	21.1		14.5	15.3	-

In the present investigation, Luping and Nilsson's (1992) experimental results were collected and combined to obtain the best correlation between chloride diffusivity and time as shown in Figure 8-2.

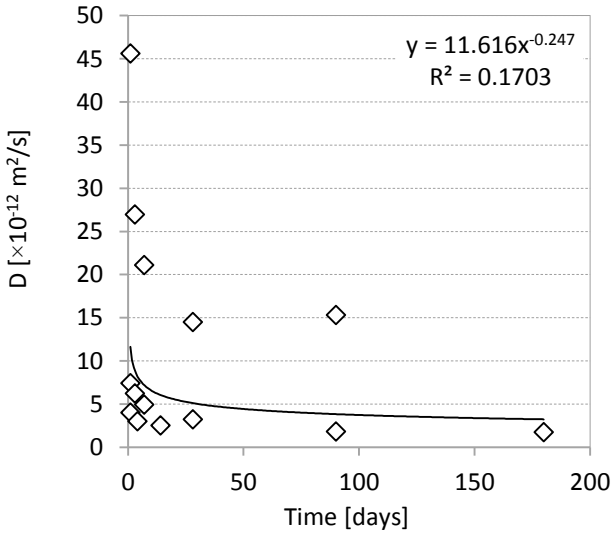

Figure 8-2 Chloride diffusivity vs. time, Luping & Nilsson (1992)

According to Figure 8-2, the best fit curve to express the relationship between D and t can be presented in Equation 8.4.

$$D = 11.616\,(t)^{-0.247} \tag{8.4}$$

8.2.3 O. Truc et al. Approach (2000)

Truc et al. (Truc et al., 2000) conducted an investigation by preparing four different concretes in accordance with the French Standard NFP18305, which specifies conditions to investigate the chloride diffusivity in the concrete when concrete structures are exposed to a marine environment. They used two types of cement with two different water/cement ratios to make the concrete specimens. They used four concrete mixes as shown in Table 8-6.

Table 8-6 Concrete mix designs, Truc et al. (2000)

Material	1	2	3	4
Cement [kg/m^3]	425 CPA-CEMI 52	425 CPA-CEMI	364 CPA-CEMI 52	364 CPA-CEMI
Gravel [kg/m^3]	1130	1130	1062	1062
Sand [kg/m^3]	750	750	708	708
Water [kg/m^3]	136	136	200	200
W/C ratio	0.32	0.32	0.55	0.55
Superplasticizer [%cement]	2	2	-	-

The results of Truc et al.'s study are summarised in Table 8-7.

Table 8-7 Chloride diffusivity vs. time (Truc et al., 2000)

Time [days]	D1	D2	D3	D4
	[$\times 10^{-12}$ m^2/s]			
4	6.5	4.5	-	-
7	3.2	3.2	1.55	1.2
11	2.1	1.97	1.1	0.75
14	2	1.1	0.8	0.45

The results, which have been collected and combined, are presented in Figure 8-3. According to Figure 8-3, the best fit curve to express the relationship between D and t can be presented in Equation 8.5.

$$D = 30.295\ (t)^{-1.317} \tag{8.5}$$

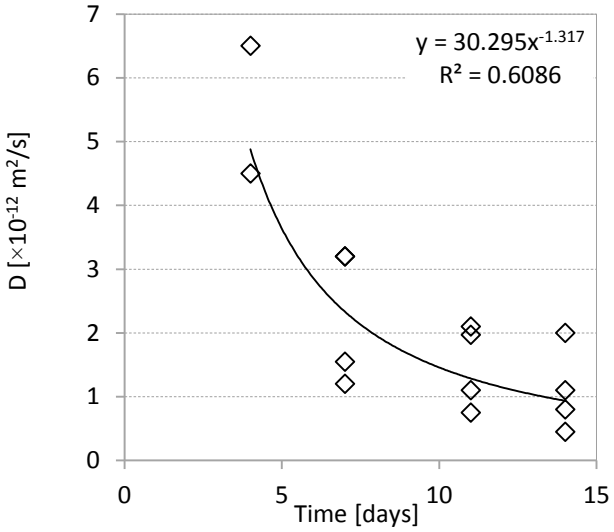

Figure 8-3 Chloride diffusivity vs. time (Truc et al., 2000)

8.2.4 Polder Approach (1995)

Polder (1995) used a constant water cement ratio of 0.4 to investigate the chloride diffusivity versus time. The data of his experimental investigation are presented in Table 8-8.

Table 8-8 Chloride diffusivity investigation, Polder (1995)

Reference	W/C	Age	Mix Design			D
			Cement	Water	Aggregates	$\times 10^{-12}$ [m^2/s]
		7 days				3
(Polder, 1995)	0.4	28 days	420	168	NG	2
		98 days				1

The output of the Polder (1995) study was examined in the present investigation to find the best relationship between D and t as shown in Figure 8-4.

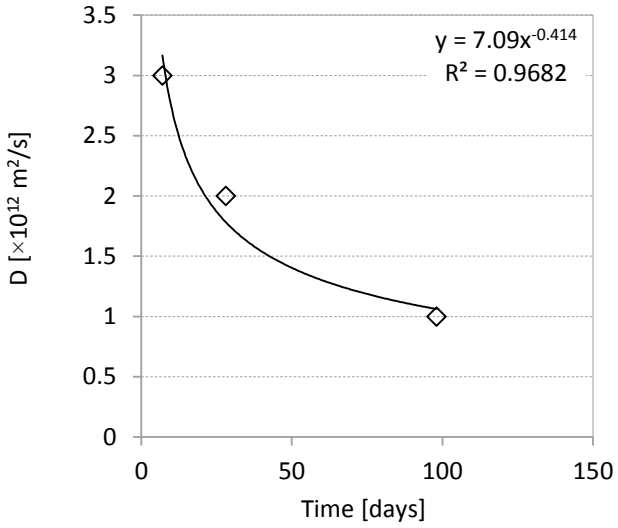

Figure 8-4 Chloride diffusivity vs. time, Polder (1995)

According to Figure 8-4, the best fit curve to express the relationship between D and t can be presented in Equation 8.6.

$$D = 7.09\ (t)^{-0.414} \tag{8.6}$$

8.2.5 Kanaya et al. Approach (1998)

Kanaya et al. (1998) used a fixed water cement ratio of 0.6 to investigate the chloride diffusivity versus time. The results of this experimental investigation are presented in Table 8-9.

Table 8-9 Chloride diffusivity investigation, Kanaya et al. (1998)

Reference	W/C	Age	Mix Design			D
			Cement	Water	Aggregates	$\times 10^{-12}$ [m^2/s]
Kanaya et al. (1998)	0.6	14 days	275	165	1867	3.2
		21 days				1.0
		90 days				0.6

The output of the Kanaya et al. (1998) study has been analysed in the present investigation to find the best correlation between D and t as shown in Figure 8-5.

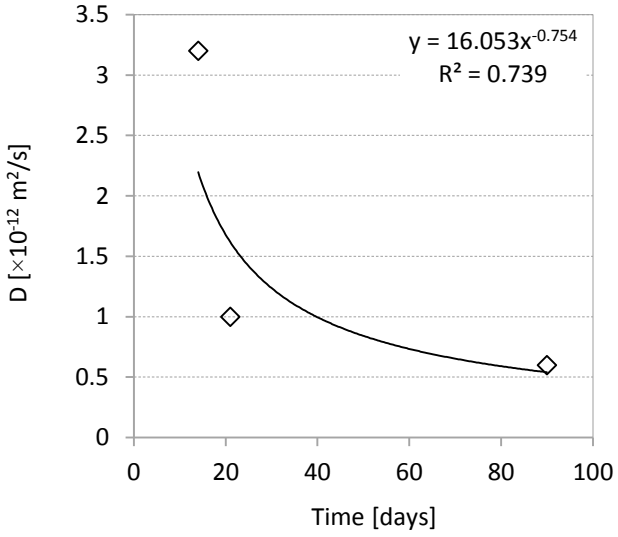

Figure 8-5 Chloride diffusivity vs. time, Kanaya (1998)

According to Figure 8-5, the best fit curve to express the relationship between D and t can be presented in Equation 8.7.

$$D = 16.53\ (t)^{-0.754} \tag{8.7}$$

8.2.6 Mangat and Molloy Approach (1994b)

Mangat and Molloy (1994b) also used a constant water cement ratio of 0.58 to investigate the chloride diffusivity versus time. The results of their experimental study are presented in Table 8-10.

Table 8-10 Chloride diffusivity investigation, Mangat & Molloy (1994b)

Reference	W/C	Age	Mix Design			D
			Cement	Water	Aggregates	$\times 10^{-12}$ [m^2/s]
Mangat and Molloy (1994b)	0.58	28 days	530	307	1309	5.3
		90 days				2.8
		270 days				1.3

The output of the Mangat and Molloy (1994b) study was analysed in the present investigation to find the preeminent relation between D and t and is shown in Figure 8-6.

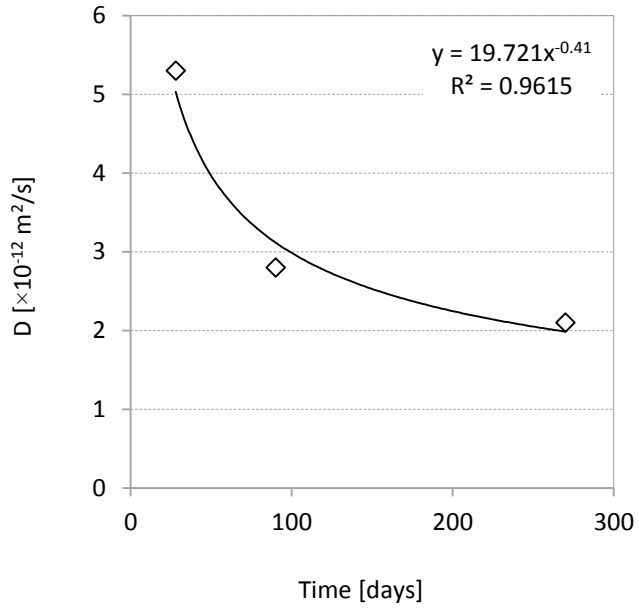

Figure 8-6 Chloride diffusivity vs. time, Mangat & Molloy (1994b)

According to Figure 8-6, the best fit curve to express the relationship between D and t can be presented in Equation 8.8.

$$D = 5.231\ (t)^{-0.851} \tag{8.8}$$

8.2.7 Luping and Nilsson Approach (1993b)

Luping and Nilsson (1993b) used a constant water cement ratio of 0.54 to investigate the chloride diffusivity versus time. The output of this experimental work is presented in Table 8-11.

The results of the Luping & Nilsson (1993b) investigation have been analysed in this study to find the best relationship between D and t which is shown in Figure 8-7.

Table 8-11 Chloride diffusivity investigation, Luping and Nilsson (1993b)

Reference	W/C	Age	Mix Design			D
			Cement	Water	Aggregates	$\times 10^{-12}$ [m^2/s]
Luping and Nilsson (1993b)	0.54	7 days	300	162	NG	4.0
		14 days				3.0
		98 days				2.5

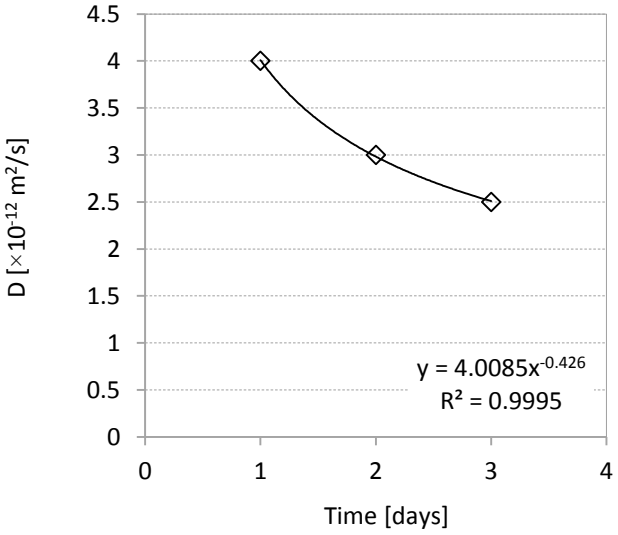

Figure 8-7 Chloride diffusivity vs. time, Luping & Nilsson (1993b)

According to Figure 8-7, the best fit curve to express the relationship between D and t can be presented in Equation 8.9.

$$D = 4.0085\ (t)^{-0.426} \tag{8.9}$$

8.3 PROPOSED NEW MODEL

Understanding of the transfer of chemicals and water in concrete is very important due to costs and environmental impact including maintenance and repair costs, increasing carbon dioxide emission, and usage of raw materials.

Therefore, accurate estimation of chloride content in concrete at any time and depth is required to predict the service life of structures precisely.

In this study, an accurate mathematical model is proposed to model the chloride diffusivity.

To develop a mathematical model for chloride diffusion coefficient, the database from literature and their different conditions are examined and accordingly the analytical model is proposed. Moreover, a parametric study is performed to investigate the influence of each affecting parameter on chloride diffusivity of concrete. Eventually, the calibrated model is verified by means of FEM and utilising ABAQUS computer software.

According to the previous studies from the literature the general form of the model can be expressed as follows:

$$D(t) = \alpha(t)^{-\beta} \tag{8.10}$$

Comparing this general format obtained from database analysis and Song et al (2004) model (Equation 8.3), the proposed model for chloride diffusion coefficient in the concrete can be rewritten as follows:

$$D(t) = D_0(t)^{-m} \tag{8.11}$$

where $\alpha = D_0$ and $\beta = m$.

In this study, to calculate the chloride diffusion coefficient (D) as a time-dependent parameter, two time phases have been assumed. These two time phases include (i) the end of curing period (t') and (ii) duration of exposure time (t). Consequently, the chloride diffusion coefficients corresponding to (i) and (ii) can be assumed as $D(t')$ and $D(t)$, respectively. Figure 8-8 explains the concept of time periods assumptions in this study.

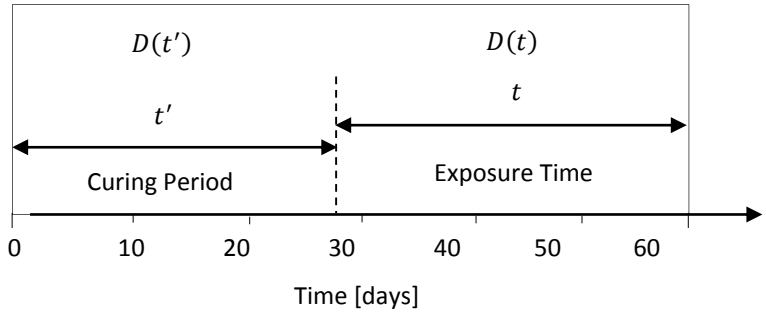

Figure 8-8 Time concept for mathematical model of D in this research

Therefore, general equation for the mathematical model of the time-dependent chloride diffusion coefficient for curing period can be presented as Equation 8.12.

$$D(t') = f(t') = a \cdot (t')^{-n} \tag{8.12}$$

where $\mathrm{D(t')}$ is the time-dependent diffusion coefficient at t', t' is the curing period, and a and n are constants which are different for different concrete mix designs (cement content, water content, and proportion of coarse aggregates).

Values of n are presented in Table 8-12.

Table 8-12 Empirical values of n

Type of cement	n
Portland cement concrete	0.264
Fly Ash Concrete	0.699
GGBF Slag concrete	0.621
Silica Fume concrete	$n = 1 - (1.10 \cdot \frac{W}{C})$

The author believes that rate of the reduction of chloride diffusion coefficient in the first 28 days is much faster than after 28 days (see Figure 8-9) due to high rate of cement hydration process. This behaviour was the main reason of dividing the total time into two phases and proposing mathematical models for each phase separately.

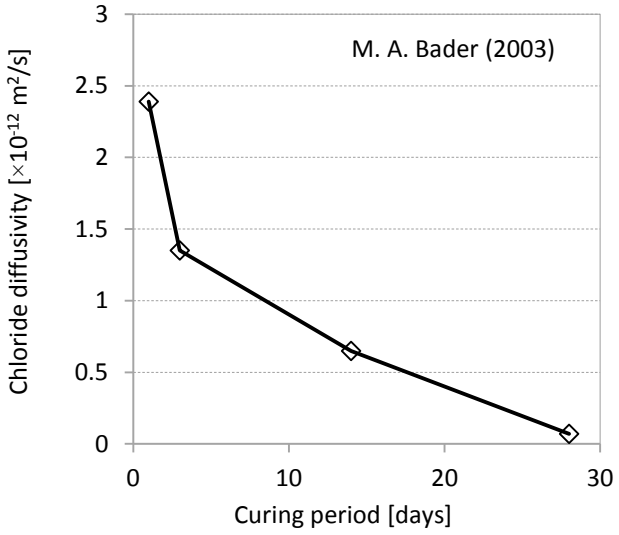

Figure 8-9 Effect of curing period on chloride diffusivity, (Bader, 2003)

Figure 8-9 illustrates the reduction of chloride diffusivity from day 1 to day 3 as 43%. In contrast, this chloride diffusivity reduction from day 14 to day 16 is only 8.3%. The average of the chloride diffusivity values during the first 28 days of the concrete age is considered as effective chloride diffusion coefficient, D_{eff}.

Therefore, assuming 28 days as the final time (upper band) for ultimate value of effective chloride diffusion coefficient $\left(D_{eff}\right)$ is logically accurate:

$$D_{eff} = \int_{t_0'}^{t_u'} D(t')\,dt' = \int_{t_0'}^{t_u'} \alpha(t')^{-n} dt' = \frac{D_0}{(1-n)} \cdot \left[\frac{{t_0'}^{(1-n)}}{{t_u'}^{(1-n)} - {t_s'}^{(1-n)}}\right] \tag{8.13}$$

where D_{eff} is the average of chloride diffusivity during 28 days, $t_s' = 7$ (days) and $t_u' = 28$ (days), $t_0 = 1\ (day)$, and D_0 is the concrete chloride diffusivity at age of one day.

To obtain a reliable mathematical model for chloride diffusivity, the effect of influencing factors on chloride diffusivity should be included in the model. Since chloride can diffuse into the concrete through the interconnected pores, the influencing parameters on pore structure of the concrete should be investigated and their effect should be included in the model.

The most important factors affecting chloride diffusivity are: water/cement ratio, cement content, cement type, and coarse aggregate proportion in the concrete mix. In following discussion the effects of these factors are investigated.

Since it has been assumed that the exposure time starts after 28 days of curing. Equation 8.15 is proposed as a mathematical model to determine the chloride diffusion coefficient.

$$D(t) = D_{eff} f(w/c)\, f(A) f(C) f(C_T) (t)^{-m} \tag{8.15}$$

where $D(t)$ is the time-dependent chloride diffusivity, $f(w/c)$ is the water cement ratio function, $f(A)$ is the aggregate size and proportion function, $f(C)$ is the cement content function, $f(C_T)$ is the cement type function, and t is the exposure time in seconds.

Among these affecting parameters the aggregate function $f(A)$ and cement content $f(C)$ are not time dependent and can be considered as influencing parameters on the effective chloride diffusion coefficient.

Increasing the coarse aggregate proportion increases the possibility of generating interconnected pores due to increasing the amount of Interfacial Transition Zone (ITZ) in the concrete.

Increasing the cement content reduces the porosity of the concrete which consequently decreases the chance of generating interconnected pores. On the other hand, increasing the coarse aggregate proportion increases the chloride diffusivity and increasing the cement content decreases the chloride diffusivity.

In addition, characteristic of the microstructure of the concrete which depends on the hydration process rate (hydration degree) is a function of cement type $f(C_T)$ and water cement ratio $f(w/c)$. Considering the abovementioned discussion for $D(t)$ and D_{eff}, the proposed models are presented in Equations 8.15 and 8.16.

$$D_{eff} = \frac{D_0}{(1-n)} \cdot \left[\frac{{t_0}^{'(1-n)}}{{t_u}^{'(1-n)} - {t_s}^{'(1-n)}} \right] \cdot f(A)/f(C) \tag{8.15}$$

$$D(t) = D_{eff} \cdot f(C_T)/f(w/c)(t)^{-m} \tag{8.16}$$

8.3.1 Effect of Aggregate, $f(A)$

Size and proportion of aggregate influence the chloride diffusion coefficient due to ITZ effect (interface effect). The high porosity property of ITZ, due to high concentration of C-H-S, causes chloride diffusivity in this area to be 10 times greater than the bulk cement matrix (Delagrave et al., 1997). Therefore, the proportion of coarse aggregate in concrete mix can affect the chloride diffusivity as increasing the coarse aggregates proportion in the mix increases the ITZ.

Consequently, increasing ITZ increases the possibility of interconnecting the pores in concrete microstructure and this phenomenon can increase the rate of chloride diffusion into concrete. Figure 8-10 illustrates that up to 30% of volume fraction of aggregate, chloride diffusivity shows a little change, but it increases considerably when the aggregate volume fraction is greater than 30% (Nilsson and Ollivier, 1995b, Asbridge et al., 2001).

Some scholars have investigated the effect of coarse aggregate proportion on the chloride diffusion coefficient in concrete, but none of them except Xi and Bazant (Xi and Bažant, 1999) have proposed a mathematical model for this factor (Basheer et al., 2005, Caré, 2003, Delagrave et al., 1997, Hobbs, 1999). The proposed model by Xi & Bazant is shown by Equation 8.17.

$$f(A) = \frac{2(1 - C_A)}{2 + C_A} \tag{8.17}$$

where C_A is the coarse aggregate content.

This model shows that even a small volume of aggregate has an influence on the chloride diffusion rate. However, the author believes that the ITZ porosity can affect the diffusion rate of chloride into the concrete only when ITZ can contribute in interconnection of the pores in the media. In other words, the effective area of ITZ should achieve a certain value to influence the chloride penetration into the concrete. Due to this phenomenon, in this study the data from the investigations conducted by Nilsson and Ollivier (Nilsson and Ollivier, 1995b) and Asbridge et al. (Asbridge et al., 2001) has been used to propose a model considering influence of aggregate on chloride diffusivity (see Figure 8-10).

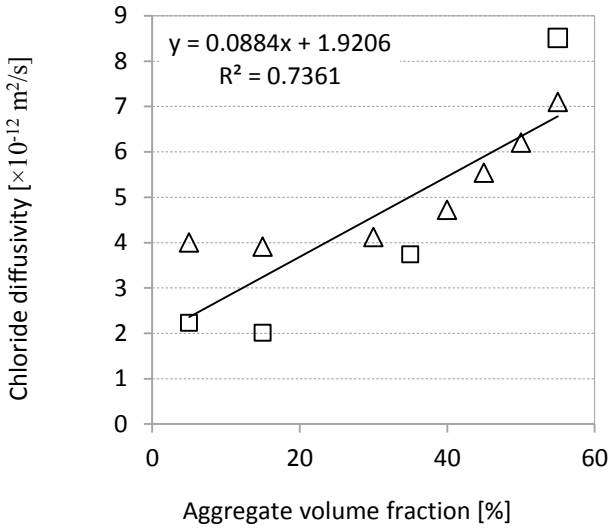

Figure 8-10 Model of aggregate proportion effect on chloride diffusivity

As a result, to consider the coarse aggregate effect, $f(A)$ on chloride diffusivity the following model has been proposed in this study:

$$if \ \frac{V_A}{V_{Con}} * 100 \ \leq 30\% \quad \rightarrow \quad f(A) = 1.00 \tag{8.18}$$

$$if \ \frac{V_A}{V_{Con}} * 100 > 30\% \quad \rightarrow \quad f(A) = \left[\frac{\left(\frac{V_A}{V_{Con}} - 30\right)}{5}\right] * 0.8 \tag{8.19}$$

where $\frac{V_A}{V_{Con}}$ is the coarse aggregate volume fraction in the mix in %.

8.3.2 Effect of Cement Content, $f(C)$

Some previous investigation results have revealed that increasing the cement content in concrete increases the rate of chloride transport into concrete. Increased activity by higher cement content brings the higher level of chloride ions into the concrete matrix as shown in Figure 8-11 (Song et al., 2010). Thus, it can be stated that the higher cement content may not always guarantee the long-life service of the concrete structures. Higher cement content increases the concrete strength, but reduces the concrete resistance to the risk of steel corrosion (Buenfeld and Okundi, 1998).

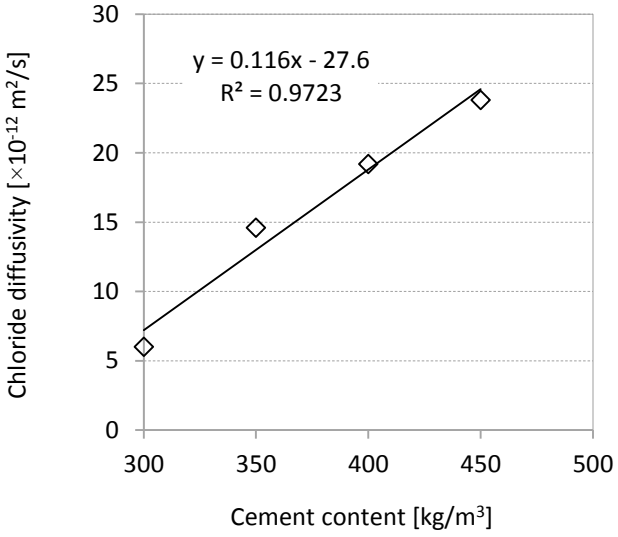

Figure 8-11 Effect of cement content on chloride diffusivity

Most studies have shown that increase in cement content in concrete mix reduces the chloride diffusion coefficient. Table 8-13 illustrates the change in chloride diffusivity by changing the cement content.

Table 8-13 Database for the relationship between cement content and chloride diffusivity

Cement content [kg/m^3]	D [$\times 10^{-12}$ m^2/s]	Reference
420	1.5	Polder (1995)
300	2.75	
250	9.8	Luping (1995)
390	5.6	
420	4.4	
450	2.8	
200	8.5	Dhir et al. (1990)
225	8.2	
285	2.8	
320	2.6	
385	1.5	
430	1.0	
369	7.1	Hooton et al. (1997)
374	5.0	
380	4.7	

This database (Table 8-13) has been used to obtain the correlation between cement content and chloride diffusivity as shown in Figure 8-12.

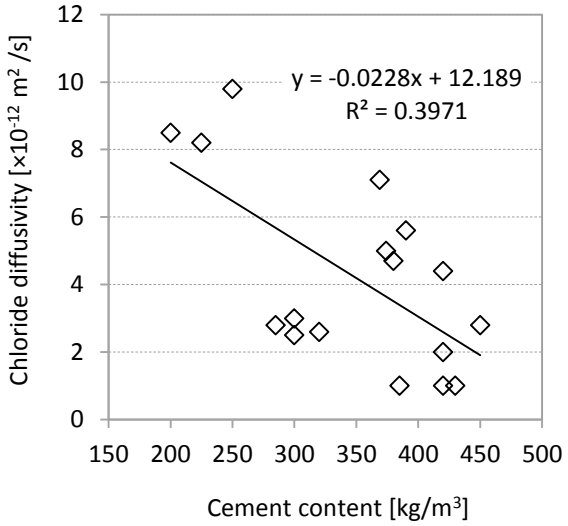

Figure 8-12 chloride diffusivity vs. cement content model

Therefore, the proposed relationship between chloride diffusivity and cement content can be expressed as follows:

$$if\ C_c < 200\ kg/m^3 \quad \rightarrow \quad f(C) = 1.00 \tag{8.20}$$

$$if\ C_c \geq 200\ kg/m^3 \quad \rightarrow \quad f(C) = \left[\frac{(C_c - 200)}{50}\right] * 1.14 \tag{8.21}$$

8.3.3 Effect of Cement Type, $f(C_T)$

Owing to differences in chemical composition of different cement types, the chloride binding capacity will be different. Chloride binding capacity of the cement influences the concrete chloride diffusivity. Generally, Portland cement type I (GP, C1) has shown smaller diffusion coefficient than Type V (Sulfate Resistance cement or SR, C5) owing to C_3A content in different type of cement (Oh and Jang, 2007). Using pozzolanic materials such as fly ash reduces the rate of chloride diffusion into the concrete as well. Table 8-14 illustrates the effect of cementitious materials on chloride diffusivity of the concrete.

Table 8-14 Effect of cement type on chloride diffusivity (Oh and Jang, 2007)

Cement type	GP	GPFA20*	SR	SRFA20**
D [$\times 10^{-12}$ m^2/s]	6.44	5.66	9.92	6.14

*Portland cement and 20% fly ash
**Sulfate resistance cement and 20% fly ash

Considering the concrete chloride diffusivity values for different types of cement, the coefficients of cement content, in the proposed model for chloride diffusion coefficient, can be expressed as shown in Table 8-15:

Table 8-15 Coefficients of cement type in mathematical models

Cement type	GP	GPFA20	SR	SRFA20
Coefficient in model	1.00	0.80	1.54	0.95

8.3.4 Effect of Water Cement Ratio, $f(w/c)$

Water cement ratio is the most important parameter related to the transport property of concrete, as it controls the permeability of concrete. Almost, all studies and investigations have achieved to a similar and common conclusion about the effect of water cement ratio on chloride diffusion coefficient. The results are shown in Figure 8-13 that confirm the similarity in this relationship.

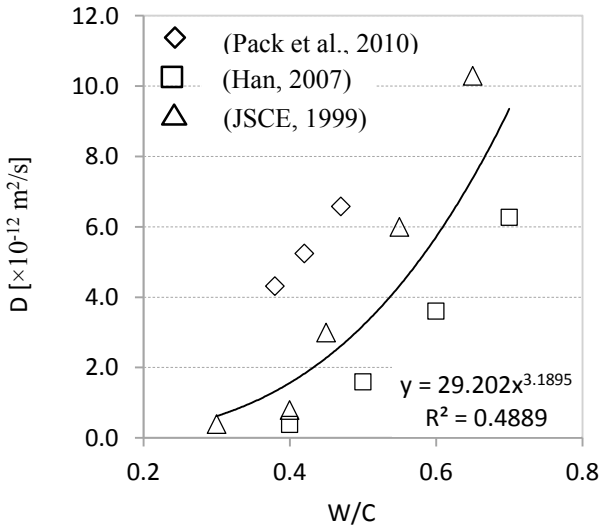

Figure 8-13 Relationship between chloride diffusivity and water cement ration

8.3.5 Determination of Age Factor, m

There is not any universal agreement about the value or mathematical model of the age factor (m) in the literature.

Some studies have proposed fixed values of m for different mix designs. Bamforth (Bamford, 1999) considered $m = 0.27$ for Portland cement concrete, Tang and Nilsson (Tang and Nilsson, 1992) proposed $m = 0.25$ for Portland cement concrete with W/C of 0.7 and $m = 0.31$ for Portland cement concrete with w/c of 0.32, and Nokken et al. (Nokken et al., 2006) suggested $m = 0.73$ for Portland cement concrete with W/C of 0.4.

Some other investigations have proposed mathematical models to determine the aging factor "m".

Mangat and Molloy (Mangat and Molloy, 1994b) have proposed the following equation:

$$m = 0.6 - 2.5\ (w/c) \tag{8.22}$$

ACI Life 365^{TM} model recommended:

$$m = 0.2 + \left[0.4\left(\frac{FA}{50} + \frac{BFS}{70}\right)\right] \tag{8.23}$$

where FA is the fly ash content [%], and BFS is the Slag content [%].

Roa-Rodriguez et al. (Roa-Rodriguez et al., 2013), by collecting the recommendations from six other published papers, concluded that:

$$m = \delta(F) + \varphi \tag{8.24}$$

where δ and φ are empirical coefficients and F is the cement content volume fraction in the concrete mix.

$$\delta = 0.0034 - 0.0015(w/c) \tag{8.25}$$

$$\varphi = 0.840 - 0.175(w/c) \tag{8.26}$$

This model can be feasible if the cement volume fraction is less than 0.5 and w/c is between 0.45 and 0.65.

Due to use of cement type factor (C_T) as an independent factor in the proposed model, ACI Life 365^{TM} model (Equation 8.23) has not been used in this study. Similarly, due to limitations of water to cement ratio in the model presented in Equation 8.24 has not been used as well. According to Australian Standard AS 4997, it is not recommended to use W/C greater than 0.4.

Consequently, in this study the model proposed by Mangat and Molloy (1994b) presented in Equation (8.22) has been used as the base model to calculate the value of "m". Considering the experimental results presented in following mentioned studies, this model also needs to be modified. The modification and calibration of the Mangat & Molloy's model is expressed as follows:

$w/c = 0.32 \quad \rightarrow \quad m = 0.31$ (Tang and Nilsson, 1992)

$w/c = 0.4 \quad \rightarrow \quad m = 0.49$ (Nokken et al., 2006)

Calculation of m using Equation 8.22 is presented as follows:

$$m = 0.6 - 2.5\,(w/c) = 0.6 - 2.5\,(0.32) = -0.2$$

$$m = 0.6 - 2.5\,(0.4) = -0.4$$

By changing 0.6 to 0.5, the results will be closer to the experimental results of other investigations. In this case for $w/c = 0.32 \rightarrow m = -0.3$ and for $w/c = 0.4 \rightarrow m = -0.5$ which shows a better match between model and experimental output.

In conclusion, a modified and calibrated model to determine the value of "m" has been proposed as shown in Equation 8-27.

$$m = 0.5 - 2.5(w/c) \tag{8.27}$$

By applying the effect of W/C ratio in the age factor, the W/C ratio coefficient in proposed model $f(w/c)$ can be eliminated.

8.3.6 Proposed Mathematical Model

Conferring the abovementioned discussions, the following mathematical models are proposed

$$D_{eff} = \frac{D_0}{(1-n)} \cdot \left[\frac{{t_0'}^{(1-n)}}{{t_u'}^{(1-n)} - {t_s'}^{(1-n)}}\right] \cdot f(A)/f(C) \tag{8.28}$$

$$D(t) = D_{eff} \cdot f(C_T) \left(\frac{t_u'}{t}\right)^m \tag{8.29}$$

where value of n is selected from Table 8-12, $f(A)$ can be calculated using Equations 8.18 and 8.19, $f(C)$ can be determined from Equations 8.20 and 8.21, $f(C_T)$ can be selected from Table 8-15, and m can be calculated using Equation 8.27.

8.4 NUMERICAL EXAMPLES

To check the proposed mathematical model, one of the experimental databases is compared with the proposed mathematical model as follows:

Example 1.

Comparing Proposed Model with Experimental Results Kanaya et al. (1998)

The experimental results are presented in Table 8-16.

Table 8-16 Experimental results conducted by Kayana et al. 1998

Reference	W/C	Age	Mix Design			D
			Cement	Water	Aggregates	$\times 10^{-12}$ [m^2/s]
Kanaya et al. (1998)	0.6	14 days	275	165	1867	3.2
		21 days				1.0
		90 days				0.6

The results of proposed mathematical model in this study are presented in Table 8-17.

Table 8-17 Proposed model results

Reference	m	Age	Mix Design				D
			n	f(C)	f(A)	$f(C_t)$	$\times 10^{-12}$ [m^2/s]
Proposed Model	1	14 days	1.71	165	1.84	1	3.02
		21 days					1.51
		90 days					0.62

Kanaya et al. (1998) experimental results and proposed mathematical model results are presented in Figure 8-14. As can be seen, the results show an excellent correlation.

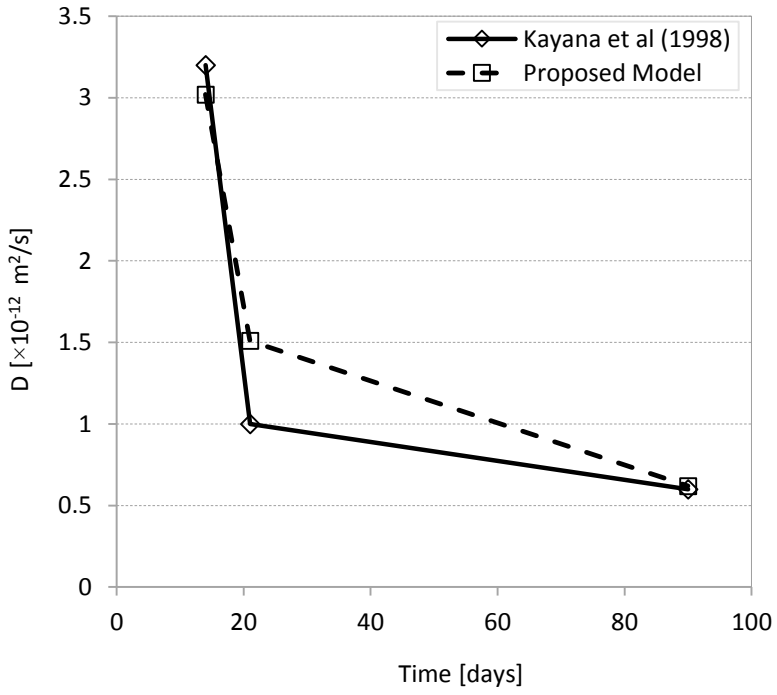

Figure 8-14 Comparing the proposed model and experimental results

Example 2.

Comparing Proposed Model with Experimental Results Luping & Nilsson (1992), Luping (1995), Zhang & Gjorv (1995), and Mangat & Molloy (1994b)

Chloride diffusion coefficient obtaining from experimental results are presented in Table 8-18. Data from these experimental investigations have been used as input data in proposed mathematical model to calculate chloride diffusion coefficient.

Table 8-18 Chloride diffusion coefficients obtaining from experimental studies

	Reference	Cement [kg/m^3]	Water [kg/m^3]	W/C	Aggregate [kg/m^3]	D [$\times 10^{-12}$ m^2/s]	Exposure Time
1	Zhang & Gjorv (1995)	330	165	0.5	2066	3.65	2 mon.
2	Luping (1995)	450	157.5	0.35	1695	3.1	2 mon.
3	Luping (1995)	420	168	0.4	1692	5.4	2 mon.
4	Luping & Nilsson (1992)	690	276	0.4	1380	1.1	3 mon.
5	Mangat & Molloy (1994b)	530	307	0.58	1309	2.8	3 mon.

Chloride diffusion coefficients calculated utilising proposed mathematical model in this study and are presented in Table 8-19.

Table 8-19 Chloride diffusion coefficient calculated by proposed mathematical model

Reference	n	t_0 [day]	t_s [day]	t_u [day]	t [mon]	$f(A)$	$f(C)$	$f(C_T)$	D_{eff} [$\times 10^{-12}$ m^2/s]	m	D [$\times 10^{-12}$ m^2/s]
1	0.264	1	7	28	2	7.36	2.96	1.00	2.00	-0.75	3.94
2	0.264	1	7	28	2	5.28	5.7	1.00	2.54	-0.35	3.38
3	0.264	1	7	28	2	5.28	5.0	1.00	3.50	-0.5	5.13
4	0.264	1	7	28	3	3.36	11.2	1.00	6.60	-0.5	1.18
5	0.264	1	7	28	3	2.88	7.52	1.00	5.80	-0.95	2.97

Comparison of experimental results and proposed mathematical model output is presented in Table 8-20. This assessment confirms that the proposed mathematical model can be used to predict the chloride diffusion coefficient reliably.

Table 8-20 Comparison of experimental results and output of proposed mathematical model

Reference	D Experimental [$\times 10^{-12}$ m^2/s]	D Mathematical [$\times 10^{-12}$ m^2/s]	Change [%]
Zhang & Gjorv (1995)	3.65	3.94	7.94
Luping (1995)	3.1	3.38	9.03
Luping (1995)	5.4	5.13	5.00
Luping & Nilsson (1992)	1.1	1.18	7.27
Mangat & Molloy (1994b)	2.8	2.97	6.07

8.5 SUMMARY

In this study a rationale mathematical model was proposed. An extensive investigation of databases regarding the relationship between chloride diffusion coefficient and time, revealed that the models proposed by Mangat and Molloy (1994b) can be a reasonable base for chloride diffusivity prediction. Mangat and Molloy (1994b) proposed an equation to determine "m" coefficient in mathematical model according to water cement ratio.

These models used "age factor, m" as the only influencing parameter on chloride diffusivity. But as the data analysis conducted in Chapter 4 indicates, this model and databases are not well matched and accurate.

In this study, the proposed model was divided into two time phases including (i) curing period, and (ii) exposure time. Also, in the proposed model the following influencing factors in addition to water cement ratio have been considered to determine chloride diffusivity more accurately:

- Coarse aggregate proportion to apply the effect of interfacial transition zone (ITZ)
- Cement content
- Cement type to apply the effect of chloride binding process,

In conclusion, the proposed model has been compared by one of the databases. This analysis indicates an excellent trend match between experimental results and the proposed model in this study.

CHAPTER 9

COMPUTER MODELING

CHAPTER 9. COMPUTER MODELLING

9.1 INTRODUCTION

Computer modelling techniques have been increasingly used to provide precise information on prediction of the chloride diffusion mechanism in concrete.

ABAQUS/CAE uses Fick's second law, as the default model, to determine the diffusion derived by the concentration gradient. Through the literature review, it has been established that both diffusivity (D) and surface chloride concentration (Cs) are time-dependent parameters. Whereas, according to the main assumptions of Fick's law both D and Cs are considered as constant parameters. In this study the abovementioned parameters are modified and defined to the software (input data) as time dependent parameters.

As discussed in previous chapters, the diffusion coefficient of chloride into reinforced concrete elements is the most vital parameter for estimating the service life of RC structures. Most of the former studies and investigations have already suggested mathematical models of predicting the service life of RC structures based on the diffusion coefficient of chloride as a constant parameter. However, according to the experimental investigations presented in literature, it has been proved that the diffusion coefficient is a time-dependent factor and it is reduced by time.

To verify the proposed mathematical model in this study, a comprehensive FE analysis by employing ABAQUS software has been conducted. ABAQUS provides analysis technics to solve traditional implicit finite element analysis, including static, dynamic; and heat and

mass diffusion, all powered with the widest range of contact and nonlinear material options.

A mass diffusion analysis models the transient or steady-state diffusion of one material through another, such as the diffusion of hydrogen through a metal. The governing equations for mass diffusion are an extension of Fick's equations: they allow for non-uniform solubility of the diffusing substance in the base material and for mass diffusion driven by gradients of temperature and pressure. Mass diffusion analysis is performed using mass diffusion elements and the *MASS DIFFUSION procedure.

A mass diffusion analysis:

- Models the transient diffusion of one material through another, such as the diffusion of hydrogen through a metal, or diffusion of chloride ion through the concrete
- Can be also used to model temperature and/or pressure-driven mass diffusion

Afterwards, the output data from the computer model will be verified by experimental results. After verifying, the computer model can be used to estimate the chloride content in the concrete at any time. Consequently, service life of reinforced concrete structures can be predicted accurately.

9.2 GOVERNING EQUATION

The commercial finite element code ABAQUS is used to model the mass diffusion process, with the governing equations for mass diffusion in ABAQUS being an extension of Fick’s law. The model allows for non-uniform solubility of the diffusing substance in the base material and for mass diffusion driven by gradients of temperature and pressure. The basic solution variable (used as the degree of freedom at the nodes of the mesh) is the “normalized concentration” (often also referred to as the “activity” of the diffusing material).

$$\emptyset = c/s \tag{9.1}$$

where $\boldsymbol{c}$ is the mass concentration of the diffusing material and $\boldsymbol{s}$ is its solubility in the base material. Therefore, when the mesh includes dissimilar materials that share nodes, the normalized concentration is continuous across the interface between the different materials.

The diffusion problem is defined from the requirement of mass conservation for the diffusing phase.

$$\int_V \frac{dc}{dt} dV + \int_S \boldsymbol{n}.\boldsymbol{J}\, dS = 0 \tag{9.2}$$

where V is any volume whose surface is S, $\mathbf{n}$ is the outward normal to S, $\mathbf{J}$ is the flux of concentration of the diffusing phase, and $\mathbf{n} \cdot \mathbf{J}$ is the concentration flux leaving S.

Diffusion is assumed to be driven by the gradient of a general chemical potential (concentration gradient):

$$\boldsymbol{J} = -s\boldsymbol{D}.\left[\frac{\partial \emptyset}{\partial x} + k_s \frac{\partial}{\partial x}\left(ln(\theta - \theta^Z)\right) + k_p \frac{\partial p}{\partial x}\right] \tag{9.3}$$

where $D(c, \theta, f)$ is the diffusivity; $s(\theta, f)$ is the solubility;$k_s(c, \theta, f)$ is the "Soret effect" factor, providing diffusion because of temperature gradient; θ is the temperature; θ^Z is the value of absolute zero on the temperature scale being used; $k_p(c, \theta, f)$ is the pressure stress factor, providing diffusion driven by the gradient of the equivalent pressure stress, and f are any predefined field variables.

$$p = -trace\,(\sigma)/3 \tag{9.4}$$

where "$\boldsymbol{\sigma}$" is stress; and "f" are any predefined field variables.

Whenever D, k_s, or k_p depends on concentration, the problem becomes nonlinear and the system of equations becomes nonsymmetric. In practical cases the dependence on concentration is quite strong, so the nonsymmetrical matrix storage and solution scheme is invoked automatically when a mass diffusion analysis is performed.

The two terms in this equation describe the normalized concentration and temperature-driven diffusion, respectively. The normalized concentration-driven diffusion term is identical to that given in the general relation. The temperature-driven diffusion term in Fick's law is recovered in the general relation if:

$$k_s = \frac{c(\theta - \theta^Z)}{s^2}\frac{\partial s}{\partial \theta}\,. \tag{9.5}$$

This conversion is done automatically in ABAQUS/Standard when you request Fick's law. An extended form of Fick's law can also be chosen by specifying a nonzero value for k_p:

$$J = -D.\left(\frac{\partial c}{\partial x} + sk_p\frac{\partial p}{\partial x}\right) \tag{9.6}$$

In this case ABAQUS/Standard will still define k_s automatically.

UNITS:

The units of concentration are commonly given as per million (P). On the basis of the applicability of Sievert's law to the mass diffusion, the units of solubility are $PLF^{1/2}$, where F is force and L is length. The units of the Soret effect factor are $F^{1/2}L^{-1}$. The units of the pressure stress factor are $LF^{1/2}$, and the units of equivalent pressure stress are FL^{-2}. The diffusivity, D, has units of L^2T^{-1}, where T is time. The concentration flux, J, then has units of PLT^{-2}; and the concentration volumetric flux, $Q = \int_s n \cdot J ds$, has units of PL^3T^{-1}.

9.3 STEADY-STATE ANALYSIS

Steady-state mass diffusion analysis provides the steady-state solution directly. In nonlinear cases, iteration may be necessary to achieve a converged solution. In the real environment the concentration of chloride ions can be considered as a time-dependent parameter. Therefore, in this research project the steady-state analysis will be used to solve the mass diffusion problem.

In steady-state analysis a "time" scale to the analysis step is assigned as shown in Figure 9-1. This time scale is often convenient for output identification and for specifying prescribed normalized concentrations and fluxes with varying magnitudes. Thus, when steady-state analysis is chosen, you specify a "time" increment and a "time" period for the step; ABAQUS/Standard then increments through the step accordingly (see Figure 9-2). If a steady-state analysis step is to be followed by a transient analysis step and total time is used in amplitude definitions, the time period should be defined to be negligibly small in the steady-state step.

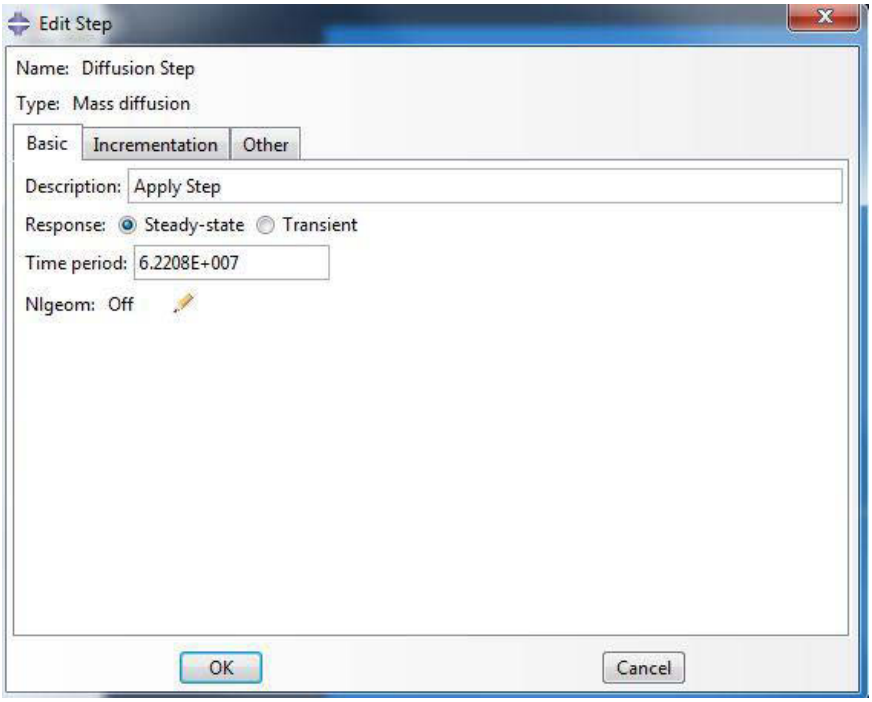

Figure 9-1 Steady-state analysis basic in mass diffusion (time period)

Automatic or fixed time incrementation can be used for transient analysis. The automatic time incrementation scheme is generally preferred because the response is usually simple diffusion and the rate of change of normalized concentration varies widely during the step and requires different time increments to maintain accuracy in the time integration.

The automatic time incrementation scheme for mass diffusion problems is based on the user-specified maximum normalized concentration change allowed at any node during an increment ΔC_{max}.

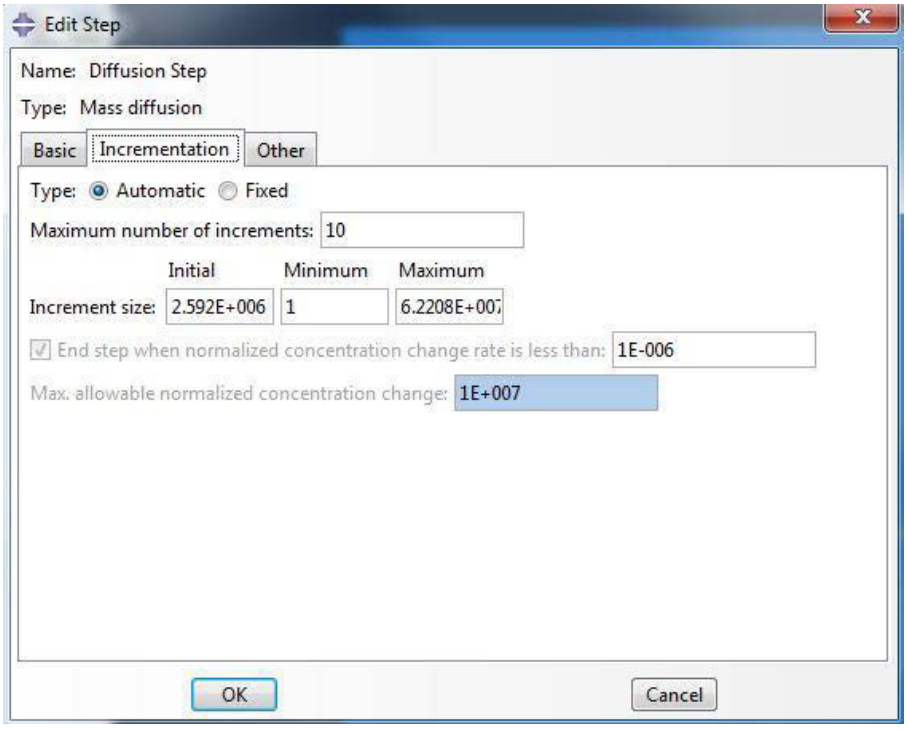

Figure 9-2 Time incrementation in steady-state analysis (Automatic time incrementation)

9.4 MODEL SIZE

The size of the model is 100 mm × 100 mm as shown in Figure 9-3.

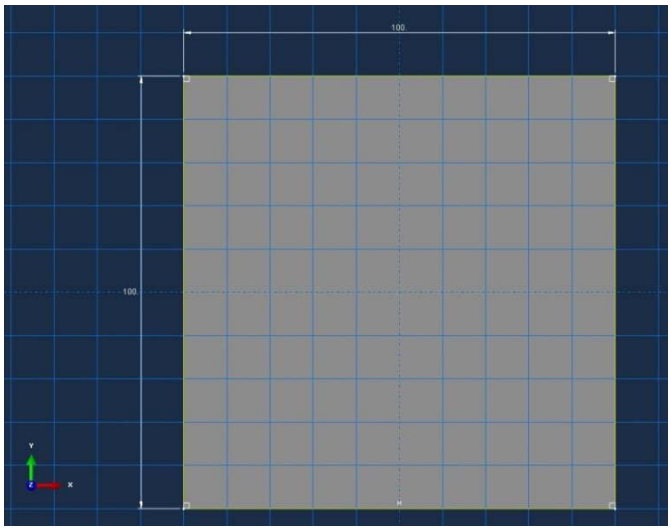

Figure 9-3 Model size in computer simulation

9.5 INITIAL CONCENTRATION

An initial normalised concentration of the diffusing material at specific nodes that belong to mass diffusion elements is defined as:

*TYPE = CONCENTRATION FOR INITIAL CONCENTRATION

9.6 BOUNDARY CONDITIONS

Boundary conditions can be applied to nodal degree of freedom of 11 in any mass diffusion element to prescribe values of normalised concentration. Such values can be specified as function of time.

Any boundary condition changes to be applied during a mass diffusion step should be given in the respective step using appropriate amplitude definitions to specify their "time" variations. If boundary conditions are specified for the step without amplitude references, they are assumed to changed either linearly with "time" during the step or instantly at the start of the step, according to the value given to the AMPLITUDE parameter of the *STEP option or its default value.

Since chloride flux diffuses into the concrete from just one surface, the boundary conditions of the model in this study is expressed as:

$$x = 0.0 \qquad Chloride\ Concentration = Surface\ Chloride\ Concentration \tag{9.7}$$

$$x = 10.0 \qquad Chloride\ Concentration = 0.0 \tag{9.8}$$

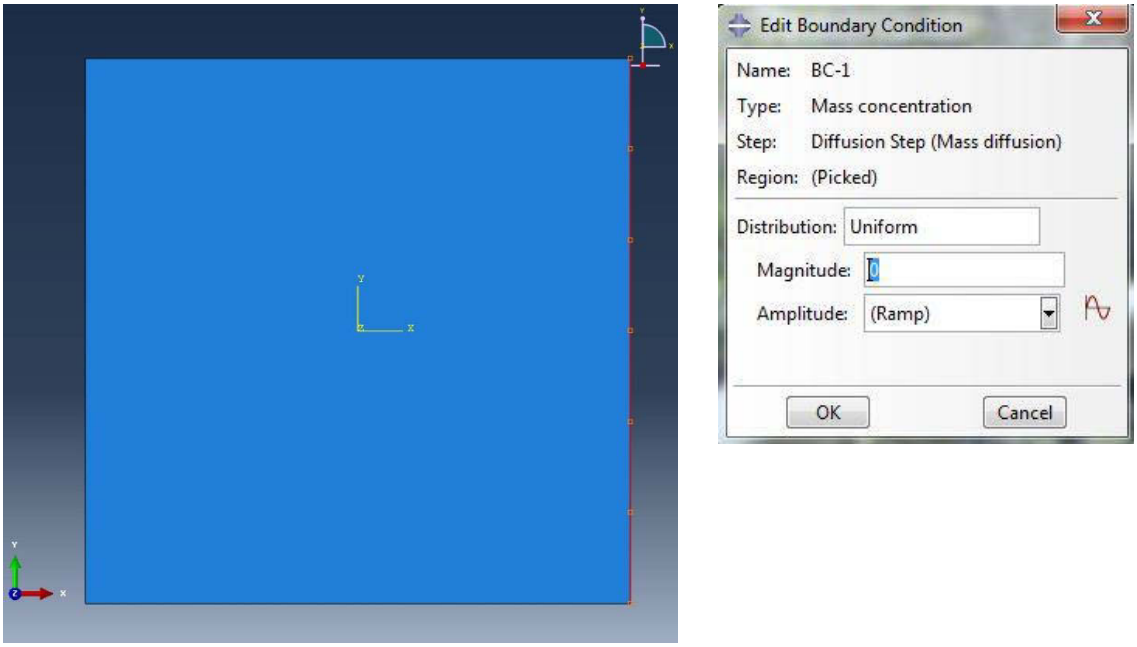

Figure 9-4 Boundary conditions

9.7 LOADING

Concentration fluxes are the only loads that can be applied in mass diffusion analysis. In transport phenomenon, flux is defined as the rate of flow of a property per unit area, which has the dimensions [quantity].[time]$^{-1}$.[area]. In the diffusion process, diffusion flux is the rate of movement of molecules across a unit area [mol].[m^{-2}].[s^{-1}].

The *CFLUX option is used to specify a concentrated concentration flux at a node. The *DFLUX option is used to specify distributed concentration fluxes acting on entire elements (body fluxes) or just on element faces (surface fluxes). The concentration flux was uniformly applied as surface fluxes (see Figure 9-5).

The concentration flux on the surface which is the model of surface chloride concentration (C_s) has been estimated based on the mathematical model (Equation 7.6) proposed by Song et al (Song et al., 2008).

$$C_s = C_0 + \alpha \cdot ln(t) \tag{9.9}$$

Surface chloride concentration (C_s) values, measured from experimental results, are thoroughly matched with Equation 9.9. C_s measured values as inputs for ABAQUS have been shown in Figure 9-6.

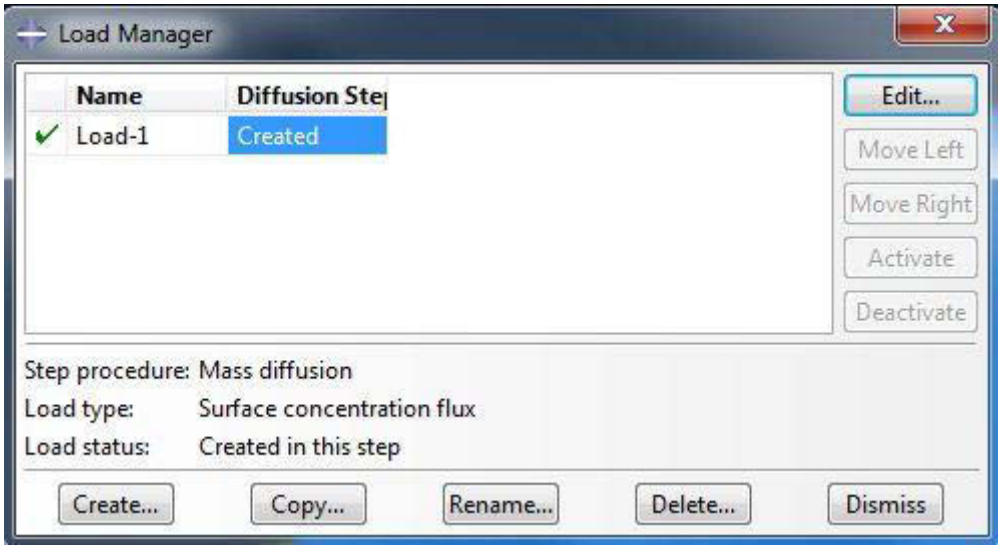

Figure 9-5 Loading surface concentration flux in ABAQUS/CAE

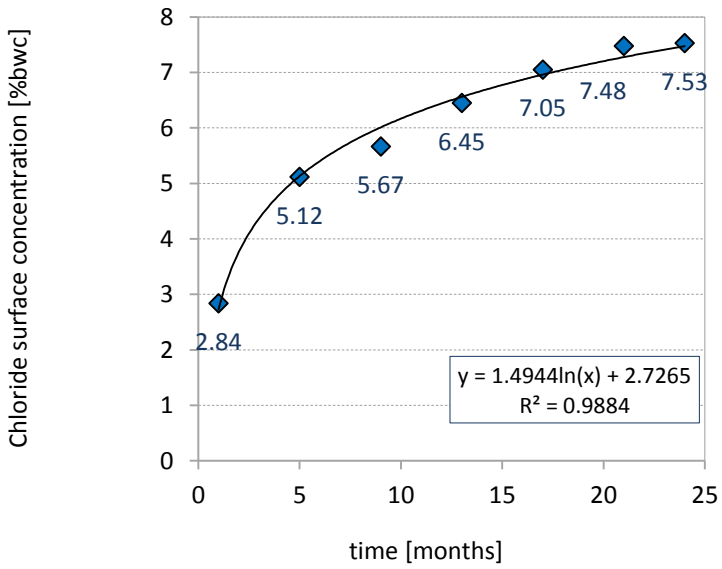

Figure 9-6 C_s values as input data for ABAQUS

Loading is presented in Figure 9-7. The initial surface chloride concentration (C_0) corresponding to $t_0 = 28\ days$ has been assumed 2.84 % by weight of cement (bwc).

$$t_0 = 28\ days \quad \rightarrow \quad C_0 = 2.84\ \%bwc \tag{9.10}$$

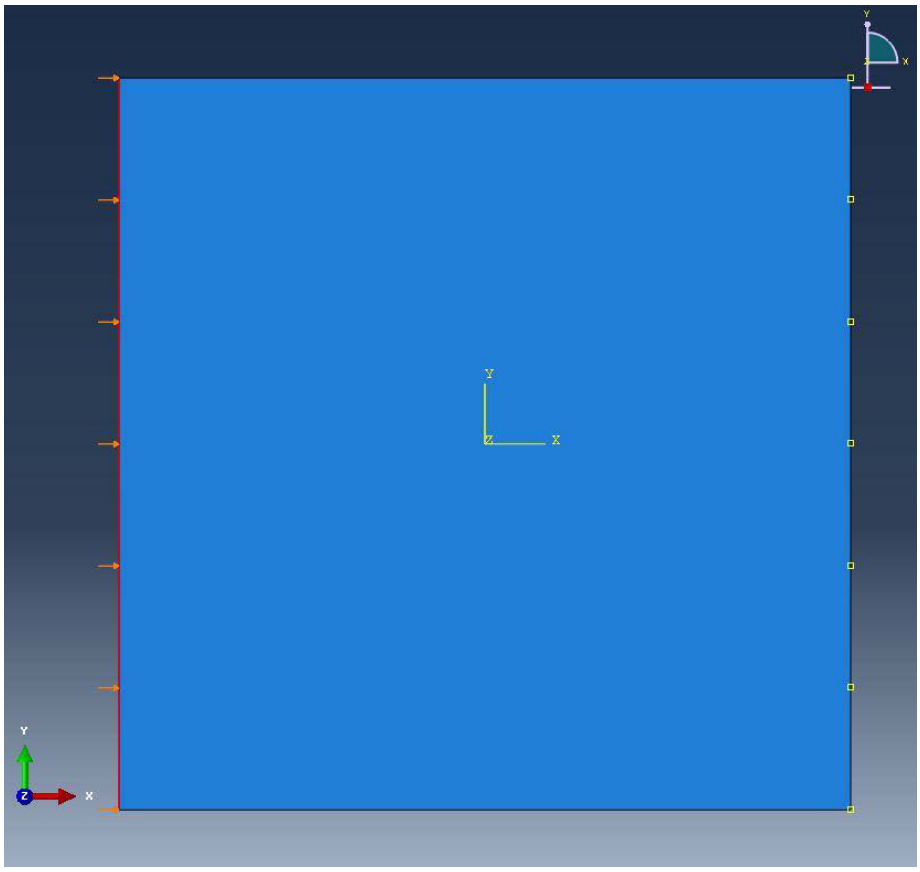

Figure 9-7 Concentration loading in one dimension (1D)

9.8 MATERIAL PROPERTIES

Conventional concrete properties including density (2400 kg/m^3), Young's modulus (32 GPa), Poisson's ratio (0.2), conductivity (0.88), concrete specific heat (800000000) have been selected.

Both diffusivity and solubility must be defined in a mass diffusion analysis. In ABAQUS material options diffusivity has been assumed as a constant parameter due to use of Fick's law. In this study, time-dependent diffusivity values, proposed in mathematical model, have been calculated by Equations 8.29 and 8.30, and then were entered as concrete properties to calculate the chloride content based on time-variable diffusivity values (see Figure 9-8).

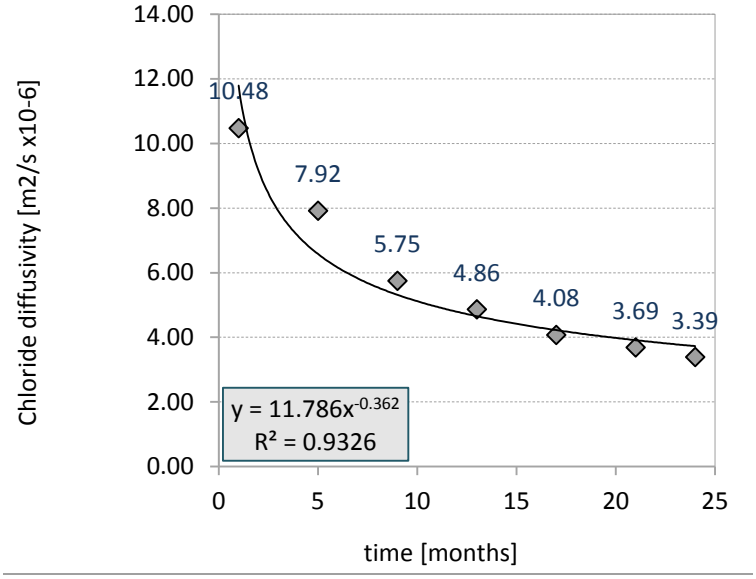

Figure 9-8 Chloride diffusivity calculated based on proposed mathematical model

The values of chloride diffusivity (D), surface chloride concentration (C_s), and time (Field 1) have been determined by proposed mathematical model in this study and proposed model by Song et al. (2008), respectively. Figure 9-9 shows the values of D and C_s as input data for computer modeling.

Using proposed mathematical model of chloride diffusion in this thesis (Equations 8.29 & 8.30), Chloride diffusion coefficient values for 24 months have been calculated and entered in the relevant column shown in Figure 9-9.

The surface chloride concentration values versus time were calculated by Equation (9.9) for 24 months and entered in "Concentration Column" in Figure 9-9.

In Figure 9-9, Field 1 is the exposure time in seconds for 24 months.

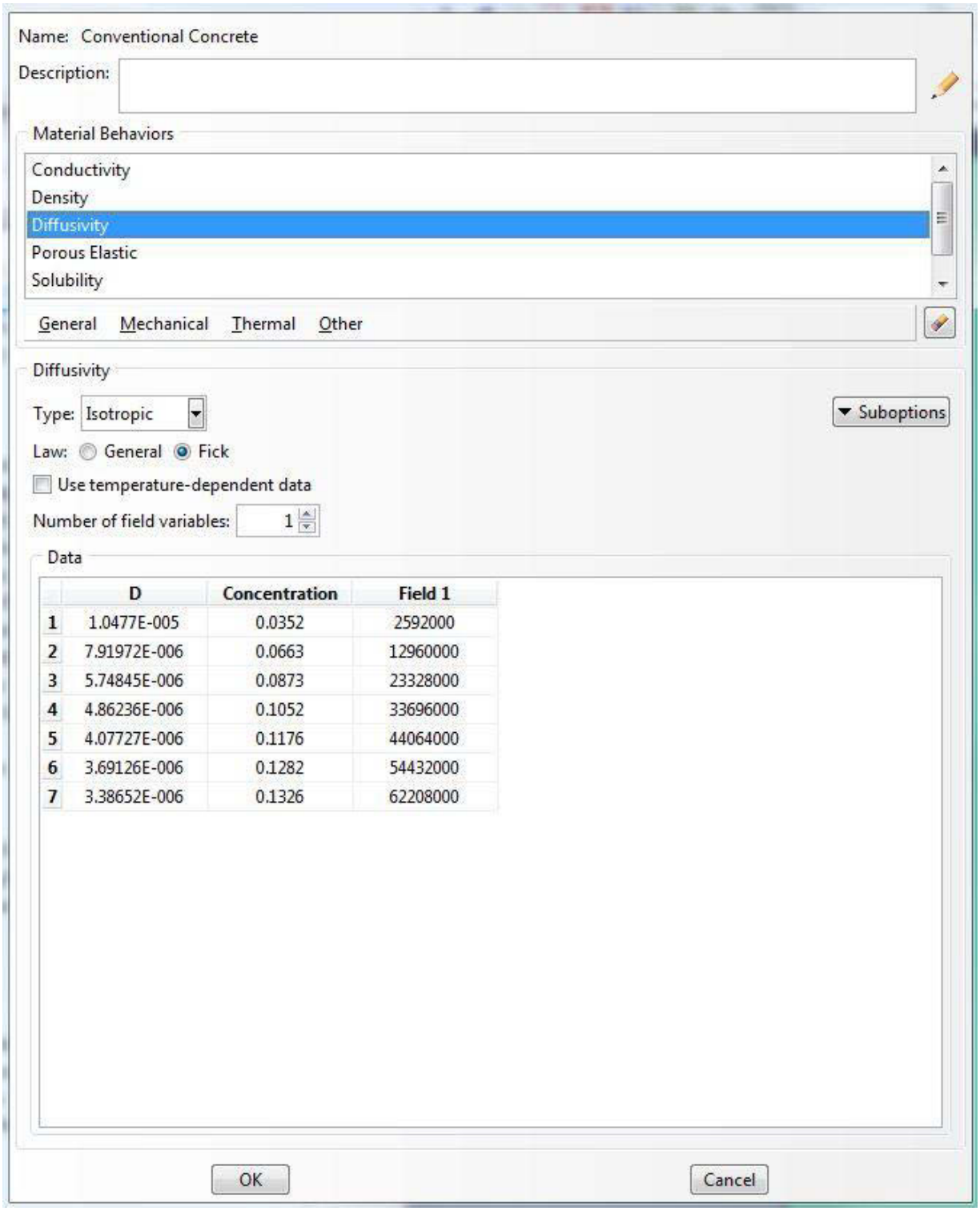

Figure 9-9 D and C_s values versus time as input data calculated by proposed model in this study and Song et al. (2008), respectively.

9.9 ELEMENTS

Mass diffusion analysis was performed in 2D environment using only one-dimensional elements to be able to verify the proposed diffusion mathematical model based on one-dimensional diffusion process (Figure 9-10).

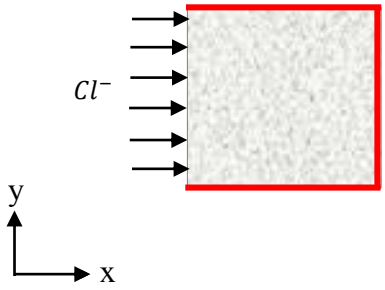

Figure 9-10 One-dimensional diffusion

The mesh size for concrete specimens generally is equal to the maximum size of the aggregate which is 20 mm. In this study, due to small cross-sectional area of specimen (100 mm), the mesh size has been selected as 10 mm as shown in Figure 9-11.

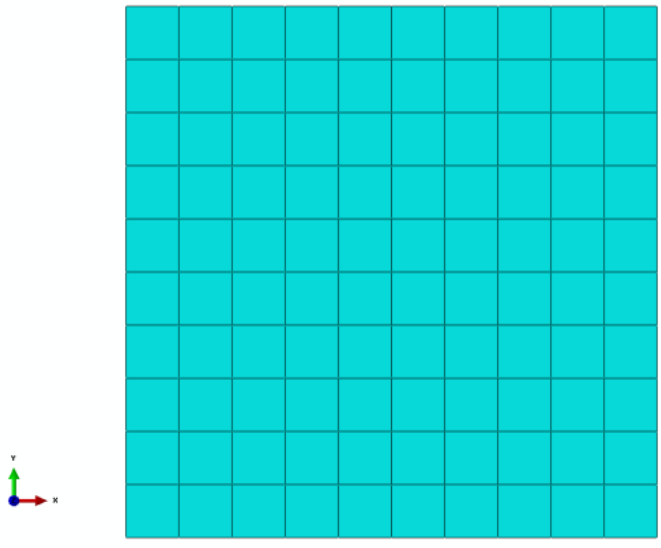

Figure 9-11 Mesh size of the computer model

9.10 PREDEFINED FIELDS

Predefined temperatures, equivalent pressure stresses, and field variables can be specified in a mass diffusion analysis. Since the diffusion of chloride into concrete occurs by concentration gradient, in this study, mass diffusion due to temperature and pressure stresses has not been considered, since they are out of the scope of this research.

Temperatures

Temperatures are applied to nodes in temperature-driven mass diffusion analysis using the *TEMPERATURE option. Absolute zero on the temperature scale used is defined as the value of the ABSOLUTE ZERO parameter on the *PHYSICAL CONSTANT option (see Figure 9-12).

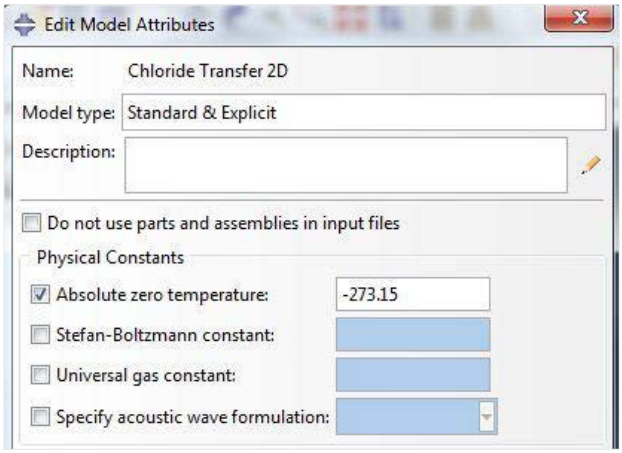

Figure 9-12 Temperature as predefine physical condition

9.11 ABAQUS OUTPUT/RESULTS

According to the aforementioned conditions, the results of the computer modelling are shown in Figure 9-13, Figure 9-14, and Figure 9-15.

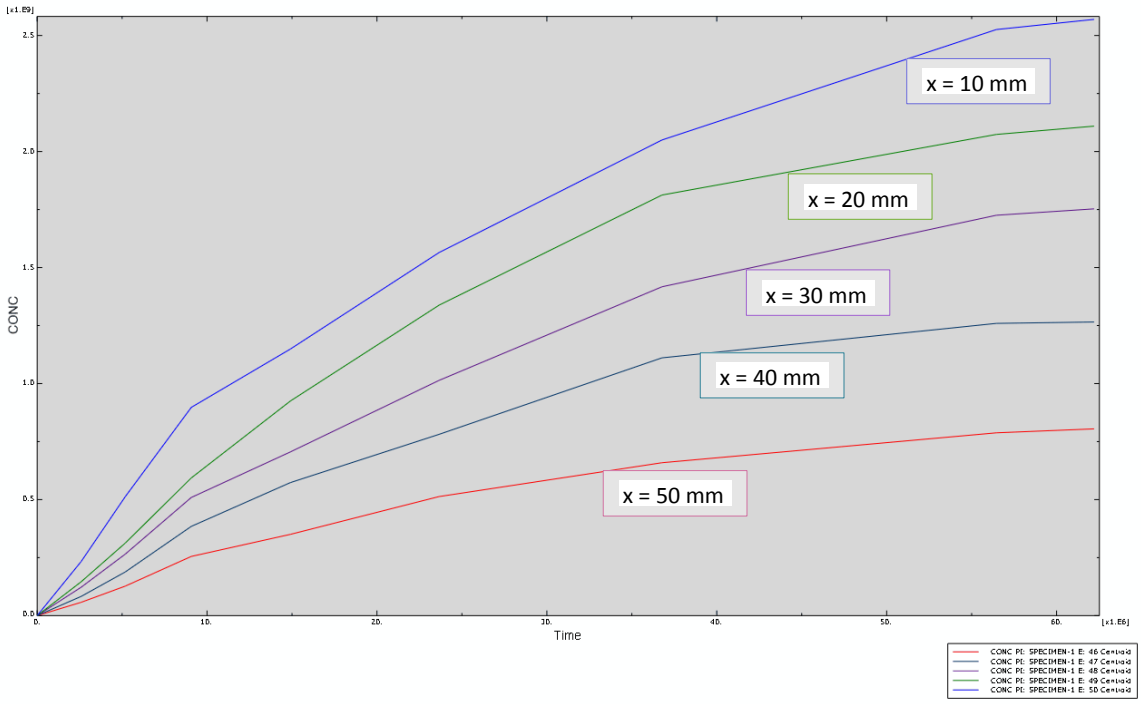

Figure 9-13 Computer modelling output, chloride content vs. time

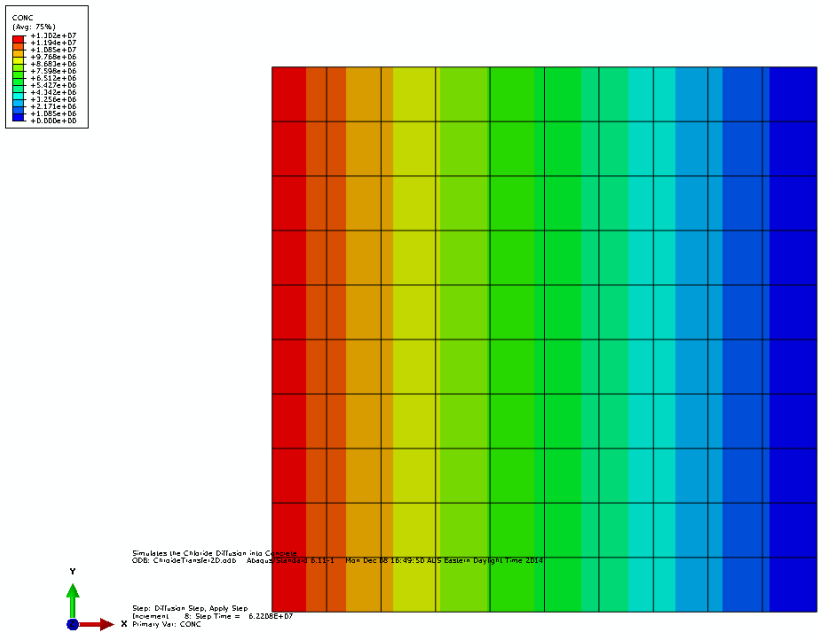

Figure 9-14 Concentration contours

The results show a reasonable agreement. Later, these results will be compared to experimental results from laboratory tests conducted in section 9-12.

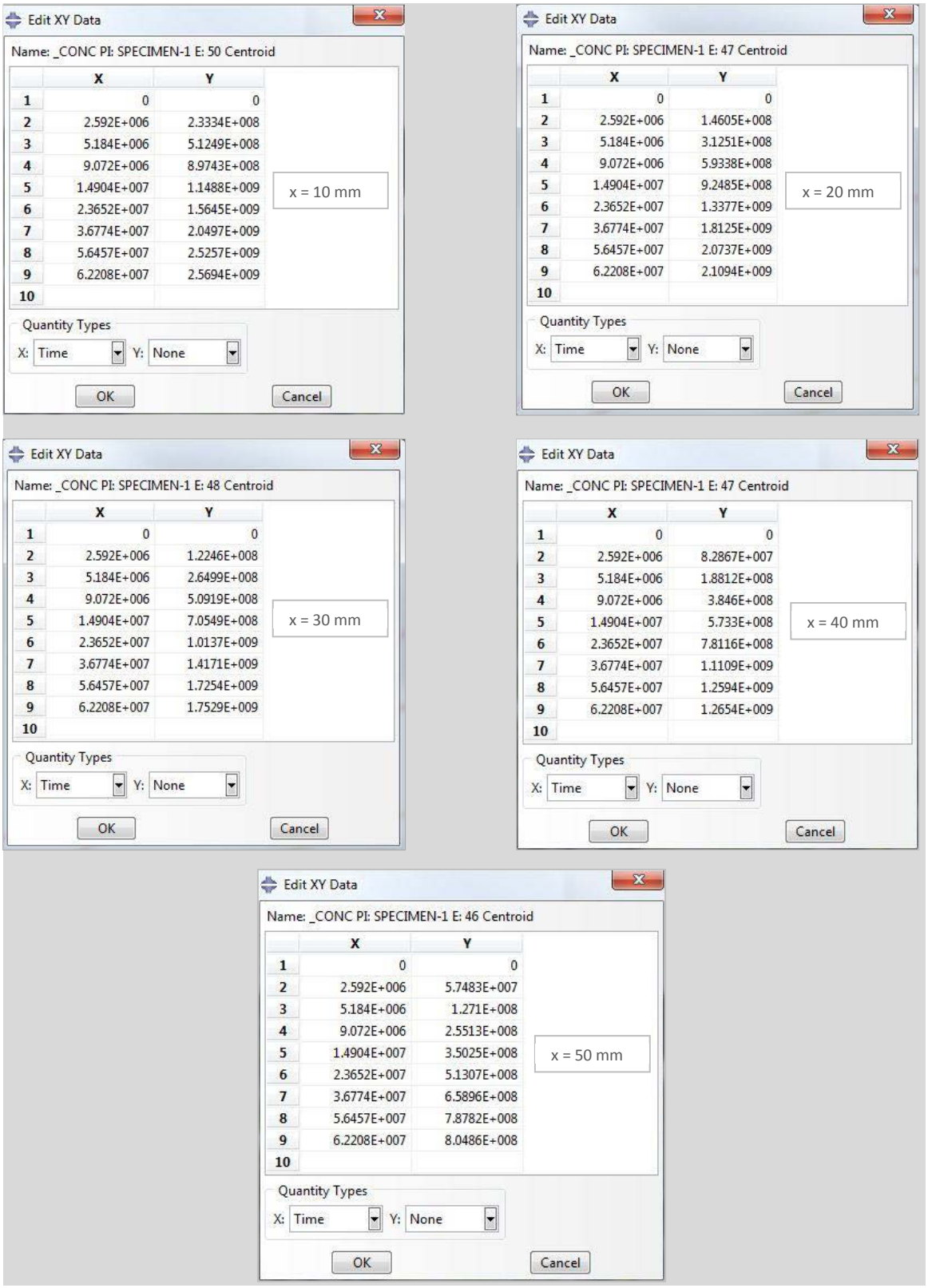

Figure 9-15 Chloride content vs. time in various depths (ABAQUS output)

9.12 VERIFICATION OF THE MATHEMATICAL MODEL

In this section, the results of computer modelling are compared and verified with the experimental results of this study for conventional concrete. The experimental results from chloride measurement in different depths over time are compared with the computer modelling results which have been obtained at the same depth and time. As mentioned earlier in this chapter, both surface chloride concentration factor and chloride diffusion coefficient have been introduced to the computer program as time-dependent parameters. To compare the correlation of the modelling results and experimental results, outcome of the both methods are plotted for different cross-sections as follows:

Figure 9-16 for $x = 10\ mm$,
Figure 9-17 for $x = 20\ mm$,
Figure 9-18 for $x = 30\ mm$,
Figure 9-19 for $x = 40\ mm$, and
Figure 9-20 for $x = 50\ mm$.

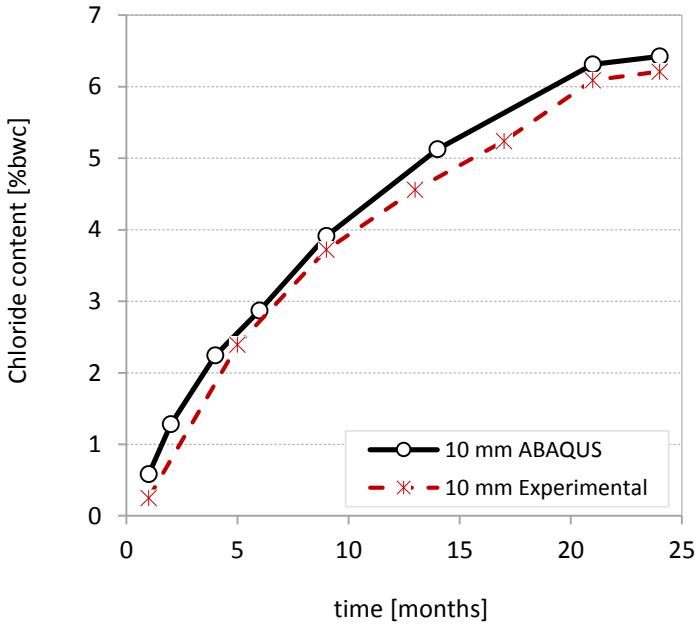

Figure 9-16 Comparing computer model and experimental results for $x = 10\ mm$

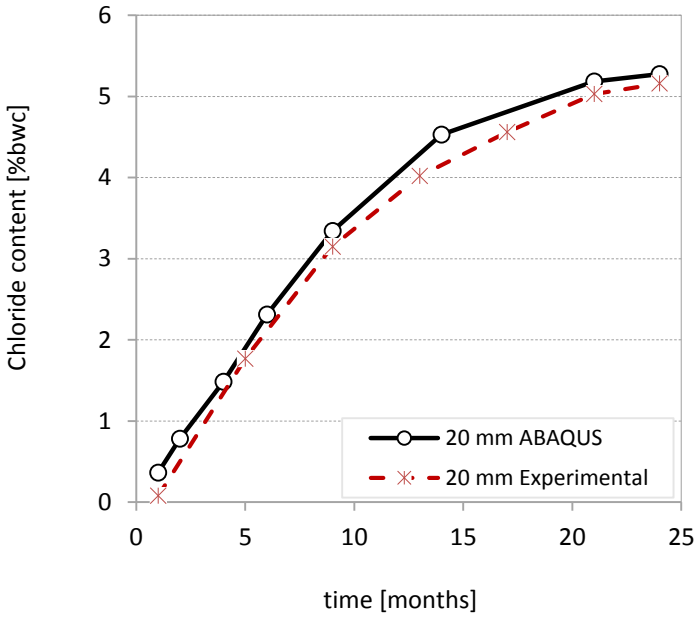

Figure 9-17 Comparing computer model and experimental results for $x = 20\ mm$

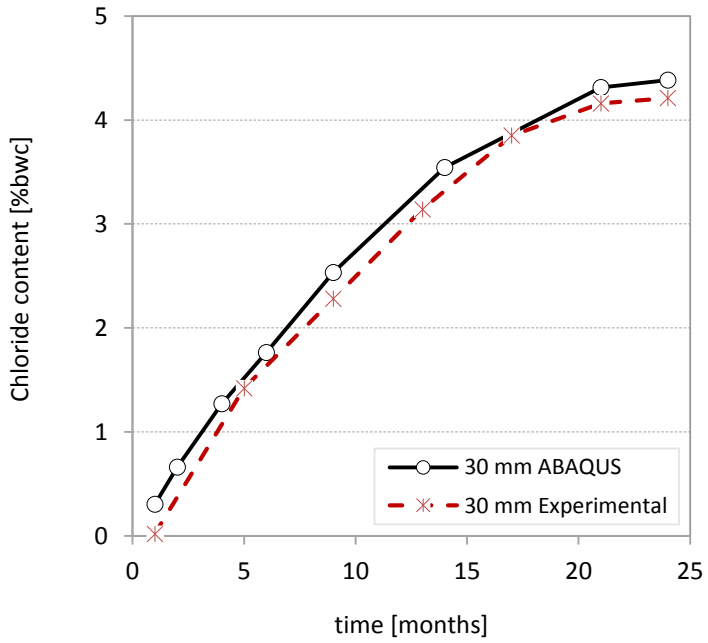

Figure 9-18 Comparing computer model and experimental results for $x = 30\ mm$

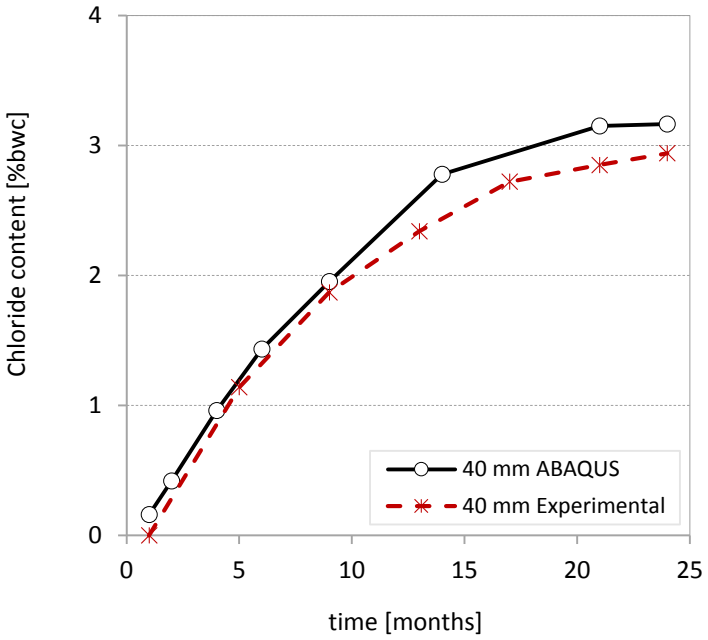

Figure 9-19 Comparing computer model and experimental results for $x = 40\ mm$

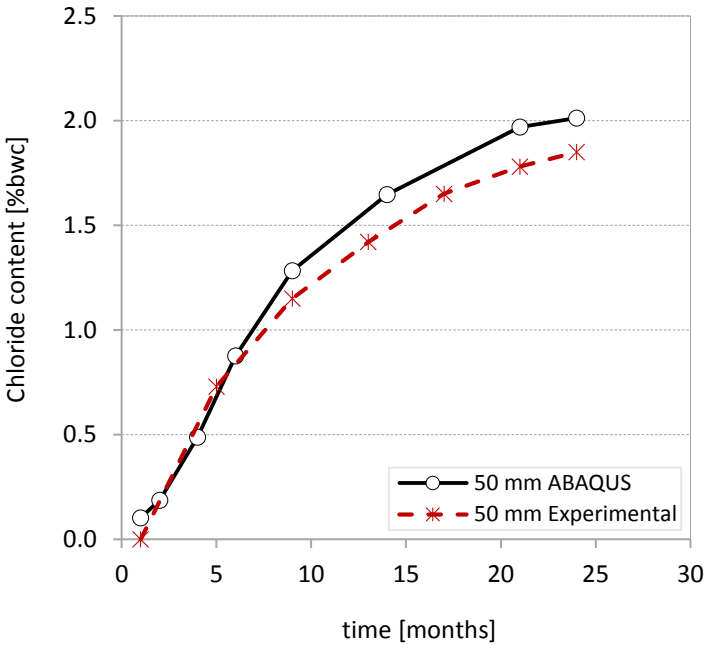

Figure 9-20 Comparing computer model and experimental results for $x = 50\ mm$

As can be observed, the computer modelling results have excellent correspondence to the experimental results.

9.13 SUMMARY

Surface chloride concentration parameter, Cs, and chloride diffusion coefficient, D, are the most important factors to estimate the chloride content of concrete at any time using Fick's second law under the pure diffusion condition.

As discussed in Chapter 2, according to the field and laboratory studies, it has been confirmed that both surface chloride concentration (C_s) and chloride diffusivity (D) are time-dependent parameters. C_s increases by time while D decreases by time.

In this investigation, the values of surface chloride concentration were determined by the available mathematical model proposed by Song et al (2008). After that, C_s values over time were introduced to the computer model as the input data of surface loading. The values of chloride diffusivity (D) were calculated utilising the proposed mathematical model in this study. These calculated values were also entered in computer model as input data.

The chloride content versus time was solved and modeled by ABAQUS software and raw output showed the predicted trend. The results of computer modelling and long-term laboratory experimental results are in reasonably good agreement.

CHAPTER 10

SUMMARY AND CONCLUSIONS

CHAPTER 10. SUMMARY AND CONCLUSIONS

10.1 SUMMARY

With increasing problems related to corrosion of reinforcing steel embedded in the concrete, service life prediction of reinforced concrete (RC) structures against corrosion damage has become a worldwide research challenge.

In this study, the influence of polymer-concrete composites on service life of reinforced concrete structures exposed to severe environment was comprehensively investigated.

An extensive literature review on the concrete microstructure including porosity and permeability, chloride diffusion concepts, corrosion of steel in concrete, concrete durability and service life was conducted and presented. Moreover, influencing parameters on chloride threshold level, surface chloride concentration, and chloride diffusion coefficient were investigated.

In addition, several corrosion prevention methods such as electrochemical protection techniques, epoxy-coated bars, galvanized steel bars, fibre reinforced polymer bars, corrosion inhibitors, were investigated in terms of technical performance and cost effect.

The mechanical properties and durability characteristics of polymer-concrete composites were examined extensively. Polymer-concrete composites are multi-phase materials produced by combining aqueous or powder state polymers and/or reinforcing fibres in order to enhance the mechanical and durability performance of the plain concrete.

In the experimental program of this study, long-term tests were conducted up to 720 days. To assess the durability of the different concrete types, two test methods including pure diffusion test and time to corrosion-induced crack by deploying accelerated chloride-induced corrosion test method were applied.

Sixteen different types of concrete including conventional concrete, fibre reinforced concrete, polymer modified concrete and fibre reinforced polymer modified concrete with different proportions of polypropylene fibres and Styrene Butadiene Rubber polymer (latex) were monitored and examined. The effects of polymer-concrete composites on both mechanical properties and durability performance of concrete were comprehensively investigated.

Several trial concrete mixes were prepared and examined to obtain the optimum mix proportions to produce high quality of structural concrete. Compressive, flexural, and tensile strengths (mechanical properties), and chloride diffusion and corrosion-induced cracking characteristics for durability assessment were tested and determined.

To investigate the effect of polymer-concrete composites on chloride diffusion characteristics of the concrete, specimens were exposed to high concentration of chloride solution for 24 months. In time intervals of 1, 5, 9, 13, 17, 21, and 28 months, chloride content were measured using titration method (NT Build 443) in different depths of 10 mm, 20 mm, 30 mm, 40 mm, and 50 mm.

To investigate the corrosion time, series of reinforced concrete specimens with dimensions of 400 mm × 100 mm × 100 mm including one 12 mm embedded steel bar with 50 mm of cover were examined using accelerated electrochemical test. In this test, specimens were located in high concentrated chloride solution and subjected to a constant DC voltage till the crack initiation on the concrete cover occurred. The corresponding time to the crack initiation, (corrosion time) was reported.

The proposed model was divided into two time phases including (i) curing period, and (ii) exposure time. Also, in the proposed model the following influencing factors in addition to water cement ratio have been considered to determine chloride diffusivity more accurately:

- Coarse aggregate proportion to apply the effect of interfacial transition zone (ITZ)
- Cement content
- Cement type to apply the effect of chloride binding process,

The results of proposed mathematical model were used as input data for a computer model to determine the chloride content in different depths over time.

Finally, the values of surface chloride concentration were determined by mathematical model proposed by Song et al (2008) and were entered to computer model as input data. The values of chloride diffusivity (D) were estimated utilising the proposed mathematical model in this study. These values were also entered in computer model as input data. This FE analysis indicates an excellent agreement between experimental results and results of the computer model conducted in this research.

10.2 CONCLUSIONS

The following conclusions can be drawn from the results presented in this study:

10.2.1 Practical Recommendations for Casting FRC and PMC

Initially, to produce PP fibres reinforced concrete and latex modified concrete some recommendations can be suggested as follows:

- PP fibers can be simply added to the concrete mix and adding at least four minutes to the mixing time in order to uniformly distribution of fibres in the mix.
- If polymer (SBR, latex) modified concrete is expected to use as a structural concrete following remedy instructions should be considered:
    - Mixing water should be reduced equal to the water content of latex, usually between 45% and 50%.
    - Antifoaming agent should be added to latex and mixed properly for two minutes and then the mixture will be added to the concrete mix.

- Usually silicon-based antifoaming agent (defoamer) has better effect on reducing the foam (bubbles). The proportion of the defoamer has to be determined by series of trial mixes.
- Polymer modified concrete is highly sensitive to the moisture especially in early ages. Therefore, especial curing method has to be conducted to achieve acceptable mechanical properties.

10.2.2 Mechanical Properties

In order to examine the effects of polymers on mechanical properties of concrete, compressive strength, flexural strength, and tensile strength were monitored and measured.

Results show that all polymer-concrete composites obtain compressive strength higher than the targeted minimum design compressive strength of 60 MPa. Test results revealed the improvement of compressive strength for all polymer-concrete composites except PMCs. Compressive strength of PMCs was enhanced by adding an appropriate antifoaming agent. As a result, FRCs and FRPMCs compressive strengths were increased up to 14% and 16%, respectively. Two empirical models proposed to predict the compressive strength of FRCs and PMCs depending on the proportion of PP fibres and latex in the concrete mix.

In addition, test results revealed the enhancement of flexural strength of FRCs and FRPMCs by 8% and 14%, respectively. However, PMCs indicated a reduction of 5% in flexural strength. Two empirical models were proposed to determine the flexural strength of FRCs and PMCs based on the proportions of PP fibres and latex in the concrete mix too.

According to the test results, PMCs do not have influence on tensile strength. Whereas, FRCs and FRPMCs tensile strength was increased approximately up to 9% and 10%. In conclusion, it can be stated that combination of PP fibres and latex can improve the mechanical properties of the concrete notably. By reducing the porosity of the concrete by using latex, bond strength of fibres and cement matrix will be improved. Improving the bond strength consequently increases the bridging effect of the fibres and enhancing concrete tensile strength.

10.2.3 Durability Performance

Since chloride ion diffusion is dominant factor in deterioration of the RC structures, the chloride diffusion rate in concrete can be measured precisely to investigate the durability of the concrete exposed to severe environment such as marine environment. In this study, 16 different types of concretes including CC, FRC, PMC, and FRPMC were constructed and exposed to high concentration of chloride solution. Then, chloride content in different depths over time was measured. The results of this investigation can be utilized to determine corrosion-free service life.

Moreover, corrosion-induced crack was monitored and studied in order to determine the end of service life of concrete structures. In this investigation, accelerated chloride-induced corrosion tests were performed to obtain the corrosion time for all concrete types simulating a long period of time.

Results revealed that all types of polymer-concrete composites showed high resistance to chloride diffusion especially PMCs and FRPMCs. For instance, average of PMCs and FRPMCs chloride content comparing to CC chloride content, could be reduced approximately up to 50% and 75%, respectively. Chloride content measurement results can be used to determine the corrosion-free service life of the structure.

The test results of this study revealed that all polymer-concrete composites (fibres, latex and combination of them) can enhance the corrosion time of conventional concrete considerably. For example, latex modified concrete enhanced the corrosion time significantly from 36% with polymer to cement ratio (P/C) of 5% to 130% with P/C of 15%. Moreover, results confirmed that the combination of PP fibres and latex in concrete improves corrosion time extraordinary up to 147%. This enhancement can be described as follows:

If we assume a design service life of 50 years for marine concrete structure, this service life can be extended up to 124 years by using a combination of PP fibres and latex polymer. Discussion has been taken place in Chapter 7.

It can be concluded that the polymer-concrete composites can significantly and reliably increase the durability and service life of the structures by fulfilling the following processes:

- Due to blockage and making discontinuous pores by latex polymer, chloride diffusion rate can be reduced significantly. This phenomenon has been clearly confirmed by chloride diffusion test results in Chapter 7.
- Reducing microcracks by increasing tensile strength of the concrete by PP fibres.

From the findings of the experimental program of this research, it is apparent that polymer-concrete composites can be classified as high performance concrete. Extending the service life of RC structures by approximately 2.5 times than design service life can extraordinary reduces maintenance and repair costs, environmental impact in terms of the consumption of raw materials, and safety issues.

10.3 MATHEMATICAL AND COMPUTER MODELS

The FE analysis results were compared with the experimental results. According to this comparison, up to 10 months FE analysis and experimental results were shown an excellent agreement with approximately ±0.06 inaccuracy. However, this error slightly increased up to ±0.11. This behaviour can be related to chloride binding property of the concrete which can be assumed as a time-dependent parameter too.

In general, the proposed mathematical model, FE analysis, and experimental results are in reasonably good agreement.

10.4 RECOMMEDATIONS FOR FUTURE STUDY

The following areas of research concerning polymer-concrete composites remain relatively unexplored and could form the basis for future studies:

- An experimental program on performance of polymer-concrete composites exposed to sulphate and acid environment.
- An experimental and analytical program to investigate the long-term behaviour of polymer-concrete composites such as creep and shrinkage.

- Additional computer modelling based on FE analysis to consider the effect of pressure on diffusion of chloride into the concrete.
- Additional computer modelling based on FE analysis to consider the effect of temperature on diffusion of chloride into the concrete
- An experimental program to compare durability performance of polymer-concrete composites with the concrete incorporating supplementary cementitious materials such as fly ash, silica fume, and GGBF Slag.
- A long-term experimental program to investigate the chloride binding capacity of polymer-concrete composites and its effect on the chloride diffusion coefficient.
- An analytical and experimental program to investigate the time dependency of chloride binding property of the concrete and polymer-concrete composites.

REFERNCE

REFERENCES

ABDALLA, H. 2006. Concrete cover requirements for FRP reinforced members in hot climates. *Composite structures,* 73**,** 61-69.

AHMAD, S. 2003. Reinforcement corrosion in concrete structures, its monitoring and service life prediction—a review. *Cement and Concrete Composites,* 25**,** 459-471.

AHMAD, S., BHATTACHARJEE, B. & WASON, R. 1997. Experimental service life prediction of rebar-corroded reinforced concrete structure. *ACI materials journal,* 94.

AL-AMOUDI, O. S. B. 2002. Durability of plain and blended cements in marine environments. *Advances in Cement Research* [Online], 14.

AL-TAYYIB, A. J., AL-ZAHRANI, M. M., RASHEEDUZZAFAR & AL-SULAIMANI, G. J. 1988. Effect of polypropylene fiber reinforcement on the properties of fresh and hardened concrete in the Arabian Gulf environment. *Cement and Concrete Research,* 18**,** 561-570.

ALDEA, C.-M. & SHAH, S. P. 1999. Effect of Cracking on Water and Chloride Permeability of Concrete. *Journal of Materials in Civil Engineering,* 11**,** 181.

ALDEA, C.-M., SHAH, S. P. & KARR, A. 1999. Effect of cracking on water and chloride permeability of concrete. *Journal of materials in civil engineering,* 11**,** 181-187.

ALHOZAIMY, A. M., SOROUSHIAN, P. & MIRZA, F. 1996. Mechanical properties of polypropylene fiber reinforced concrete and the effects of pozzolanic materials. *Cement and Concrete Composites,* 18**,** 85-92.

ALONSO, C., ANDRADE, C., CASTELLOTE, M. & CASTRO, P. 2000. Chloride threshold values to depassivate reinforcing bars embedded in a standardized OPC mortar. *Cement and Concrete Research,* 30**,** 1047-1055.

ALONSO, C., CASTELLOTE, M. & ANDRADE, C. 2002. Chloride threshold dependence of pitting potential of reinforcements. *Electrochimica Acta,* 47**,** 3469-3481.

ALONSO, M. C. & SANCHEZ, M. 2009. Analysis of the variability of chloride threshold values in the literature. *Materials and Corrosion,* 60**,** 631-637.

ALTOUBAT, S. A. & LANGE, D. A. 2001. Creep, shrinkage, and cracking of restrained concrete at early age. *ACI Materials Journal,* 98.

AMBLER, H. R. & BAIN, A. A. J. 1955. Corrosion of metals in the tropics. *Journal of Applied Chemistry,* 5**,** 437-467.

AMEY, S. L., JOHNSON, D. A., MILTENBERGER, M. A. & FARZAM, H. 1998. Predicting the service life of concrete marine structures: an environmental methodology. *ACI Structural Journal,* 95.

ANDRADE, C. 1993. Calculation of chloride diffusion coefficients in concrete from ionic migration measurements. *Cement and Concrete Research,* 23**,** 724-742.

ANDRADE, C., CASTELLOTE, M., ALONSO, C. & GONZÁLEZ, C. 2000. Non-steady-state chloride diffusion coefficients obtained from migration and natural diffusion tests. Part I: Comparison between several methods of calculation. *Materials and Structures,* 33**,** 21-28.

ANDRADE, C., DíEZ, J. M. & ALONSO, C. 1997. Mathematical Modeling of a Concrete Surface "Skin Effect" on Diffusion in Chloride Contaminated Media. *Advanced Cement Based Materials,* 6**,** 39-44.

ANDRADE, C., SANJUÁN, M., RECUERO, A. & RIO, O. 1994. Calculation of chloride diffusivity in concrete from migration experiments, in non steady-state conditions. *Cement and concrete research,* 24**,** 1214-1228.

ANGST, U., ELSENER, B., JAMALI, A. & ADEY, B. 2012. Concrete cover cracking owing to reinforcement corrosion – theoretical considerations and practical experience. *Materials and Corrosion,* 63**,** 1069-1077.

ANGST, U., ELSENER, B., LARSEN, C. K. & VENNESLAND, Ø. 2009. Critical chloride content in reinforced concrete — A review. *Cement and Concrete Research,* 39**,** 1122-1138.

ANN, K., SONG, H., LEE, C. & LEE, K. 2006. Build-up of surface chloride and its influence on corrosion initiation time of steel in concrete. *Structural engineering and construction. Bangkok, Thailand***,** 767-72.

ANN, K. Y., AHN, J. H. & RYOU, J. S. 2009. The importance of chloride content at the concrete surface in assessing the time to corrosion of steel in concrete structures. *Construction and Building Materials,* 23**,** 239-245.

ANN, K. Y. & SONG, H.-W. 2007. Chloride threshold level for corrosion of steel in concrete. *Corrosion Science,* 49**,** 4113-4133.

ANWAR HOSSAIN, K. M., EASA, S. M. & LACHEMI, M. 2009. Evaluation of the effect of marine salts on urban built infrastructure. *Building and Environment,* 44**,** 713-722.

APOSTOLOPOULOS, C. A. & PAPADAKIS, V. G. 2008. Consequences of steel corrosion on the ductility properties of reinforcement bar. *Construction and Building Materials,* 22**,** 2316-2324.

ARYA, C., BUENFELD, N. R. & NEWMAN, J. B. 1990. Factors influencing chloride binding in concrete. *Cement & Concrete Research,* 20.

ARYA, C. & XU, Y. 1995. Effect of cement type on chloride binding and corrosion of steel in concrete. *Cement and Concrete Research,* 25**,** 893-902.

ASBRIDGE, A., CHADBOURN, G. & PAGE, C. 2001. Effects of metakaolin and the interfacial transition zone on the diffusion of chloride ions through cement mortars. *Cement and Concrete Research,* 31**,** 1567-1572.

BADER, M. A. 2003. Performance of concrete in a coastal environment. *Cement and Concrete Composites,* 25**,** 539-548.

BAKIS, C., BANK, L., BROWN, V., COSENZA, E., DAVALOS, J., LESKO, J., MACHIDA, A., RIZKALLA, S. & TRIANTAFILLOU, T. 2002. Fiber-Reinforced Polymer Composites

for Construction—State-of-the-Art Review. *Journal of Composites for Construction,* 6**,** 73-87.

BALÁZS, G. & KOVÁCS, K. 1982. Polymer-impregnated concrete. *Civil Engineering,* 26**,** 89-98.

BALÁZS, G. L. & BOROSNYÓI, A. Long-term behavior of FRP. Composites in Construction@ sA Reality, 2001. ASCE, 84-91.

BAMFORD, P. B. 1999. The derivation of input data for modeling chloride ingress from eight-year UK coastal exposure trials. *Magazine of Concrete Research.*

BAMFORTH, P. 1993. Concrete classification for RC structures exposed to marine and other salt-laden environments. *Structural Faults and Repair,* 93**,** 31-40.

BAMFORTH, P. & PRICE, W. 1993. Factors influencing chloride ingress into marine structures. *Concrete 2000***,** 1105.

BAMFORTH, P., PRICE, W. F. & EMERSON, M. 1997. An international review of chloride ingress into structural concrete. *CONTRACTOR REPORT 359*.

BANK, L. C., GENTRY, T. R. & BARKATT, A. 1995. Accelerated test methods to determine the long-term behavior of FRP composite structures: environmental effects. *Journal of Reinforced Plastics and Composites,* 14**,** 559-587.

BARLUENGA, G. & HERNÁNDEZ-OLIVARES, F. 2004. SBR latex modified mortar rheology and mechanical behaviour. *Cement and Concrete Research,* 34**,** 527-535.

BARNES, B. D., DIAMOND, S. & DOLCH, W. L. 1979. Micromorphology of the interfacial zone around aggregates in Portland cement mortar. *Journal of American Ceramic Society,* 62**,** 21-34.

BASHEER, L., BASHEER, P. A. M. & LONG, A. E. 2005. Influence of coarse aggregate on the permeation, durability and the microstructure characteristics of ordinary Portland cement concrete. *Construction and Building Materials,* 19**,** 682-690.

BASHEER, L., KROPP, J. & CLELAND, D. J. 2001. Assessment of the durability of concrete from its permeation properties: a review. *Construction and Building Materials,* 15**,** 93-103.

BASHEER, P. A. M., CHIDIACT, S. E. & LONG, A. E. 1996. Predictive models for deterioration of concrete structures. *Construction and Building Materials,* 10**,** 27-37.

BÄUMEL, A. 1959. Die Auswirkung von Betonzusatzmitteln auf das Korrosionsverhalten von Stahl in Beton. *Zement-Kalk-Gips,* 12**,** 294-305.

BAZANT, Z. P. 1979. Physical model for steel corrosion in concrete sea structures—theory. *Journal of the Structural Division,* 105**,** 1137-1153.

BEAUDOIN, J. & RAMACHANDRAN, V. S. 1989. Effect of water dispersible polymers on the properties of superplasticized cement paste, mortar, and concrete. *ACI SP***,** 221-242.

BENNETT, J. E. & SCHUE, T. J. 1995. Cathodic protection field trials on prestressed concrete components.

BENTUR, A. 1982. Properties of polymer latex-cement composites. *International Journal of Cement Composites and Lightweight Concrete,* 4**,** 57-65.

BENTUR, A., BERKE, N. & DIAMOND, S. 1997. *Steel corrosion in concrete: fundamentals and civil engineering practice*, Taylor & Francis.

BENTUR, A. & MINDESS, S. 2006. *Fibre reinforced cementitious composites*, CRC Press.

BENTZ, E., THOMAS, M. & EVANS, C. 1996. Chloride diffusion modelling for marine exposed concretes. *SPECIAL PUBLICATION-ROYAL SOCIETY OF CHEMISTRY,* 183**,** 136-145.

BERKE, N. S. & HICKS, M. C. 2004. Predicting long-term durability of steel reinforced concrete with calcium nitrite corrosion inhibitor. *Cement and Concrete Composites,* 26**,** 191-198.

BERKELEY, K. & PATHMANABAN, S. 1990. *Cathodic protection of reinforcement steel in concrete*.

BERMAN, H. A. 1972. Determination of chloride in hardened Portland cement paste, mortar, and concrete. *Journal of Materials in Civil Engineering,* 7.

BERTOLINI, L. 2008. Steel corrosion and service life of reinforced concrete structures. *Structure and Infrastructure Engineering,* 4**,** 123-137.

BERTOLINI, L., ELSENER, B., PEDEFERRI, P., REDAELLI, E. & POLDER, R. B. 2013. *Corrosion of steel in concrete: prevention, diagnosis, repair*, John Wiley & Sons.

BERTOLINI, L., GASTALDI, M., PEDEFERRI, M. & REDAELLI, E. 2002. Prevention of steel corrosion in concrete exposed to seawater with submerged sacrificial anodes. *Corrosion Science,* 44**,** 1497-1513.

BHARGAVA, K., GHOSH, A. K., MORI, Y. & RAMANUJAM, S. 2006. Analytical model for time to cover cracking in RC structures due to rebar corrosion. *Nuclear Engineering and Design,* 236**,** 1123-1139.

BODDY, A., BENTZ, E., THOMAS, M. D. A. & HOOTON, R. D. 1999. An overview and sensitivity study of a multimechanistic chloride transport model. *Cement and Concrete Research,* 29**,** 827-837.

BRANDT, A. M. 2008. Fibre reinforced cement-based (FRC) composites after over 40 years of development in building and civil engineering. *Composite Structures,* 86**,** 3-9.

BREIT, W. 2003. Kritischer korrosionsauslösender Chloridgehalt – Untersuchungen an Mörtelelektroden in chloridhaltigen alkalischen Lösungen. *Materials and Corrosion,* 54**,** 430-439.

BRENNA, A., BOLZONI, F., BERETTA, S. & ORMELLESE, M. 2013. Long-term chloride-induced corrosion monitoring of reinforced concrete coated with commercial polymer-modified mortar and polymeric coatings

Construction and Building Materials, 48**,** 734-744.

BROWN, M. C. 2002. *Corrosion protection service life of epoxy coated reinforcing steel in Virginia bridge decks.* Virginia Polytechnic Institute and State University.

BROWN, R., SHUKLA, A. & NATARAJAN, K. R. 2002. Fiber reinforcement of concrete structures.

BROWNE, R. D. 1980. Mechanisms of corrosion of steel in concrete in relation to design, inspection, and repair of offshore and coastal structures. *ACI Special Publication,* 65.

BUENFELD, N. & OKUNDI, E. 1998. Effect of cement content on transport in concrete. *Magazine of Concrete Research,* 50.

BUENFELD, N. R. & GLASS, G. K. 1998. Chloride Transport in Concrete Subjected to Electric Field. *Journal of Materials in Civil Engineering,* 10**,** 220.

BUENFELD, N. R. & NEWMAN, J. B. 1987. Examination of the three methods for studying ion diffusion in cement pasts, mortars and concrete. *Mater. Struct.,* 20**,** 3-10.

BULLARD, J. W., JENNINGS, H. M., LIVINGSTON, R. A., NONAT, A., SCHERER, G. W., SCHWEITZER, J. S., SCRIVENER, K. L. & THOMAS, J. J. 2011. Mechanisms of cement hydration. *Cement and Concrete Research,* 41**,** 1208-1223.

BYE, G. C. 1999. *Portland cement: composition, production and properties*, Thomas Telford.

BYFORS, K., HANSSON, C. M. & TRITTHART, J. 1986. Pore solution expression as a method to determine the influence of mineral additives on chloride binding. *Cement and Concrete Research,* 16**,** 760-770.

CABRERA, J. G. 1996. Deterioration of concrete due to reinforcement steel corrosion. *Cement and Concrete Composites,* 18**,** 47-59.

CARÉ, S. 2003. Influence of aggregates on chloride diffusion coefficient into mortar. *Cement and Concrete Research,* 33**,** 1021-1028.

CARINO, N. 1999. Nondestructive Techniques to Investigate Corrosion Status in Concrete Structures. *Journal of Performance of Constructed Facilities,* 13**,** 96-106.

CASTELLOTE, M., ANDRADE, C. & ALONSO, C. 2001. Measurement of the steady and non-steady-state chloride diffusion coefficients in a migration test by means of monitoring the conductivity in the anolyte chamber. Comparison with natural diffusion tests. *Cement and Concrete Research,* 31**,** 1411-1420.

CASTELLOTE, M., ANDRADE, C. & ALONSO, C. 2002. Accelerated simultaneous determination of the chloride depassivation threshold and of the non-stationary diffusion coefficient values. *Corrosion Science,* 44**,** 2409-2424.

CASTRO-BORGES, P., BALANC, #XE1, N-ZAPATA, M., #XF3, PEZ-GONZ & LEZ, A. 2013. Analysis of Tools to Evaluate Chloride Threshold for Corrosion Onset of Reinforced Concrete in Tropical Marine Environment of Yucatán, México. *Journal of Chemistry,* 2013**,** 8.

CASTRO, P., DE RINCON, O. T. & PAZINI, E. J. 2001. Interpretation of chloride profiles from concrete exposed to tropical marine environments. *Cement and Concrete Research,* 31**,** 529-537.

CERONI, F., COSENZA, E., GAETANO, M. & PECCE, M. 2006. Durability issues of FRP rebars in reinforced concrete members. *Cement and Concrete Composites,* 28**,** 857-868.

CHANDRA KISHEN, J. M. & RAO, P. S. 2007. Fracture of cold jointed concrete interfaces. *Engineering Fracture Mechanics,* 74**,** 122-131.

CHATTERJI, S. 1994. Transportation of ions through cement based materials. Part 1 fundamental equations and basic measurement techniques. *Cement and Concrete Research,* 24**,** 907-912.

CHEN, D. & MAHADEVAN, S. 2008. Chloride-induced reinforcement corrosion and concrete cracking simulation. *Cement and Concrete Composites,* 30**,** 227-238.

CHINDAPRASIRT, P., HOMWUTTIWONG, S. & SIRIVIVATNANON, V. 2004. Influence of fly ash fineness on strength, drying shrinkage and sulfate resistance of blended cement mortar. *Cement and Concrete Research,* 34**,** 1087-1092.

CHITTY, W.-J., DILLMANN, P., L'HOSTIS, V. & LOMBARD, C. 2005. Long-term corrosion resistance of metallic reinforcements in concrete—a study of corrosion mechanisms based on archaeological artefacts. *Corrosion Science,* 47**,** 1555-1581.

CHOI, Y. & YUAN, R. L. 2005. Experimental relationship between splitting tensile strength and compressive strength of GFRC and PFRC. *Cement and Concrete Research,* 35**,** 1587-1591.

CHONG, K. P., CARINO, N. J. & WASHER, G. 2003. Health monitoring of civil infrastructures. *Smart Materials and structures,* 12**,** 483.

CLEAR, K. C. 1976. Time-to-corrosion of reinforcing steel in concrete slabs. Volume 3: Performance after 830 daily salt applications.

CLEAR, K. C., HARTT, W. H., MCINTYRE, J. & LEE, S. K. 1995. Performance of Epoxy-Coated Reinforcing Steel in Highway Bridges. National Research Council. *Transportation Research Board. NCHRP Report,* 370.

COHEN, M. D., OLEK, J. & DOLCH, W. L. 1990. Mechanism of plastic shrinkage cracking in portland cement and portland cement-silica fume paste and mortar. *Cement and Concrete Research,* 20**,** 103-119.

ÇOLAK, A. 2005. Properties of plain and latex modified Portland cement pastes and concretes with and without superplasticizer. *Cement and Concrete Research,* 35**,** 1510-1521.

COLLEPARDI, M., MARCIALIS, A. & TURRIZIANI, R. 1970. The kinetics of penetration of chloride ions into the concrete. *Il cemento,* 67**,** 157-164.

COLLEPARDI, M., MARCIALIS, A. & TURRIZIANI, R. 1972. Penetration of Chloride Ions into Cement Paste and Concrete. *Journal of American Ceramic Society,* 55**,** 534.

CONCIATORI, D., SADOUKI, H. & BRÜHWILER, E. 2008. Capillary suction and diffusion model for chloride ingress into concrete. *Cement and Concrete Research,* 38**,** 1401-1408.

COPPOLA, L. 2000. Concrete durability and repair technology. *ENCO Engineering and Concrete Spresiano (TV)*.

CORVO, F., BETANCOURT, N. & MENDOZA, A. 1995. The influence of airborne salinity on the atmospheric corrosion of steel. *Corrosion Science,* 37**,** 1889-1901.

COSENZA, E., MANFREDI, G. & REALFONZO, R. 1997. Behavior and Modeling of Bond of FRP Rebars to Concrete. *Journal of Composites for Construction,* 1**,** 40.

COSTA, A. & APPLETON, J. 1999. Chloride penetration into concrete in marine environment—Part I: Main parameters affecting chloride penetration. *Materials and Structures,* 32**,** 252-259.

COSTA, A. & APPLETON, J. 2002. Case studies of concrete deterioration in a marine environment in Portugal. *Cement and Concrete Composites,* 24**,** 169-179.

CRANK, J. 1975. The Mathematics of Diffusion. *Clarendon Press,* 2.

DARWIN, D., BROWNING, J., O'REILLY, M., LIHUA, X. & JIANXIN, J. 2009. Critical Chloride Corrosion Threshold of Galvanized Reinforcing Bars. *ACI Materials Journal,* 106**,** 176-183.

DE LHONEUX, B., KALBSKOPF, R., KIM, P., LI, V. C., LIN, Z., VIDTS, D., WANG, S. & WU, H.-C. 2002. Development of high tenacity polypropylene fibers for cementitious composites.

DE RINCÓN, O., ANDRADE, C. & KROPP, J. Comparison between chloride ion threshold and electrochemical measurements for reinforcement corrosion. Third International RILEM Workshop on Testing and Modelling Chloride Ingress into Concrete, 2004a. RILEM Publications SARL, 361-380.

DE RINCÓN, O. T., CASTRO, P., MORENO, E. I., TORRES-ACOSTA, A. A., DE BRAVO, O. M., ARRIETA, I., GARCíA, C., GARCíA, D. & MARTíNEZ-MADRID, M. 2004b. Chloride profiles in two marine structures—meaning and some predictions. *Building and Environment,* 39**,** 1065-1070.

DE SARKAR, M., DE, P. P. & BHOWMICK, A. K. 2000. Diimide reduction of carboxylated styrene-butadiene rubber in latex stage. *Polymer,* 41**,** 907-915.

DEB, S. 2012. Critical Chloride Content in Reinforced Concrete. *The Materbuilder***,** 9.

DELAGRAVE, A., BIGAS, J. P., OLLIVIER, J. P., MARCHAND, J. & PIGEON, M. 1997. Influence of the interfacial zone on the chloride diffusivity of mortars. *Advanced Cement Based Materials,* 5**,** 86-92.

DHIR, R. K., JONES, M. R., AHMED, H. E. H. & SENEVIRATNE, A. M. G. 1990. Rapid estimation of chloride diffusion coefficient in concrete. *Magazine of Concrete Research* [Online], 42. Available: http://www.icevirtuallibrary.com/content/article/10.1680/macr.1990.42.152.177.

DIAB, A. M., ELYAMANY, H. E. & ALI, A. H. 2013. Experimental investigation of the effect of latex solid/water ratio on latex modified co-matrix mechanical properties. *Alexandria Engineering Journal,* 52**,** 83-98.

DIAB, A. M., ELYAMANY, H. E. & ALI, A. H. 2014. The participation ratios of cement matrix and latex network in latex cement co-matrix strength. *Alexandria Engineering Journal,* 53**,** 309-317.

DIAB, H., BENTUR, A., HEITNER-WIRGUIN, C. & BEN-DOR, L. 1988. The diffusion of Cl−ions through portland cement and portland cement-polymer pastes. *Cement and Concrete Research,* 18**,** 715-722.

DIAMOND, S. 2004. The microstructure of cement paste and concrete—a visual primer. *Cement and Concrete Composites,* 26**,** 919-933.

EL MAADDAWY, T. & SOUDKI, K. 2007. A model for prediction of time from corrosion initiation to corrosion cracking. *Cement and Concrete Composites,* 29**,** 168-175.

ELBADRY, M. M., ABDALLA, H. & GHALI, A. 2000. Effects of temperature on the behaviour of fiber reinforced polymer reinforced concrete members: experimental studies. *Canadian Journal of Civil Engineering,* 27**,** 993-1004.

ELSENER, B. & BÖHNI, H. Corrosion of steel in mortar studied by impedance measurements. Materials Science Forum, 1986. Trans Tech Publ, 363-372.

ENRIGHT, M. & FRANGOPOL, D. 1998. Service-Life Prediction of Deteriorating Concrete Bridges. *Journal of Structural Engineering,* 124**,** 309-317.

ENRIGHT, M. P. & FRANGOPOL, D. M. 2000. Survey and Evaluation of Damaged Concrete Bridges. *Journal of Bridge Engineering,* 5**,** 31.

FAGERLUND, G. Service life of structures. Proceedings of the Second International Rilem Symposium, 1979.

FANG, C., LUNDGREN, K., CHEN, L. & ZHU, C. 2004. Corrosion influence on bond in reinforced concrete. *Cement and Concrete Research,* 34**,** 2159-2167.

FERREIRA, R. M. 2010. Optimization of RC structure performance in marine environment. *Engineering Structures,* 32**,** 1489-1494.

FITZGERALD, J. W. 1991. Marine aerosols: A review. *Atmospheric Environment. Part A. General Topics,* 25**,** 533-545.

FOWLER, D. W. 1999. Polymers in concrete: a vision for the 21st century. *Cement and Concrete Composites,* 21**,** 449-452.

FRIEDMANN, H., AMIRI, O., AïT-MOKHTAR, A. & DUMARGUE, P. 2004. A direct method for determining chloride diffusion coefficient by using migration test. *Cement and Concrete Research,* 34**,** 1967-1973.

FUNAHASHI, M. I. 1990. Predicting corrosion-free service life of a concrete structure in a chloride environment. *ACI Materials journal,* 87.

GALATI, N., NANNI, A., DHARANI, L. R., FOCACCI, F. & AIELLO, M. A. 2006. Thermal effects on bond between FRP rebars and concrete. *Composites Part A: Applied Science and Manufacturing,* 37**,** 1223-1230.

GELEJI, F., KÓCZY, L., FÜLÖP, I. & BODOR, G. Properties of polypropylene fibers made from polymer homologue mixtures. Journal of Polymer Science: Polymer Symposia, 1977. Wiley Online Library, 253-273.

GJØRV, O. E. 2009. *Durability of Concrete Structures in Severe Environments,* NY, Taylor & Francis Group.

GJØRV, O. E. & VENNESLAND, Ø. 1979. Diffusion of chloride ions from seawater into concrete. *Cement and Concrete Research,* 9**,** 229-238.

GLASS, G. K. & BUENFELD, N. R. 1997. The presentation of the chloride threshold level for corrosion of steel in concrete. *Corrosion Science,* 39**,** 1001-1013.

GLASS, G. K. & BUENFELD, N. R. 2000a. Chloride-induced corrosion of steel in concrete. *Progress in Structural Engineering and Materials,* 2**,** 448-458.

GLASS, G. K. & BUENFELD, N. R. 2000b. The influence of chloride binding on the chloride induced corrosion risk in reinforced concrete. *Corrosion Science,* 42**,** 329-344.

GLASS, G. K., REDDY, B. & BUENFELD, N. R. 2000. The participation of bound chloride in passive film breakdown on steel in concrete. *Corrosion Science,* 42**,** 2013-2021.

GLASSER, F. P., MARCHAND, J. & SAMSON, E. 2008. Durability of concrete — Degradation phenomena involving detrimental chemical reactions. *Cement and Concrete Research,* 38**,** 226-246.

GOLTERMANN, P., SCHLANGEN, E. & DE SCHUTTER, G. Chloride ingress: modelling, sampling and predicting service life. International RILEM Symposium on Concrete Modelling-ConMod'08, 2008. RILEM Publications SARL, 753-760.

GOÑI, S. & ANDRADE, C. 1990. Synthetic concrete pore solution chemistry and rebar corrosion rate in the presence of chlorides. *Cement and Concrete Research,* 20**,** 525-539.

GOUDA, V. 1970. Corrosion and corrosion inhibition of reinforcing steel: I. Immersed in alkaline solutions. *British Corrosion Journal,* 5**,** 198-203.

GOUDA, V. & HALAKA, W. 1970. Corrosion and corrosion inhibition of reinforcing steel: II. Embedded in concrete. *British Corrosion Journal,* 5**,** 204-208.

GOWRIPALAN, N. & MOHAMED, H. M. 1998. Chloride-ion induced corrosion of galvanized and ordinary steel reinforcement in high-performance concrete. *Cement and Concrete Research,* 28**,** 1119-1131.

GULIKERS, J. 1997. Development of a galvanic monitoring probe to improve service life prediction of reinforced concrete structures with respect to reinforcement corrosion. *Construction and Building Materials,* 11**,** 143-148.

GÜNEYISI, E., GESOĞLU, M., ÖZTURAN, T. & ÖZBAY, E. 2009. Estimation of chloride permeability of concretes by empirical modeling: Considering effects of cement type, curing condition and age. *Construction and Building Materials,* 23**,** 469-481.

GUSTAFSSON, M. E. R. & FRANZÉN, L. G. 1996. Dry deposition and concentration of marine aerosols in a coastal area, SW Sweden. *Atmospheric Environment,* 30**,** 977-989.

GUZMÁN, S., GÁLVEZ, J. C. & SANCHO, J. M. 2011. Cover cracking of reinforced concrete due to rebar corrosion induced by chloride penetration. *Cement and Concrete Research,* 41**,** 893-902.

HA, T.-H., MURALIDHARAN, S., BAE, J.-H., HA, Y.-C., LEE, H.-G., PARK, K.-W. & KIM, D.-K. 2007. Accelerated short-term techniques to evaluate the corrosion performance of steel in fly ash blended concrete. *Building and Environment,* 42**,** 78-85.

HAN, S.-H. 2007. Influence of diffusion coefficient on chloride ion penetration of concrete structure. *Construction and Building Materials,* 21**,** 370-378.

HANSSON, C. M. 1984. Comments on electrochemical measurements of the rate of corrosion of steel in concrete. *Cement and Concrete Research,* 14**,** 574-584.

HANSSON, C. M. & SORENSEN, B. 1988. The threshold concentration of chloride in concrete for the initiation of reinforcement corrosion. *Corrosion rates of steel in concrete***,** 3-16.

HAUSMANN, D. A. 1967. STEEL CORROSION IN CONCRETE - HOW DOES IT OCCUR. *Materials Protection,* 6**,** 19-&.

HAYNES, H. H. 1982. Permeability of Concrete in Sea Water. *ACI Mater J*.

HILSDORF, H. & KROPP, J. 2004. *Performance criteria for concrete durability*, CRC Press.

HOBBS, D. W. 1999. Aggregate influence on chloride ion diffusion into concrete. *Cement and Concrete Research,* 29**,** 1995-1998.

HOLLAWAY, L. 1993. *Polymer composites for civil and structural engineering*, Springer.

HONG, K. & HOOTON, R. D. 1999. Effects of cyclic chloride exposure on penetration of concrete cover. *Cement and Concrete Research,* 29**,** 1379-1386.

HOOTON, R., PUN, P., KOJUNDIC, T. & FIDJESTOL, P. Influence of silica fume on chloride resistance of concrete. Proceeding International Symposium of High Performance Concrete, Chicago,(P. Johal, Precast Prestressed Concrete Institute) pp, 1997. 245-249.

HOOTON, R. D., GEIKER, M. R. & BENTZ, E. C. 2002. Effects of curing on chloride ingress and implications on service life. *ACI Materials journal,* 99.

HOOTON, R. D. & MCGRATH, P. F. Issues related to recent developments in service life specifications for concrete structures. *In:* NILSON, L. O. & OLLIVIER, J. P., eds. International RILEM Workshop: Chloride penetration into Concrete, 1995 Saint-Remy-Les-Chevreuse. 388-397.

HOPE, B. B. & IP, A. K. 1987. Chloride corrosion threshold in concrete. *ACI Materials Journal,* 84.

HOSSEIN M. SHODJA , K. K., ALIREZA HASHEMIAN 2010. <A model for the evolution of concrete deterioration due to reinforcement corrosion.pdf>. *Mathematical and Computer Modelling,* 52**,** 1403-1422.

HSU, K. L., TAKEDA, H. & MARUYA, T. Numerical simulation on corrosion of steel in concrete structures under chloride attack. PROCEEDINGS-JAPAN SOCIETY OF CIVIL ENGINEERS, 2000. DOTOKU GAKKAI, 143-157.

HUANG, W.-H. 2001. Improving the properties of cement–fly ash grout using fiber and superplasticizer. *Cement and Concrete Research,* 31**,** 1033-1041.

HUSSAIN, R. R. & ISHIDA, T. 2011. Enhanced electro-chemical corrosion model for reinforced concrete under severe coupled action of chloride and temperature. *Construction and Building Materials,* 25**,** 1305-1315.

HUSSAIN, S. E., RASHEEDUZZAFAR, AL-MUSALLAM, A. & AL-GAHTANI, A. S. 1995. Factors affecting threshold chloride for reinforcement corrosion in concrete. *Cement and Concrete Research,* 25**,** 1543-1555.

JAFFER, S. J. & HANSSON, C. M. 2008. The influence of cracks on chloride-induced corrosion of steel in ordinary Portland cement and high performance concretes subjected to different loading conditions. *Corrosion Science,* 50**,** 3343-3355.

JAPAN SOCIETY OF CIVIL ENGINEERS, J. 1999. *Standard Specification for Durability of Concrete.*

JASTRZEBSKI, Z. D. 1976. *Nature and properties of engineering materials*.

JOHANNESSON, B. F. 2003. A theoretical model describing diffusion of a mixture of different types of ions in pore solution of concrete coupled to moisture transport. *Cement and Concrete Research,* 33**,** 481-488.

KAESCHE, H. 1959. Die Prüfung der Korrosionsgefährdung von Stahlarmierungen durch Betonzusatzmittel. *Zement-Kalk-Gips,* 7**,** 289-294.

KAKOOEI, S., AKIL, H. M., JAMSHIDI, M. & ROUHI, J. 2012. The effects of polypropylene fibers on the properties of reinforced concrete structures. *Construction and Building Materials,* 27**,** 73-77.

KALOUSEK, G. L. Fundamental factors in the drying shrinkage of concrete block. ACI Journal Proceedings, 1954. ACI.

KANAYA, M., MASUDA, Y., ABE, M. & NISHIYAMA, N. 1998. Diffusion of Chloride Ions in Concrete Exposed in the Coastal Area. *Concrete Under Severe Conditions,* 2**,** 242-249.

KARDON, J. B. 1997. Polymer-modified concrete: Review. *Journal of Materials in Civil Engineering,* 9**,** 85.

KAYYALI, O. A. & HAQUE, M. N. 1995. The Cl^- - OH^- ratio in chloride contaminated concrete - a most importatnt criterion. *Magazine of Concrete research.*

KELLY, J. W. 1981. Cracks in Concrete. *Concrete Construction,* 26.

KEPLER, J. L., DARWIN, D. & LOCKE, C. E. 2000. Evaluation of corrosion protection methods for reinforced concrete highway structures. Kansas Department of Transportation.

KHATRI, R. P. & SIRIVIVATNANON, V. 2004. Characteristic service life for concrete exposed to marine environments. *Cement and Concrete Research,* 34**,** 745-752.

KHAYAT, K. H., TAGNIT-HAMOU, A. & PETROV, N. 2005. Performance of concrete wharves constructed between 1901 and 1928 at the Port of Montréal. *Cement and Concrete Research,* 35**,** 226-232.

KHITAB, A., LORENTE, S. & OLLIVIER, J. P. 2005. Predictive model for chloride penetration through concrete. *Magazine of Concrete Research* [Online], 57.

KNAPEN, E. & VAN GEMERT, D. 2009. Cement hydration and microstructure formation in the presence of water-soluble polymers. *Cement and Concrete Research,* 39**,** 6-13.

KOCH, G. H., BRONGRERS, M. P. H., THOMPSON, N. H., VIRMANI, Y. P. & PRAYER, J. H. 2001. *Corrosion Cost and Preventive Strategies in United States*, Springfield, VA: National Technical Information Service.

KOLEVA, D. A., HU, J., FRAAIJ, A. L. A., VAN BREUGEL, K. & DE WIT, J. H. W. 2007. Microstructural analysis of plain and reinforced mortars under chloride-induced deterioration. *Cement and Concrete Research,* 37**,** 604-617.

KOLLEK, J. 1989. The determination of the permeability of concrete to oxygen by the Cembureau method—a recommendation. *Materials and structures,* 22**,** 225-230.

KONDRATOVA, I., MONTES, P. & BREMNER, T. 2003. Natural marine exposure results for reinforced concrete slabs with corrosion inhibitors. *Cement and Concrete Composites,* 25**,** 483-490.

KOOTSOOKOS, A. & MOURITZ, A. P. 2004. Seawater durability of glass- and carbon-polymer composites. *Composites Science and Technology,* 64**,** 1503-1511.

KRAAI, P. P. 1985. A proposed test to determine the cracking potential due to drying shrinkage of concrete. *Concrete construction,* 30**,** 775-778.

KRABBENHØFT, K. & KRABBENHØFT, J. 2008. Application of the Poisson–Nernst–Planck equations to the migration test. *Cement and Concrete Research,* 38**,** 77-88.

KROPP, J. 1995. Chlorides in concrete. In: Performance criteria for concrete durability. *RILEM report,* 12**,** 27.

KUHLMANN, L. A. 1985. Latex modified concrete for the repair and rehabilitation of bridges. *International Journal of Cement Composites and Lightweight Concrete,* 7**,** 241-247.

KWON, S. J., NA, U. J., PARK, S. S. & JUNG, S. H. 2009. Service life prediction of concrete wharves with early-aged crack: Probabilistic approach for chloride diffusion. *Structural Safety,* 31**,** 75-83.

LAMBERT, P., PAGE, C. & VASSIE, P. 1991. Investigations of reinforcement corrosion. 2. Electrochemical monitoring of steel in chloride-contaminated concrete. *Materials and Structures,* 24**,** 351-358.

LARBI, J. & POLDER, R. 2007. Effects of polypropylene fibres in concrete: Microstructure after fire testing and chloride migration. *HERON-ENGLISH EDITION-,* 52**,** 289.

LEWIS, W. J. & LEWIS, G. 1990. The influence of polymer latex modifiers on the properties of concrete. *Composites,* 21**,** 487-494.

LI, V. C. 2003. On Engineered Cementitious Composites (ECC)

A Review of the Material and Its Applications. *Journal of Advanced Concrete Technology,* 1**,** 215-230.

LI, Y., ZHU, Y., ZHU, X., GE, Y. & LAURA, S. 2007. Chloride ion critical content in reinforced concrete. *Journal of Wuhan University of Technology-Mater. Sci. Ed.,* 22**,** 737-740.

LIAM, K. C., ROY, S. K. & WOOD, D. O. N. 1992. Chloride ingress measurements and corrosion potential mapping study of a 24-year-old reinforced concrete jetty structure in a tropical marine environment. *Magazine of Concrete Research* [Online], 44. Available: http://www.icevirtuallibrary.com/content/article/10.1680/macr.1992.44.160.205.

LIANG, M., LIN, L. & LIANG, C. 2002. Service Life Prediction of Existing Reinforced Concrete Bridges Exposed to Chloride Environment. *Journal of Infrastructure Systems,* 8**,** 76-85.

LIANG, M. T., WANG, K. L. & LIANG, C. H. 1999. Service life prediction of reinforced concrete structures. *Cement and Concrete Research,* 29**,** 1411-1418.

LIAO, K., ALTKORN, R. I., MILKOVICH, S. M., FILDES, J. M., GOMEZ, J., SCHULTHEISZ, C. R., HUNSTON, D. L. & BRINSON, L. 1997. Long-term durability of glass-fiber reinforced composites in infrastructure applications. *Journal of advanced materials,* 28**,** 54-63.

LIM, Y., KIM, M., SHIN, S. & LI, V. C. 2001. Numerical simulation for quasi-brittle interface fracture in cementitious bi-material system. *Proceedings of FramCos-4. ACI, Cachan, France***,** 127-32.

LIN, G., LIU, Y. & XIANG, Z. 2010. Numerical modeling for predicting service life of reinforced concrete structures exposed to chloride environments. *Cement and Concrete Composites,* 32**,** 571-579.

LIZARAZO-MARRIAGA, J. & CLAISSE, P. 2009. Determination of the concrete chloride diffusion coefficient based on an electrochemical test and an optimization model. *Materials Chemistry and Physics,* 117**,** 536-543.

LOCKE, C. & SIMAN, A. 1980. Electrochemistry of reinforcing steel in salt-contaminated concrete. *ASTM special technical publication***,** 3-16.

LOVETT, R. F. 1978. Quantitative measurement of airborne sea-salt in the North Atlantic. *Tellus,* 30**,** 358-364.

LU, C., JIN, W. & LIU, R. 2011. Reinforcement corrosion-induced cover cracking and its time prediction for reinforced concrete structures. *Corrosion Science,* 53**,** 1337-1347.

LU, X. 1997. Application of the Nernst-Einstein equation to concrete. *Cement and Concrete Research,* 27**,** 293-302.

LUC THE NGOC, D., VINH THE NGOC, D., SANG-HYO, K. & KI YONG, A. 2010. Modelinmg Steel Corrosion in Concrete Structures - Part 1: A New Inverse Relation between Current Density and Potentialfor the Cathodic Reaction. *International Journal of ELECTROCHEMICAL SCIENCE,* 5**,** 302-313.

LUIKOV, A. V. 1975. Systems of differential equations of heat and mass transfer in capillary-porous bodies (review). *International Journal of Heat and Mass Transfer,* 18**,** 1-14.

LUNDGREN, K. 2002. Modelling the effect of corrosion on bond in reinforced concrete. *Magazine of Concrete Research* [Online], 54.

LUO, R., CAI, Y., WANG, C. & HUANG, X. 2003. Study of chloride binding and diffusion in GGBS concrete. *Cement and Concrete Research,* 33**,** 1-7.

LUPING, T. 2008. Engineering expression of the ClinConc model for prediction of free and total chloride ingress in submerged marine concrete. *Cement and Concrete Research,* 38**,** 1092-1097.

LUPING, T. & GULIKERS, J. 2007. On the mathematics of time-dependent apparent chloride diffusion coefficient in concrete. *Cement and Concrete Research,* 37**,** 589-595.

LUPING, T. & NILSSON, L.-O. 1993a. Chloride binding capacity and binding isotherms of OPC pastes and mortars. *Cement and Concrete Research,* 23**,** 247-253.

LUPING, T. & NILSSON, L. O. 1992. Chloride diffusivity in high strength concrete at different ages. *NORDIC CONCRETE RESEARCH. PUBLICATION NO 11*.

LUPING, T. & NILSSON, L. O. 1993b. Rapid determination of the chloride diffusivity in concrete by applying an electric field. *ACI Materials journal,* 89.

MA, H., TIAN, Y. & LI, Z. 2011. Interactions between Organic and Inorganic Phases in PA-and PU/PA-Modified-Cement-Based Materials. *Journal of Materials in Civil Engineering,* 23**,** 1412-1421.

MAAGE, M., HELLAND, S., POULSEN, E., VENNESLAND, O. & CARL, J. E. 1996. Service life prediction of existing concrete structures exposed to marine environment. *ACI Materials Journal,* 93.

MACIAS, A. & ANDRADE, C. 1987. Corrosion of galvanized steel reinforcements in alkaline solutions: Part 2: SEM study and identification of corrosion products. *British Corrosion Journal,* 22**,** 119-130.

MACKNICK, A. B., MASIA, M. & STEWART, R. F. 1985. Corrosion protection method. Google Patents.

MANERA, M., VENNESLAND, Ø. & BERTOLINI, L. 2008. Chloride threshold for rebar corrosion in concrete with addition of silica fume. *Corrosion Science,* 50**,** 554-560.

MANGAT, P. & MOLLOY, B. 1994a. Prediction of long term chloride concentration in concrete. *Materials and Structures,* 27**,** 338-346.

MANGAT, P. S. & GURUSAMY, K. 1987. Chloride diffusion in steel fibre reinforced marine concrete. *Cement and Concrete Research,* 17**,** 385-396.

MANGAT, P. S. & MOLLOY, B. T. 1994b. Prediction of long term chloride concentration in concrete. *Materials and Structures,* 27**,** 338-346.

MANNING, D., ESCALANTE, E. & WHITING, D. 1982. Panel Report—Galvanized Rebars as Long-Term Protective System. *Washington, DC*.

MANNING, D. G. 1996. Corrosion performance of epoxy-coated reinforcing steel: North American experience. *Construction and Building Materials,* 10**,** 349-365.

MARKESET, I. G. 2008. Modelling of reinforcement corrosion in concrete-State of the art.

MARTíN-PÉREZ, B., PANTAZOPOULOU, S. J. & THOMAS, M. D. A. 2001. Numerical solution of mass transport equations in concrete structures. *Computers & Structures,* 79**,** 1251-1264.

MARTíN-PÉREZ, B., ZIBARA, H., HOOTON, R. D. & THOMAS, M. D. A. 2000. A study of the effect of chloride binding on service life predictions. *Cement and Concrete Research,* 30**,** 1215-1223.

MASSOUD, M. T., ABOU-ZEID, M. N. & FAHMY, E. H. Polypropylene Fibers and Silica Fume Concrete for Bridge Overlays. Transportation Research Board annual meeting, 2003.

MCCRUM, R. & ARNOLD, C. 1993. Evaluation of Simulated Bridge Deck Slabs Using Uncoated, Galvanized, and Epoxy Coated Reinforcing Steel.

MCDONALD, R., UNNI, C. & DUCE, R. 1982. Estimation of atmospheric sea salt dry deposition: Wind speed and particle size dependence. *Journal of Geophysical Research: Oceans (1978–2012),* 87**,** 1246-1250.

MCGRATH, P. F. & HOOTON, R. D. 1996. Influence of voltage on chloride diffusion coefficients from chloride migration tests. *Cement and Concrete Research,* 26**,** 1239-1244.

MEHTA, P. K. 2001. Reducing the environmental impact of concrete. *Concrete international,* 23**,** 61-66.

MEHTA, P. K. 2002. Greening of the Concrete Industry for Sustainable Development. *Concrete International,* 24**,** 6.

MEHTA, P. K. & MONTERIO, P. J. M. 1993. *Concrete structure, properties and materials,* New Jersey, Prentice Hall.

MEIRA, G. R., ANDRADE, C., ALONSO, C., BORBA JR, J. C. & PADILHA JR, M. 2010. Durability of concrete structures in marine atmosphere zones – The use of chloride deposition rate on the wet candle as an environmental indicator. *Cement and Concrete Composites,* 32**,** 427-435.

MEIRA, G. R., ANDRADE, C., PADARATZ, I. J., ALONSO, C. & BORBA JR, J. C. 2007. Chloride penetration into concrete structures in the marine atmosphere zone – Relationship between deposition of chlorides on the wet candle and chlorides accumulated into concrete. *Cement and Concrete Composites,* 29**,** 667-676.

MELCHERS, R. E. & LI, C. Q. 2009. Reinforcement corrosion initiation and activation times in concrete structures exposed to severe marine environments. *Cement and Concrete Research,* 39**,** 1068-1076.

MICELLI, F. & NANNI, A. 2004. Durability of FRP rods for concrete structures. *Construction and Building Materials,* 18**,** 491-503.

MINDESS, S. & VONDRAN, G. 1988. Properties of concrete reinforced with fibrillated polypropylene fibres under impact loading. *Cement and Concrete Research,* 18**,** 109-115.

MINDESS, S. & YOUNG, J. F. 1981. Concrete, 1981. *qsy ujot^ og^ uau,* 3**,** 114.

MOHAMMED, T. U., HAMADA, H. & YAMAJI, T. 2004. Concrete After 30 Years of Exposure-Part 1: Minearlogy, Microstructure, and Interfaces. *ACI Materials Journal,* 101.

MOHAMMED, T. U., YAMAJI, T. & HAMADA, H. 2002. Chloride diffusion, microstructure, and mineralogy of concrete after 15 years of exposure in tidal environment. *ACI Materials Journal,* 99.

MORCILLO, M., CHICO, B., OTERO, E. & MARIACA, L. 1999. Effect of marine aerosol on atmospheric corrosion. *Materials Performance,* 38**,** 72.

MORINAGA, S. Life prediction of reinforced concrete structures in hot and salt-laden environments. CONCRETE IN HOT CLIMATES. PROCEEDINGS OF THE THIRD INTERNATIONAL CONFERENCE HELD BY RILEM (THE INTERNATIONAL UNION OF TESTING AND RESEARCH LABORATORIES FOR MATERIALS AND TESTING), SEPTEMBER 21-25, 1992, TORQUAY, ENGLAND, 1992.

MORRIS, W., VICO, A. & VÁZQUEZ, M. 2004. Chloride induced corrosion of reinforcing steel evaluated by concrete resistivity measurements. *Electrochimica Acta,* 49**,** 4447-4453.

MUHAMMAD, B. & ISMAIL, M. 2012. Performance of natural rubber latex modified concrete in acidic and sulfated environments. *Construction and Building Materials,* 31**,** 129-134.

MULLARD, J. A. & STEWART, M. G. 2011. Corrosion-Induced Cover Cracking: New Test Data and Predictive Models. *ACI Structural Journal,* 108**,** 71-79.

MUSTAFA, M. A. & YUSEF, K. M. 1994. Atmosphoric chloride penetration into concrete in semi-tropical marine environment. *Cement & Concrete Research,* 24**,** 661-670.

MUTHUKUMAR, M. & MOHAN, D. 2004. Optimization of mechanical properties of polymer concrete and mix design recommendation based on design of experiments. *Journal of Applied Polymer Science,* 94**,** 1107-1116.

NANNI, A. & MEAMARIAN, N. 1991. Distribution and opening of fibrillated polypropylene fibers in concrete. *Cement and Concrete Composites,* 13**,** 107-114.

NEVILLE, A. 1991. *Properties of Concrete*.

NEVILLE, A. M. & BROOKS, J. J. 1987. *Concrete technology*.

NEVILLE, K. & LEE, H. 1967. Handbook of epoxy resins. *MacGraw-Hill, Inc***,** 2-2.

NGUYEN, T. Q., PETKOVIĆ, J., DANGLA, P. & BAROGHEL-BOUNY, V. 2008. Modelling of coupled ion and moisture transport in porous building materials. *Construction and Building Materials,* 22**,** 2185-2195.

NILSSON, L.-O. 2009. Models for chloride ingress into concrete – from Collepardi to today. *International Journal of Modelling, Identification and Control,* 7**,** 129-134.

NILSSON, L. 2006. Modelling of chloride ingress. WP4-report of EU-project GRD1-2002-71808 ChlorTest, Resistance of Concrete to Chloride Ingress–From Laboratory Tests to In-field Performance, available at http://www. chlortest. org.

NILSSON, L. & OLLIVIER, J. Chloride diffusion and resistivity testing of five. RILEM International Workshop on Chloride Penetration into Concrete, 1995a. RILEM Publications SARL, 225-233.

NILSSON, L. & OLLIVIER, J. Steady-state diffusion characteristics of cementitious materials. RILEM International Workshop on Chloride Penetration into Concrete, 1995b. RILEM Publications SARL, 77-84.

NMAI, C. K. 2004. Multi-functional organic corrosion inhibitor. *Cement and Concrete Composites,* 26**,** 199-207.

NOGUEIRA, C. G. & LEONEL, E. D. 2013. Probabilistic models applied to safety assessment of reinforced concrete structures subjected to chloride ingress. *Engineering Failure Analysis,* 31**,** 76-89.

NOKKEN, M., BODDY, A., HOOTON, R. D. & THOMAS, M. D. A. 2006. Time dependent diffusion in concrete—three laboratory studies. *Cement and Concrete Research,* 36**,** 200-207.

NYGAARD, P. V. & GEIKER, M. R. 2005. A method for measuring the chloride threshold level required to initiate reinforcement corrosion in concrete. *Materials and Structures,* 38**,** 489-494.

O'CONNOR, C. 2007. Historic bridges and roads of Norfolk Island. *Australian Journal of Civil Engineering,* 3**,** 75.

O'CONNOR, D. N. & SAIIDI, M. 1993. Compatibility of polyester-styrene polymer concrete overlays with Portland cement concrete bridge decks. *ACI Materials Journal,* 90.

OH, B. H. & JANG, S. Y. 2007. Effects of material and environmental parameters on chloride penetration profiles in concrete structures. *Cement and Concrete Research,* 37**,** 47-53.

OH, B. H., JANG, S. Y. & SHIN, Y. S. 2003. Experimental investigation of the threshold chloride concentration for corrosion initiation in reinforced concrete structures. *Magazine of Concrete Research* [Online], 55. Available: http://www.icevirtuallibrary.com/content/article/10.1680/macr.2003.55.2.117.

OHAMA, Y. 1987. Principle of Latex Modification and Some Typical Properties of Latex-Modified Mortars and Concretes Adhesion; Binders (materials); Bond (paste to aggregate); Carbonation; Chlorides; curing; diffusion. *ACI Materials Journal,* 84.

OHAMA, Y. 1995. *Handbook of polymer-modified concrete and mortars: properties and process technology*, William Andrew.

OHAMA, Y. 1998. Polymer-based admixtures. *Cement and Concrete Composites,* 20**,** 189-212.

OHAMA, Y., DEMURA, K., KOBAYASHI, K., SATOH, Y. & MORIKAWA, M. 1991. Pore size distribution and oxygen diffusion resistance of polymer-modified mortars. *Cement and Concrete Research,* 21**,** 309-315.

OKBA, S. H., EL-DIEB, A. S. & REDA, M. M. 1997. Evaluation of the corrosion resistance of latex modified concrete (LMC). *Cement and Concrete Research,* 27**,** 861-868.

ORELLAN, J. C., ESCADEILLAS, G. & ARLIGUIE, G. 2004. Electrochemical chloride extraction: efficiency and side effects. *Cement and Concrete Research,* 34**,** 227-234.

OTIENO, M. B., BEUSHAUSEN, H. D. & ALEXANDER, M. G. 2011. Modelling corrosion propagation in reinforced concrete structures – A critical review. *Cement and Concrete Composites,* 33**,** 240-245.

PACK, S.-W., JUNG, M.-S., SONG, H.-W., KIM, S.-H. & ANN, K. Y. 2010. Prediction of time dependent chloride transport in concrete structures exposed to a marine environment. *Cement and Concrete Research,* 40**,** 302-312.

PAGE, C., LAMBERT, P. & VASSIE, P. 1991. Investigations of reinforcement corrosion. 1. The pore electrolyte phase in chloride-contaminated concrete. *Materials and Structures,* 24**,** 243-252.

PAGE, C. & SERGI, G. 2000. Developments in Cathodic Protection Applied to Reinforced Concrete. *Journal of Materials in Civil Engineering,* 12**,** 8-15.

PAGE, C. L., SHORT, N. R. & EL TARRAS, A. 1981. Diffusion of chloride ions in hardened cement pastes. *Cement and Concrete Research,* 11**,** 395-406.

PANTAZOPOULOU, S. J. & ZANGANEH, M. 2001. Triaxial Tests of Fiber-Reinforced Concrete. *Journal of Materials in Civil Engineering,* 13**,** 340-348.

PEDERSEN, V. & ARNTSEN, B. Effect of Early-age Curing on Penetration of Chloride Ions Into Concrete in the Tidal Zone. Proc. of the 2nd Intl. Conf. on Concrete under Severe Conditions, CONSEC, 1998. 21-24.

PERIS MORA, E. 2007. Life cycle, sustainability and the transcendent quality of building materials. *Building and Environment,* 42**,** 1329-1334.

PETTERSSON, K. 1992. Corrosion threshold value and corrosion rate in reinforced concrete. *CBI REPORT 2: 92*.

PFEIFER, D. 2000. High performance concrete and reinforcing steel with a 100-year service life. *PCI journal,* 45**,** 46-54.

PHILIBERT, J. 2005. One and a Half century of Diffusion: Fick, Einstein, before and beyond. *The Open-Access Journal for the Basic principles of Diffusion Theory, Experiment and Application,* 2**,** 10.

PHONG, L. 1997. Plastic Composites in Civil Engineering Structures. *California Engineer,* 76**,** 20-24.

PIKE, R. 1973. Nonmetallic coatings for concrete reinforcing bars. *Public Roads,* 37.

POLDER, R. B. 1995. Chloride Diffusion and Resistivity Testing of Five Concrete Mixes for Marine Environment. *International Conference, Chloride Penetration into Concrete.* Paris: RILEM.

POLDER, R. B. & PEELEN, W. H. A. 2002. Characterisation of chloride transport and reinforcement corrosion in concrete under cyclic wetting and drying by electrical resistivity. *Cement and Concrete Composites,* 24**,** 427-435.

POWERS, T. C., COPELAND, L., HAYES, J. & MANN, H. Permeablity of Portland Cement Paste. ACI Journal Proceedings, 1954. ACI.

PULLAR-STRECKER, P. 1987. *Corrosion damaged concrete: assessment and repair*, Construction Industry Research and Information Association.

PYC, W. A. 1998. *Corrosion Protection Performance of Corrosion Inhibitors and Epoxy-Coated Reinforcing Steel in a Simulated Concrete Pore Water Solution.* Virginia Polytechnic.

QIAN, C. X. & STROEVEN, P. 2000. Development of hybrid polypropylene-steel fibre-reinforced concrete. *Cement and Concrete Research,* 30**,** 63-69.

QING LI, C. 2004. Reliability Based Service Life Prediction of Corrosion Affected Concrete Structures. *Journal of Structural Engineering,* 130**,** 1570-1577.

RAMAKRISHNAN, V. 1992. *Latex-modified concretes and mortars*, Transportation Research Board.

RAMAKRISHNAN, V., GOLLAPUDI, S. & ZELLERS, R. 1987. Performance characteristics and fatigue strength of polypropylene fiber reinforced concrete. *ACI Special Publication,* 105.

RAMLI, M., TABASSI, A. A. & HOE, K. W. 2013. Porosity, pore structure and water absorption of polymer-modified mortars: An experimental study under different curing conditions. *Composites Part B: Engineering,* 55**,** 221-233.

RASHEEDUZZAFAR, EHTESHAM HUSSAIN, S. & AL-SAADOUN, S. S. 1991. Effect of cement composition on chloride binding and corrosion of reinforcing steel in concrete. *Cement and Concrete Research,* 21**,** 777-794.

RAUPACH, M. 1996. Chloride-induced macrocell corrosion of steel in concrete—theoretical background and practical consequences. *Construction and Building Materials,* 10**,** 329-338.

RAY, I., GUPTA, A. & BISWAS, M. 1994a. Effect of latex and superplasticiser on Portland cement mortar in the fresh state. *Cement and concrete composites,* 16**,** 309-316.

RAY, I., GUPTA, A. P. & BISWAS, M. 1994b. Effect of latex and superplasticiser on Portland cement mortar in the fresh state. *Cement and Concrete Composites,* 16**,** 309-316.

REBEIZ, K. 1996. Precast use of polymer concrete using unsaturated polyester resin based on recycled PET waste. *Construction and Building Materials,* 10**,** 215-220.

REDDY, B., GLASS, G. K., LIM, P. J. & BUENFELD, N. R. 2002. On the corrosion risk presented by chloride bound in concrete. *Cement & Concrete Composites,* 24.

RIBEIRO, M., GONÇALVES, A. & BRANCO, F. 2008. Styrene-butadiene polymer action on compressive and tensile strengths of cement mortars. *Materials and Structures,* 41**,** 1263-1273.

RICHARTZ, W. 1969. Die Bindung von Chlorid bei der Zementerhärtung. *Zement-Kalk-Gips,* 22**,** 447-456.

RILEM, T. 178-TMC (2002). Recommendation for analysis of total chloride in concrete. *Mat. Struct,* 35**,** 583-585.

ROA-RODRIGUEZ, G., APERADOR, W. & DELGADO, A. 2013. Calculation of Chloride Penetration Profile in Concrete Structures. *Int. J. Electrochem. Sci,* 8**,** 5022-5035.

ROBERT, M., COUSIN, P. & BENMOKRANE, B. 2009. Durability of GFRP Reinforcing Bars Embedded in Moist Concrete. *Journal of Composites for Construction,* 13**,** 66-73.

ROSSIGNOLO, J. A. & AGNESINI, M. V. C. 2004. Durability of polymer-modified lightweight aggregate concrete. *Cement and Concrete Composites,* 26**,** 375-380.

ROY, D. M., BROWN, P., SHI, D., SCHEETZ, B. & MAY, W. 1993a. CONCRETE MISCROSTRUCTURE POROSITY AND PERMEABILITY.

ROY, S. K., LIAM KOK, C. & NORTHWOOD, D. O. 1993b. Chloride ingress in concrete as measured by field exposure tests in the atmospheric, tidal and submerged zones of a tropical marine environment. *Cement and Concrete Research,* 23**,** 1289-1306.

SAETTA, A. V. 2005. Deterioration of Reinforced Concrete Structures due to Chemical–Physical Phenomena: Model-Based Simulation. *Journal Of Materials in Civil Engineering,* 17**,** 313-319.

SALPARANTA, L. 1988. Epoxy-coated concrete reinforcements.

SAMSON, E. & MARCHAND, J. 2008. Modeling the transport of ions in unsaturated cement based materials. *Comput Struct***,** 17.

SAMSON, E., MARCHAND, J. & SNYDER, K. A. 2003. Calculation of ionic diffusion coefficients on the basis of migration test results. *Materials and Structures,* 36**,** 156-165.

SANDBERG, P., TANG, L. & ANDERSEN, A. 1998. Recurrent studies of chloride ingress in uncracked marine concrete at various exposure times and elevations. *Cement and Concrete Research,* 28**,** 1489-1503.

SANJUÁN, M. A. & MORAGUES, A. 1997. Polypropylene-fibre-reinforced mortar mixes: Optimization to control plastic shrinkage. *Composites Science and Technology,* 57**,** 655-660.

SAREMI, M. & MAHALLATI, E. 2002. A study on chloride-induced depassivation of mild steel in simulated concrete pore solution. *Cement and Concrete Research,* 32**,** 1915-1921.

SARJA, A. 2000. Durability design of concrete structures—Committee report 130-CSL. *Materials and Structures,* 33**,** 14-20.

SCHIESSL, P. & BREIT, W. 1996. 51 Local repair measures at concrete structures damaged by reinforcement corrosion-Aspects of durability. *Special Publications of the Royal Society of Chemistry,* 183**,** 525-534.

SCHIESSL, P. & RAUPACH, M. 1990. *INFLUENCE OF CONCRETE COMPOSITION AND MICROCLIMATE ON THE CRITICAL CHLORIDE CONTENT IN CONCRETE,* Barking Essex, Elsevier Appl Sci Publ Ltd.

SCRIVENER, K. L. Use of back scattered electron microscopy and image analysis to study the porosity of cement paste. Materials Research Society, 1989. 129-140.

SCRIVENER, K. L. & NONAT, A. 2011. Hydration of cementitious materials, present and future. *Cement and Concrete Research,* 41**,** 651-665.

SCULLY, J. R. 2000. Polarization resistance method for determination of instantaneous corrision rates. *Corrosion,* 56**,** 199.

SEYMOUR, R. B. & MARK, H. F. 1990. *Handbook of organic coatings: a comprehensive guide for the coatings industry*, Elsevier.

SHAFEI, B., ALIPOUR, A. & SHINOZUKA, M. 2012. Prediction of corrosion initiation in reinforced concrete members subjected to environmental stressors: A finite-element framework. *Cement and Concrete Research,* 42**,** 365-376.

SHAKER, F. A., EL-DIEB, A. S. & REDA, M. M. 1997. Durability of Styrene-Butadiene latex modified concrete. *Cement and Concrete Research,* 27**,** 711-720.

SHERMAN, M. R., CARRASQUILLO, R. & FOWLER, D. W. 1993. Field evaluation of bridge corrosion protection measures.

SHETTY, M. 2005. Concrete technology: theory and practice, S. Chand.

SHIN, C. B. & KIM, E. K. 2002. Modeling of chloride ion ingress in coastal concrete. Cement and Concrete Research, 32**,** 757-762.

SIEMES, T., POLDER, R. & DE VRIES, H. 1998. Design of concrete structures for durability. Heron, 43**,** 227-44.

SILVA, D. A. & MONTEIRO, P. J. M. 2006. The influence of polymers on the hydration of portland cement phases analyzed by soft X-ray transmission microscopy. Cement and Concrete Research, 36**,** 1501-1507.

SINGH, D. D. N. & GHOSH, R. 2005. Unexpected Deterioration of Fusion-Bonded Epoxy-Coated Rebars Embedded in Chloride-Contaminated Concrete Environments. Corrosion, 61**,** 815-829.

SINGHAL, D., AGRAWAL, R. & NAUTIYAL, B. Chloride resistance of SFRC. FIBRE REINFORCED CEMENT AND CONCRETE. PROCEEDINGS OF THE FOURTH INTERNATIONAL SYMPOSIUM HELD BY RILEM, JULY 20-23 1992, UNIVERSITY OF SHEFFIELD, 1992.

SMITH, J. L. & VIRMANI, Y. P. 1996. Performance of epoxy coated rebars in bridge decks.

SONG, H.-W., ANN, K. Y., PACK, S.-W. & LEE, C.-H. 2010. Factors influencing chloride transport and chloride threshold level for the prediction of service life of concrete structures. International Journal of Structural Engineering, 1**,** 131-144.

SONG, H.-W. & KWON, S.-J. 2009. Evaluation of chloride penetration in high performance concrete using neural network algorithm and micro pore structure. Cement and Concrete Research, 39**,** 814-824.

SONG, H.-W., LEE, C.-H. & ANN, K. Y. 2008. Factors influencing chloride transport in concrete structures exposed to marine environments. Cement and Concrete Composites, 30**,** 113-121.

SONG, P. S., WU, J. C., HWANG, S. & SHEU, B. C. 2005. Statistical analysis of impact strength and strength reliability of steel–polypropylene hybrid fiber-reinforced concrete. Construction and Building Materials, 19**,** 1-9.

SOROUSHIAN, P. & FAIZ MIRZA, A. A. 1993. Plastic shrinkage cracking of polypropylene fiber reinforced concrete. ACI Materials Journal, 92.

SÖYLEV, T. A. & RICHARDSON, M. G. 2008. Corrosion inhibitors for steel in concrete: State-of-the-art report. Construction and Building Materials, 22**,** 609-622.

STANISH, K., HOOTON, R. & THOMAS, M. 1997. Testing the chloride penetration resistance of concrete: a literature review. FHWA contract DTFH61**,** 19-22.

STANISH, K. & THOMAS, M. 2003. The use of bulk diffusion tests to establish time-dependent concrete chloride diffusion coefficients. Cement and Concrete Research, 33**,** 55-62.

STECKEL, G., HAWKINS, G. & BAUER, J. Environmental durability of composites for seismic retrofit of bridge columns. Second International Conference on Composites in Infrastructure, 1998.

STIPANOVIC OSLAKOVIC, I., BJEGOVIC, D. & MIKULIC, D. 2010. Evaluation of service life design models on concrete structures exposed to marine environment. Materials and Structures, 43**,** 1397-1412.

SU, Z., BIJEN, J. M. J. M. & LARBI, J. A. 1991. Influence of polymer modification on the hydration of portland cement. Cement and Concrete Research, 21**,** 242-250.

SUE, Y., MATSUSHITA, H. & TSURUTA, H. Effects of construction joint on bending strength reduction. CONSEC'01: Third International Conference on Concrete Under Severe Conditions, 2001. 1117-1124.

SUKONTASUKKUL, P. & BOONPRADIT, N. 2006. to Improve Watertightness at the Hardening Stage. Thammasat Int. J. Sc. Tech, 11**,** 41-46.

SURYAVANSHI, A. K., SWAMY, R. N. & MCHUGH, S. 1998. Chloride penetration into reinforced concrete slabs. Canadian Journal of Civil Engineering, 25**,** 87-95.

TAKEWAKE, K. & MASTUMOTO, S. Quality and cover thickness of concrete based on the estimation of chloride penetration in marine environments. In: MALHOTRA, V. M., ed. 2nd Int. Conf. Concr. Marine Envir., 1988. ACI, 381-400.

TANG, L. & NILSON, L. O. 1993. Chloride binding capacity and binding isotherms of OPC pastes and mortars Cement & Concrete Research, 23.

TANG, L. & NILSSON, L. O. 1992. Chloride Diffusivity in High Strength Concrete at Different Ages Nordic Concr. Res.

TANG, L. P. & GULIKERS, J. P. 2007. On the mathematics of time-dependent apparent chloride diffusion coefficient in concrete. Cement & Concrete Research, 37**,** 6.

TAZAWA, E. & KOBAYASHI, S. 1973. Properties and Applications of Polymer Impregnated Cementitious Materials. American Concrete Institute, Journal of, 70.

THOMAS, M. D. A. & BAMFORTH, P. B. 1999. Modelling chloride diffusion in concrete: Effect of fly ash and slag. Cement and Concrete Research, 29**,** 487-495.

TOUTANJI, H., MCNEIL, S. & BAYASI, Z. 1998. Chloride permeability and impact resistance of polypropylene-fiber-reinforced silica fume concrete. Cement and Concrete Research, 28**,** 961-968.

TOUTANJI, H. A. 1999. Properties of polypropylene fiber reinforced silica fume expansive-cement concrete. Construction and Building Materials, 13**,** 171-177.

TREJO, D. & MONTEIRO, P. J. 2005. Corrosion performance of conventional (ASTM A615) and low-alloy (ASTM A706) reinforcing bars embedded in concrete and exposed to chloride environments. Cement and Concrete Research, 35**,** 562-571.

TREJO, D. & PILLAI, R. G. 2003. Accelerated chloride threshold testing: Part I-ASTM A 615 and A 706 Reinforcement. ACI Materials Journal, 100.

TRÉPANIER, S. M., HOPE, B. B. & HANSSON, C. M. 2001. Corrosion inhibitors in concrete: Part III. Effect on time to chloride-induced corrosion initiation and subsequent corrosion rates of steel in mortar. Cement and Concrete Research, 31**,** 713-718.

TRITTHART, J. 1989. Chloride binding in cement II. The influence of the hydroxide concentration in the pore solution of hardened cement paste on chloride binding. Cement and Concrete Research, 19**,** 683-691.

TROCÓNIS DE RINCÓN, O. 2006. Durability of concrete structures: DURACON, an iberoamerican project. Preliminary results. Building and Environment, 41**,** 952-962.

TROCÓNIS DE RINCÓN, O., SÁNCHEZ, M., MILLANO, V., FERNÁNDEZ, R., DE PARTIDAS, E. A., ANDRADE, C., MARTÍNEZ, I., CASTELLOTE, M., BARBOZA, M., IRASSAR, F., MONTENEGRO, J. C., VERA, R., CARVAJAL, A. M., DE GUTIÉRREZ, R. M., MALDONADO, J., GUERRERO, C., SABORIO-LEIVA, E., VILLALOBOS, A. C., TRES-CALVO, G., TORRES-ACOSTA, A., PÉREZ-QUIROZ, J., MARTÍNEZ-MADRID, M., ALMERAYA-CALDERÓN, F., CASTRO-BORGES, P., MORENO, E. I., PÉREZ-LÓPEZ, T., SALTA, M., DE MELO, A. P., RODRÍGUEZ, G., PEDRÓN, M. & DERRÉGIBUS, M. 2007. Effect of the marine environment on reinforced concrete durability in Iberoamerican countries: DURACON project/CYTED. Corrosion Science, 49**,** 2832-2843.

TRUC, O., OLLIVIER, J. P. & CARCASSÈS, M. 2000. A new way for determining the chloride diffusion coefficient in concrete from steady state migration test. Cement and Concrete Research, 30**,** 217-226.

TUUTTI, K. 1982. Corrosion of Steel in Concrete. Swedish Cement and Concrete Research Institute**,** 6.

UJI, K., MATSUOKA, Y. & MARUYA, T. 1990. Formation of an equation for surface chloride content of concrete due to permeation of chloride Corrosion of reinforcement in concrete. UK: Elsevier Applied Science.

UNO, P. J. 1998. Plastic Shrinkage Cracking and Evaporation Formulae. ACI Mater J, 95**,** 11.

USTABAS, I. 2012. The effect of capillarity on chloride transport and the prediction of the accumulation region of chloride in concretes with reinforcement corrosion. Construction and Building Materials, 28**,** 640-647.

VAL, D. 2007. Deterioration of Strength of RC Beams due to Corrosion and Its Influence on Beam Reliability. Journal of Structural Engineering, 133**,** 1297-1306.

VAL, D., CHERNIN, L. & STEWART, M. 2009. Experimental and Numerical Investigation of Corrosion-Induced Cover Cracking in Reinforced Concrete Structures. Journal of Structural Engineering, 135**,** 376-385.

VAL, D. V. & STEWART, M. G. 2003. Life-cycle cost analysis of reinforced concrete structures in marine environments. Structural Safety, 25**,** 343-362.

VAN DER WAGEN, G., POLDER, R. B. & VAN BREUGEL, K. 2012. Guideline for service life design of structural concrete, A performance based approach. HERON, 57**,** 153-167.

VAN GEMERT, D. Cement-concrete and concrete-polymer composites: Two merging worlds. XIIth Interantional Congress on Polymers in Concrete, 2007. 3-15.

VASSIE, P., SWENSON, D. L., GREGG, D. J., VINELOTT, K. M. & ARSHAD, M. 1985. REINFORCEMENT CORROSION AND THE DURABILITY OF CONCRETE

BRIDGES - DISCUSSION. Proceedings of the Institution of Civil Engineers Part 1-Design and Construction, 78**,** 1253-1256.

VILLAIN, G., SBARTAÏ, Z. M., DÉROBERT, X., GARNIER, V. & BALAYSSAC, J.-P. 2012. Durability diagnosis of a concrete structure in a tidal zone by combining NDT methods: Laboratory tests and case study. *Construction and Building Materials,* 37**,** 893-903.

VIRMANI, Y. 2002. Corrosion costs and preventive strategies in the United States. *Federal Highway Administration, Report FHWA-RD-01-156 BIOGRAPHICAL SKETCH*.

VIRMANI, Y. P. & CLEMENA, G. G. 1998. Corrosion Protection-Concrete Bridges.

VON BAECKMANN, W., SCHWENK, W. & PRINZ, W. 1997. *Handbook of Cathodic corrosion protection*, Gulf Professional Publishing.

WALTERS, D. G. 1987. What are latexes. *Concrete International,* 9**,** 44-47.

WALTON, P. & MAJUMDAR, A. J. 1975. Cement-based composites with mixtures of different types of fibres. *Composites,* 6**,** 209-216.

WANG, R., LI, X.-G. & WANG, P.-M. 2006. Influence of polymer on cement hydration in SBR-modified cement pastes. *Cement and Concrete Research,* 36**,** 1744-1751.

WANG, X. & ZHAO, H. 1993. The residual service life prediction of RC structures. *Durability of building materials and components,* 6**,** 1107-1114.

WANG, Y., LI, L.-Y. & PAGE, C. L. 2005. Modelling of chloride ingress into concrete from a saline environment. *Building and Environment,* 40**,** 1573-1582.

WEE, T. H., SURYAVANSHI, A. K. & TIN, S. S. 1999. Influence of aggregate fraction in the mix on the reliability of the rapid chloride permeability test. *Cement and Concrete Composites,* 21**,** 59-72.

WEST, R. E. & HIME, W. G. 1985. Chloride profiles in salty concrete. *Materials Performance,* 24**,** 29-36.

WEYERS, R. E. 1998. Service life model for concrete structures in chloride laden environments. *ACI materials journal,* 95.

WEYERS, R. E., PYC, W., ZEMAJTIS, J., LIU, Y., MOKAREM, D. & SPRINKEL, M. M. 1997. Field investigation of corrosion-protection performance of bridge decks constructed with epoxy-coated reinforcing steel in Virginia. *Transportation Research Record: Journal of the Transportation Research Board,* 1597**,** 82-90.

WHITING, D. 1981. Rapid determination of the chloride permeability of concrete. *Final Report Portland Cement Association, Skokie, IL. Construction Technology Labs.,* 1.

WIN, P. P., WATANABE, M. & MACHIDA, A. 2004. Penetration profile of chloride ion in cracked reinforced concrete. *Cement and Concrete Research,* 34**,** 1073-1079.

WINSLOW, D. N., COHEN, M. D., BENTZ, D. P., SNYDER, K. A. & GARBOCZI, E. J. 1994. Percolation and pore structure in mortars and concrete. *Cement and Concrete Research,* 24**,** 25-37.

XI, Y. & ABABNEH, A. Prediction of the onset of steel corrosion in concrete by multiscale chloride diffusion. Proc. of the International Symposium on High Performance Concrete: Workability, Strength and Durability, Hong Kong and Shenzhen, China, 2000. Prentice-Hall Inc., 181-6.

XI, Y. & BAŽANT, Z. 1999. Modeling Chloride Penetration in Saturated Concrete. *Journal of Materials in Civil Engineering,* 11**,** 58-65.

XU, J., JIANG, L. & WANG, J. 2009. Influence of detection methods on chloride threshold value for the corrosion of steel reinforcement. *Construction and Building Materials,* 23**,** 1902-1908.

YANG, C. C. & CHO, S. W. 2003. An electrochemical method for accelerated chloride migration test of diffusion coefficient in cement-based materials. *Materials Chemistry and Physics,* 81**,** 116-125.

YANG, C. C. & CHO, S. W. 2004. The relationship between chloride migration rate for concrete and electrical current in steady state using the accelerated chloride migration test. *Materials and Structures,* 37**,** 456-463.

YANG, C. C., CHO, S. W. & HUANG, R. 2002. The relationship between charge passed and the chloride-ion concentration in concrete using steady-state chloride migration test. *Cement and Concrete Research,* 32**,** 217-222.

YANG, Z., SHI, X., CREIGHTON, A. T. & PETERSON, M. M. 2009. Effect of styrene–butadiene rubber latex on the chloride permeability and microstructure of Portland cement mortar. *Construction and Building Materials,* 23**,** 2283-2290.

YE, H., JIN, N., JIN, X. & FU, C. 2012. Model of chloride penetration into cracked concrete subject to drying–wetting cycles. *Construction and Building Materials,* 36**,** 259-269.

YEOMANS, S. Galvanized steel reinforcement in concrete. First National Structural Engineering Conference 1987: Preprints of Papers, 1987. Institution of Engineers, Australia, 662.

YIĞITER, H., YAZıCı, H. & AYDıN, S. 2007. Effects of cement type, water/cement ratio and cement content on sea water resistance of concrete. *Building and Environment,* 42**,** 1770-1776.

YUAN, Q., SHI, C., DE SCHUTTER, G., AUDENAERT, K. & DENG, D. 2009. Chloride binding of cement-based materials subjected to external chloride environment – A review. *Construction and Building Materials,* 23**,** 1-13.

YUNPING XI, Z. K. P. B. A. 1999. Modelling Chloride Penetration in Saturated Concrete. *JOURNAL OF MATERIALS IN CIVIL ENGINEERING,* 11**,** 58-65.

ZHANG, J. & LOUNIS, Z. 2006. Sensitivity analysis of simplified diffusion-based corrosion initiation model of concrete structures exposed to chlorides. *Cement and Concrete Research,* 36**,** 1312-1323.

ZHANG, J. & LOUNIS, Z. 2009. Nonlinear relationships between parameters of simplified diffusion-based model for service life design of concrete structures exposed to chlorides. *Cement and Concrete Composites,* 31**,** 591-600.

ZHANG, R., CASTEL, A. & FRANÇOIS, R. 2010. Concrete cover cracking with reinforcement corrosion of RC beam during chloride-induced corrosion process. *Cement and Concrete Research,* 40**,** 415-425.

ZHANG, T. & GJØRV, O. E. 1994. An electrochemical method for accelerated testing of chloride diffusivity in concrete. *Cement and Concrete Research,* 24**,** 1534-1548.

ZHANG, X., GROVES, G. W. & RODGER, S. A. 1988. The microstructure of cement aggregate interface, Bonding in cementitious composites. *Materials Research Society*

ZHAO, Y.-X., CHEN, C., GAO, X.-J. & JIN, W.-L. 2013. Seasonal Variation of Surface Chloride Ion Content and Chloride Diffusion Coefficient in a Concrete Dock. *Advances in Structural Engineering,* 16**,** 395-404.

ZHENG, J.-J., WONG, H. S. & BUENFELD, N. R. 2009. Assessing the influence of ITZ on the steady-state chloride diffusivity of concrete using a numerical model. *Cement and Concrete Research,* 39**,** 805-813.

ZHENG, J. J. & ZHOU, X. Z. 2007. Prediction of the chloride diffusion coefficient of concrete. *Materials and Structures,* 40**,** 693-701.

ZHENG, Z. & FELDMAN, D. 1995. Synthetic fibre-reinforced concrete. *Progress in Polymer Science,* 20**,** 185-210.

ZHONG, S. & CHEN, Z. 2002. Properties of latex blends and its modified cement mortars. *Cement and Concrete Research,* 32**,** 1515-1524.

ZIMMERMANN, L., ELSENER, B. & BOHNI, H. 2000. Critical factors for the initiation of rebar corrosion. *European Federation of Corrosion Publications(UK),* 31**,** 25-33.

ZORNOZA, E., GARCÉS, P., PAYÁ, J. & CLIMENT, M. A. 2009. Improvement of the chloride ingress resistance of OPC mortars by using spent cracking catalyst. *Cement and Concrete Research,* 39**,** 126-139.

APPENDICES

APPENDIX.A

In this section the detail of chloride content measurement tables for all type of concrete are presented.

Table A- 1 Results of chloride content measurement for CC

Depth [mm]	Time [months]						
	1	5	9	13	17	21	24
2.5	2.84	5.12	5.67	6.45	7.05	7.48	7.63
10	0.25	2.39	3.72	4.56	5.24	6.09	6.21
20	0.08	1.77	3.15	4.02	4.56	5.03	5.16
30	0.02	1.42	2.28	3.14	3.85	4.16	4.21
40	0	1.14	1.87	2.34	2.72	2.85	2.94
50	0	0.73	1.15	1.42	1.65	1.78	1.85

Table A- 2 Results of chloride content measurement for FRC1

Depth [mm]	Time [months]						
	1	5	9	13	17	21	24
2.5	2.84	5.12	5.67	6.45	7.05	7.48	7.63
10	0.21	2.27	3.63	4.37	5.12	5.82	6.02
20	0.05	1.65	2.85	3.58	4.31	4.78	4.95
30	0	1.12	2.37	2.65	3.41	3.83	4.01
40	0	0.95	1.56	2.14	2.25	2.66	2.82
50	0	0.32	0.91	1.35	1.52	1.68	1.75

Table A- 3 Results of chloride content measurement for FRC2

Depth [mm]	Time [months]						
	1	5	9	13	17	21	24
2.5	2.84	5.12	5.67	6.45	7.05	7.48	7.63
10	0.23	2.31	3.68	4.31	5.16	5.94	6.11
20	0.06	1.7	2.93	3.64	4.26	4.73	5.03
30	0	1.32	2.3	2.82	3.71	3.95	4.22
40	0	1.01	1.67	2.1	2.35	2.71	2.82
50	0	0.63	1.05	1.44	1.55	1.7	1.78

Table A- 4 Results of chloride content measurement for FRC3

Depth	Time [months]						
[mm]	1	5	9	13	17	21	24
2.5	2.84	5.12	5.67	6.45	7.05	7.48	7.63
10	0.21	2.33	3.66	4.22	5.15	5.67	5.79
20	0.06	1.72	3.1	3.71	4.36	4.75	4.92
30	0	1.38	2.18	2.77	3.68	3.84	4.11
40	0	1.1	1.58	2.15	2.31	2.66	2.74
50	0	0.67	1.1	1.37	1.56	1.67	1.75

Table A- 5 Results of chloride content measurement for PMC1

Depth	Time [months]						
[mm]	1	5	9	13	17	21	24
2.5	2.1	4.25	5.15	5.65	6.12	6.53	6.64
10	0.15	2.51	3.45	4.15	4.59	4.87	4.96
20	0.00	1.98	2.98	3.68	4.13	4.43	4.55
30	0.00	1.56	2.25	3.05	3.45	3.57	3.75
40	0.00	1.09	1.58	1.88	2.36	2.79	2.85
50	0.00	0.62	0.99	1.11	1.56	1.65	1.69

Table A- 6 Results of chloride content measurement for PMC2

Depth	Time [months]						
[mm]	1	5	9	13	17	21	24
2.5	1.56	3.21	4.17	4.68	5.27	5.56	5.66
10	0.12	1.55	2.35	2.92	3.28	3.70	3.80
20	0.00	1.20	1.87	2.61	2.94	3.12	3.20
30	0.00	1.06	1.47	2.12	2.60	2.75	2.83
40	0.00	0.75	1.29	1.64	1.92	2.13	2.20
50	0.00	0.47	0.77	1.01	1.20	1.32	1.43

Table A- 7 Results of chloride content measurement for PMC3

Depth	Time [months]						
[mm]	1	5	9	13	17	21	24
2.5	1.26	2.56	3.42	3.75	4.23	4.68	4.74
10	0.09	1.37	1.90	2.24	2.69	2.93	3.03
20	0.00	1.02	1.62	1.90	2.21	2.33	2.42
30	0.00	0.69	1.11	1.41	1.67	1.88	1.94
40	0.00	0.42	0.55	0.81	1.22	1.39	1.55
50	0.00	0.26	0.39	0.55	0.63	0.75	0.83

Table A- 8 Results of chloride content measurement for FRPMC1

Depth [mm]	Time [months]						
	1	5	9	13	17	21	24
2.5	2.45	4.78	5.24	6.12	6.57	7.23	7.32
10	0.15	2.13	3.36	4.15	4.37	5.43	5.55
20	0.04	1.58	2.64	3.23	3.55	4.21	4.3
30	0	1.18	1.88	2.42	2.84	3.21	3.28
40	0	0.87	1.44	1.73	2.12	2.34	2.42
50	0	0.35	0.82	1.17	1.33	1.46	1.52

Table A- 9 Results of chloride content measurement for FRPMC2

Depth [mm]	Time [months]						
	1	5	9	13	17	21	24
2.5	2.18	4.21	4.52	5.23	5.68	6.24	6.31
10	0.13	1.88	2.42	3.22	3.76	4.23	4.32
20	0	1.31	2.02	2.74	3.16	3.47	3.54
30	0	1.16	1.65	2.15	2.56	2.84	2.92
40	0	0.74	1.22	1.57	1.92	2.16	2.24
50	0	0.5	0.74	1.05	1.24	1.38	1.43

Table A- 10 Results of chloride content measurement for FRPMC3

Depth [mm]	Time [months]						
	1	5	9	13	17	21	24
2.5	1.87	3.54	4.13	4.78	5.32	5.84	5.91
10	0.1	1.65	2.28	2.91	3.37	3.75	3.84
20	0	1.14	1.75	2.37	2.91	3.23	3.32
30	0	0.83	1.27	1.86	2.37	2.68	2.75
40	0	0.51	0.91	1.31	1.64	1.92	2.04
50	0	0.2	0.53	0.85	1.12	1.28	1.35

Table A- 11 Results of chloride content measurement for FRPMC4

Depth [mm]	Time [months]						
	1	5	9	13	17	21	24
2.5	2.36	4.66	5.12	5.85	6.32	6.64	6.73
10	0.16	2.16	2.67	3.21	3.68	3.84	3.91
20	0	1.58	2.23	2.71	3.14	3.42	3.53
30	0	1.25	1.81	2.23	2.66	2.91	3.07
40	0	0.91	1.28	1.64	2.12	2.35	2.42
50	0	0.55	0.82	1.14	1.32	1.42	1.51

Table A- 12 Results of chloride content measurement for FRPMC5

Depth	Time [months]						
[mm]	1	5	9	13	17	21	24
2.5	1.56	3.21	4.17	4.68	5.27	5.56	5.66
10	0.18	1.63	2.16	2.73	3.15	3.36	3.44
20	0	1.24	1.83	2.37	2.66	2.81	2.88
30	0	1.02	1.47	1.86	2.21	2.34	2.42
40	0	0.68	1.18	1.47	1.73	1.91	2.06
50	0	0.43	0.82	1.1	1.23	1.31	1.38

Table A- 13 Results of chloride content measurement for FRPMC6

Depth	Time [months]						
[mm]	1	5	9	13	17	21	24
2.5	1.36	2.76	3.55	4.13	4.38	4.88	4.93
10	0.08	1.38	1.68	2.04	2.35	2.62	2.71
20	0	0.94	1.28	1.66	1.82	2.11	2.18
30	0	0.68	0.96	1.22	1.45	1.57	1.65
40	0	0.46	0.67	0.82	0.95	1.12	1.21
50	0	0.23	0.38	0.58	0.71	0.84	0.9

Table A- 14 Results of chloride content measurement for FRPMC7

Depth	Time [months]						
[mm]	1	5	9	13	17	21	24
2.5	2.1	4.55	5.15	5.65	6.12	6.53	6.64
10	0.18	2.03	2.57	3.18	3.51	3.81	3.88
20	0	1.62	2.15	2.55	2.98	3.24	3.35
30	0	1.24	1.83	2.32	2.58	2.74	2.84
40	0	0.92	1.31	1.55	1.86	2.14	2.21
50	0	0.51	0.75	0.92	1.25	1.32	1.37

Table A- 15 Results of chloride content measurement for FRPMC8

Depth	Time [months]						
[mm]	1	5	9	13	17	21	24
2.5	1.56	3.21	4.17	4.68	5.27	5.56	5.66
10	0.14	1.32	1.82	2.42	2.81	3.12	3.18
20	0	1.11	1.43	1.88	2.28	2.57	2.66
30	0	0.72	1.07	1.36	1.64	1.83	1.9
40	0	0.43	0.74	0.91	1.16	1.27	1.32
50	0	0.15	0.35	0.54	0.63	0.74	0.78

Table A- 16 Results of chloride content measurement for FRPMC9

Depth [mm]	Time [months]						
	1	5	9	13	17	21	24
2.5	1.26	2.56	3.42	3.75	4.23	4.88	5.13
10	0.09	0.95	1.42	1.66	1.81	2.11	2.16
20	0	0.68	0.91	1.14	1.42	1.57	1.61
30	0	0.42	0.62	0.78	0.94	1.14	1.18
40	0	0.27	0.43	0.51	0.68	0.75	0.79
50	0	0.11	0.18	0.25	0.3	0.37	0.41

APPENDIX.B

The results of corrosion time obtaining from the digital data logger are presented in this section (Anodic Current).

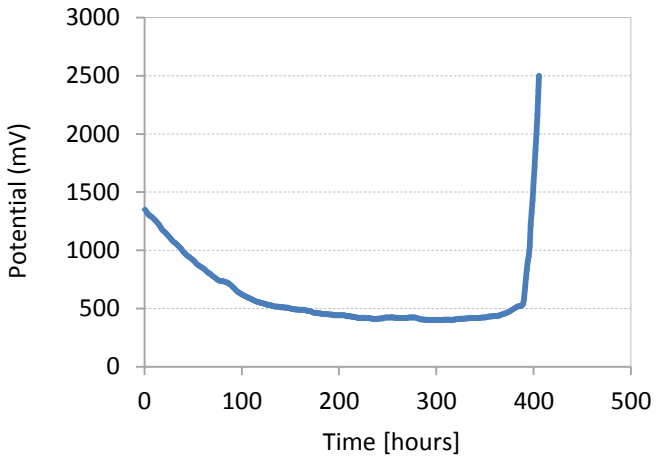

Figure B-1 Time to corrosion-induced crack for CC

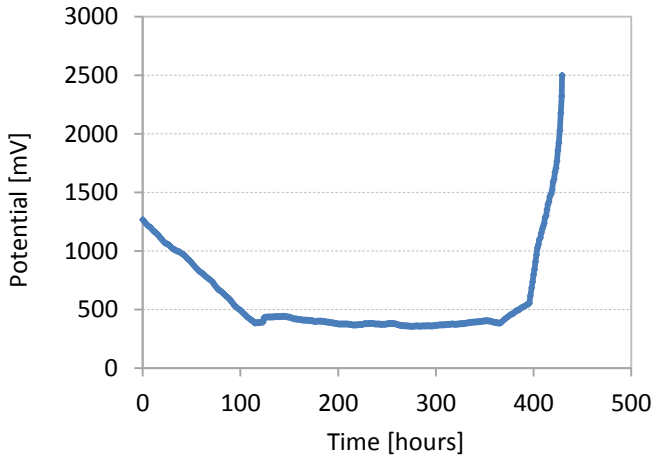

Figure B-2 Time to corrosion-induced crack for FRC1-1

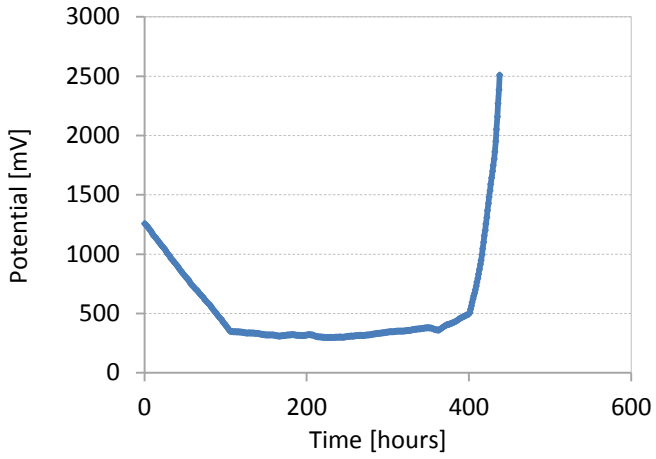

Figure B-3 Time to corrosion-induced crack for FRC1-2

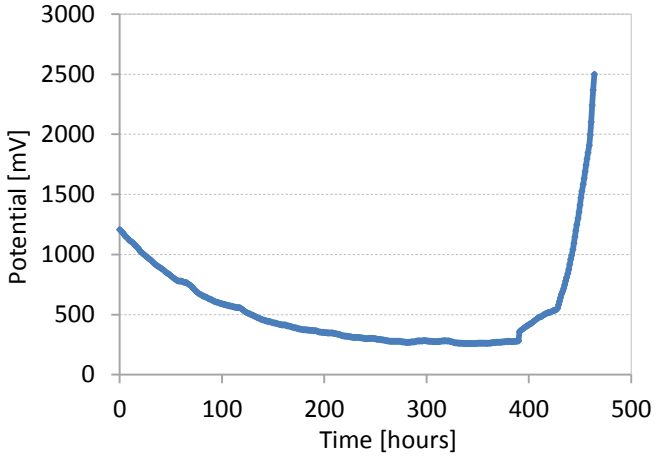

Figure B-4 Time to corrosion-induced crack for FRC2-1

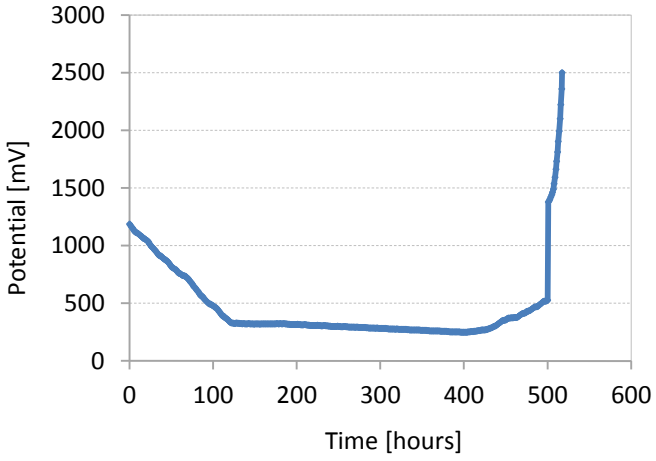

Figure B-5 Time to corrosion-induced crack for FRC3-1

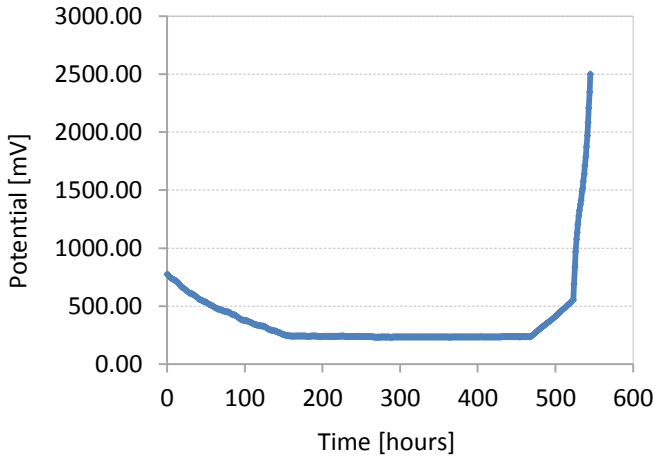

Figure B-6 Time to corrosion-induced crack for PMC1-1

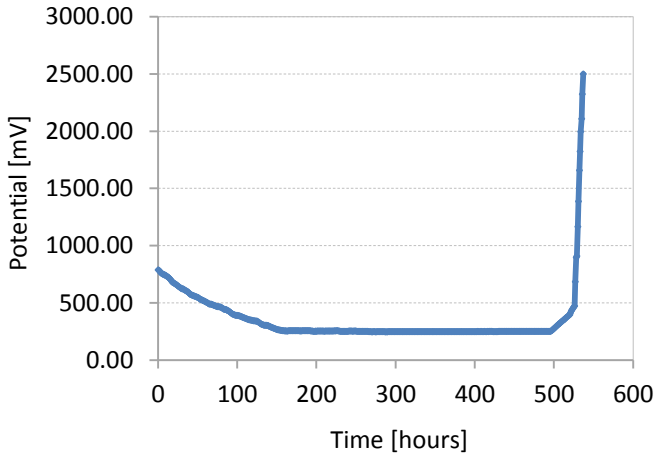

Figure B-7 Time to corrosion-induced crack for PMC1-2

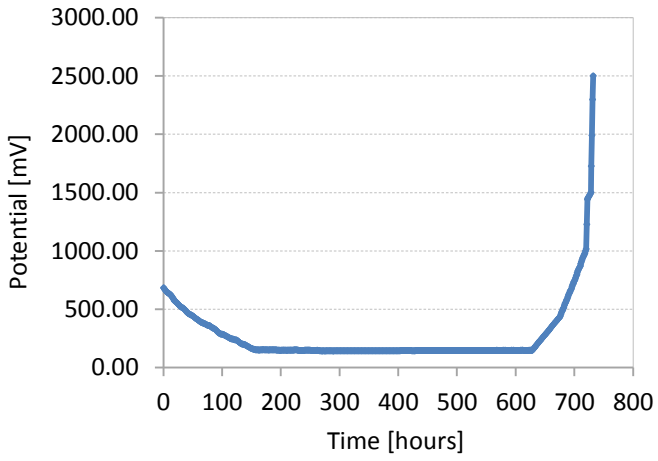

Figure B-8 Time to corrosion-induced crack for PMC2-1

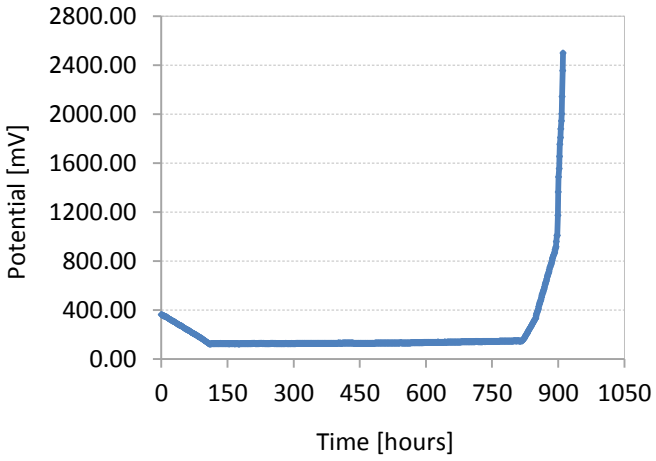

Figure B-9 Time to corrosion-induced crack for PMC3-2

APPENDIX.C

Changes of chloride diffusion coefficient over time determined for some samples based on chloride content measurements from experimental program of this study are presented in this section.

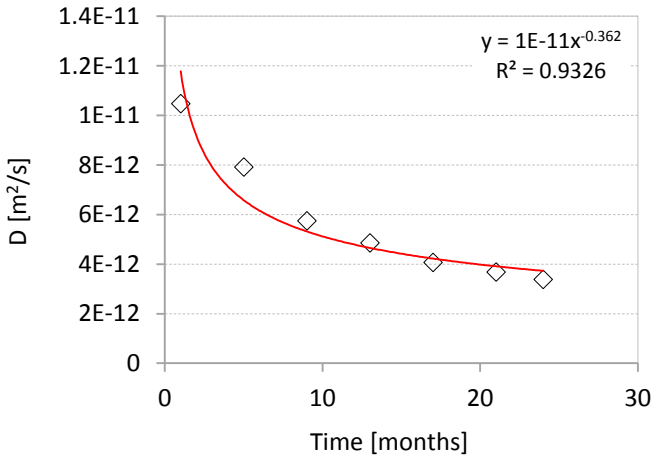

Figure C-1 Chloride diffusion coefficient of CC for x=10mm

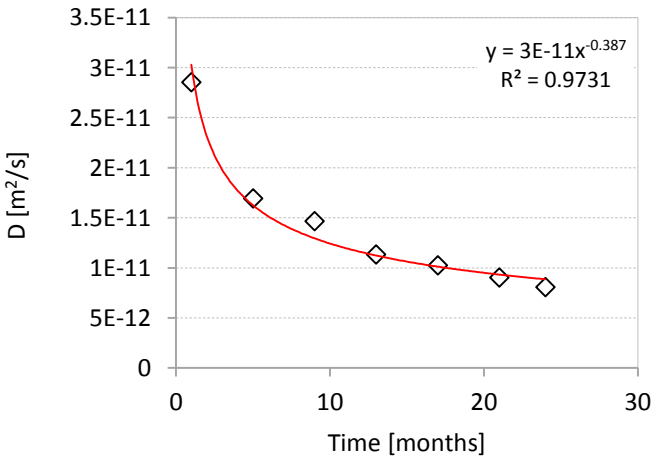

Figure C-2 Chloride diffusion coefficient of CC for x=20mm

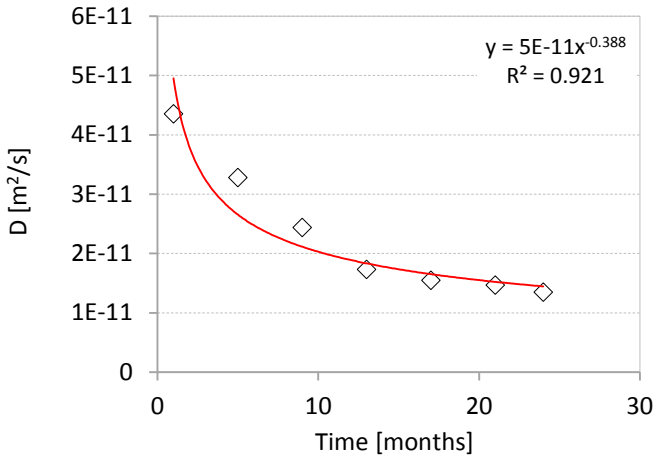

Figure C-2 Chloride diffusion coefficient of CC for x=30mm

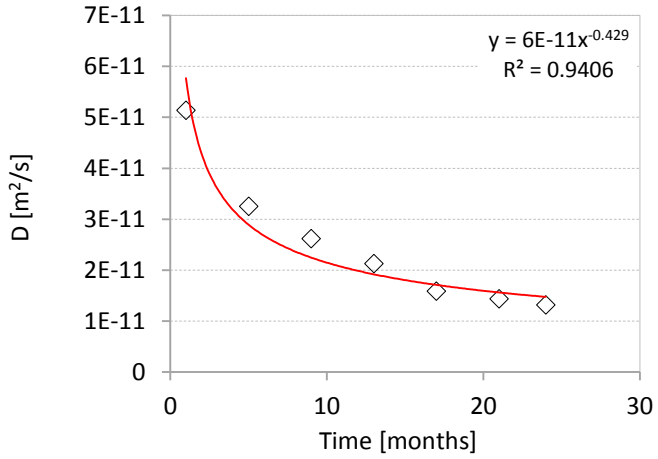

Figure C-2 Chloride diffusion coefficient of CC for x=40mm

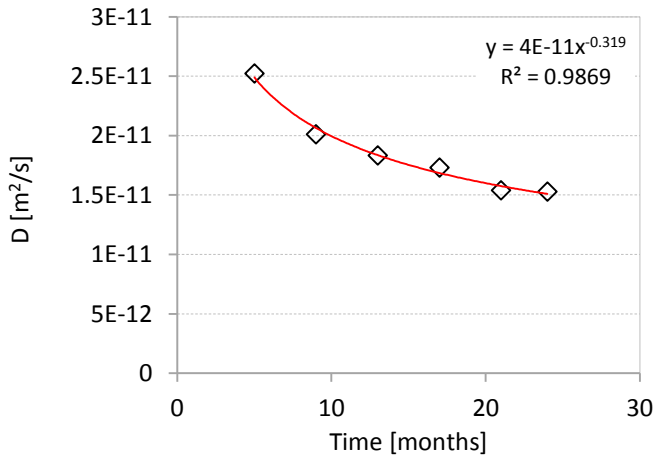

Figure C-2 Chloride diffusion coefficient of CC for x=50mm

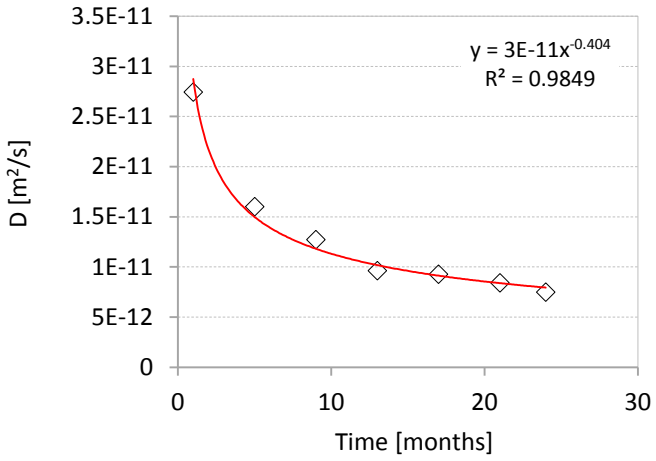

Figure C-2 Chloride diffusion coefficient of FRC1 for x=20mm

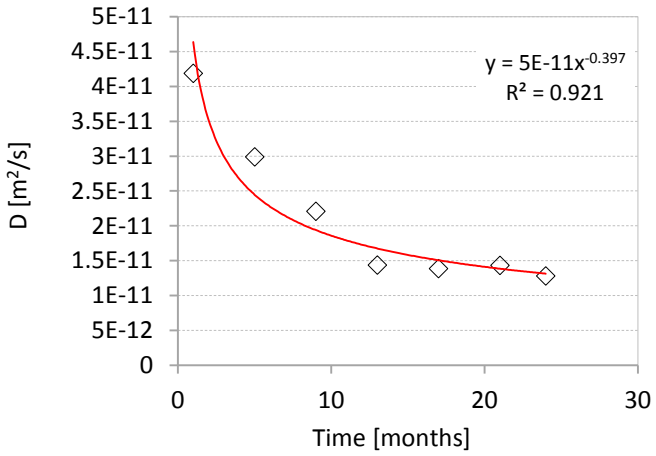

Figure C-2 Chloride diffusion coefficient of FRC1 for x=30mm

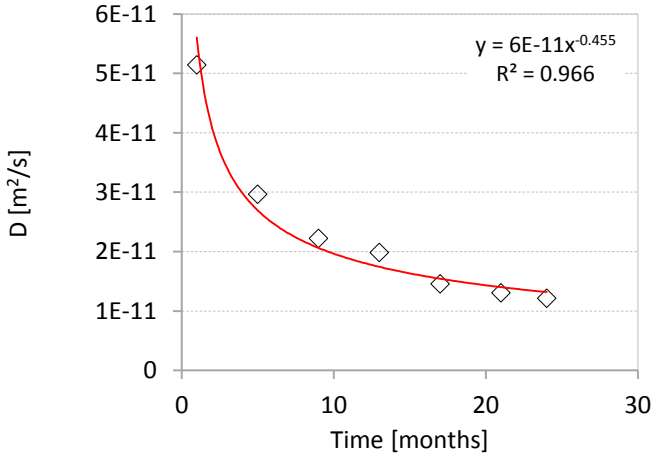

Figure C-2 Chloride diffusion coefficient of FRC1 for x=40mm

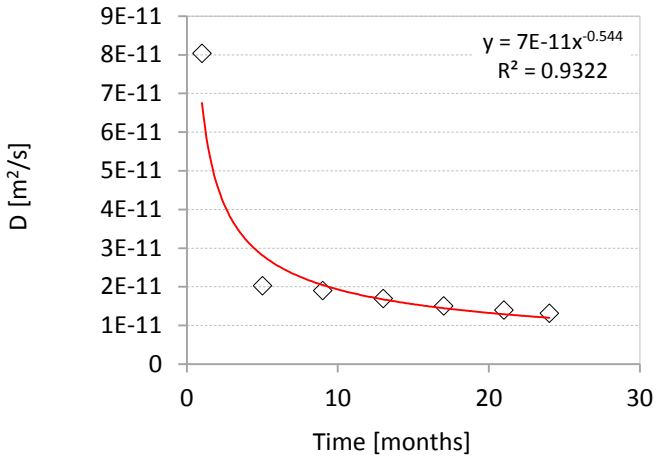

Figure C-2 Chloride diffusion coefficient of FRC1 for x=50mm

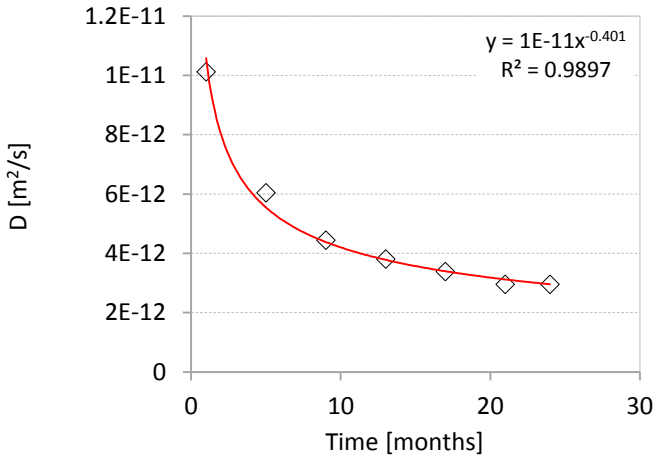

Figure C-2 Chloride diffusion coefficient of FRC2 for x=10mm

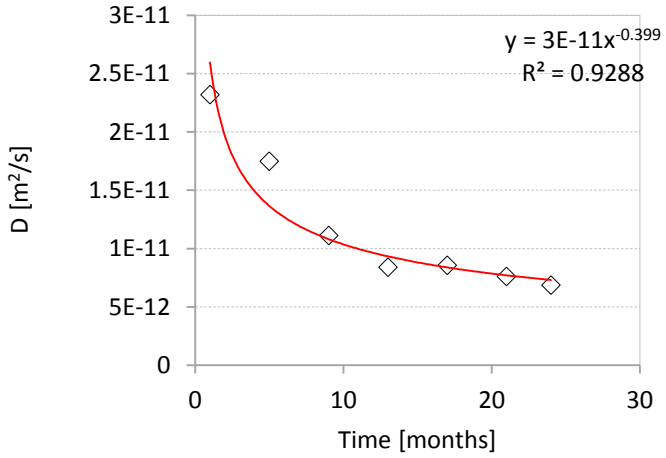

Figure C-2 Chloride diffusion coefficient of FRC2 for x=20mm

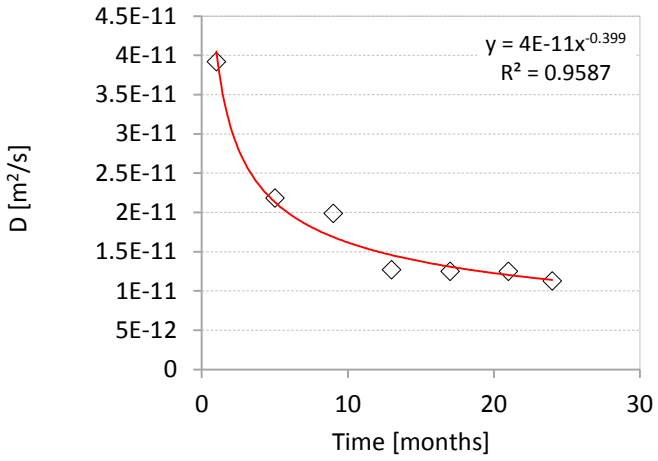

Figure C-2 Chloride diffusion coefficient of FRC2 for x=30mm

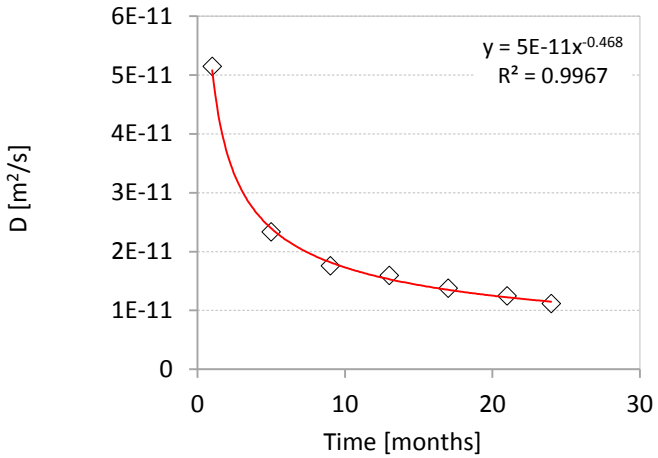

Figure C-2 Chloride diffusion coefficient of FRC2 for x=40mm

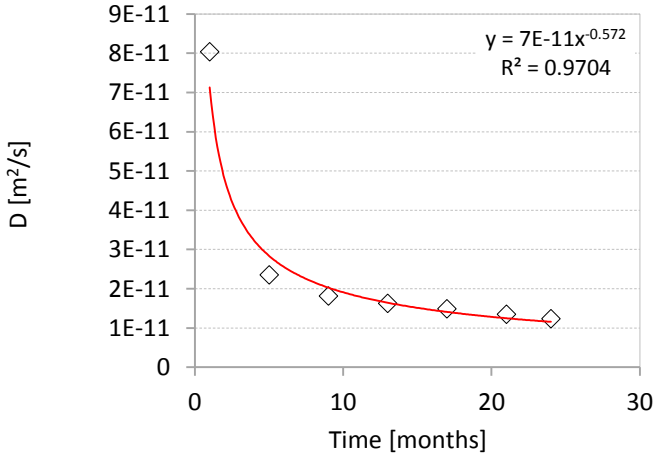

Figure C-2 Chloride diffusion coefficient of FRC2 for x=50mm

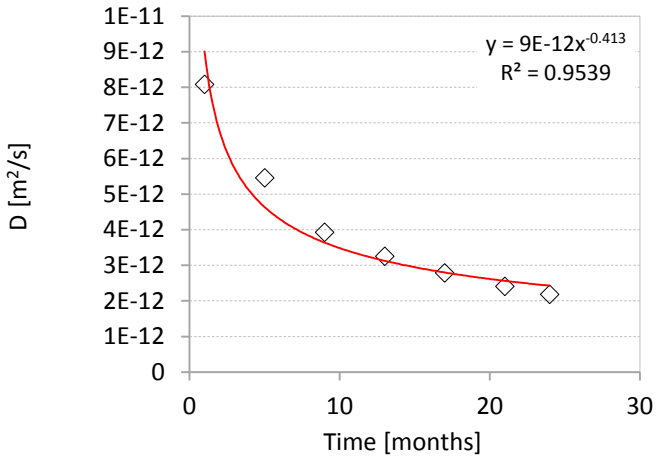

Figure C-2 Chloride diffusion coefficient of FRC3 for x=10mm

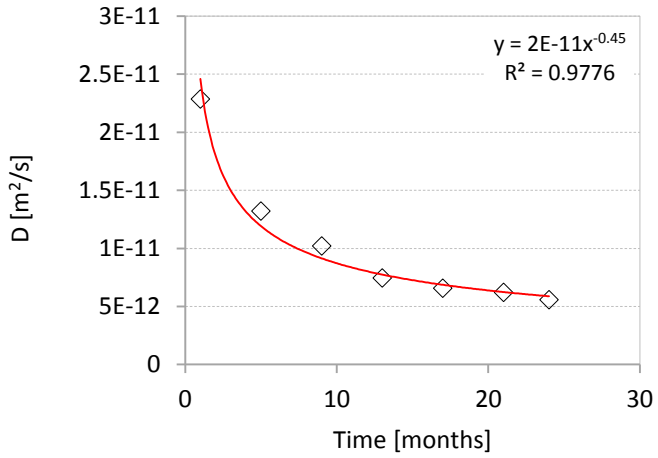

Figure C-2 Chloride diffusion coefficient of FRC3 for x=20mm

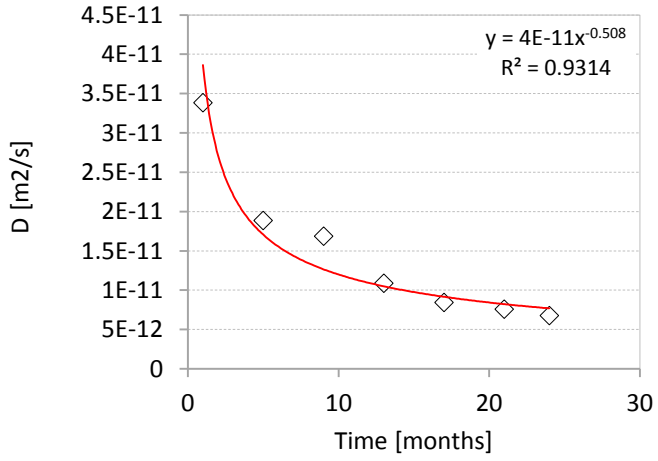

Figure C-2 Chloride diffusion coefficient of FRC3 for x=30mm

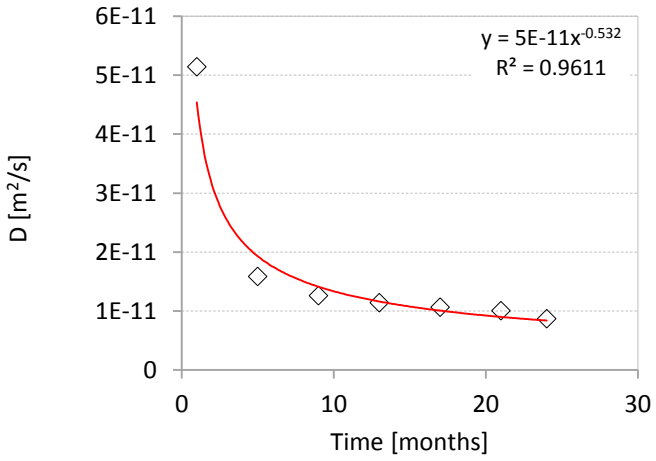

Figure C-2 Chloride diffusion coefficient of FRC3 for x=40mm

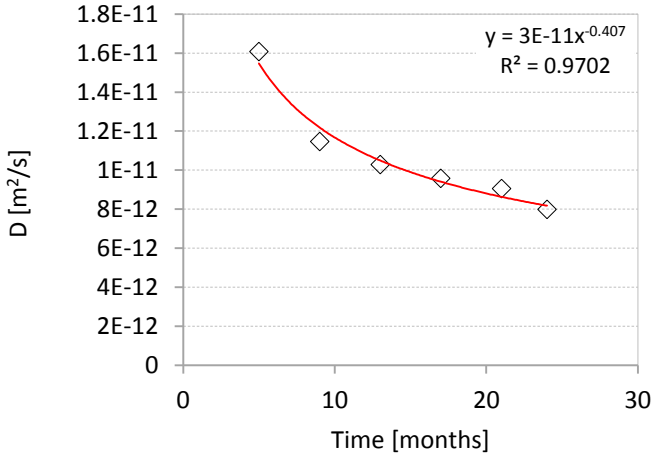

Figure C-2 Chloride diffusion coefficient of FRC3 for x=50mm

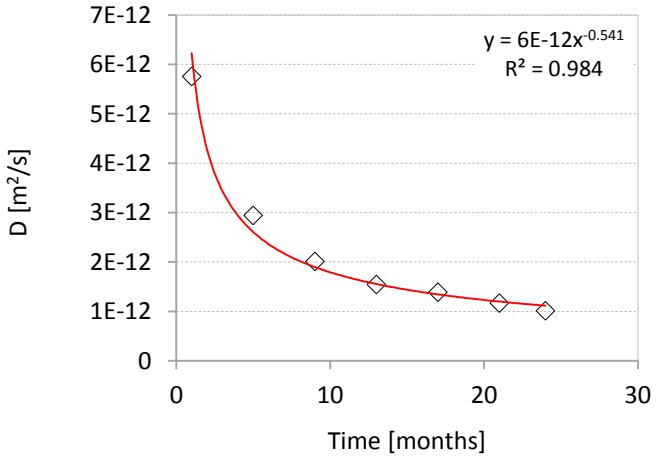

Figure C-2 Chloride diffusion coefficient of PMC1 for x=10mm

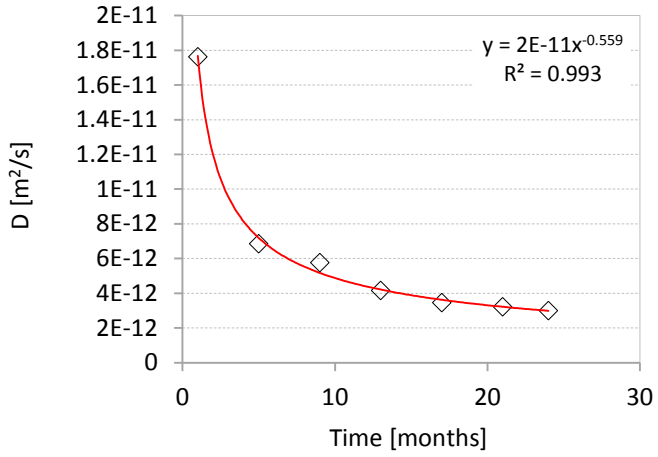

Figure C-2 Chloride diffusion coefficient of PMC1 for x=20mm

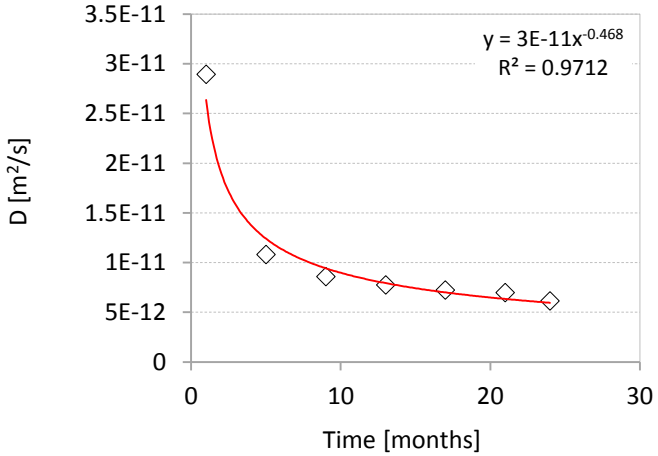

Figure C-2 Chloride diffusion coefficient of PMC1 for x=30mm

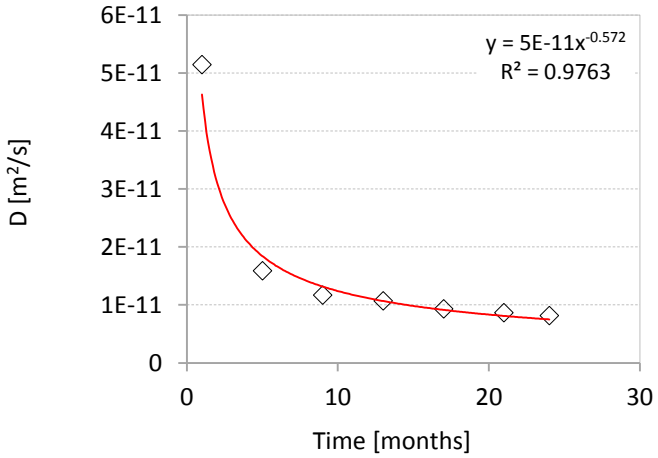

Figure C-2 Chloride diffusion coefficient of PMC1 for x=40mm

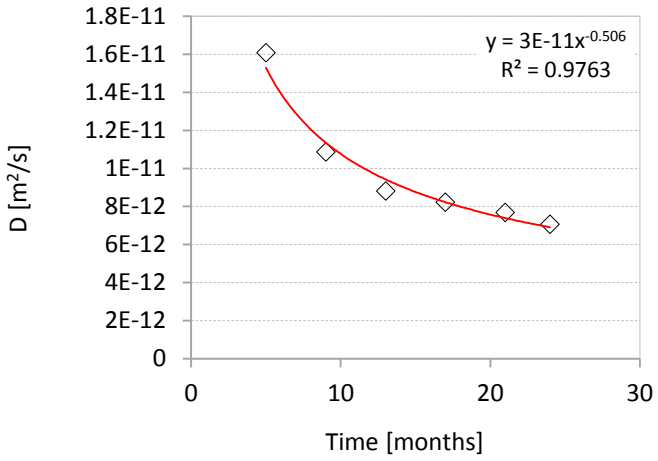

Figure C-2 Chloride diffusion coefficient of PMC1 for x=50mm